Roughans Point
Coastal Flood Damage Reduction Project
Revere, Massachusetts

Design Memorandum No. 2
Hydrology and Hydraulics

April 1991

US Army Corps of Engineers
New England Division

REPORT DOCUMENTATION PAGE

Form Approved
OMB No. 0704-0188

1. AGENCY USE ONLY (Leave blank)	2. REPORT DATE	3. REPORT TYPE AND DATES COVERED
	April 1991	Design Memorandum No.2

4. TITLE AND SUBTITLE
Water Resources Development Project Roughans Point Coastal Flood Damage Reduction, Revere, Massachusetts, Design Memorandum No.2, Hydrology and Hydraulics

5. FUNDING NUMBERS

6. AUTHOR(S)
U.S. Army Corps of Engineers
New England Division

7. PERFORMING ORGANIZATION NAME(S) AND ADDRESS(ES)
U.S. Army Corps of Engineers, New England Division
Hydraulics and Water Quality Branch,
Hydrologic Engineering Branch, Water Control Division
Engineering Directorate
424 Trapelo Road, Waltham, MA 02254-9149

8. PERFORMING ORGANIZATION REPORT NUMBER

9. SPONSORING/MONITORING AGENCY NAME(S) AND ADDRESS(ES)
U.S. Army Corps of Engineers, New England Division
424 Trapelo Road
Waltham, MA 02254-9149

10. SPONSORING/MONITORING AGENCY REPORT NUMBER

11. SUPPLEMENTARY NOTES
The project was congressionally authorized by Public Law 99-662 on November 17, 1986.

12a. DISTRIBUTION/AVAILABILITY STATEMENT
Approved for public release
Distribution is unlimited

12b. DISTRIBUTION CODE

13. ABSTRACT (Maximum 200 words)

This memorandum presents the hydrologic and hydraulic criteria and analysis pertinent to the design of coastal flood damage reduction improvements for Roughans Point in Revere, Massachusetts. Included are the results of physical and mathematical model investigations and analysis, descriptions of the hydraulic features, and hydrologic effects of the proposed project. This memorandum which includes the results of model studies completed in 1986 is intended to serve as an update to earlier hydrologic and hydraulic studies conducted during the feasibility investigation which was completed in 1983. Geotechnical and civil design studies needed for the General Design Memorandum (GDM) have been ongoing since completion of model studies. This memorandum, a companion document to the GDM, is being submitted for HQUSACE review on a concurrent basis.

14. SUBJECT TERMS
Roughans Point; Revere, Massachusetts; hydrology; sea walls; coastal regions; shore protection

15. NUMBER OF PAGES
250

16. PRICE CODE

17. SECURITY CLASSIFICATION OF REPORT	18. SECURITY CLASSIFICATION OF THIS PAGE	19. SECURITY CLASSIFICATION OF ABSTRACT	20. LIMITATION OF ABSTRACT
Unclassified	Unclassified	Unclassified	

DEPARTMENT OF THE ARMY
NEW ENGLAND DIVISION, CORPS OF ENGINEERS
424 TRAPELO ROAD
WALTHAM, MASSACHUSETTS 02254-9149

REPLY TO
ATTENTION OF

CENED-ED-WH

30 April 1991

MEMORANDUM FOR CDRUSACE (CECW-EP-E)/Mr. Phil Brown, 20 MASS. AVE., N.W., WASH DC 20314-1000

SUBJECT: Roughans Point, Coastal Flood Damage Reduction Project, Revere, Massachusetts, Design Memorandum No. 2, Hydrology and Hydraulics

In accordance with ER 1110-2-1150, dated 24 June 1985, Design Memorandum No. 2, Hydrology and Hydraulics for the Roughans Point Project, Revere, Massachusetts is submitted for review and approval.

FOR THE COMMANDER:

RICHARD D. REARDON
Director of Engineering

Encl (20 cys)

WATER RESOURCES DEVELOPMENT PROJECT
ROUGHANS POINT COASTAL FLOOD DAMAGE REDUCTION
REVERE, MASSACHUSETTS

DESIGN MEMORANDA INDEX

No.	Title	Anticipated Submission Date	Date Submitted	Date Approved
1	General Design	3/91	4/91	
2	Hydrology and Hydraulics	4/91	4/91	

WATER RESOURCES DEVELOPMENT PROJECT
ROUGHANS POINT COASTAL FLOOD DAMAGE REDUCTION
REVERE, MASSACHUSETTS

DESIGN MEMORANDUM NO. 2
HYDROLOGY AND HYDRAULICS

BY
HYDRAULICS AND WATER QUALITY BRANCH
AND
HYDROLOGIC ENGINEERING BRANCH
WATER CONTROL DIVISION
ENGINEERING DIRECTORATE

DEPARTMENT OF THE ARMY
NEW ENGLAND DIVISION, CORPS OF ENGINEERS
WALTHAM, MASSACHUSETTS 02254-9149

APRIL 1991

WATER RESOURCES DEVELOPMENT PROJECT
ROUGHANS POINT COASTAL FLOOD DAMAGE REDUCTION
REVERE, MASSACHUSETTS

DESIGN MEMORANDUM NO. 2
HYDROLOGY AND HYDRAULICS

TABLE OF CONTENTS

LIST OF TABLES

LIST OF FIGURES

LIST OF PLATES

LIST OF APPENDICES

PERTINENT DATA

1. Purpose: Hurricane and Storm Damage Reduction

2. Location:

   State: Massachusetts

   County: Suffolk

   City: Revere

   Water Body: Broad Sound

3. Design Conditions:

   Design Ocean Stillwater Level: 10.3 feet NGVD (100-year)

   Design Wave Height: 3.7 feet (Locally generated in Broad Sound)
   9.6 feet (Deep ocean generated)

   Design Freeboard: 5.0 feet (North Wall, reach A)
   3.7 feet (North revetment, reaches B-D)
   9.3 feet (East Wall, reaches E & F)
   0.7 foot (Backwater)

4. Existing Seawall (Reach A):

   Slope: Vertical

   Top Level: 15.3 feet NGVD

   Length: 805 feet

5. Armor Stone Revetment:

   Slope: 1 on 3

   Top Level: 8 feet NGVD (East Wall, portions of reach E will be overbuilt up to 10 ft, NGVD to allow for settlement. See Geotechnical Appendix, DM. No. 1)

   14 feet NGVD (North revetment, reaches B-D)

   Length: 3,125 feet

Berm Width: Varies between 5 and 25 feet

6. Concrete Seawall Cap and Existing Seawall:

Cap Height: 2 feet (East Wall, reaches E & F)

Top Level: 19.6 feet NGVD (with existing seawalls)

7. Backwater Protection:

Berm Height: 1 foot

Berm Length: 200 feet

Berm Top Level: 11.0 feet NGVD

Sluice Gate: 42-inch diameter on existing 42-inch storm drain

8. New Emergency Gravity Drain:

Diameter: 48 inches transitioning to a 5 by 5-foot box culvert

Gates: 48-inch sluice

9. Improvement to Existing Pumping Station Entrance:

Pumps: 2 @ 15 mgd, 1 @ 1 mgd (all existing)

Capacity: Nominal 48 cfs (with improved entrance structure)

10. Improved Flood Warning and Evacuation Plan

A plan has been developed by the city of Revere that provides for warning and evacuation of the area if necessary. This plan, activated prior to severe flooding, calls for close monitoring of conditions, road closure, and evacuation depending on storm severity.

HYDROLOGIC AND HYDRAULIC DESIGN CRITERIA REFERENCES

Corps of Engineers References:

EC 1105-2-86	"Flood Damage Prevention: Level of Protection"
EC 1105-2-186	"Guidance on The Incorporation of Sea Level Rise Possibilities in Feasibility Studies," April 1989
EC 1110-2-249	"Hydrologic Frequency Analysis," June 1985
EC 1110-2-265	"Engineering and Design For Civil Works Projects," September 1989
EM 1110-2-1411	"Standard Project Flood Determinations," Revised March 1965
EM 1110-2-1412	"Engineering and Design Storm Surge Analysis," April 1986
EM 1110-2-1413	"Hydrologic Analysis of Interior Areas," January 1987
EM 1110-2-1414	"Water Levels and Wave Heights for Coastal Engineering Design," July 1989
ER 1110-2-1150 (Draft)	"Engineering After Feasibility Studies"
ER 1165-2-21	"Flood Damage Reduction Measures in Urban Areas," October 1980
ETL 1110-2-230	"Hydrologic and Hydraulic Engineering for Survey Investigations," May 1978
	"Shore Protection Manual," Volumes 1 and 2, 1984
	"Tides and Tidal Datums in the United States," CERC, February 1981
	"Atlantic Coast Hindcast, Shallow-Water, Significant Wave Information," WES, January 1983

Other Selected References:

	Guidelines for Determining Flood Flow Frequency, Bulletin 17B
	U.S. Weather Bureau Technical Paper 40
Army TM5-820-4	"Drainage for Areas Other Than Airfields," October 1983
Brater and King	"Handbook of Hydraulics," 1976

WATER RESOURCES DEVELOPMENT PROJECT
ROUGHANS POINT COASTAL FLOOD DAMAGE REDUCTION
REVERE, MASSACHUSETTS

DESIGN MEMORANDUM NO. 2
HYDROLOGY AND HYDRAULICS

1. PURPOSE

This memorandum presents the hydrologic and hydraulic criteria and analysis pertinent to the design of coastal flood damage reduction improvements for Roughans Point in Revere, Massachusetts. Included are the results of physical and mathematical model investigations and analysis, descriptions of the hydraulic features, and hydrologic effects of the proposed project. This memorandum which includes the results of model studies completed in 1986 is intended to serve as an update to earlier hydrologic and hydraulic studies conducted during the feasibility investigation which was completed in 1983. Geotechnical and civil design studies needed for the General Design Memorandum (GDM) have been ongoing since completion of model studies. This memorandum, a companion document to the GDM, is being submitted for HQUSACE review on a concurrent basis. Duplication has intentionally been minimized.

2. AUTHORIZATION

The project was Congressionally authorized by Public Law 99-662 on 17 November 1986. However, funds to initiate Continued Planning and Engineering, included model studies that were in previous Congressional appropriations under the Southeastern New England (SENE) authorization adopted by the Committee on Public Works of the United States Senate on 12 September 1969.

3. PROJECT DESCRIPTION

a. General. The Roughans Point coastal flood damage reduction project is described in the feasibility report approved by the Board of Engineers for Rivers and Harbors in December 1983, and in Design Memorandum No. 1, "General Design".

Overtopping of existing walls and dikes by wind-generated waves is the principal agent of coastal flooding in the Roughans Point area of Revere, Massachusetts (figures 2-1 and

2-2). Rainfall runoff also contributes to interior flooding, although to a lesser degree. The amount of wave overtopping is significantly affected by wave characteristics, local winds, geometry of protective works and ocean level. Substantial variations in water level can be produced by astronomical tides and by storm surges caused by a combination of high onshore winds and low atmospheric pressure. The coincidence of high water levels, large waves, and strong onshore winds create a threat of very serious flooding due to wave overtopping.

The recommended plan to provide protection for Roughans Point from wave overtopping consists of the existing seawall (reach A) extending southerly from a point 400 feet north of Eliot Circle and stabilizing the existing facilities (reaches B through F) along the shore with a 3,125-foot long armor stone revetment to dissipate incoming waves. The revetment would extend from the southerly end of reach A 320 feet from Eliot Circle, easterly then southerly to a point 200 feet south of the intersection of Winthrop Parkway and Leverett Avenue. The height of the existing easterly seawall (reaches E and F) would be increased by adding a 2-foot concrete cap. The plan also calls for backwater protection by constructing an earth berm 1 foot high and 200 feet long on the existing median strip between Bennington Street and State Road. An improved flood warning and evacuation plan is also part of the project.

Interior drainage improvements consist of the existing pump station, a new intake structure, a new emergency gravity drain and two sluice gates. Plate 1 of the GDM depicts the General Plan.

Following is a general description of project elements with reference to GDM plates. A complete project description is contained in the GDM.

b. Existing Seawall. Section stations 19+20 to 27+25, shown on plates 2 and 3 of the GDM, are called reach A. This reach includes the existing concrete seawall with a top elevation of 15.3 feet NGVD. It is not necessary to further reduce project wave overtopping in this area, only to insure that the existing wall remains intact throughout the design flood and project life.

c. Armor Stone Revetments. Stations 27+25 to 29+95 (reach B) are shown on plates 2, 3, and 4 of the GDM, and consist of steel sheet piling as a "cutoff" barrier driven along the centerline of a new armor stone revetment. This new structure will be 10 feet wide at elevation 14.0 feet

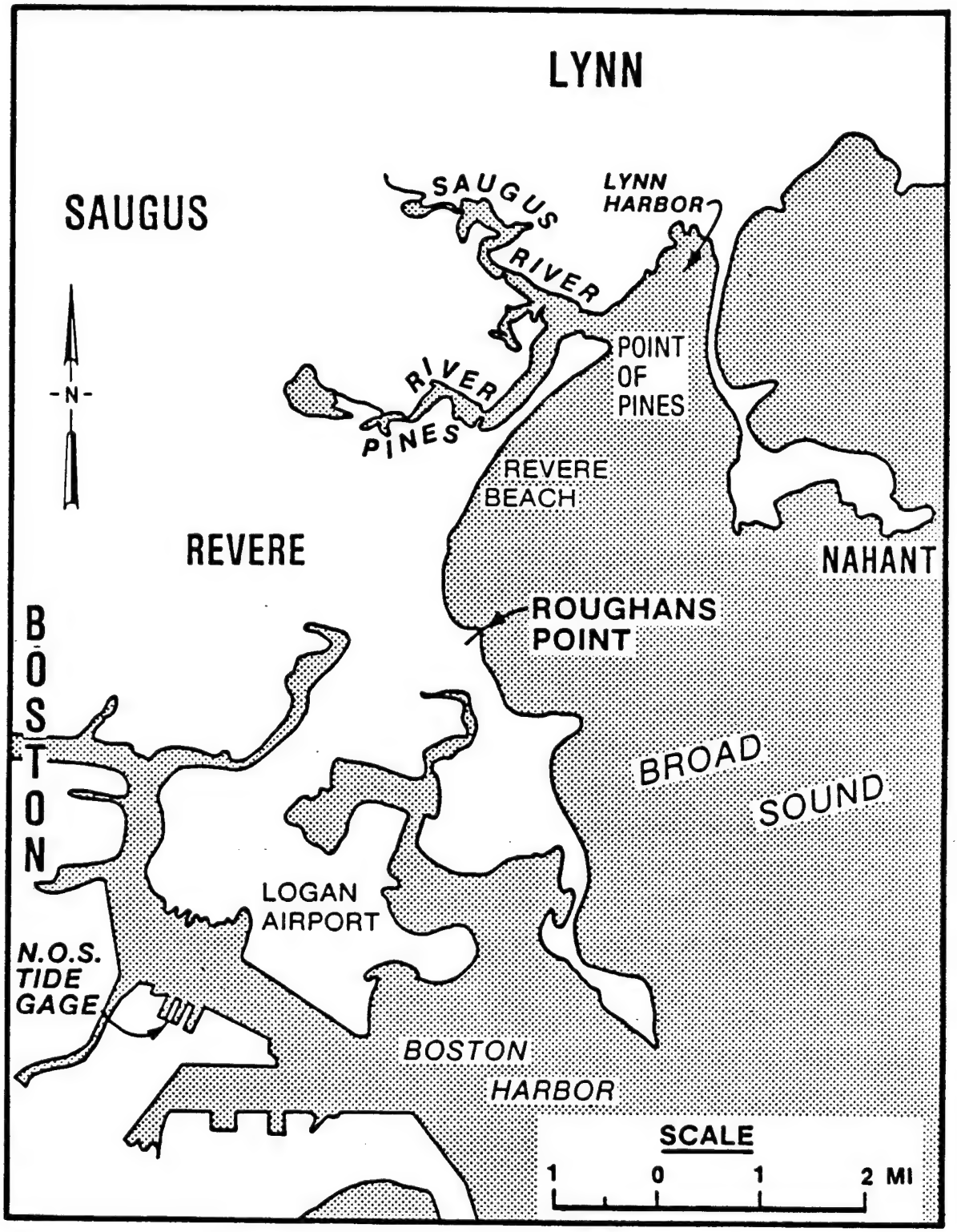

Figure 2-1. Location and vicinity map

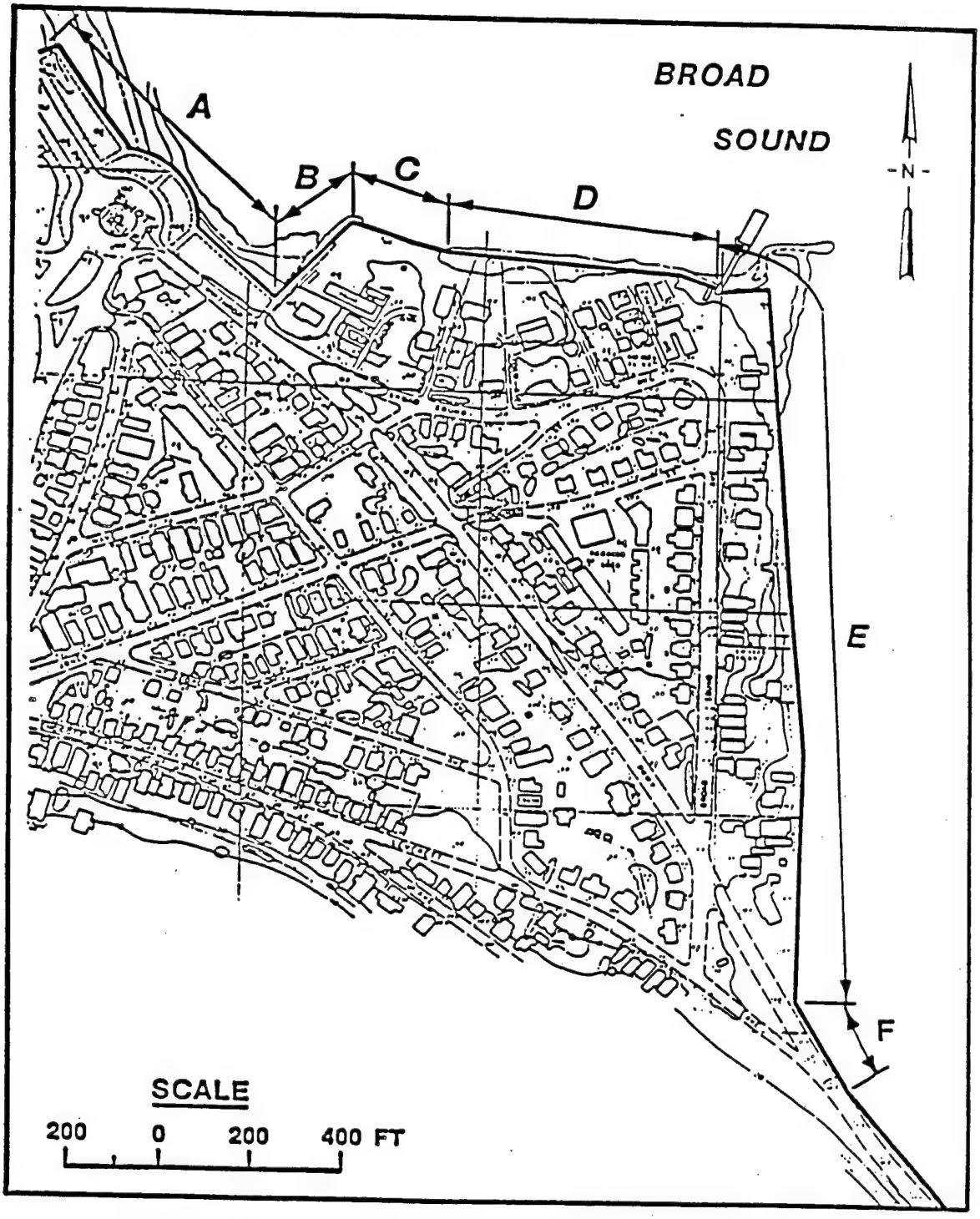

Figure 2-2. Location of Reaches A through F at Roughans Point

NGVD also with a seaward slope of 1 on 3 down to the beach. The landside of the revetment is sloped 1 on 2 down to the original ground surface, and serves as design ocean storm stillwater protection for the project area and also protects against localized turbulence and wave action.

The existing granite wall comprises reach C and runs from stations 29+95 to 32+00 and is shown on plates 2 and 5 of the GDM. The new section is similar to reach B, except that the sheet piling is driven along the face of the existing wall. The top of this revetment is also at elevation 14.0 feet NGVD. This reach reduces major wave overtopping and protects against design ocean stillwater.

Reach D, running from stations 32+00 to 38+45, is shown on plates 2 and 6, and has a steel sheet pile "cutoff" wall and new stone revetment which is 10 feet wide at top elevation 14.0 feet NGVD. Protection is provided against design ocean stillwater level and major wave overtopping is reduced.

The concrete seawall from stations 38+45 to 56+25 makes up reach E, shown on plates 7 through 9 of the GDM, and consists of stone protection in front of the vertical face of the existing concrete wall. This rock revetment will be 25 feet wide at top elevation of 8.0 to 10.0 feet NGVD, with a seaward slope of 1 on 3. Although hydraulic design calls for a 25.5-foot wide berm at elevation 8.0 feet NGVD, the height has been increased up to 2 feet at some locations to account for expected settlement due to poor foundation conditions. This is further discussed in the GDM. Reduction of wave overtopping and protection from design ocean stillwater are the purpose of this reach. The overbuilding of the berm for settlement was determined to have minimal effect on wave overtopping.

Lastly, reach F runs from stations 56+25 to 58+50 and completes the shore protection. This section is shown on plates 9 and 10 of the GDM, and is identical to reach E except that the rock berm is 25 feet wide at elevation 8.0 feet NGVD. Settlement was not identified as a problem here. This is principally a tie-in reach needed to interconnect with a sandbag emergency closure.

d. Concrete Cap and Existing Seawall. Along reaches E and F, a 2.0-foot high concrete cap will be added to the existing concrete wall, bringing the top elevation to 19.6 feet NGVD (see plates 9 and 10 of GDM).

e. Backwater Protection. An earth berm, about 1-foot high and 200 feet long with a top elevation of 11.0 feet NGVD

would be constructed on the existing median strip between Bennington Street and State Road. The berm would start at high ground on the Revere Beach Parkway bridge embankment and terminate at the intersection of Bennington and State Road (plate 11 of GDM). The intersection would be appropriately raised with new bituminous concrete to reach high ground, which is at the middle of the intersection, opposite the west end of Endicott Avenue. The existing parkway and road embankments from the north end of the proposed 1,150-foot berm to the Eliot Circle seawall are needed to prevent backwater flooding into Roughans. Backwater protection has been kept to a minimum to allow escape of wave overtopping waters coming from the east and north during a coastal storm exceeding design conditions such as a Standard Project Northeaster (SPN).

A sandbag closure may be needed, depending on the severity of a storm, to prevent floodwaters from flowing north on Winthrop Parkway and into the project area (plate 10 of GDM). The closure would be up to 3 feet high (elevation 18 feet) and located at the south end of the shore protection at reach F and extending across Winthrop Parkway to high ground, a distance of about 60 feet.

Other options to sandbag closures such as road raising may be considered during final design.

f. Interior Drainage. Interior drainage provisions include the existing pumping station with an improved intake structure to serve the pumping station and a new emergency gravity drain (plates 12 and 13 of GDM). A sluice gate would be provided on the existing drainage pipe which discharges into Sales Creek (plate 11 of GDM). During intense rainfall runoff conditions, drainage could be both to Sales Creek and through the existing Broad Sound Avenue pumping station. The Sales Creek sluice gate could be closed to prevent higher water in the creek from entering the project area. The new 48-inch (concrete pipe) gravity drain at the pumping station will transition to a 5 by 5-foot concrete box conduit and pass through the existing reach E seawall and the proposed rock revetment. Outletting on the revetment structure, the emergency gravity drain will have a positive closure sluice gate landside of the seawall.

g. Pumping Station. The existing Broad Sound Avenue pumping station (plates 12 and 13 of GDM) is located landside of the shore protection line along reach E. Three pumps (2 at 15 mgd and 1 at 1 mgd) with a nominal capacity of 48 cfs, along with diesel powered generators, are the main features of the facility. Access to the station is from

Broad Sound Avenue, and discharge to the ocean is through 30-inch and 4-inch cast iron discharge pipes. Normally the sluice gate on the new emergency gravity drain will be closed and the drainage pumped to the ocean. With low ground at about 4 feet NGVD near the pumping station and with a pipe invert of -2 feet NGVD, this is necessary to prevent ocean backflow through the emergency drain.

h. Improved Flood Warning and Evacuation Plan. A plan has been developed by the city of Revere that provides for warning and evacuation of the area if necessary. This plan is activated prior to severe flood conditions and calls for close monitoring of conditions, road closure, and evacuation depending on storm severity.

4. CLIMATOLOGY

a. General. The city of Revere, Massachusetts, located at 42 degrees north latitude, has a cool, semi-humid, and most variable climate, typical of New England. It is somewhat less harsh than in the higher inland areas of New England due to the moderating effect of adjacent ocean waters. Its location on the easterly-facing coast of New England exposes the Roughans Point area of Revere to coastal storms that move northeasterly up the Atlantic Coast with accompanying intense rainfall, winds, and flood producing storm tides and waves.

b. Temperature. The mean annual temperature at Revere is 51 degree Fahrenheit. Mean monthly temperatures vary from a high of 72 degrees in July to 29 degrees Fahrenheit in January and February. Extremes in temperature vary from summertime highs in the nineties to wintertime lows in the minus teens. Mean, maximum, and minimum monthly temperatures as recorded over a 109-year period at neighboring Boston are listed in table 2-1.

c. Precipitation. The mean annual precipitation at Revere is 42 inches based on 110 continuous years of record at neighboring Boston. Precipitation is distributed quite uniformly throughout the year, averaging about 3.5 inches per month. Short duration intense rainfall often results from fast moving frontal systems, thunderstorms, and coastal storms. Also, most winter precipitation occurs as snowfall. Mean, maximum, and minimum monthly precipitation recorded at Boston, Massachusetts is listed in table 2-2.

TABLE 2-1

MONTHLY TEMPERATURE
BOSTON, MASSACHUSETTS

Elevation 15 feet NGVD
109 Years of Record
(Degrees Fahrenheit)

Month	Mean	Maximum	Minimum
January	29.0	72	-13
February	29.3	68	-11
March	37.7	86	- 8
April	47.4	89	11
May	57.9	97	31
June	67.3	100	42
July	72.5	104	46
August	71.6	101	47
September	64.4	102	34
October	54.9	90	25
November	44.5	83	- 2
December	32.9	69	-14
ANNUAL	50.8	104	-14

TABLE 2-2

MONTHLY PRECIPITATION
BOSTON, MASSACHUSETTS

Elevation 15 Feet NGVD
110 Years of Record
(Inches)

Month	Mean	Maximum	Minimum
January	3.67	10.55	0.35
February	3.35	9.98	0.45
March	3.84	11.75	Trace
April	3.55	10.83	0.20
May	3.24	13.38	0.25
June	3.13	9.13	0.27
July	3.12	12.38	0.52
August	3.64	17.09	0.37
September	3.23	11.95	0.21
October	3.27	8.84	0.06
November	3.80	11.63	0.59
December	3.70	9.74	0.26
ANNUAL	41.54	67.72	23.71

d. Snowfall. The average annual snowfall at Revere is 43 inches. Mean monthly and annual snowfall recorded at Boston is listed in table 2-3. Data on seasonal snowpack is not available for Revere. However, snow surveys by the Corps of Engineers in the Blackstone River Basin, about 20 miles south and 15 miles inland from Boston, indicate maximum water equivalent occurs about 1 March, ranging from near zero to about 6 inches, with an average of approximately 2.7 inches.

5. TIDAL HYDROLOGY

a. Astronomical Tides. At Revere, tides are semidiurnal, with two high and two low waters occurring during each lunar day (approximately 24 hours 50 minutes). The resulting tide range is constantly varying in response to the relative positions of the earth, moon, and sun; the moon having the primary tide producing effect. Maximum tide ranges occur when the orbital cycles of these bodies are in phase. A complete sequence of tide ranges is approximately repeated over an interval of 19 years, which is known as a tidal epoch. At the National Ocean Survey (NOS) tide gage in Boston, Massachusetts (the one nearest to Revere), the mean range of tide and mean spring range of tide are 9.5 feet and 11.0 feet, respectively (see figure 2 and 3). However, the maximum and minimum predicted astronomic tide ranges at Boston have been estimated at about 14.7 and 5.0 feet, respectively, using the Coastal Engineering Research Center (CERC) report, entitled: "Tides and Tidal Datums in the United States", SR No. 7, 1981. The variability of astronomical tide ranges is a very significant factor in tidal flooding potentials at Revere. This is explained further in section 5d.

Because of the continual variation in water level due to the tides, several reference planes, called tidal datums, have been defined to serve as a reference zero for measuring elevations of both land and water. Tidal datum information for Boston is presented on figure 2-3 and table 2-4. These were compiled using currently available NOS tidal benchmark data for Boston along with the previously mentioned report. As well, the frequency of predicted astronomic high water and hourly tide values were determined using the CERC report and are shown in figure 2-3A. This information will be useful in exploring rock berm construction scenarios since work will be tidally affected.

The epoch for which the National Ocean Survey has published tidal datum information for Boston is 1960-78. A phenomenon that has been observed through tide gaging and tidal benchmark measurements is that sea level is apparently rising with respect to the land along most of the U.S. coast.

TABLE 2-3

MEAN MONTHLY SNOWFALL
BOSTON, MASSACHUSETTS

Elevation 15 Feet NGVD
110 Years of Record
(Average Depth in Inches)

Month	Snowfall
January	11.9
February	12.5
March	7.7
April	1.6
May	Trace
June	0
July	0
August	0
September	0
October	Trace
November	1.4
December	8.0
ANNUAL	43.1

TIDAL DATUM PLANES
BOSTON, MASSACHUSETTS
NATIONAL OCEAN SURVEY TIDE GAGE

(BASED UPON 1960-78 NOS TIDAL EPOCH)

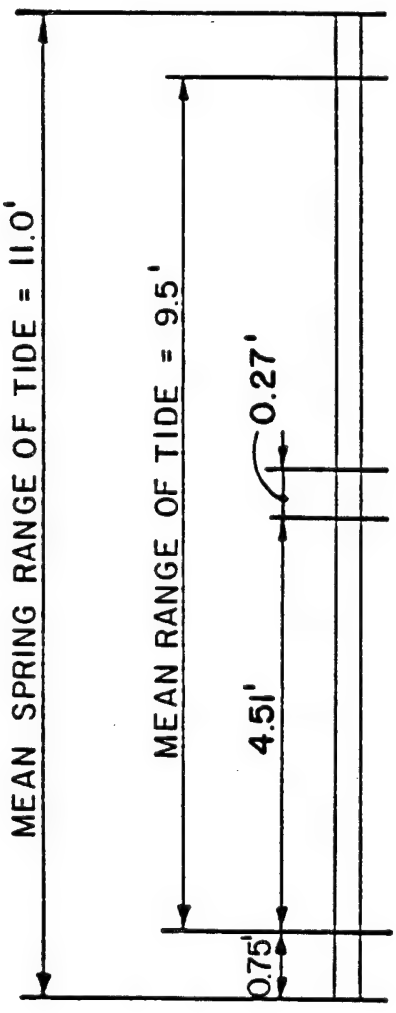

MEAN SPRING HIGH WATER (MHWS)

MEAN HIGH WATER (MHW)

MEAN TIDE LEVEL (MTL)

NATIONAL GEODETIC VERTICAL DATUM (NGVD)

MEAN LOW WATER (MLW)

MEAN SPRING LOW WATER (MLWS)

NEW ENGLAND DIVISION
U.S. ARMY, CORPS OF ENGINEERS
WALTHAM, MASS. MARCH 1985

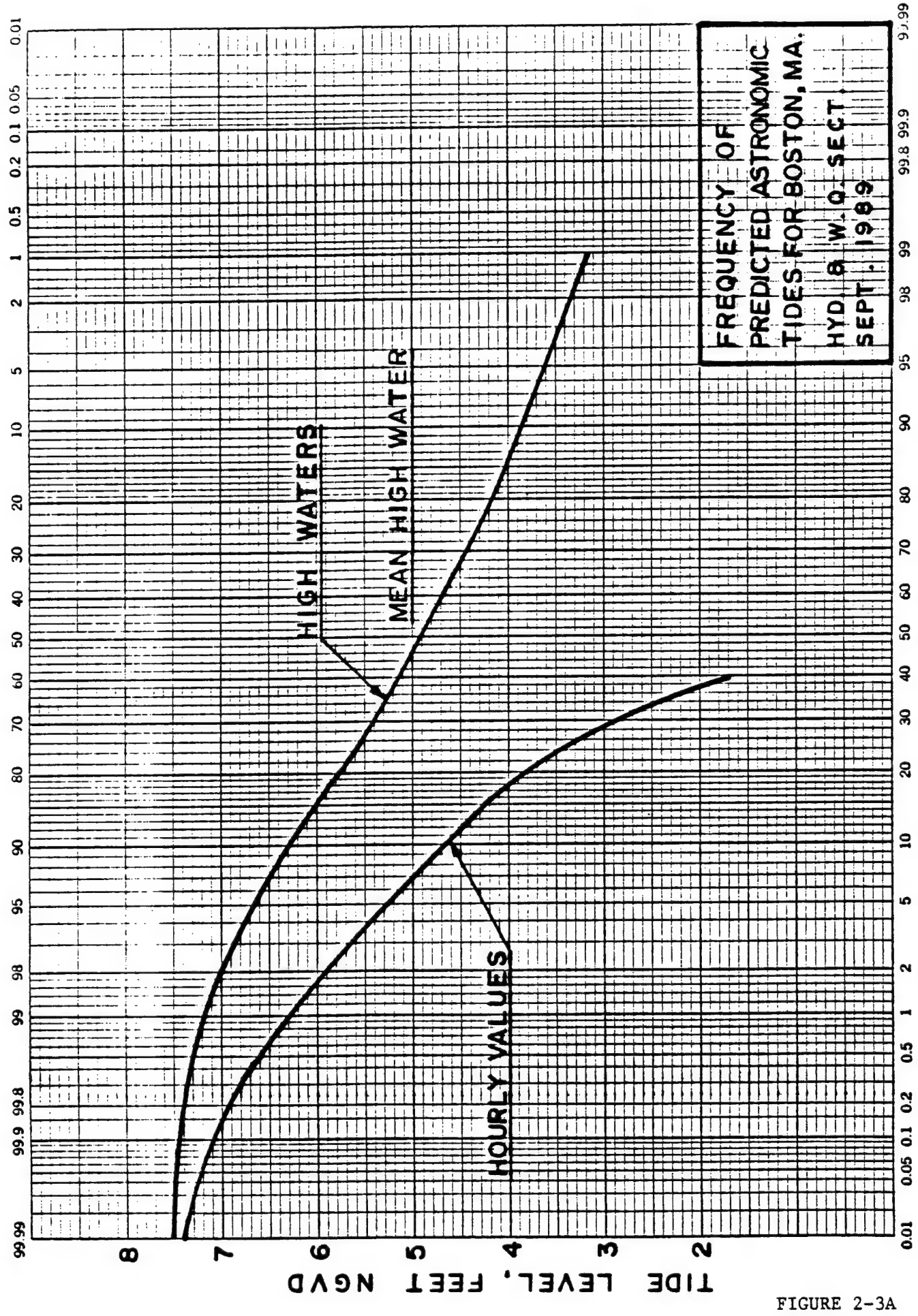
FREQUENCY OF
PREDICTED ASTRONOMIC
TIDES FOR BOSTON, MA.
HYD & W.Q. SECT.
SEPT. 1989
HIGH WATERS
MEAN HIGH WATER
HOURLY VALUES
TIDE LEVEL, FEET NGVD
PERCENT OF VALUES EQUALLING OR EXCEEDING
99.99 0.01
99.9 99.8 0.1 0.2
99 0.5 1
98 2
95 5
90 10
80 20
70 30
60 40
50
40 60
30 70
20 80
10 90
5 95
2 98
1 99
0.5
0.2 99.8
0.1 99.9
0.05
0.01 99.99
8
7
6
5
4
3
2

FIGURE 2-3A

At the Boston National Ocean Survey tide gage, the rise has been observed to be slightly less than 0.1 foot per decade. Sea level determination is generally revised at intervals of about 25 years to account for the changing sea level phenomenon (see section 9).

TABLE 2-4

BOSTON TIDAL DATUM PLANES
NATIONAL OCEAN SURVEY TIDE GAGE
(BASED UPON 1960-78 NOS TIDAL EPOCH)

	Tide Level (ft, NGVD)
Maximum Predicted Astronomic High Water	7.5
Mean Spring High Water (MHWS)	5.8
Mean High Water (MHW)	5.0
Minimum Predicted Astronomic High Water	2.7
Mean Tide Level (MTL)	0.3
National Geodetic Vertical Datum (NGVD)	0.0
Maximum Predicted Astronomic Low Water	-2.4
Mean Low Water (MLW)	-4.5
Mean Spring Low Water (MLWS)	-5.2
Minimum Predicted Astronomic Low Water	-7.1

b. Storm Types. Two distinct types of storms, distinguished primarily by their place of origin as being extratropical and tropical cyclones, influence coastal processes in New England. These storms can produce above normal water levels and waves and must be recognized in studying New England coastal problems.

(1) Extratropical Cyclones. These are the most frequently occurring variety of cyclones in New England. Low pressure centers frequently form or intensify along the boundary between a cold dry continental air mass and a warm moist marine air mass just off the coast of Georgia or the

Carolinas and move northeastward more or less parallel to the coast. These storms derive their energy from temperature contrast between cold and warm air masses. The organized circulation pattern associated with this type of storm may extend for 1,000 to 1,500 miles from the storm center. The wind field in an extratropical cyclone is generally asymmetric with the highest winds in the northeastern quadrant. When the storm center passes parallel and to the southeast of the New England coastline and highest onshore wind speeds are from the northeast, these storms are called "northeasters" or "nor'easters" by New Englanders. As the storm passes, local wind directions may vary from southeast to slightly west of north. Coastlines exposed to these winds can experience high waves and extreme storm surges. Such storms are the principal tidal flood producing events at Revere. Other storms which take a more inland track can have high winds from the southeast, and are referred to as "southeasters". At Revere, these storms do not generally produce as much storm surge and wave action as "northeasters" due to more limited fetch. However, "southeasters" can produce very turbulent ocean conditions. The prime season for severe extratropical storms in New England is November through April.

(2) Tropical Cyclones. These storms form in a warm moist air mass over the Caribbean and the waters adjacent to the West Coast of Africa. The air mass is nearly uniform in all directions from the storm center. The energy for the storm is provided by the latent heat of condensation. When the maximum windspeed in a tropical cyclone exceeds 75 mph, it is labeled a hurricane. Wind velocity at any position can be estimated based upon the distance from the storm center and the forward speed of the storm. The organized wind field may not extend more than 300 to 500 miles from the storm center. Recent hurricanes affecting New England generally have crossed Long Island Sound and proceeded landward in a generally northerly direction. However, hurricane tracks can be erratic. The storms lose much of their strength after landfall. For this reason the southern coast of New England experiences the greatest surge and wave action from the strong southerly to easterly hurricane winds. However, on very rare occasions, reaches of coastline in eastern and northern New England may experience some storm surge and wave action from the weakened storm. Hurricanes have not been a principal cause of tidal flooding at Revere. However, hurricane rainfall can cause serious ponding. The hurricane and tropical storm season in New England generally extends from August through October.

c. Winds. An estimate of windspeed is one of the essential ingredients in any wave hindcasting effort. The most

accurate estimate of winds at sea, which generate waves and propel them landward, is obtained by utilizing isobars of barometric pressure recorded during a given storm. However, actual recorded windspeed and direction data observed at a land based coastal meteorological station can serve as a useful guide when more locally generated waves and currents are of interest. The disadvantage with using land based wind records is that they may not be totally indicative of wind velocities at the sea-air interface where waves are generated. However, often they are the only available source of information and adjustments must be made to develop overwater estimates from the land based records. Also, when estimating wave overtopping of coastal structures, it is necessary to utilize local wind conditions. These local winds help determine how much of the runup from breaking waves is blown over the structures.

(1) Percent Occurrence of Wind Direction and Speed. The National Weather Service (NWS) has recorded 31 years of hourly one-minute average windspeed and direction data at Logan International Airport in Boston, Massachusetts from 1945 through 1979. Logan Airport, which is adjacent to Revere, is the closest location to the project for which relatively complete, systematically recorded, wind data are available. The windspeed data were adjusted to a standard 33-foot observation height and 1-minute average windspeeds were converted to 1-hour average windspeeds. Since Logan International Airport is almost directly adjacent to the ocean, no land to sea conversion was applied. However, a wide stability correction was made for all fetches of interest. All adjustments were made in accordance with ETL 1110-2-305 on the subject of determining wave characteristics on sheltered waters. Utilizing these 1-hour average wind data, the percent occurrence of wind direction and windspeed range were computed. Since only onshore winds at Revere are of interest, the wind directions utilized in this analysis were limited to those between northeast (NE) and southeast (SE). This analysis, the results of which are shown in table 2-5 and figure 2-4, indicated that the principal onshore wind direction for windspeeds $\leq$ 5 mph is from the SE and, for windspeeds > 5 and $\leq$ 15 mph, is from the ESE. Winds > 15 and $\leq$ 20 mph generally come from the E. Winds > 20 mph come from the NE. The maximum average windspeed (11.8 mph) is from the NE, and the greatest maximum speed was 68.7 mph from the SE. Overall average speed is 10.5 mph. Table 2-5 also shows the resultant wind direction for various windspeed ranges. The resultant wind direction is a vector quantity computed using the product of windspeed and direction. It is an indicator of net air movement past a given location. Overall, the resultant wind direction is from the E. However, winds > 20

TABLE 2-5

ADJUSTED HOURLY WIND OBSERVATIONS BETWEEN NE AND SE AT BOSTON, MASSACHUSETTS
(One-Hour Average Values)

PERCENT OF ONSHORE WINDSPEED AND DIRECTION OBSERVATIONS (X 10)

Direction	Windspeed Range (Miles Per Hour) 0-5	5-10	10-15	15-20	20-25	25-30	30-35	Over 35	All Inclusive	Avg Speed (mph)	Max Speed (mph)
NE	19	46	55	31	16	8	3	2	179	11.8	54.3
ENE	20	52	59	31	13	7	2	2	185	11.3	49.2
E	23	69	91	33	10	5	2	1	234	10.7	55.3
ESE	22	73	92	30	7	2	1	0	227	10.0	49.2
SE	24	72	63	13	2	1	0	0	174	8.7	68.7
NE-SE	108	313	360	136	48	22	7	5	1,000	10.5	68.7
Resultant Direction:	E	E	E	E	ENE	ENE	ENE	ENE	E		

NOTES:
1. Windspeed ranges include values greater than the lower limit and less than or equal to the higher limit.
2. Onshore winds occur 21 percent of the time; therefore, average annual number of occurrence (A) = percent occurrence times 18.654 (for example: a windspeed range of 0-5 mph from the ENE, A = 2.0 (18.654) = 37).

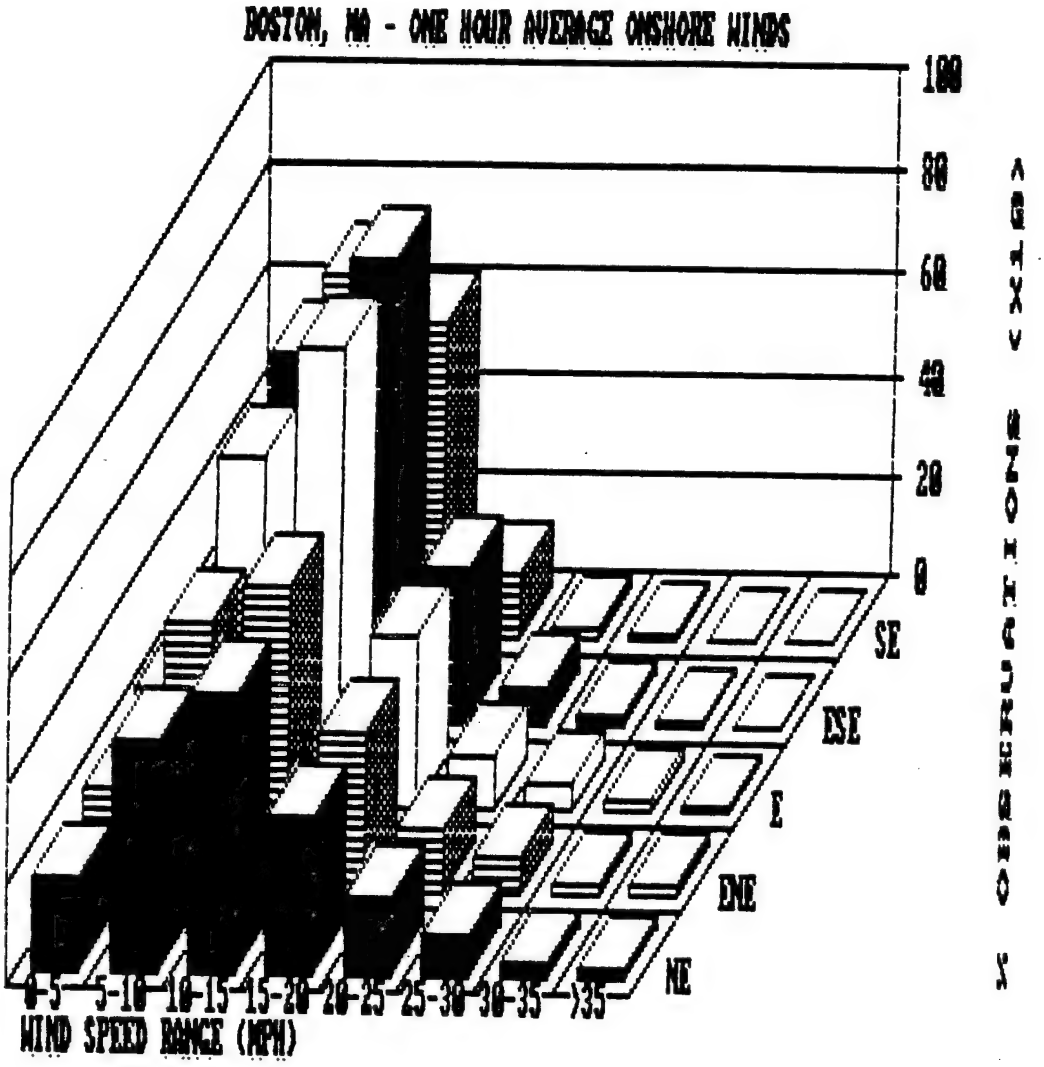
BOSTON, MA - ONE HOUR AVERAGE ONSHORE WINDS
100
80
60
40
20
0
SE
ESE
E
ENE
NE
0-5 5-10 10-15 15-20 20-25 25-30 30-35 >35
WIND SPEED RANGE (MPH)
% OBSERVATIONS EXCEEDING

FIGURE 2-4

mph have a more ENE resultant. The greatest percentage of windspeeds is shown to be > 10 and ≤ 15 mph.

(2) Windspeed Persistence. Additionally, actual windspeed persistence was determined on a directional basis. The resulting maximum windspeed persistence data, shown on figures 2-5A through 2-5E, for directions northeast through southeast, indicate the maximum number of consecutive hourly windspeed observations that occurred at a given average speed from a particular direction. This analysis demonstrated that high onshore winds can occur for extended periods of time in the study area. High speed-long duration winds are usually associated with northeasters and, therefore, come from the northeastern quadrant. High intensity-short duration winds have come from the southeast due to hurricane events.

(3) Winds During Historic Storms. When studying overtopping of coastal structures it is useful to examine wind conditions occurring during past flood events in order to get an appreciation for the severity of experienced wave overtopping conditions. Table 2-6 presents National Weather Service (NWS) wind observations recorded at Logan Airport in Boston during notable tidal floods. From these data it can be seen that the strongest winds recorded during flood events generally originated from directions between northeast and east. The greatest fastest-mile (approximately equal to 1-minute average speed) listed, 61 mph from the northeast was recorded on 6 February 1978 during the great "Blizzard of '78". By comparing table 2-6 with table 2-9, it can be seen that the stillwater tide levels recorded during these storm events ranged between 10.3 and 8.3 feet, respectively. However, extremely severe onshore winds have occurred during storm events which produced significantly lower observed maximum stillwater tide levels in the study area.

Since the astronomic tide range at Revere is so variable, as explained in section 5a, many severe coastal storms occur during periods of relatively low astronomic tides. Thus, even though a storm may produce exceptionally high onshore winds, waves, and a tidal surge, the resulting tide level may be less than that occurring during a time of high astronomic tide and no meteorological influence. Table 2-7 presents wind data recorded at Logan Airport during storms which produced annual maximum surge values of three feet or more. For comparison, table 2-8 lists maximum annual storm surges and associated observed tide levels. It can be seen that the recurrence intervals of the maximum observed tide levels recorded on days of maximum annual storm surge were generally less than one year, with only a few storms producing significant tidal flood levels. Some of the most severe

Northeast

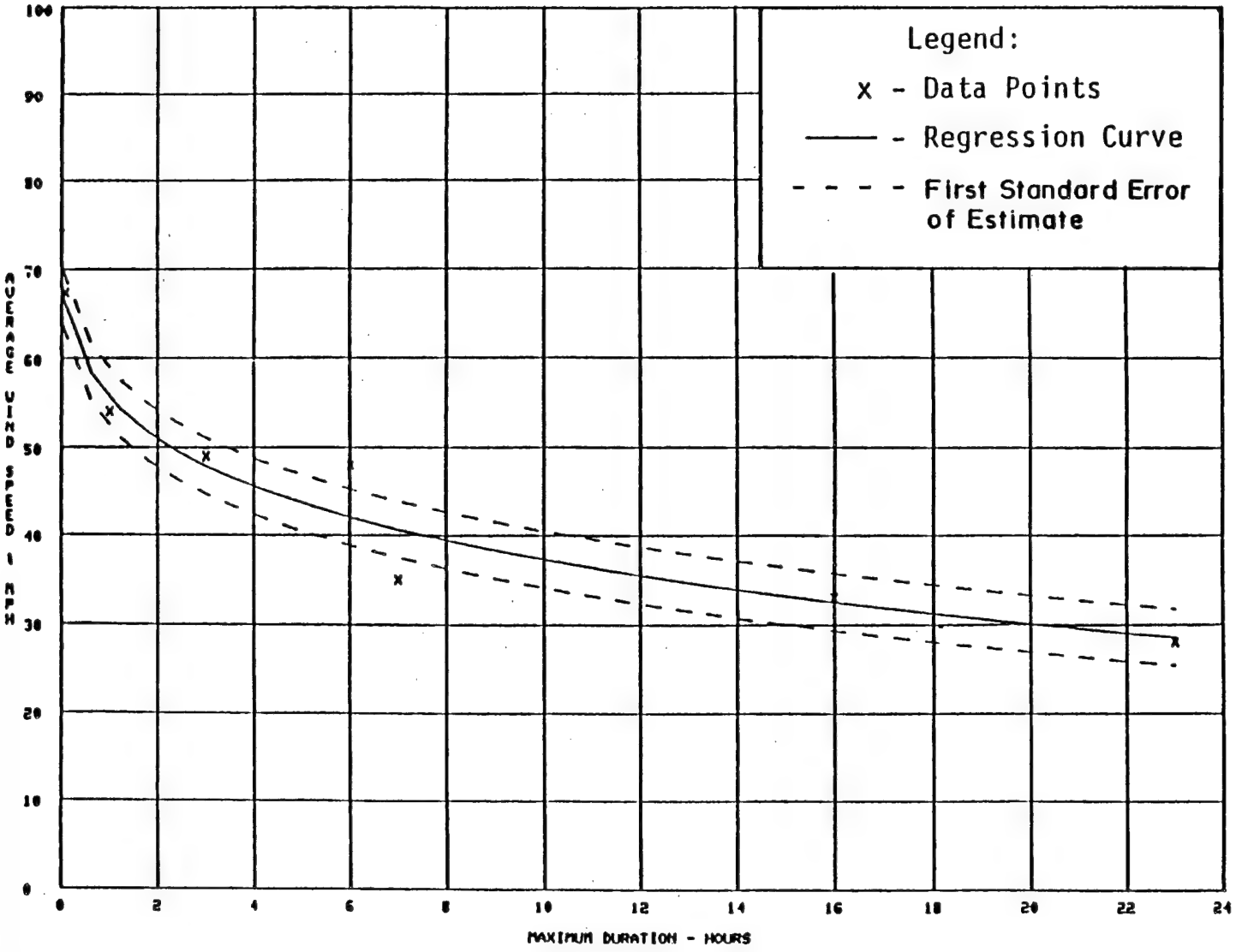

WIND PERSISTENCE
MEASURED AT BOSTON M
HYD.& W.Q. SECT. JUNE 1988

FIGURE 2-5A

East-Northeast

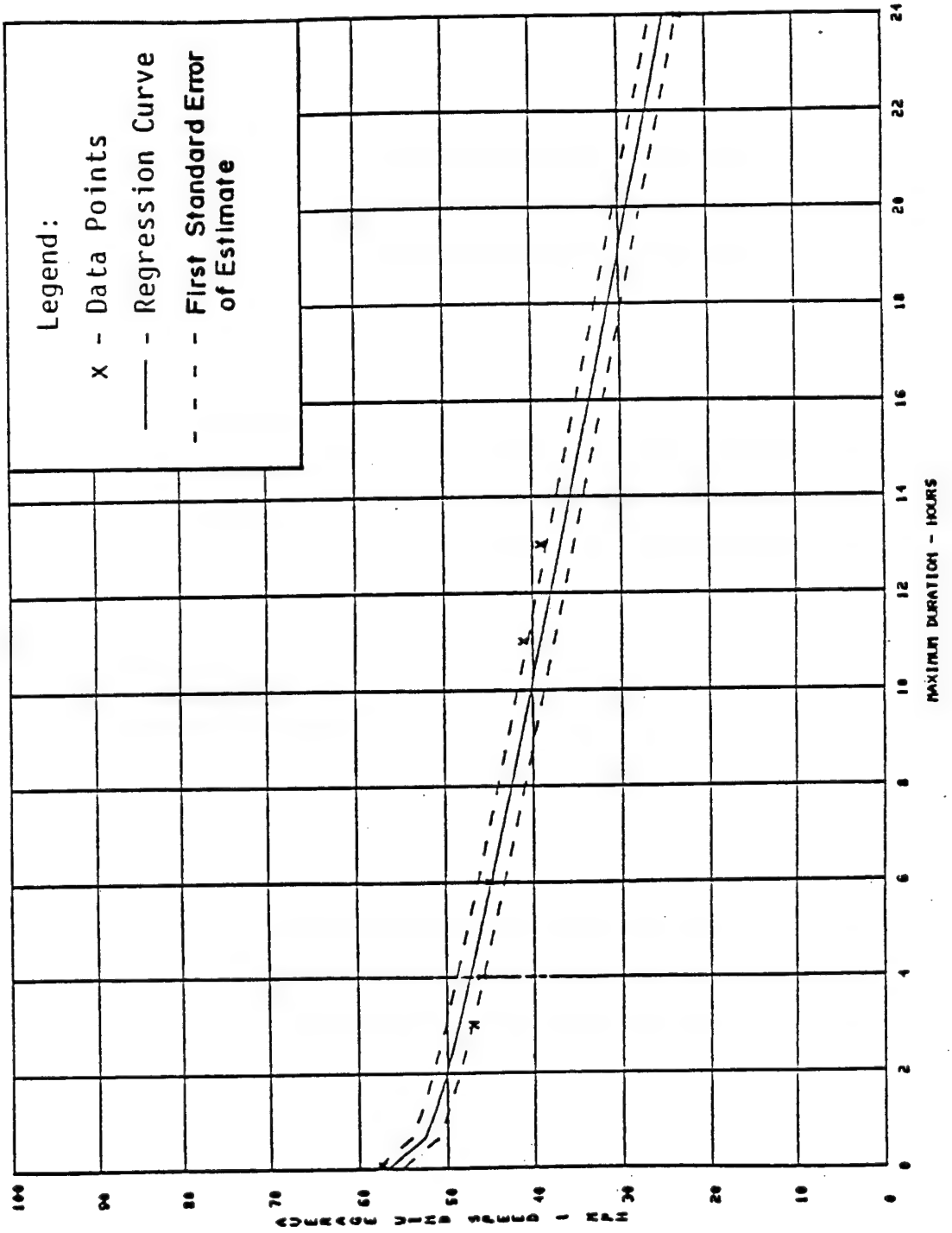

WIND PERSISTENCE
MEASURED AT BOSTON, MA.
HYD. & W.Q. SECT. JUNE 1988

FIGURE 2-5B

East

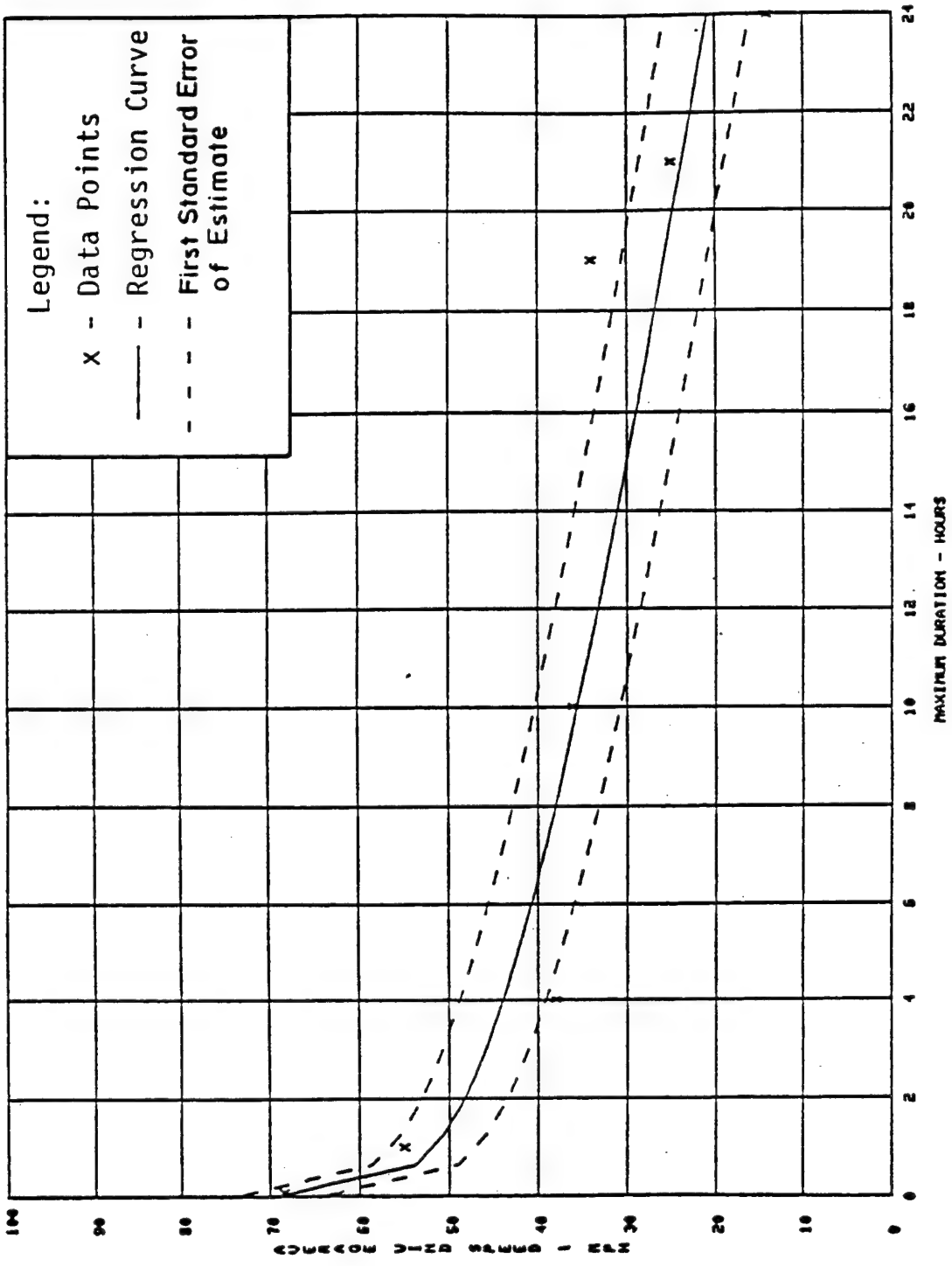

WIND PERSISTENCE
MEASURED AT BOSTON, [redacted]
HYD. & W.Q. SECT. JUNE 1988

FIGURE 2-5C

East-Southeast

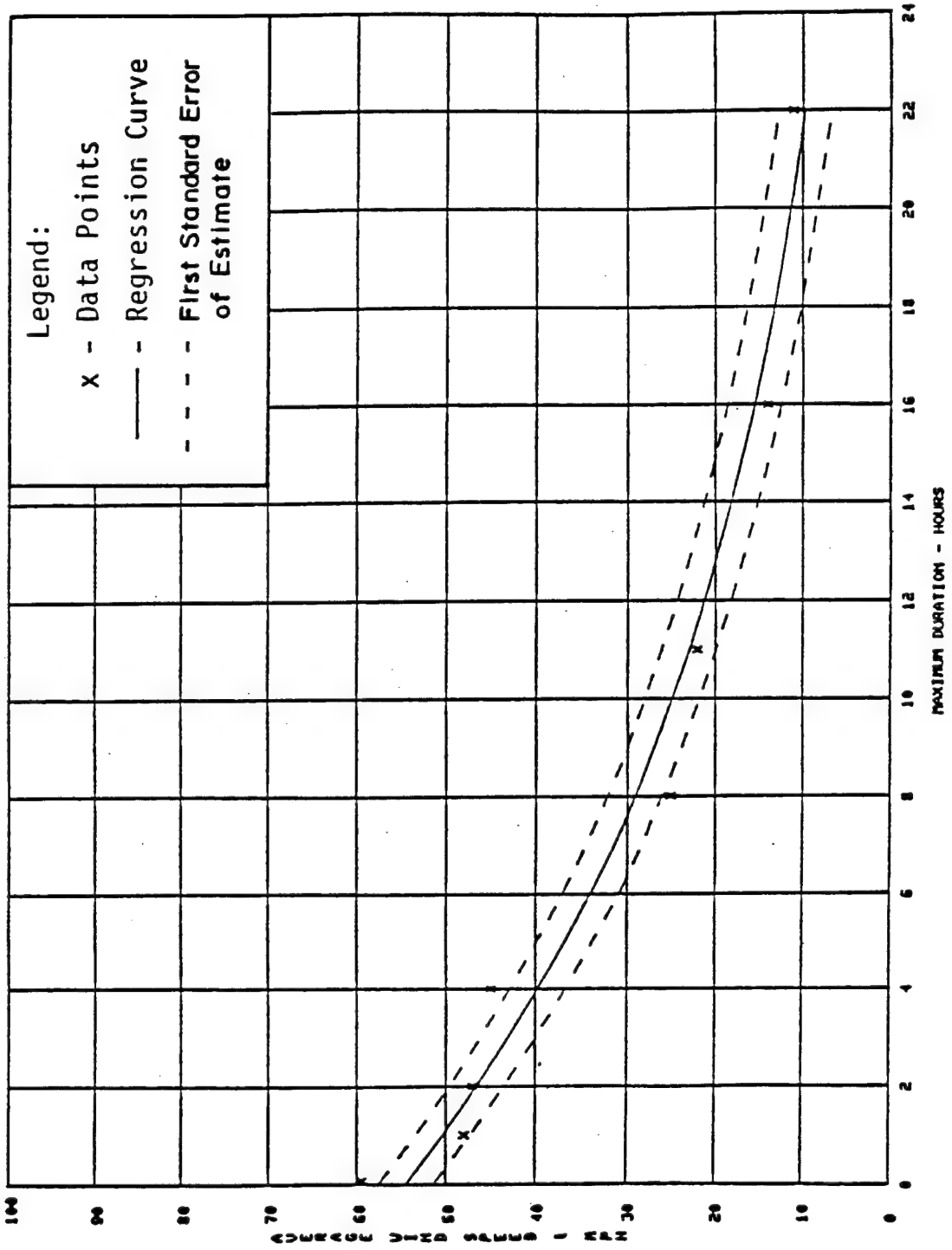

WIND PERSISTENCE
MEASURED AT BOSTON, MA.
HYD. & W.Q. SECT. JUNE 1988

FIGURE 2-5D

Southeast

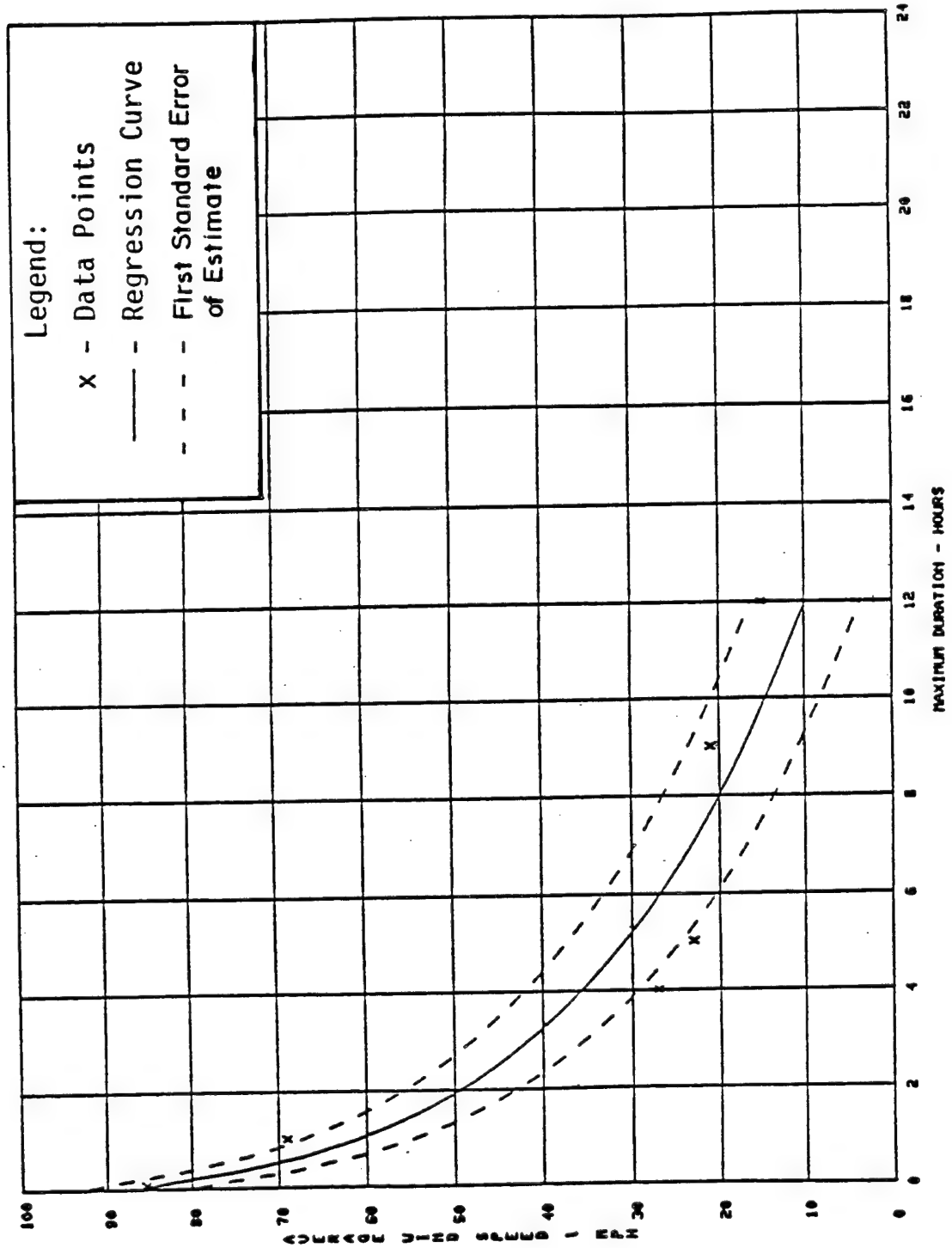

WIND PERSISTENCE
MEASURED AT BOSTON, MA.
HYD. & W.Q. SECT. JUNE 1988

FIGURE 2-5E

TABLE 2-6

BOSTON - LOGAN INTERNATIONAL AIRPORT
NATIONAL WEATHER SERVICE
WIND OBSERVATIONS RECORDED
DURING NOTABLE TIDAL FLOODS

Date	Resultant Direction	Resultant Speed (mph)	Average Speed (mph)	Fastest-Mile Speed (mph)	Fastest-Mile Direction
6 Feb 1978	ENE	28.4	29.3	61	NE
2 Jan 1987	N	15.5	21.8	35	NE
25 Jan 1979	ENE	23.2	24.2	45	E
29 Dec 1959	NE*	--	20.7	34	E
19 Feb 1972	NE	21.1	24.2	47	NE
25 May 1967	NE	34.3	34.7	50	NE
21 Apr 1940	-	--	13.3	43**	NE
20 Jan 1961	NNW*	--	26.7	41	NNE
30 Nov 1944	-	--	13.4	48**	NE
9 Jan 1978	SSW	22.8	28.8	43	SW
16 Mar 1976	ENE	15.4	20.4	35	NE
16 Mar 1956	ENE*	--	28.1	54	NE
6 Apr 1958	WSW*	--	13.8	32	SSE
26 Feb 1979	NE	19.1	19.6	30	NE
2 Dec 1974	ENE	15.7	20.7	38	E
7 Mar 1962	NE*	--	31.6	42	ENE
4 Apr 1973	E	13.0	13.5	31	E
22 Dec 1972	N	13.3	13.5	21	N

* Resultant speed and direction not available for the period prior to 1964; direction shown is prevailing wind direction.

**Fastest-mile not available; value shown is five-minute average speed.

NOTE: Listing is in order of decreasing observed stillwater tide level to provide uniformity with table 2-9.

TABLE 2-7

BOSTON LOGAN INTERNATIONAL AIRPORT
NATIONAL WEATHER SERVICE
WIND OBSERVATIONS RECORDED
DURING ANNUAL MAXIMUM SURGE
PRODUCING STORMS
(1922-1979)

Date	Fastest-Mile Speed (mph)	Fastest-Mile Direction	Average Speed (mph)	Prevailing Direction
29 Nov 1945	63*	NE	40.5	-
13 Apr 1961	42	ENE	25.0	NE
6 Feb 1978	61	NE	29.3	ENE
14 Feb 1940	51*	NE	12.7	-
17 Nov 1935	54*	NE	14.9	-
19 Feb 1972	47	NE	24.2	NE
3 Mar 1947	50*	E	13.4	-
4 Mar 1960	45	NE	28.0	N
30 Jan 1966	43	S	22.3	SSE
12 Nov 1968	54	NE	23.9	E
25 Jan 1979	45	E	24.2	ENE
22 Mar 1977	60	NE	19.3	E
25 Nov 1950	74	E	42.4	E
31 Aug 1954	86	SE	31.8	ENE
16 Feb 1958	45	E	28.0	E
15 Nov 1962	37	NW	28.5	NW
16 Mar 1956	54	NE	28.1	ENE
27 Dec 1969	26	E	17.3	WNW
11 Mar 1924	--	-	--	-
30 Jan 1939	43*	NE	12.7	-
17 Feb 1952	50	NE	29.8	NE
7 Mar 1923	--	-	--	-
20 Feb 1927	--	-	--	-
19 Jan 1936	40*	NE	12.6	-
7 Nov 1953	67	NE	30.5	NE
14 Aug 1971	18	E	9.6	E
28 Jan 1973	23	NE	19.4	NE
12 Mar 1959	42	ESE	23.9	SE
16 Apr 1929	--	-	--	-
8 Mar 1931	--	-	--	-

* Fastest-mile not available; value shown is five-minute average speed.

NOTE: Listing in order of decreasing annual maximum storm surge to allow comparison with table 2-8.

TABLE 2-8

ANNUAL MAXIMUM STORM SURGE
BOSTON, MASSACHUSETTS
(1922-1979)

Date	Annual Maximum Storm Surge (feet)	Maximum Observed Tide Level for the Day (feet, NGVD)	Recurrence* Interval (years)
30 Nov 1945	4.9	7.6	LT 1
13 Apr 1961	4.7	8.0	1
6 Feb 1978	4.6	10.0	50
14 Feb 1940	4.2	5.0	LT 1
17 Nov 1935	4.1	6.5	LT 1
19 Feb 1972	4.0	9.1	10
3 Mar 1947	3.8	7.2	LT 1
4 Mar 1960	3.8	8.1	2
30 Jan 1966	3.8	5.5	LT 1
12 Nov 1968	3.7	7.7	LT 1
25 Jan 1979	3.7	9.2	13
22 Mar 1977	3.6	5.3	LT 1
25 Nov 1950	3.6	6.4	LT 1
31 Aug 1954	3.5	8.2	2
16 Feb 1958	3.5	7.9	1
15 Nov 1962	3.5	7.9	1
16 Mar 1956	3.4	5.6	LT 1
27 Dec 1969	3.3	6.7	LT 1
11 Mar 1924	3.2	6.2	LT 1
31 Jan 1939	3.2	6.9	LT 1
18 Feb 1952	3.2	7.9	1
7 Mar 1923	3.1	6.9	LT 1
20 Feb 1927	3.1	6.9	LT 1
19 Jan 1936	3.1	5.9	LT 1
7 Nov 1953	3.0	7.4	LT 1
14 Aug 1971	3.0	5.4	LT 1
29 Jan 1973	3.0	6.1	LT 1
12 Mar 1959	2.9	6.5	LT 1
16 Apr 1929	2.8	6.6	LT 1
8 Mar 1931	2.8	6.5	LT 1

* Recurrence interval of observed tide elevations. Obtained from tide stage-frequency relationship, figure 2-8.

NOTE: LT = Less Than

TABLE 2-9

MAXIMUM STILLWATER TIDE HEIGHTS
BOSTON, MASSACHUSETTS

Date	Observed Elevation (feet, NGVD)	Adjusted Elevation* (feet, NGVD)	Recurrence*** Interval (years)
7 Feb 1978	10.3	10.4	91
16 Apr 1851	10.1	10.4	63
26 Dec 1909	9.9	10.5	42
2 Jan 1987	9.4	9.4	17
25 Jan 1979	9.3	9.4	14
29 Dec 1959	9.3	9.5	14
27 Dec 1839	9.2**	--	13
15 Dec 1839	9.2**	--	13
19 Feb 1972	9.1	9.2	11
24 Feb 1723	9.1**	--	11
26 Mar 1830	9.0**	--	9
26 May 1967	8.9	9.0	7
21 Apr 1940	8.9	9.2	7
29 Dec 1853	8.9	9.2	7
4 Dec 1786	8.9**	--	7
20 Jan 1961	8.8	9.0	6
30 Nov 1944	8.8	9.1	6
4 Mar 1931	8.8	9.2	6
3 Dec 1854	8.8	9.1	6
3 Nov 1861	8.7	9.1	5
9 Jan 1978	8.6	8.7	4
16 Mar 1976	8.6	8.7	4
17 Mar 1956	8.6	8.8	4
7 Apr 1958	8.5	8.7	4
15 Nov 1871	8.5	9.0	4
23 Nov 1858	8.5	8.9	4
26 Feb 1979	8.4	8.5	3
2 Dec 1974	8.4	8.5	3
7 Mar 1962	8.4	8.6	3
4 Apr 1973	8.3	8.4	2
22 Dec 1972	8.3	8.4	2
28 Jan 1933	8.3	8.7	2

*Observed values after adjustment for changing mean sea level; adjustment made to 1987 mean sea level.
**Approximate value based upon historical account. Record not sufficient to document change of sea level for this time.
***Recurrence interval of observed tide elevations. Obtained from tide stage-frequency relationship, figure 2-8.

NOTE: Events occurring within about 30 days of a greater tide producing event are excluded from this list. Events recorded during years for which only partial records are available were also excluded.

onshore winds, waves, and storm surges have produced minor tidal flooding, owing to their coincidence with low astronomic tides. A good example of this is the 29 November 1945 event which produced the maximum storm surge of record at Boston; extremely high onshore winds occurred during low astronomic tide and resulted in only a minor tidal flood level of 7.6 feet NGVD.

Conversely, rather significant tidal flood levels can result from the coincidence of relatively high astronomic tides and only minor meteorological events. Astronomic high tide level in Boston alone can reach 7.5 feet NGVD (see table 2-4). With such a condition, a coincident storm surge of only 2 to 3 feet can produce major tidal flood levels. The 7 February 1978 storm tide at Boston reached 10.3 feet NGVD, the greatest of record, but was produced by the combination of a 6.9-foot NGVD astronomic tide and a 3.4-foot surge, the latter being of only moderate magnitude (see table 2-8 which shows that a surge of 3.4 feet is not extreme).

Windspeed observations recorded by the NWS at Boston's Logan Airport during the great Blizzard of '78 are shown on figure 2-6. Gusts are shown in excess of 55 knots (63 mph) for about 4 hours from the ENE. Average windspeeds were sustained above 43 knots (49 mph) for nearly 4 hours from the same direction.

d. Storm Tides and Tide Stage-Frequency. The total effect of astronomical tide combined with storm surge produced by wind, wave, and atmospheric pressure contributions is reflected in actual tide gage measurements. Since the astronomical tide is so variable at the study area, the time of storm surge occurrence greatly affects the magnitude of the resulting tidal flood level. Obviously, a storm surge of 3 feet occurring at a low astronomic tide would not produce as high a water level as if it occurred at a higher tide. It is important to note that the storm surge itself varies with time, thus introducing another variable into the makeup of the total flood tide. The variation in observed tide, and surge at Boston during the "Blizzard of '78", is shown in figure 2-7. It is interesting to note that the maximum surge (4.7 feet) occurred just before 10 p.m. on 6 February. However, the maximum observed tide occurred about 10:30 a.m. the following day when the surge had dropped 1.3 feet. Had the maximum surge recorded during the storm occurred at 10:30 a.m. on 7 February, the observed tide would have been 11.6 feet NGVD, and would have resulted in even more catastrophic flooding at Revere. Annual maximum surge values of greater than or equal to 3.0 feet measured at the Boston, Massachusetts, National Ocean Survey (NOS) tide gage are shown in

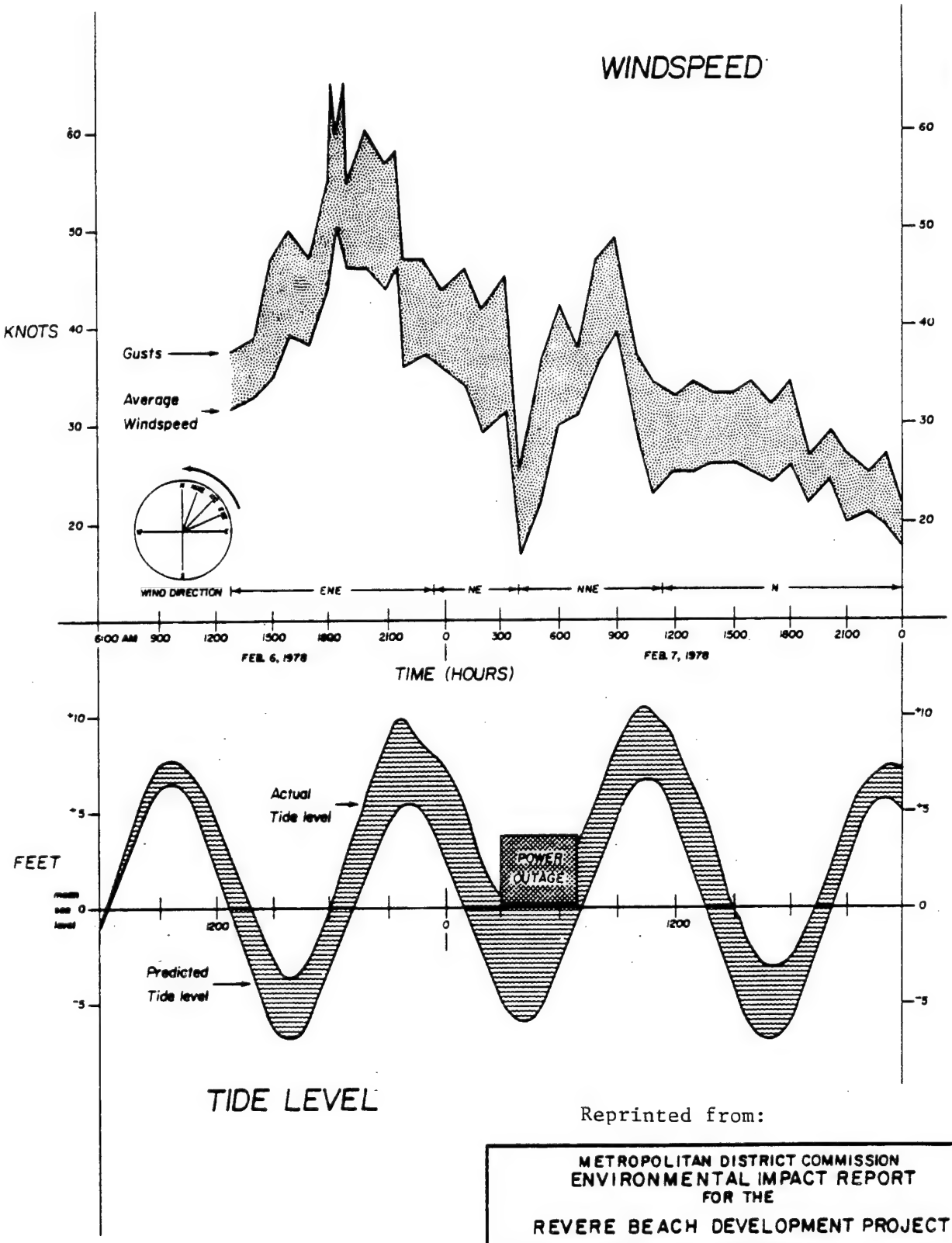

Reprinted from:

METROPOLITAN DISTRICT COMMISSION
ENVIRONMENTAL IMPACT REPORT
FOR THE
REVERE BEACH DEVELOPMENT PROJECT

TIDE LEVEL AND WINDSPEED VS. TIME FOR THE STORM OF FEBRUARY 6 AND 7, 1978.

Camp, Dresser & McKee, Inc.
In Association With
Alan M. Voorhees & Assoc., Inc. Bolt Beranek & Newman

FIG. J-1

Source: U.S. Weather Bureau Stations, Boston, MA
NOAA, National Climatic Center, Asheville, NC

FIGURE 2-6

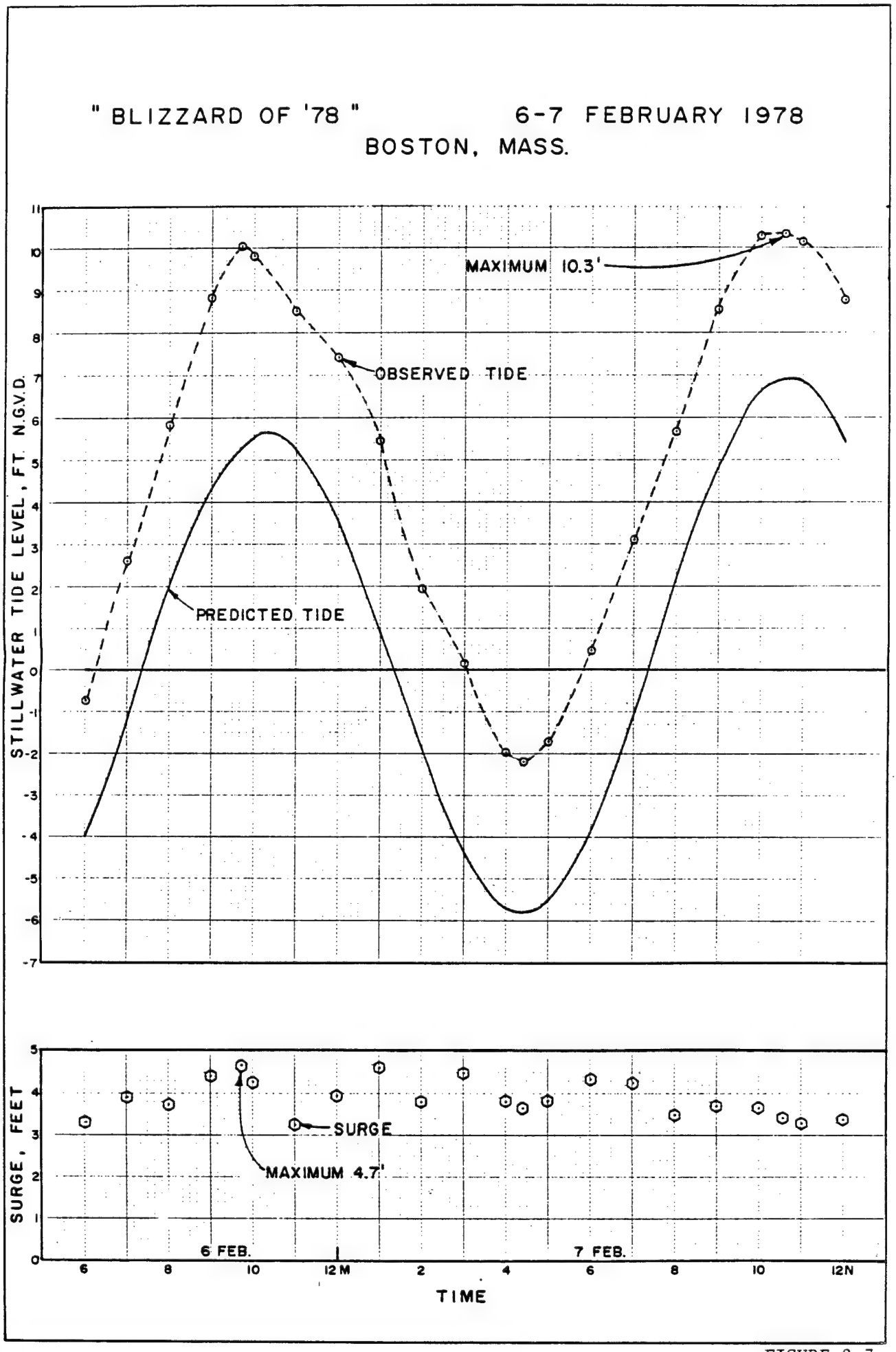
" BLIZZARD OF '78 "
6-7 FEBRUARY 1978
BOSTON, MASS.
MAXIMUM 10.3'
OBSERVED TIDE
PREDICTED TIDE
STILLWATER TIDE LEVEL, FT. N.G.V.D.
SURGE
MAXIMUM 4.7'
SURGE, FEET
6 FEB.
7 FEB.
6
8
10
12 M
2
4
6
8
10
12N
TIME

FIGURE 2-7

table 2-8. This table shows the importance of coincident astronomic tide in producing significant tidal flooding. (See the discussion in section 5c, which deals with the wind observations recorded during these events).

The National Ocean Survey has systematically recorded tide heights at Boston since 1922. The record prior to that time was developed utilizing staff gage measurements and historical accounts. Maximum observed stillwater tide heights (measurements taken in protected areas where waves are dampened out) recorded up to 1987 are shown in table 2-9. Also shown are tide heights with an adjustment applied to account for the effect of rising sea level (see section 9). The greatest observed stillwater tide level recorded occurred during the "Blizzard of 78". No hurricanes or tropical storms have produced extreme tide heights at Boston, thus indicating that the principal threat of tidal flooding in the study area is due to storms of the extratropical variety.

A tide stage-frequency relationship for Boston was previously developed utilizing a composite of: (1) a Pearson type III distribution function, with expected probability adjustment, for analysis of historic and systematically observed annual maximum stillwater tide levels, and (2) a graphical solution of Weibull plot positions for partial duration series data. The resulting tide stage-frequency curve is shown on figure 2-8.

NOS tide gage records and high watermark data gathered after major storms have been utilized in the development of profiles of tidal floods along the New England coast. Additionally, profiles of storm tides for selected recurrence intervals have been developed utilizing tide stage-frequency curves and high watermark information. A location map and profile for the reach of the New England coast bounding Revere are shown on figures 2-9 and 2-10, respectively.

6. TIDAL HYDRAULICS

a. General. During the course of feasibility planning investigations for the Roughans Point project, it became apparent that confidence in estimates of interior stage frequency relationships was somewhat limited. This uncertainty can be attributed to several factors: (1) the geometry of existing and proposed protective works is not truly like those presented in the Shore Protection Manual (SPM) for use in estimating wave overtopping rates, (2) the frequency of wave overtopping is not truly a function of stillwater tide level alone, but is also related to coincident wave conditions which can vary, and (3) wave overtopping volumes theoretically computed during the feasibility study for the 1978

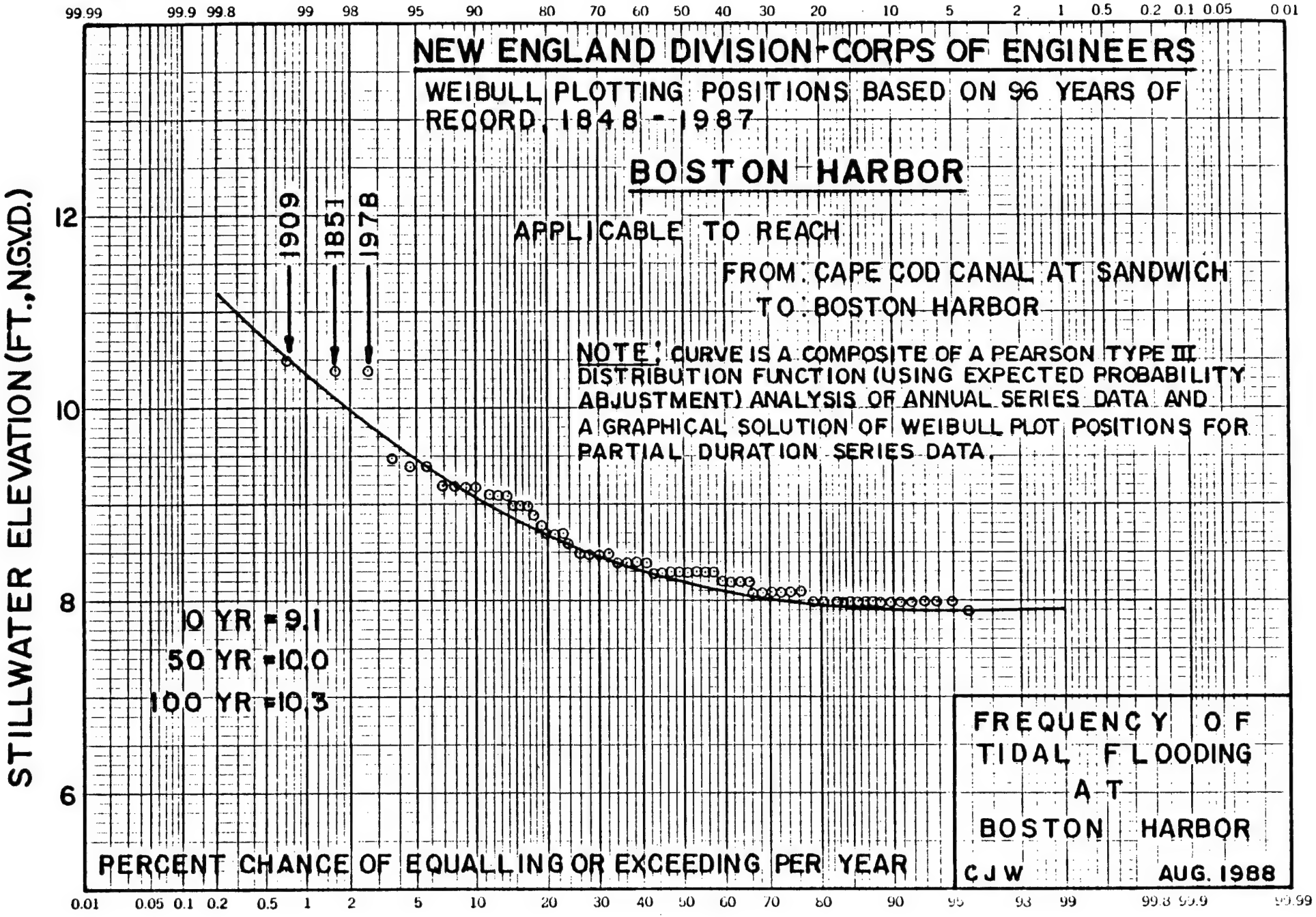

WITH 1 OUTLIER

BASE MAP FOR TIDAL FLOOD PROFILE

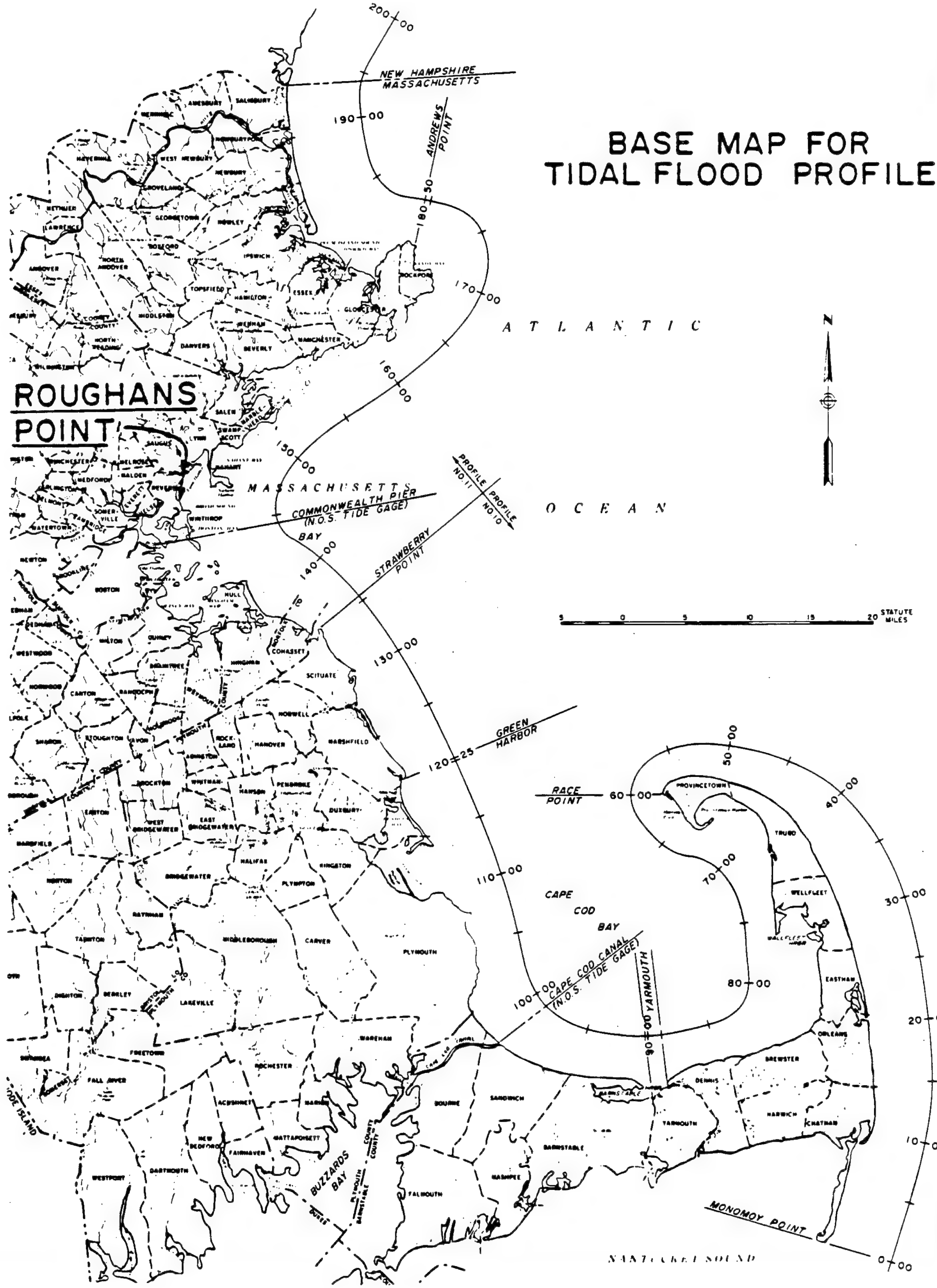

FIGURE 2-9

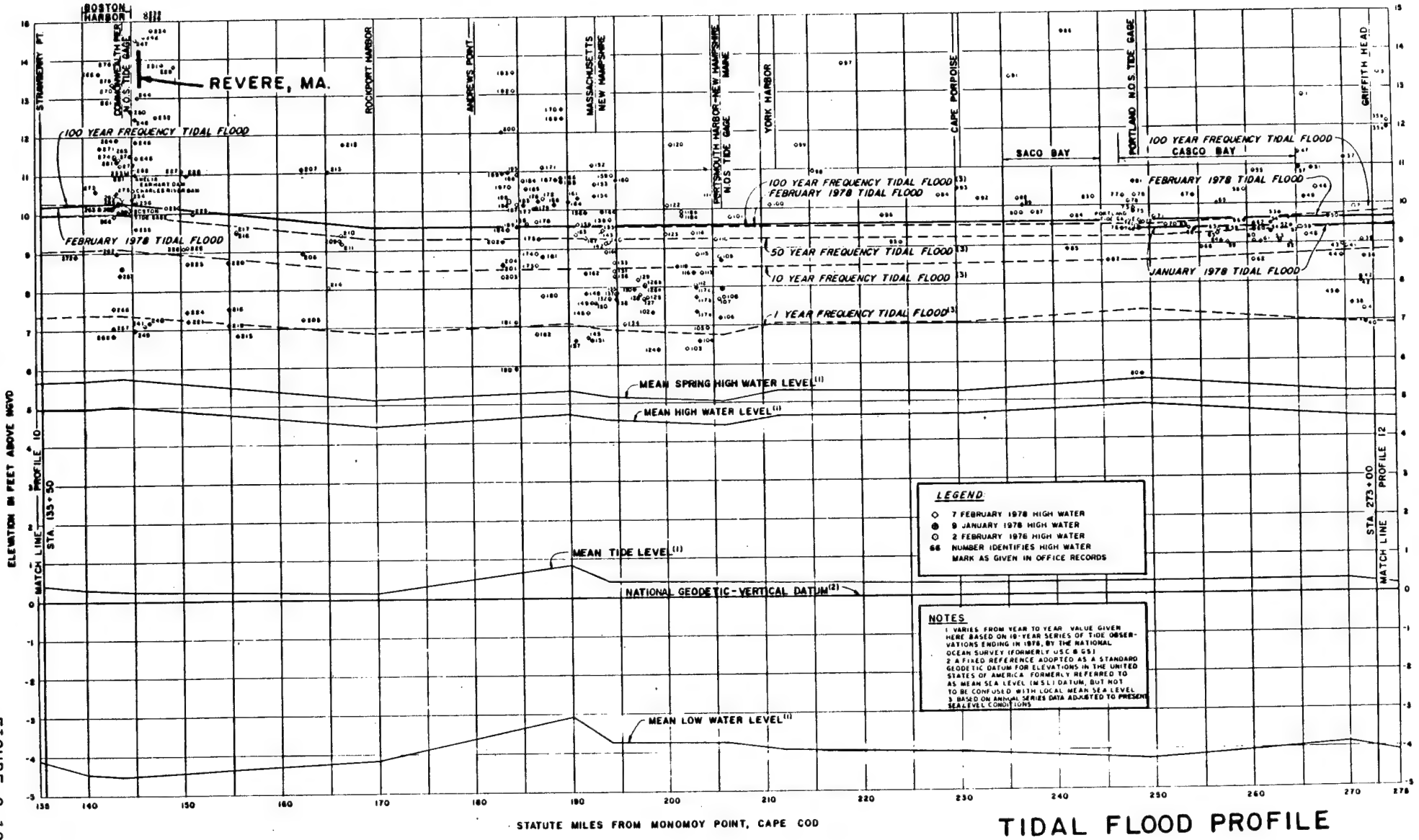
BOSTON HARBOR
REVERE, MA.
100 YEAR FREQUENCY TIDAL FLOOD
FEBRUARY 1978 TIDAL FLOOD
STRAWBERRY PT
ROCKPORT HARBOR
ANDREWS POINT
MASSACHUSETTS NEW HAMPSHIRE
PORTSMOUTH HARBOR-NEW HAMPSHIRE MAINE
YORK HARBOR
CAPE PORPOISE
SACO BAY
PORTLAND N.O.S. TIDE GAGE
CASCO BAY
GRIFFITH HEAD
100 YEAR FREQUENCY TIDAL FLOOD
FEBRUARY 1978 TIDAL FLOOD
50 YEAR FREQUENCY TIDAL FLOOD (3)
10 YEAR FREQUENCY TIDAL FLOOD (3)
1 YEAR FREQUENCY TIDAL FLOOD (3)
JANUARY 1978 TIDAL FLOOD
MEAN SPRING HIGH WATER LEVEL (1)
MEAN HIGH WATER LEVEL (1)
MEAN TIDE LEVEL (1)
NATIONAL GEODETIC-VERTICAL DATUM (2)
MEAN LOW WATER LEVEL (1)
MATCH LINE STA 135+50 PROFILE 10
MATCH LINE STA 273+00 PROFILE 12
LEGEND
◇ 7 FEBRUARY 1978 HIGH WATER
◉ 9 JANUARY 1978 HIGH WATER
○ 2 FEBRUARY 1976 HIGH WATER
66 NUMBER IDENTIFIES HIGH WATER MARK AS GIVEN IN OFFICE RECORDS
NOTES
1 VARIES FROM YEAR TO YEAR VALUE GIVEN HERE BASED ON 19-YEAR SERIES OF TIDE OBSERVATIONS ENDING IN 1978, BY THE NATIONAL OCEAN SURVEY (FORMERLY USC & GS)
2 A FIXED REFERENCE ADOPTED AS A STANDARD GEODETIC DATUM FOR ELEVATIONS IN THE UNITED STATES OF AMERICA FORMERLY REFERRED TO AS MEAN SEA LEVEL (MSL) DATUM, BUT NOT TO BE CONFUSED WITH LOCAL MEAN SEA LEVEL
3 BASED ON ANNUAL SERIES DATA ADJUSTED TO PRESENT SEA LEVEL CONDITIONS
ELEVATION IN FEET ABOVE NGVD
STATUTE MILES FROM MONOMOY POINT, CAPE COD
TIDAL FLOOD PROFILE

FIGURE 2-10

and 1972 storm events were much greater than indicated by interior high watermarks. A project design conference was held 26 March 1984 involving representatives from NED, WES, and OCE to discuss possible physical and mathematical modeling which could be done to provide greater confidence in the flood reducing ability of the proposed rock revetment (reference 1st Ind from DAEN-CWH-Y, dated 5 March 1984, and 2nd Ind from NEDED-WQ, dated 11 April 1984, subject: Hydrologic Criteria - Roughans Point Coastal Flood Protection, Revere, Massachusetts). Subsequently, the detailed scope of a proposed joint physical and mathematical modeling effort was prepared by WES and approved by OCE (reference 1st Ind from DAEN-CWH-D, dated 25 April 1984, subject: Proposed Model Testing - Roughans Point Coastal Flood Protection, Revere, Massachusetts).

b. Physical Modeling. Laboratory tests to determine irregular wave overtopping rates on coastal structures were conducted at the Coastal Engineering Research Center (CERC), in Vicksburg, Mississippi. These tests were intended to solve a site-specific problem at Roughans Point, Massachusetts. The results have yielded specific information for Roughans Point and a general approach to calculating irregular wave overtopping rates which are superior to the method in the Shore Protection Manual (SPM, 1984).

Model tests were conducted in CERC's 3 by 3 foot by 150 foot long wave tank at a 1:16 (model: prototype) undistorted Froude scale. A JONSWAP type spectrum was produced at the wave generator blade. Prototype water depths at the wave blade were typically about 34 feet, and about 13 feet near the structure. Wave shoaling and breaking between the blade and structure was quite conspicuous for most tests. Due to wave breaking, the spectra near the structure were wider than normally associated with JONSWAP spectra. Wave conditions included periods of peak energy density of the spectra, T_p between 5 and 12 seconds prototype and zero-moment wave heights, H_{mo}, near the structure between 5 and 8 feet prototype. Ten different seawall/revetment configurations were tested, ranging from a seawall with no fronting revetment, to capped seawalls having a wide berm riprap revetment (see table 2-10). Model tests were principally made for reach E seawall configurations where most overtopping occurs. However, one configuration (No. 10) was tested for use in the lower wave environment of the north seawall (reaches B through D). Numerous configurations were tried for reach E since it was found that the original proposal (configuration 2) did not reduce overtopping as well as had been estimated in the feasibility report. It was, therefore, necessary to try other options to get an acceptable reduction in

TABLE 2-10

List of Various Seawall/Revetment Configurations, Figure Numbers, and Overtopping Coefficients

Configuration Designation Number	Description of Seawall/Revetment Configuration	Figures Showing Configuration	Plates Showing Data	Overtopping Coefficients Regression Q_o / C_1	Overtopping Coefficients Non-Regression Q_o / C_1	Configuration Overtopping Rating Coefficient, A_q Regression	Configuration Overtopping Rating Coefficient, A_q Non-Regression
1	Existing Roughans Point seawall with no riprap revetment.	5	1	76.554 -14.078		.0797	
2*	Roughans Point seawall with standard riprap revetment.	6,7	2	30.539 -13.431		.0404	
3	Roughans Point seawall with a wave absorber riprap revetment.	10	3	485.413 -20.845		.0448	
4	Roughans Point seawall with riprap revetment having a wide berm at +8 ft NGVD.	11	4	1157.479 -25.461	439.220 -21.621	.0219	.0310
5	Roughans Point seawall with riprap revetment having a double berm at +6 and +10 ft NGVD.	13	5	758.240 -25.226		.0155	
6	Roughans Point seawall with riprap revetment having a berm at +10 ft NGVD and 1.0 ft cap on seawall.	14	6	353.541 -23.943		.0112	
7	Roughans Point seawall with riprap revetment having a wide berm at +8 ft NGVD and a 1.0 ft cap on seawall.	15	7	57.628 -19.569	305.821 -23.073	.0083	.0131
8	Roughans Point seawall with riprap revetment having a wide berm at +8 ft NGVD and a 2.0 ft cap on seawall.	16	8	93.037 -22.154		.0055	
9	Roughans Point seawall with beach breakwater.	18	9	15.226 -14.410	109.508 -18.654	.0140	.0218
10	Sheetpile seawall with standard riprap revetment, designed for less severe wave conditions.	20	10	75.189 -17.783		.0204	

* Plan recommended by NED in planning investigations

Figure and plate numbers refer to Appendix A.

overtopping. It was found that configuration 8, a wide berm at +8 feet NGVD, with a 2.0-foot concrete cap, reduced overtopping to amounts comparable to that originally estimated in the feasibility study without a significant change in overall project slope. The GDM plates for reaches B through F referenced in section 3 of this report represent the recommended plan (configurations 8 and 10). Figure 2-11 is a schematic of the required protection for reaches E and F. (Geotechnical interests require up to a 2-foot overbuilding of the berm to account for settlement -- see the GDM for details). All configurations are shown in Appendix A. These engineering design refinements will provide flood reduction similar to that approved in the feasibility report.

Findings from this study have shown that overtopping rates are strongly dependent on a dimensionless freeboard parameter, F', which is the ratio of the freeboard of the seawall to the severity of the incident wave conditions. F' is defined as

$$F' = \frac{F}{(H_{mo}^2 \, L_p)^{1/3}} \qquad (1)$$

where F, the freeboard, is the difference between the crest elevation of the seawall and the local water level and L_p is the Airy wave length calculated using T_p and the water depth at or near the structure. A simple exponential model incorporating F' was used to evaluate and compare the performance of the various seawall/revetment configurations. Comparisons were made graphically using the exponential model and numerically using the integral of the exponential model. From these comparisons of the configuration overtopping rating coefficient, Aq (table 2-10), it can be seen that configuration 8 allowed the smallest amount of overtopping to occur and configuration 1 allowed the greatest. Between these two extremes, eight other configurations were represented. The irregular wave overtopping model is written as

$$Q = Q_0 \, e^{C_1 F'} \qquad (2)$$

where Q is the overtopping rate in cubic feet per second per lineal foot of seawall crest length and Q_o and C_1 are coefficients. Both Q_o and C_1 were determined from the test data using regression analysis for each seawall/revetment configuration.

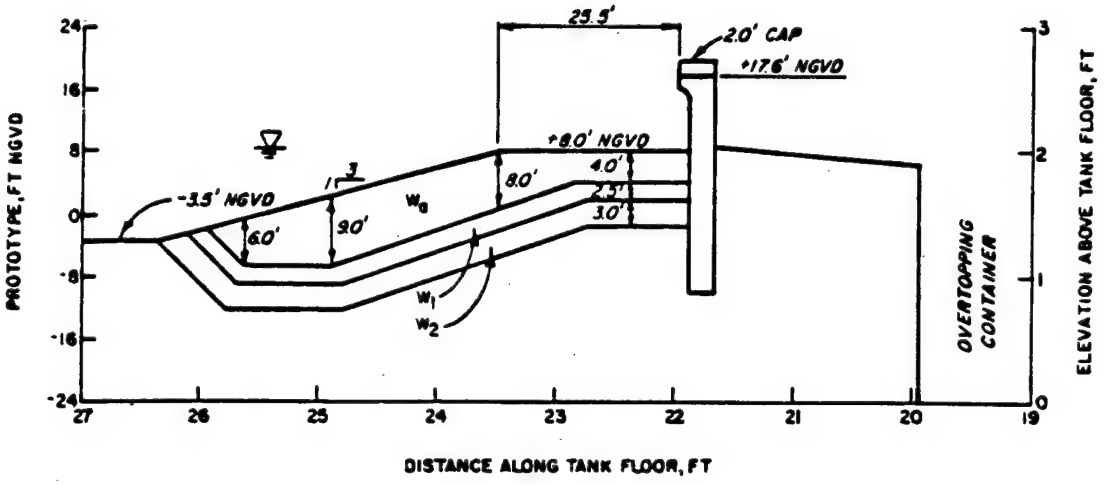

LEGEND

SYMBOL	STONE WEIGHT, W_{50}
W_0	2551 LB
W_1	347 LB
W_2	45 LB

Figure 2-11. Configuration 8, seawall with riprap revetment having a wide berm at +8 ft NGVD and a 2.0-ft cap on seawall

An additional analysis was performed of earlier monochromatic overtopping data gathered by Saville. Coefficients were developed to allow approximation of existing north wall overtopping in reaches A through D (see table 2-11).

Repetition of testing procedures has been kept to a minimum here and we suggest that Appendix A be referred to for further details.

c. Revetment Design. Although the physical model was not conducted to specifically observe stone stability, the stone gradation represented in the Feasibility Report was simulated in the model. The physical model test (Appendix A) showed some small movement of stone during severe storm events, but the stone size tested was generally satisfactory. Rock size used in the final design will be based on a combination of model observations, shore protection manual guidance, and prototype experience in the New England area. Details of revetment design will be presented in DM No. 1, General Design.

d. Mathematical Modeling. The establishment of interior stage-frequency curves for Roughans Point required the conjunctive use of several modeling components including probability, numerical storm surge, numerical wave, physical, and flood routing models.

The probability model was designed to complete four tasks: select tidal flood events for simulation by the other models, assign probabilities to these events, create stage-frequency curves, and determine a measure of confidence in the final results. The numerical storm surge model simulated the storm plus tide events producing a time history of still-water levels at specific locations throughout the study area. A numerical, spectral wave model simulated the wave field which accompanied each event simulated by the storm surge model. Also, a monochromatic wave model estimated the locally generated waves which were not considered in the spectral model. The wave parameters of height, period, and direction were calculated at selected sites throughout the study area. The physical model, previously discussed, determined coefficients for an overtopping rate equation by testing multiple combinations of water level and spectral wave characteristics for several existing and proposed structures at Roughans Point. The flood routing model calculated the maximum stage caused by each event in the interior of Roughans Point. Maximum stage was determined after outflows from drainage, pumping, seepage, and weir flow over low lying boundaries were considered.

TABLE 2-11

Overtopping Coefficients for Saville's Monochromatic Data, Saville (1955)

Structure Configuration	Water Depth d_s, ft	Overtopping Coefficients $Q = Q_o^{e^{C_1 F'}}$ *		Configuration Overtopping Rating A_q**
		Q_o, ft^2/sec	C1	
Vertical wall	0.0	3.47	-10.074	0.0168
	4.5	3.82	-5.762	0.1177
	9.5	10.58	-6.776	0.2045
Riprap 1 on 1.5	0.0	6.88	-11.434	0.0195
	4.5	8.66	-9.751	0.0476
	9.0	18.86	-9.762	0.1033

* The range of F' is from 0.094 to 1.277.

** Refer to Appendix A, Paragraph 17.

Figure 2-12 is a flow chart which depicts the conjunctive use of the above models for the establishment of stage-frequency curves. Basically, the probability model selected and assigned probability to the surge-tide-wave events simulated. Then the surge model simulated the stillwater level. At this point stage-frequency curves were generated for ocean stillwater locations. To develop the flood levels caused by wave overtopping inside Roughans Point, wave, physical, and flood routing models were necessary. The wave model simulated the parameters, height, period, and direction. Outputs of the two numerical models (surge and wave) were the main inputs to the physical model's overtopping rate equation, which produced the overtopping rate for each required time increment. The water volume due to overtopping was then hydrologically routed through the Roughans Point area and a maximum stage was calculated for each event. Finally, a stage-frequency curve was created for interior flood levels induced by wave overtopping alone. Additional refinements were then required by NED to include the effects of precipitation and runoff.

The mathematical modeling process is fully explained in Appendix B. Interior stage-frequency curves reflecting combined wave overtopping and rainfall for the recommended plan (configurations 8 and 10) are discussed in the upcoming section on Interior Flood Analysis. Numerical modeling also found less than expected overtopping along reaches A through D. This allowed elimination of a revetment to reduce overtopping in reach A as well as a reduced height of revetment (from 17 to 14 feet NGVD) in reaches B through D. The net result of the engineering design refinements is a project of similar overall scope and flood capability to that authorized by Congress.

e. Standard Project Northeaster (SPN) - Ocean Stillwater. Previous analysis conducted during the feasibility investigation resulted in an estimated ocean stillwater level of 13.0 feet NGVD for the SPN. OCE approved use of this estimated value pending formal development of the SPN stillwater level (reference 1st Ind from DAEN-CWE-H, dated 17 November 1980, subject: Hydrologic Criteria - Revere, Massachusetts Coastal Flood Protection). During a subsequent meeting between NED, WES, and OCE it was agreed that a less formal analysis of the SPN would be conducted by WES for use in the Revere area along with previously mentioned physical and mathematical modeling of wave overtopping (reference 1st Ind from DAEN-CWH-Y, dated 5 March 1984, and 2nd Ind from NEDED-WQ, dated 11 April 1984, subject: Hydrologic Criteria - Roughans Point Coastal Flood Protection, Revere, Massachusetts). The following summarizes the WES evaluation of Standard Project Northeaster Ocean Stillwater.

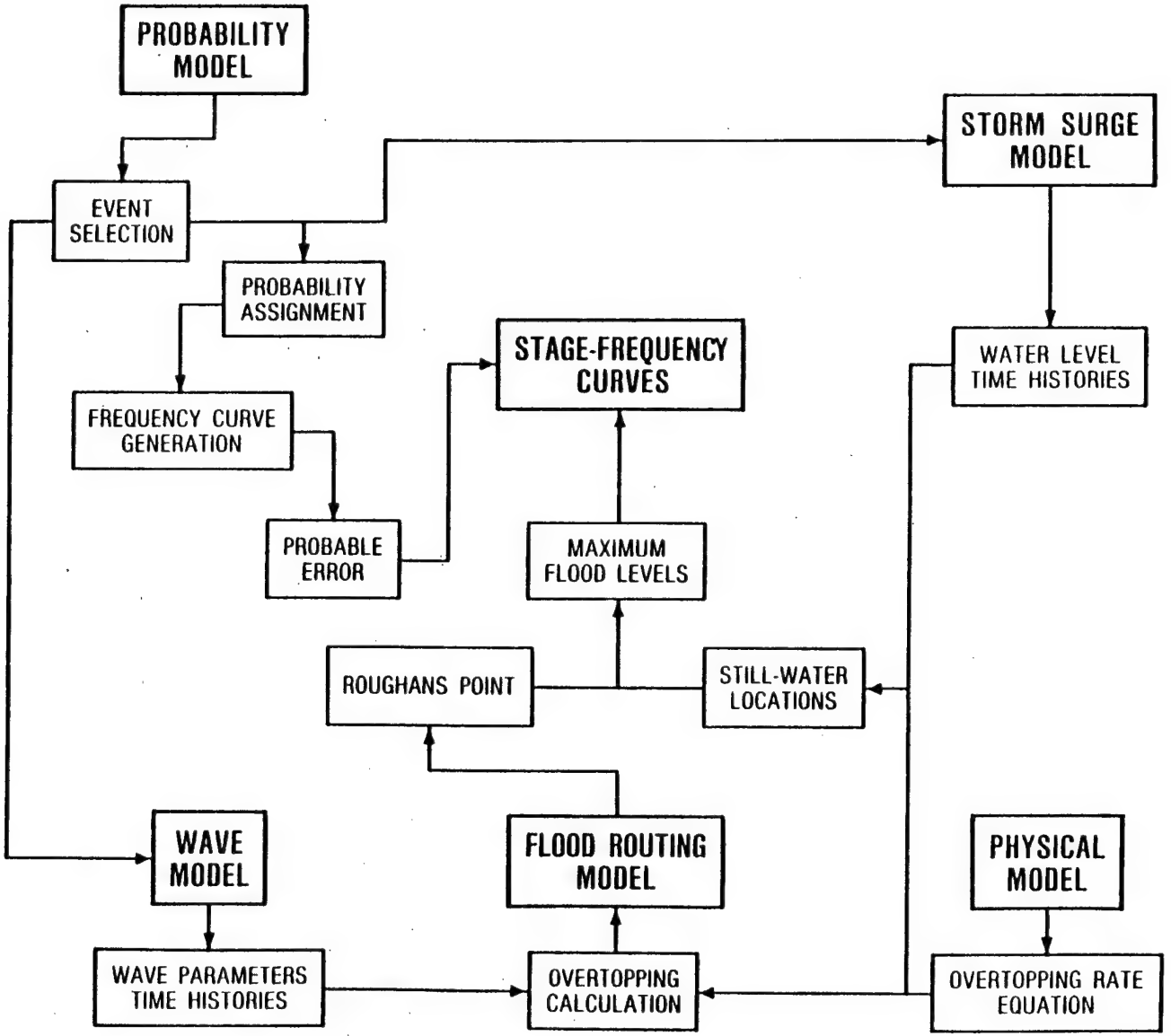

FLOW CHART OF PROJECT TECHNIQUE

FIGURE 2-12

The Standard Project Northeaster (SPN) definition can be determined from the definition for the Standard Project Storm (EM 1110-2-1411) as the northeaster which results from the "most severe combinations of meteorologic" and tidal "conditions that are considered reasonably characteristic of the geographical region involved, excluding extremely rare combinations." For this report two processes are important in considering the specification of an SPN, stillwater level and wave overtopping. It is possible that a separate SPN would have to be defined for each process. The SPN which would produce the highest ocean stillwater level might not produce the highest waves at Roughans Point and, therefore, not the highest overtopping rates. Nonetheless, due to the complexity in defining the joint occurrence of waves and stillwater level, our SPN analysis has focused on stillwater level as the principal agent. We have then assumed coincident waves at the highest level experienced in Wave Information Study hindcasting efforts.

The SPN stillwater level was estimated to be 13.0 feet NGVD in NED's feasibility studies by adding together the maximum surge recorded at Boston, about 5 feet, and the maximum predicted tide, 7.5 feet NGVD, and then rounding up to the next foot of elevation. This resulted in a stillwater ocean elevation which was almost 3 feet higher than the maximum ever recorded at the Boston gage. Given the unlikely event that a tide with a maximum elevation near the maximum predicted astronomic tide were to occur sometime during the maximum surge-producing northeaster, the probability that the hour of maximum surge (using hour increments) would occur at the hour of maximum tide is only one twenty-fourth (assuming a semidiurnal tide with unequal highs). Consequently, this combination might fall under the "excluding extremely rare" clause in the definition of the SPN. A better specification of the SPN stillwater level might be closer to 12.0 feet NGVD.

Therefore, based on the extensive WES studies of the history of storm surge and tide levels in the Revere area, 12 feet NGVD was adopted as the SPN stillwater tide level.

7. INTERIOR FLOOD ANALYSIS

a. General. Roughans Point is a low level 55-acre area, generally lying below elevation 10 feet NGVD. The interior section also receives drainage from about 30 acres of higher level Beachmont area to the south, making up a total interior drainage area of about 85 acres. A general plan and existing interior drainage facilities for the area are shown on plates 2-1 and 2-2, respectively. Existing limited storm drainage

facilities in the area generally drain to the west (away from the ocean), discharging to Sales Creek through a 42-inch diameter drain beneath Revere Beach Parkway. There is also an 18-inch flapgated storm drain at the south end of Broad Sound Avenue that discharges through the existing line of protection to the ocean, tide level permitting. The capacity of the entire existing system is affected by ocean tide. During storm tides there is no gravity drainage from the area and interior runoff, plus any wave overtopping, ponds throughout the low level area. Temporary ponding depths of 1 to 2 feet, in low areas, are reportedly an annual event with depths as great as 6 to 8 feet on rare occasions, as experienced in February 1978. A pumping station was non-Federally constructed in 1975 on Broad Sound Avenue for the purpose of pumping ponded waters from the street, through the line of protection to the ocean. This station has three pumps with a combined capacity of about 48 cfs (two at 15 mgd and one at 1 mgd); however, station capacity is reportedly limited to about 39 cfs with present inlets and outlets. This station proved quite inadequate and ineffective during the February 1978 event due to high wave overtopping rates.

Sales Creek, which receives most of the normal interior drainage from Roughans Point, is a tidal estuary that originally drained west to the Chelsea River. However, the creek now drains west about 2,000 feet and then reverses direction draining southeast a distance of about 3,000 feet through Suffolk Downs Racetrack, and discharging to the Belle Isle Inlet of Boston Harbor at Bennington Street. There is a tide gate and pumping station on the stream at Bennington Street.

There is a history of flooding along Sales Creek due both to the poor hydraulic characteristics of the creek and its many culverts, and also to the absence of drainage during high tide. A plan of improvement for Sales Creek was developed in 1974 by Andrew Christo Engineers for the Commonwealth of Massachusetts, Division of Waterways. The plan includes channel and conduit improvements plus construction of a pumping station and new tide gate at Bennington Street. The pumping station and tide gate have been completed but major channel-conduit improvements have not started. The completion of this plan and continued operation and maintenance of its extensive channel-conduit station system, would result in an improved drainage outlet for the Roughans Point area provided improvements were made in its own local storm drainage system. Discussions with personnel from the Massachusetts Division of Waterways indicate that the original planned channel and conduit improvements have been reduced in scope due to environmental concerns associated with excavation of

sediments. The current minimal plan is to clean the creek in the Garfield School area including the culvert under Winthrop Parkway, and minimal excavation from Winthrop Parkway to the Green Creek tributary from the north.

Sales Creek has a total watershed area of about 550 acres and the pumping station has a design capacity of 300 cfs, providing a pumping capacity equivalent to a runoff rate of over 1/2-inch per hour. This is a highly adequate capacity, considering the character of the watershed, its limited capacity storm drainage systems, and extremely limited gradient of the creek for moving the water to the station. The pumping station was sized by the designers based on the estimated maximum runoff rate resulting from a 4 percent chance (25-year) storm rainfall (reference: "Flood Control Study - Sales Creek, Revere," Andrew Christo Engineers, February 1974).

Completion of the once planned comprehensive Sales Creek drainage improvements would provide improved interior storm drainage in the Roughans Point area; however, the need for protection against tidal flooding will not be eliminated.

b. Analysis of Floods

(1) General. Six relatively recent and significant flood events at Roughans Point occurred in May 1967, November 1968, February 1972, February 1978 January 1979, and January 1987. Based on field interviews, photographs, and other available information, the resulting interior flood levels were determined to be about 8.0, 8.9, 11.8, 7.1, and 7.8 feet NGVD, respectively. Start of damage is about 4 feet NGVD. The resulting interior flood levels were believed to be a function of: (a) interior rainfall runoff, (b) saltwater intrusion by drain backflow or ground seepage, and (c) seawater overtopping. All six events had accompanying high winds and storm rainfall. Pertinent data for these events are listed in table 2-12. Historically, the most serious flooding has resulted from storms with associated wave overtopping; however, flooding is aggravated by interior runoff and if overtopping were minimized, there would still be a potential for minor to moderate street flooding if provisions for improved interior drainage are not provided. However, interior drainage provisions are a local responsibility and would be desirable after improvements are made for protection against tidal overtopping. An analysis was made of experienced and potential storm rainfall-runoff, seawall overtopping, and interior ponding storage capacity in assessing the interior drainage needs at Roughans Point.

(2) Storm Rainfall. Twenty-four hour rainfall amounts and maximum hourly rainfall rates recorded at Boston

TABLE 2-12

RECENT FLOODS AT ROUGHANS POINT
COMPARATIVE HYDROLOGIC DATA

Flood Event	7 Feb 1978	19 Feb 1972	26 May 1967	12 Nov 1968	25 Jan 1979	2 Jan 1987
Approx. Interior Level (ft. NGVD)	11.8-12	8.8-9	8	8	7-7.2	7.8
Annual Freq. Est. (%)	1	10	15	15	33	19
Approx. Flood Volume (ac.-ft.)	210	80	50	50	30	45
Ocean Tide (ft. NGVD)	10.3	9.1	8.9	7.7	9.3	9.4
Tide Freq., Est. (%)	1	10	13	80	7	6
Max. 1 Hr. Rainfall (in.)	0.2	0.5	0.3	0.3	0.3	0.4
Storm Rainfall (in.)	2.8/48 hr	2.5/24 hr	3.1/24 hr	1.8/24 hr	2.1/24 hr	2.2/24 hr
Rainfall Volume (ac.-ft.)	19	18	20	12	15	16
Max. Wind (Fastest-mile, MPH)	44	47	50	54	45	35
Wind Direction	NE	NE	NE	NE	E	NE

On 6 Feb '78, the ocean tide was 10.0 feet NGVD and maximum wind 61 MPH

during the six most recent significant flood events, as reported by the National Oceanic and Atmospheric Administration, are listed in table 2-12. Comparative rainfall-frequency-duration data, as reported in U.S. Weather Bureau TP 40, are listed in table 2-13. The experienced storm rainfall and rates were in the order of 2 to 3 inches, and 0.3 and 0.5 inch per hour, respectively. In comparison, the all-season 20 percent chance (5-year frequency) 24-hour rainfall is 4.0 inches and the 1 hour rainfall rate is reportedly 1.5 inches per hour.

(3) Runoff. Interior runoff and resulting ponding levels at Roughans Point are more a function of rainfall volume than rate. Minimum elevations in the area are about plus 4 feet NGVD, well below normal high tide, and interior runoff must pond or be pumped during high tide periods. Although rainfall rates were not intense during past flood events, rainfall runoff along with overtopping likely accumulated in the interior area even during ebb tides due to limited gravity storm drain capacity. Computed storm runoff and flood volumes stored during recent flood events are summarized in table 2-12. With sufficient gravity drain capacity, ponding would likely be limited to 3 to 4 hours duration -- the interval of high tide. Interior runoff volumes were estimated assuming runoff equaled rainfall, less an initial 0.2 inch infiltration. Because of the high water table, infiltration losses would be small. Peak runoff rates were estimated by "rational" formula using the maximum 1 hour rainfall rate and a runoff coefficient "C" of 0.7. The resulting maximum runoff rates during the 4 recent flood events were only 20 to 30 cfs, and the maximum 2-hour volumes only about 4 to 7 acre-feet. The 24-hour storm rainfalls represented 12 to 20 acre-feet of runoff volume.

(4) Ponding Capacity. Ponding elevation-capacity relations for the Roughans Point interior area were developed by planimetering available 2-foot contour maps of the area. The developed storage-capacity curve is shown on plate 2-3. Storage commences at about elevation 4 feet NGVD and storage at elevation 11.8, the 1978 flood level, would approximate 200 acre-feet. Maximum 24-hour rainfall during the six recent flood events was not more than 20 acre-feet, or 10 percent of total interior floodwaters.

(5) Overtopping. Past flood levels, interior flood volumes, and potential rainfall runoff, experienced during six recent flood events were analyzed. This data indicates that ocean water inflow by seawall wave overtopping, plus any drain backflow and seepages, probably ranged from 15 to 200 acre-feet and represented 50 to 90 percent of the total interior floodwaters.

TABLE 2-13

RAINFALL - FREQUENCY - DURATION
USWB TECHNICAL PAPER 40
BOSTON, MASSACHUSETTS
(In Inches)

Annual Frequency	Duration in Hours				
	1	2	6	12	24
20 Percent (5-Year Frequency)	1.5	2.0	2.8	3.4	4.0
10 Percent	1.8	2.3	3.3	3.9	4.6
2 Percent	2.4	3.1	4.3	5.1	6.0
1 Percent (100-Year Frequency)	2.6	3.3	4.7	5.8	6.8
SPS	3.5	4.8	9.0	10.6	12.4

(6) Pumping Station. A pumping station with a capacity of about 48 cfs, with surface water inlet located on Broad Sound Avenue, was non-Federally constructed in 1975 at Roughans Point. This capacity is equivalent to a runoff rate of 0.6 inch per hour from the 85-acre watershed. This discharge capacity would therefore be adequate to convey the peak rainfall runoff rates of the six most recent flood events, provided there were no other sources of inflow and drainage, and facilities were adequate to convey the runoff to the station. However, inflow rates during the record flood of February 1978, probably in excess of 1,000 cfs, far exceeded the capacity of the station, and personnel operating the station had to be evacuated.

c. Interior Flood-Stages

(1) Existing Condition Stage-Frequencies. An existing condition interior flood stage-frequency curve, the basic curve for determining flood damage frequencies, is shown on plate 2-4. This curve was developed by analysis of the history of experienced flood events in recent years, both in numbers and magnitude. The lack of a long-term systematic record of historical flood level data did not permit derivation by statistical analysis alone, and the curve was based on both analytical and subjective analysis along with considerable engineering judgment.

Stage-frequency curves were originally developed during the feasibility study concluded in 1982. Existing condition stage-frequency relationships were developed, based on the then available four historic flood elevations. Those four flood events were February 1978, February 1972, November 1968, and January 1979. In general, the existing condition stage-frequency curve was developed by assigning the 1978 interior flood elevation a 1 percent chance of occurrence (based on analysis of tidal records at the Boston gage) and assigning the three additional flood elevations Weibull plotting positions based on the then available 12 years of data.

The current investigation reviewed the four flood events previously used, along with information obtained for the more recent January 1987 event, and information concerning a flood event during May 1967. The recently obtained data on the 1967 flood was not known when the feasibility study was conducted. The revised existing condition, stage-frequency curve was developed by using the same technique as that used during the feasibility study.

Over the 24-year period, 1967 through 1990, the Roughans Point area experienced six significant flood events.

The greatest occurred in February 1978, with a reported experienced interior flood level of approximately 11.8 feet NGVD, followed by the events of February 1972, May 1967, November 1968, January 1987, and January 1979. These flood events had reported elevations of 9.0, 8.0, 8.0, 7.8, and 7.2 feet NVGD, respectively. Simply assigning Weibull plotting positions to these events per 24-year period would suggest frequencies of 1/25 (4%), 2/25 (8%), 3/25 (12%), 4/25 (16%), 5/23 (20%), and 6/25 (24%) for the experienced levels of 11.8, 9.0, 8.0, 8.0, 7.8, and 7.2 feet NVGD, respectively. However, the 1978 experienced level of 11.8 was the greatest ever known in the Roughans Point area, significantly exceeding any other, and was the result of one of the greatest coastal storms ever experienced along the New England coast, based on storm accounts extending over a 300-year historic period. Engineering judgment thus ruled out assigning a 4 percent frequency to an event the magnitude of the 1978. Instead, the 1978 interior flood stage was assigned a 1 percent frequency, the frequency of the 1978 storm tide based on a statistical analysis of long term storm tide records for Boston Harbor, including adjustment of historical data for the gradual long term rise in ocean level.

The experienced February 1972 level of 9.0 feet NGVD, was the second highest event in the 24-year period and could justifiably be assigned 2/25 (8%) annual probability Weibull plotting position. This frequency was considered the higher limit for the 1972 event. However, if the 1978 event was treated as a statistical outlier, then the frequency of the 1972 event could be as low as 1/25 (4%). Therefore, it was concluded that the frequency of the experienced 1972 stage of 9.0 feet was probably between the limits of 4 and 8 percent. The frequency of the 1972 event on the finally adopted curve was 7 percent.

The remaining flood events of May 1967, November 1968, January 1987, and January 1979 with elevations of 8.0, 8.0, 7.8, and 7.2 feet, respectively, were the third through sixth in the 24-year period and these Weibull plotting positions were adopted without adjustment in the development of the adopted interior stage-frequency curve.

The plotting positions of the six flood events, after the above adjustments, plus the statement of residents that ponding of 1 to 2 feet (4 to 5 feet NGVD) in the streets occurred annually, was the basis for developing the adopted "existing condition" interior stage-frequency curve. This curve was then compared to the existing condition stage-frequency curve developed by the Waterways Experiment Station

and reported in CERC-86-8 Technical Report entitled: "Frequency of Coastal Flooding at Roughans Point, Broad Sound, Lynn Harbor, and the Saugus-Pines River System, Appendix B." This report presented the results of numerical and physical models of the Roughans Point area. In general, there was close agreement for the rarer flood frequencies (i.e., 10- to 200-year); however, for the more frequent flood events (2- to 10-year) the WES curve was somewhat lower than the adopted curve. A review of the WES report reveals that the only source of flooding considered in their analysis was from wave overtopping. Coincident runoff from rainfall, which would contribute to flooding was not considered. The WES study team recognized this and point out in paragraph 68 of CERC-86-8 Report: "Runoff from rainfall was not considered. This will have an effect on the resulting stage-frequency curve, especially at the lower return periods. This contribution will be determined by NED." Since the historic flood events used to develop the NED stage-frequency curve have coincident rainfall runoff along with tidal overtopping, the developed curve is considered reasonable.

(2) Modified Condition Stage-Frequencies. Modified interior stage-frequency curves have been developed for improvements that would include:

(a) Rock revetment scheme that will reduce tidal overtopping and a 2-foot cap on the floodwalls of reaches E and F.

(b) New 48-inch emergency gravity outlet at the existing pumping station.

(c) New inlet to the pumping station to enable full utilization of the 48 cfs pumping capacity.

The WES report (Appendix A) screened numerous wave overtopping reduction schemes. The scheme that provided interior stage reductions comparable to those estimated during the feasibility study, was a wide berm with a 2-foot cap on the floodwalls of reaches E and F. The WES report presents modified interior flood stage-frequencies due to reduced overtopping attributable to the scheme described above. However, it is again noted that interior rainfall runoff was not considered.

(3) Wide Berm With 2-Foot Cap Engineered Refinement. A review of the modified WES stage-frequency curve indicates that overtopping volume begins to exceed pumping capacity at about a 4 to 5 percent chance event; however, it does not become significant in terms of interior ponding levels, until

about a 2 percent chance event. Therefore, any rainfall runoff coincident with a 4 percent chance or rarer tidal frequency events would result in increased interior ponding. In addition, a review of more frequent flood events shows that the existing 48 cfs pumping capacity should be adequate, with minor street ponding, for interior/runoff events up to about a 10-year frequency. Therefore, the following analysis was conducted to estimate coincident interior rainfall runoff for the project condition.

Peak interior runoff hydrographs were estimated using the "rational" formula with an adopted C of 0.7. Peak rates were determined by using 1-hour initial rainfall as determined from TP 40 with an assumed loss of 0.2 inch. Total hydrograph volume was determined based on 2-hour rainfall volumes from TP 40. Runoff hydrographs are shown on plate 2-3. First, it was assumed that a 4 percent chance (25-year) rainfall runoff would occur coincident with the peak 4 percent chance tide level. Similarly, it was assumed that peak 2 and 1 percent chance rainfall runoff would occur coincident with peak 2 and 1 percent chance tide level. The interior runoff volume was then added to the volume resulting from the modified interior levels developed by WES. This resulted in a modified interior stage-frequency relationship slightly higher than that estimated during feasibility studies. We recognize, however, that the probability of these two joint occurrences would be rarer than the frequency of individual events and the resulting modified interior stage-frequency relationship might be somewhat overestimated. Therefore, a second approach was undertaken. An adjusted storm tide runoff-duration curve was developed by determining recorded runoff rates at nearby gaged streams for a series of storm tide periods. This curve is shown on plate 2-5. We found that runoff (streamflow) during storm tides, on average, was about eight times greater than the all time average runoff. Flow durations for the gaged Old Swamp River in South Weymouth, Massachusetts (D.A.= 4.5 square miles) for periods during storm tides were developed. The 4 percent of time streamflow at the time of storm tide was applied, by a drainage area ratio, with the 4 percent chance interior level resulting from overtopping. Similarly, the 2 and 1 percent of time storm tide flow was applied with the 1 percent chance interior overtopping level. Computed interior runoff volumes, added to overtopping volumes, resulted in interior levels only slightly lower than those developed assuming coincident peak runoff conditions. This second approach was adopted for determining coincident runoff associated with high tide frequencies. The modified interior stage-frequency curve for the wide berm with 2-foot cap engineering refinement is shown on plate 2-4. The north wall was adopted at elevation 14.0 feet NGVD.

(4) Standard Project Northeaster - Interior Flood Level. This section is mainly concerned with the effect of the SPN on the interior of Roughans Point. In considering interior floods at Roughans Point, the effect of a SPN is straightforward; the interior of Roughans Point would fill to overflowing. The interior water level (approximately 1 to 2 feet higher than the stillwater level in Broad Sound) would be determined by how fast overtopping volumes would flow over roadways at the west boundary of Roughans Point. The evidence seems clear that given an ocean water level on the order of 12 to 13 feet, NGVD and with the waves appropriate for a SPN, all proposed alternatives considered at Roughans Point would be swamped. Larger and longer waves caused by the effect of deeper water in front of the structure and the higher windspeeds of the SPN would create enormous wave overtopping. Although the proposed improvements at Roughans Point would offer considerable protection against lesser northeasters, WES states it is possible that interior flood levels for the SPN might be slightly higher after the improvements. Without the improvements, water will begin returning to the ocean over the north wall with a low point at approximately 11 feet NGVD. This outflow of water lessens the probability of extreme interior flood levels; however, it must be noted that interior 1978 flood elevations (1 percent chance of occurrence) approached elevation 12 feet NGVD. With the improvements, this outflow would be prevented by the increased wall height to 14.0 feet NGVD. The lack of data to ascertain the relative importance of outflow over the walls versus the outflow at the western edge of the Roughans Point area at extreme interior flood levels such as the SPN makes definitive conclusions difficult. The approximate extent of flooding during the SPN is shown on plate 2-6.

(5) Residual Flooding. The selected design stillwater tide level is 10.3 feet NGVD (100-year). Minor ocean wave overtopping will begin at approximately a 4 to 5 percent chance event; however, will not become significant in terms of interior ponding levels, until about a 2 percent chance (50-year) event. This overtopping coincident with interior rainfall runoff which exceeds the 48 cfs pumping capacity will result in residual flooding. For the 1 percent chance project design flood residual interior flood levels will be about 7 feet NGVD with resulting maximum depth in low areas of about 3 feet with average depths throughout the area in the order of 1 foot. Approximate limits of residual flooding for the project design flood is shown on plate 2-7. Flooding will occur gradually and consist of temporary ponding which will be evacuated during receding tides using either the emergency drain alone or in combination with pumping. The 1 percent chance design flood is comparable to the 1978 flood

of record. Residual flooding resulting from a SPN tide level will inundate the entire Roughans Point area full to overflowing with estimated flood limits shown on plate 2-6.

(6) Flood Warning and Evacuation. A Flood Warning and Evacuation Plan has been developed by the city of Revere. This plan is described in the GDM and involves closing of low lying roads and evacuation of residents to the Revere High School located on high ground about 1.5 miles from Roughans Point. In general, considerable warning time should be available for floods of the magnitude of the Project Design Flood (Blizzard of 1978). In February 1978, the National Weather Service provided weather and storm bulletins to the public concerning the possibility of severe weather, strong winds, and high tides some 36 to 48 hours in advance of the onslaught of the storm. There should be sufficient lead time to coordinate any required evacuation. In addition, we note that residual wave overtopping will be gradual with resulting shallow flood depths in the order of 1 to 3 feet.

d. Interior Drainage Design

(1) General. During the feasibility investigation a number of interior drainage improvements were studied with the recommended plan having no added pumping and no interior collector drain improvements. It does provide for an emergency gate closure on the Sales Creek outlet, an improved surface water inlet at the existing pumping station, and a new emergency gravity drain through the line of protection at the existing station. Though an improved storm drain collector in the area would still be desirable, it would be a local decision and cost.

(2) Interior Drainage Collectors. Improved interior drainage collectors should be considered by local interests to provide the greatest degree of protection to the area. An interior drainage collector, as a minimum, might consist of a 42-inch trunk line storm drain from the existing drain under the Revere Beach Parkway extending east to the southerly end of Broad Sound Avenue (1,800 feet) and then continuing as a 48-inch drain north on Broad Sound Avenue to the existing 48 cfs pumping station (1,000 feet). Such a trunk line drain would have surface inlets and serve as a main outlet for existing feeder drains. It would have a very flat gradient with normal drainage to the west; however, during intense runoff, drainage could be both to Sales Creek and Broad Sound Avenue pumping station. As part of the recommended project a sluice gate will be provided at the Sales Creek discharge so that, in the event of high stages, the gate could be closed and reverse flow would convey all drainage to the Broad Sound

pumping station, where it would be pumped or discharged by gravity, tide permitting. Assuming conveyance velocities of about 4 feet per second, the minimum collector system would have drainage capacity of about 40 to 50 cfs, comparable to existing pumping capacity, under nongravity discharge conditions. Under gravity flow, both to Sales Creek and Broad Sound Avenue, the collector system would have total capacity of 70 to 80 cfs, equivalent to the estimated 20 percent chance (5-year frequency) maximum rainfall-runoff rate. We conclude that completion of the comprehensive Sales Creek improvements previously discussed (Section 7a) plus an improved Roughans Point collector system would provide residual flood relief comparable to that of an added 50 cfs pumping station at Roughans Point.

Estimated limits of interior ponding with a Standard Project interior storm runoff and a 100-year frequency storm runoff, with and without interior drainage improvements, were presented in Appendix A of the Feasibility Report. Since the principal object of this project is coastal flood reduction, these analyses are not presented in the report.

(3) Existing Pumping Station. The existing pumping station has a total capacity of 48 cfs which is equivalent to a runoff rate of 0.6 inch per hour from the 85-acre interior area. This station has considerable capacity to discharge interior rainfall-runoff provided there are adequate facilities to convey the flow to the station. As part of the recommended project, an improved surface water inlet will be provided at the existing Roughans Point pumping station. Since the existing pumping station with improvements will be part of the overall Corps protection, its hydraulic, mechanical, and electrical integrity must be assured. Results of this analysis will be presented in DM No. 1, General Design. In addition, as part of the feasibility studies, additional pumping capabilities were investigated as shown on plate 2-3. but were not considered as part of the adopted plan.

(4) Emergency Gravity Drain. Included as part of the recommended plan is a 48-inch emergency gravity drain through the line of protection to be located at the existing Roughans Point station. This drain would serve as an emergency discharge in the event of greater than design interior runoff or wall overtopping and provide a means of rapid evacuation of any accumulated ponding during receding tide.

During periods of high tailwater, this drain will have a capacity of 70 cfs with a 2-foot head differential, assuming a Mannings "n" of 0.013 and entrance, expansion, contraction, bend, gate, and exit loss coefficients totalling

3.35. During periods of low tailwater, a maximum capacity of about 135 cfs could be reached with the interior filled to overflowing at 11+ feet NGVD. In addition, a modified curb inlet will be provided for the gravity drain intake and increased inflow capacity to the pumping station. This inlet will be 66 feet long and have a total grated inlet area of 38.06 square feet with individual openings of 1-7/8 by 6-5/8 inches. A curb inlet weir length of 60.5 feet with 6-inch vertical clearance will provide a hydraulic capacity of 50 cfs with a 0.5 foot head, assuming the curb inlet is about 25 percent clogged and using a weir coefficient of 3.0. This system will: (a) assure that water can reach the pumping station so it can operate at maximum capacity, and (b) allow emergency evacuation of ponded water during events exceeding the design flood condition in less than a day after the storm abates.

(5) Ponding Levels. Significant ponding in the interior area commences at about elevation 4+ feet NGVD, the level of many streets, and appreciable flood damages commence at about elevation 5+ feet NGVD. Interior flood damages to residential, commercial, and public buildings are in the order of $10,000 at 5+ feet NGVD and $80,000 at 6+ feet NGVD. The existing pumping station with a capacity of about 48 cfs would maintain the 10-year frequency runoff below elevation 6 feet NGVD.

8. DEPARTURES FROM APPROVED PLAN

The principal departures from the plan approved in the feasibility investigation resulted from physical and mathematical modeling of wave overtopping and associated interior flooding. Changes include a lowered, wide berm along the easterly seawall, a cap on the easterly seawall, and lowered height of protection on the north seawall. The rock berm in reaches E and F was lowered from elevation 14 to 8 feet NGVD and the width was changed from 5 feet to 25 feet. Also, a concrete cap two feet high is to be added to the concrete seawall in these reaches. These changes were required to reduce wave overtopping to acceptable levels. Conversely, in reaches A through D, model overtopping was not as great as previous estimates; therefore, the height of revetment could be lowered from 17 to 14 feet NGVD. In reach A, overtopping was small; therefore, only the existing seawall is required with the revetment not being needed to further reduce overtopping.

9. SEA LEVEL RISE

a. Historic Rise. Sea level has been rising worldwide at varying rates for thousands of years. Since the maximum

advance of the last glacier around 13,000 B.C., sea level has risen between 330 to 490 feet (Shepard, 1963) or approximately 430 feet (Meade). With retreat of the glacial ice, the phenomenon of "rebound" of the landmass has accounted for more than 600 feet increased elevation in northern areas of New England where the ice sheet was very thick. The mean height of the sea, with respect to adjacent land, has been rising in the United States with the exception of Alaska and possibly northernmost New England where rebound may still be occurring. The overall long term historic rate of rise on the east coast has generally been 1 to 1-1/2 feet per century. This apparent change in sea level has been ascribed to a combination of increased water volume in the ocean from melting glaciers and subsidence of the land in some regions. Figure 2-13 depicts the historic relative sea level from 1940 to 1980 along the northern east coast (Hicks, 1983). At the Boston Harbor National Ocean Survey tide gage, the rise relative to the land has been estimated to be 0.008 ft/yr from 1922 through 1980. Sea level determination has generally been revised at intervals of about 25 years to account for the changing sea level phenomenon. The National Ocean Survey is presently finishing the process of reducing tide data from the 1960 to 1978 tidal datum epoch to make such a revision. Thus, the present local mean level of the sea at a given location along the coast can be expected to be several tenths of a foot higher than the National Geodetic Vertical Datum that was established as the mean sea level in 1929 and which remains basically fixed in time and space.

b. Future Sea Level Rise. In recent years there has been much discussion regarding a potential increased rate of future sea level rise. This phenomenon is related to a gradual warming of the earth's atmosphere associated with increased emissions of carbon dioxide and other gases on earth. The warmed atmosphere may promote expansion of near surface ocean water and increase the rate of glacier melting, thereby hastening the rate at which ocean levels appear to be rising. The scientific community is generally in agreement that the rate of global sea level rise will increase; however, there is lack of precision and agreement as to how much the increase will be. Several scientists have made projections employing mathematical models which simulate the processes involved. These global sea level rise forecasts by others are summarized in table 2-14. It can be seen that the increase in global sea level by the year 2100 could be about as little as 0.7 foot or as much as 11.3 feet. A middle estimate of 2 to 3 feet, based on 1990 studies by the International Panel on Climate Change, is now accepted by many experts. This middle ground would yield an increase of nearly threefold over historic rates in New England. The

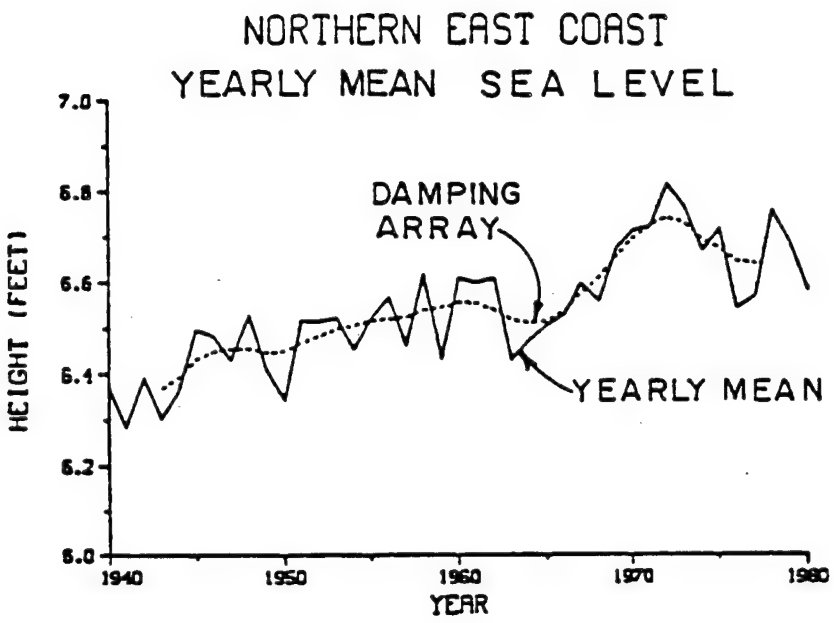

Northern east coast area mean with damping array.

Northern East Coast		
Trend	2.6 mm/yr	.009 ft/yr
Standard Error of Trend	± .3 mm/yr	±.0011 ft/yr
Variability[c]	±24.5 mm	±.080 ft

Northern East Coast to Cape Hatteras

Portland, ME
Seavey Island, ME (Portsmouth, NH)
Boston, MA
Newport, RI
Willets Pt., NY
New York (The Battery), NY
Atlantic City, NJ
Baltimore, MD
Annapolis, MD
Solomons Island, MD
Washington, DC
Hampton Roads (Norfolk), VA
Portsmouth, VA

Source:
Sea Level Variations for the United States 1855-1980
National Ocean Service

[redacted]

FIGURE 2-13

TABLE 2-14

ESTIMATES OF FUTURE SEA LEVEL RISE (FEET)

Investigator	Total Rise in Specific Years					
	2000	2025	2050	2075	2085	2100
Revelle (1983)	-	-	-	-	2.3	-
Hoffman et al. (1983)						
Low	0.2	0.4	0.8	1.2	-	1.8
Mid-Range Low	0.3	0.9	1.7	3.0	-	4.7
Mid-Range High	0.4	1.3	2.6	4.5	-	7.1
High	0.6	1.8	5.8	7.0	-	11.3
NRC (1985)						
Low	-	-	-	-	-	1.3
High	-	-	-	-	-	6.4
Hoffman et al. (1986)						
Low	0.1	0.3	0.7	1.2	1.4	1.9
High	0.2	0.7	1.8	6.3	8.5	12.1
Robin (1986)						
Low	-	-	-	-	-	0.7
High	-	-	-	-	-	5.2
IPCC (1990)						
Low	-	-	0.7	-	-	1.1
High	-	-	1.0	-	-	3.6

National Research Council (NRC, 1987) recently suggested that the sensitivity of design calculations and policy decisions be evaluated based on three plausible variations in sea level rise to the year 2100, all showing greater rate of rise in the distant future than in the next decade and all with an increased rate of rise relative to the present: 1.6, 3.3, and 4.9 feet. These estimates represent "Eustatic" or global changes. The local component which varies greatly from subsidence to uplift must also be included in estimating the total rise at a specific location. The NRC suggests the following equation for estimating total rise: $T(t) = (0.0012+M/1,00)t+bt^2)/.3048$ in which M = 1.0 mm/yr at Boston, t = years from 1987, and b = 0.000028, 0.000066 or 0.000105 m/yr^2 for global rises of 1.6, 3.3, and 4.9 feet by the year 2100. The result here is converted to feet. Figure 2-14 presents NRC total plausible rise at Boston for the three cases.

c. General Policy Regarding Sea Level Rise. The Corps policy regarding sea level rise is one of concern rather than alarm. The Corps is keeping aware of ongoing developments to further define the complex issue, keeping in mind the inherent uncertainty in any projections. A 21 March 1986 letter from OCE stated our policy as follows:

(1) Predicting future sea level rise is risky because there are so many variables and, as yet undefined interrelationships.

(2) Until substantial evidence indicates otherwise, we will maintain the procedure of considering only local regional history of sea level changes to project a rise or fall for a specific project.

(3) Where long periods of tidal records exist and are used in determining the exceedance frequency relationship for coastal flood levels, it may be necessary to adjust the water level records for relative sea level changes when such changes are significant.

(4) Prudence may require an allowance in a project design for continuation over the project design life of an established significant long-term trend in relative sea level rise.

(5) Consideration must be given to the relative magnitude of the suggested allowance and the confidence band of the data the designer is using and the tolerance allowed in constructing the project.

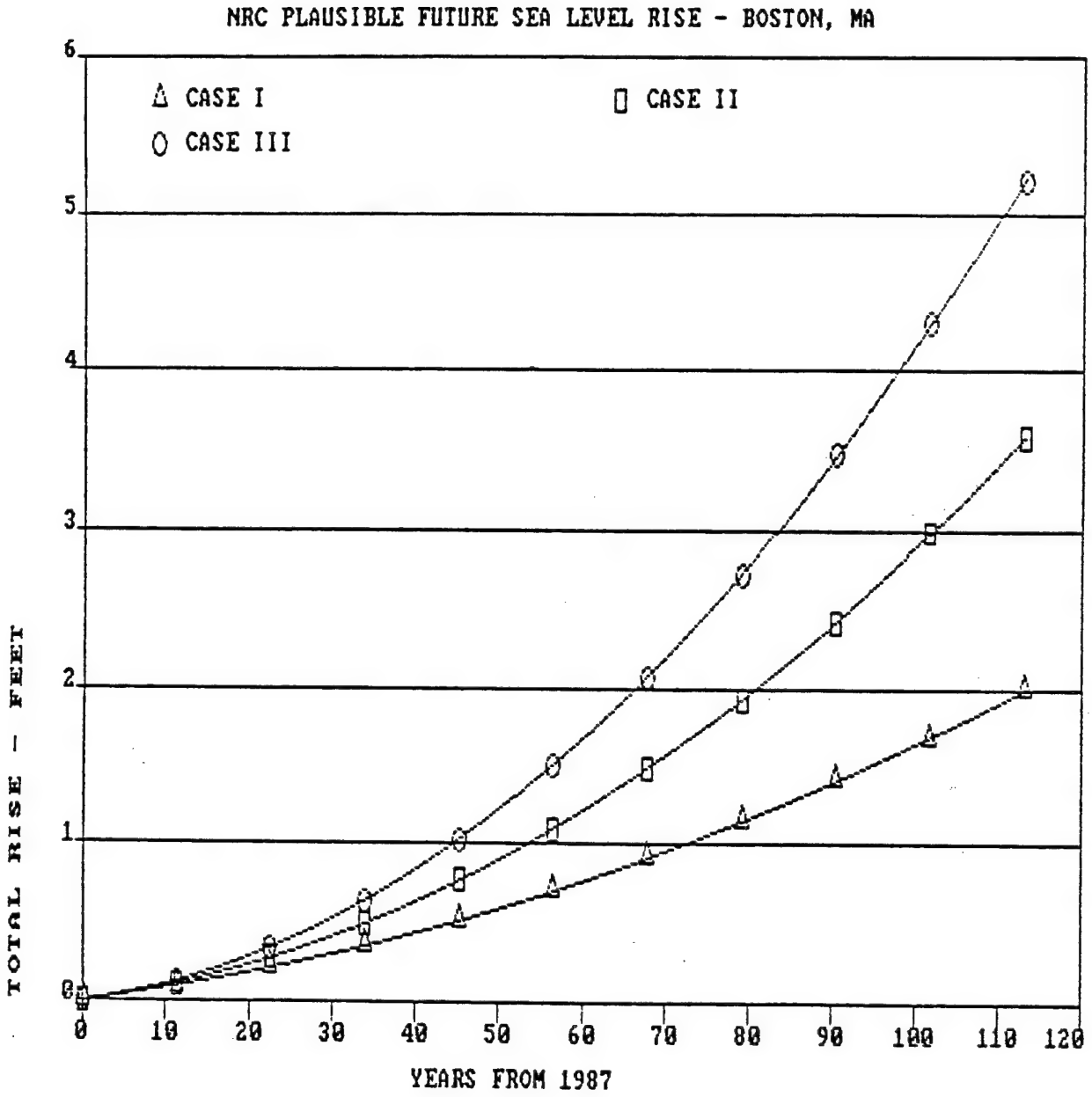

PLAUSIBLE SEA LEVEL RISE FROM NATIONAL RESEARCH COUNCIL-1987

FIGURE 2-14

(6) Consider whether it is more cost effective to include the allowance for significant sea level rise in the initial construction or to plan for modification later after the need for such is demonstrated.

Guidance on the incorporation of sea level rise possibilities in Feasibility Studies (EC 1105-2-186) was issued 21 April 1989. This document included a recommendation that a sensitivity analysis be conducted to look at effects of accelerated sea level rise on plan evaluation and selection. As well, a draft policy from Massachusetts Coastal Zone Management in December 1989 requested an evaluation of project structural integrity/engineering performance and related natural resources due to sea level rise of 3 feet, when project life is expected to be over 50 years.

As events continue to unfold and more precision is gained in estimating future sea level rise, additional policy guidance is sure to follow. In an effort to make informed policy judgements, the Corps Coastal Engineering Research Center has completed an annotated bibliography on sea level rise. As well, plans have been made to embark on a study to determine the impacts of sea level rise on coastal engineering; however, funding to initiate this effort has not been provided as yet.

d. Effects of Rising Sea Level on Future Tidal Flood Frequency. Storm surges, the increased water levels induced by wind stresses and barometric pressure reduction associated with hurricanes, tropical storms, and extratropical storms will be modified by sea level rise mostly in areas of very mild offshore slopes, as is typical of many Southeastern States. The large expanse of shallow water resulting from higher sea levels will cause increased storm surge elevations, compared to areas of steep offshore slopes, because surge heights are proportional to both the length and inverse slope of the offshore bottom. However, if the shoreline is fixed and offshore water depths increase, as is typical of the study area, then the storm surges will be less, as the surge also varies inversely with absolute water depth (NRC, 1987). Reduction of the wind stress component of the storm surge can be estimated by the relationship of Dean and Dalrymple (1984) where

$$\frac{\Delta n_{max}}{S} = \left(\frac{-n_{max}/h_o}{1+n_{max}/h_o}\right).$$

S = sea level increase, n_{max} = maximum wind stress storm surge, and h_o = a representative depth. By way of illustration, for a representative water depth of 30 feet, a 5-foot

maximum storm surge (approximately the greatest observed at Boston) would be reduced by about 0.1, 0.2, 0.4, and 0.6 foot for respective sea level increases over the next 100 years of 0.8, 1.6, 2.9, and 4.2 feet, assuming the barometric component of storm surge is about 20 to 30 percent of the total. Lesser, more frequent, surges would be reduced a progressively smaller amount. Of course, relative to an absolute datum, a total flood elevation would increase by 0.7, 1.4, 2.5, and 3.6 feet, respectively. Figure 2-15 shows the natural Boston stillwater tide stage-frequency curve as adjusted for continued historic rate of rise and for NRC cases I, II, and III rates of rise over the next 100 years with the reduction in storm surge due to increased depth included.

Table 2-15 compares the frequency of tidal flooding in the year 2087 to that in 1987 assuming that the historic rate of rise of 0.08 foot per decade were to continue, accounting for the reduction of storm surge with depth as previously discussed. Even under these conditions today's 100-year flood could become about a 25-year event. Considerable flooding and resulting economic and environmental losses will surely be associated with increasing ocean levels.

TABLE 2-15

FUTURE FREQUENCY OF TIDAL FLOODING
BOSTON, MASSACHUSETTS

Average Return Period (years)	1987 Stillwater Elevation (ft, NGVD)	2087* Projected Stillwater Elevation (ft, NGVD)
10	9.1	9.8
50	10.0	10.7
100	10.3	11.0

* Based on projecting a historic rise in relative sea level of about 0.1 foot per decade, including estimated surge reduction due to increased depth.

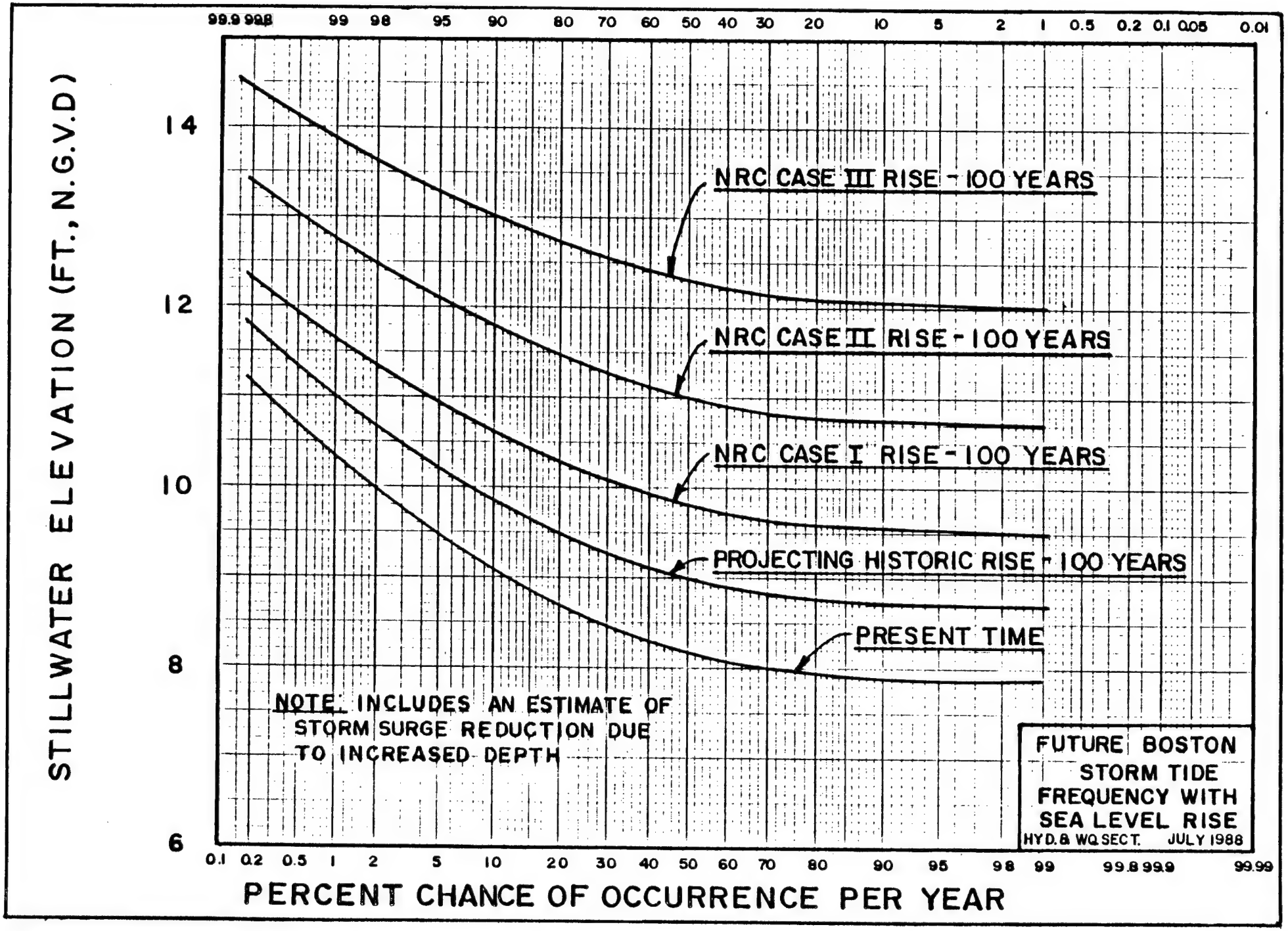
STILLWATER ELEVATION (FT., N.G.V.D)
14
12
10
8
6
99.9 99.8 99 98 95 90 80 70 60 50 40 30 20 10 5 2 1 0.5 0.2 0.1 0.05 0.01
0.1 0.2 0.5 1 2 5 10 20 30 40 50 60 70 80 90 95 98 99 99.8 99.9 99.99
PERCENT CHANCE OF OCCURRENCE PER YEAR
NRC CASE III RISE - 100 YEARS
NRC CASE II RISE - 100 YEARS
NRC CASE I RISE - 100 YEARS
PROJECTING HISTORIC RISE - 100 YEARS
PRESENT TIME
NOTE: INCLUDES AN ESTIMATE OF STORM SURGE REDUCTION DUE TO INCREASED DEPTH
FUTURE BOSTON STORM TIDE FREQUENCY WITH SEA LEVEL RISE
HYD. & WQ SECT. JULY 1988

FIGURE 2-15

It is recommended, in accordance with the previously referenced policy, that the natural stillwater tide stage-frequency relationship for the Roughans Point Project at least include an estimate to account for projection of the long term uniform historic rate of sea level rise (0.008 ft/yr) over the project life, approaching an increase in stage of 0.8 foot over a 100-year period. As well, qualitative consideration should be given to the possible future effects that accelerated rise (NRC cases I, II, and III) could have on the project and environs. The evaluation of 3 feet of rise over 100 years seems appropriate. We should not design for accelerated rise now, however, since any needed additional protection could be built over a relatively short period of time, once substantial sea level increase is confirmed (NRC, 1987). Rather, the sensitivity of the protective scheme should be qualitatively evaluated for a plausible sea level rise scenario, keeping in mind the probability of increasing sea level and keeping all response options open. Alternatives ill-suited for retrofitting should be avoided. The effectiveness of any flood protection scheme built today and subjected to significant sea level rise in the future would be a function of the project's durability and height. Obviously, significant sea level rise could cause greater wave or sea level overtopping as well as undermining of the structural integrity of any flood protection device. It is also important to assess the effects of sea level rise on the study area if no project is built.

e. Effects of Rising Sea Level on Waves. Two differing phenomena need to be considered when examining the effect of increased sea level on wave propagation. First, when waves are generated in deep ocean waters and progress shoreward over the Continental Shelf, the waves are dampened. This dampening is related to the width of the shelf and depth of water. The physics involved are quite complex. The NRC (1987) has shown as an example (Dean and Dalrymple, 1984) that for a depth of 33 feet, shelf width of 6.2 miles, wave period of 8 seconds, initial wave height of 6.6 feet, friction coefficient of 0.01 and sea level rise of 3.3 feet, a 0.2 foot or about 3 percent increase in wave height would be expected. The NRC indicates that this small increase is not likely to cause changes of substantial engineering significance.

The second case involves waves which are generated by the wind as it passes across the Continental Shelf waters. Here, wave growth will be enhanced by the deeper water due to the diminished effect of bottom friction. This effect can be estimated for the case of very long fetch using the Shore

Protection Manual (Corps of Engineers, 1984), shallow water wave forecasting relationship. Simplifying,

$$DH = (0.75 \frac{H}{h})S$$

where DH = change in wave height, S = increase in water depth, H = original wave height, and h = representative water depth. For the same values of the previous example, wave height would increase about 0.5 foot or 7.5 percent.

The combined effect of reduced wave dampening and augmented wave generation would result in larger wave heights in the surf zone. Larger amounts of sediment would be moved and greater wave forces and potential for overtopping would exist. In the coastal area of the project, this could mean accelerated beach erosion along Revere Beach. With excessive sea level rise and no continuing maintenance, undermining and failure of existing seawalls and revetments may occur. Minor sea level rise, in the order of historic rates, will at least create greater wave overtopping and flooding behind coastal structures. The amount of impact will increase as sea level rise increases. Major structural actions or abandonment may be necessary in the future in the study area and all along the United States coast, if large accelerated sea level increases occur.

f. Effects of Future Sea Level Rise on Interior Tidal Flood Frequencies

(1) General. It was requested that the effects of future sea level rise on existing natural and modified stage frequencies for the Roughans Point area be examined. This was to be used by others to qualitatively discuss any economic benefits, attributable to the project, due to future rising sea level. As previously discussed, estimates of future rates of rise vary considerably. However, Corps of Engineers policy is to consider only local regional history of sea level changes in discussing economic benefits. Therefore, the historic rate of rise of about 0.1 foot per decade was used for this cursory assessment.

(2) Effects of a 1-Foot Rise on Existing Boston Stillwater Curve. Recognizing the difficulties in trying to precisely determine the impacts of a future gradual rise in sea level on existing stage-frequency relationships we decided, for simplicity sake, to estimate stage-frequency relationships at a distant future time (say 100 years hence).

Since the historic rate of rise is about 0.1 foot per decade, the future sea level condition elevation frequencies would be the existing condition elevations plus approximately 1 foot. We note that this assumption is not precisely correct as discussed earlier in this section; however, we feel it is adequate for this investigation. Thus, based on the above assumptions, the adopted future sea level conditions on Boston stillwater elevation frequencies would be as follows in 100 years.

TABLE 2-16

FUTURE SEA LEVEL CONDITIONS
BOSTON STILLWATER ELEVATION FREQUENCIES

Percent Chance Occurrence	Existing Condition Elevation (ft, NGVD)	1-Foot Rise Future Condition (100 Years) Elevation (ft, NGVD)
SPN	12.0	13.0
0.2 (500-yr)	11.2	12.2
1.0 (100-yr)	10.3	11.3
10 (10-yr)	9.1	10.1
50 (2-yr)	8.3	9.3

(3) Effects on Natural Stage-Frequencies for Roughans Point. Existing condition stage-frequencies were developed by analyzing historic flood data for the interior Roughans Point area. We note that the flood problem at Roughans Point is principally ocean overtopping by wind-generated waves. Therefore, wind and wave conditions must be considered along with stillwater tide levels. Reviewing WES backup data, which was developed in support of Appendix B, indicates that for WES mathematical modeling, 150 historic storms with an entire range of wind, wave, and stillwater tide levels were analyzed. Ocean stillwater levels were plotted versus the resulting interior elevation in Roughans Point. WES calibrated this model to reproduce the existing stage frequencies which are shown in the following table. The array of WES data was again analyzed for future sea level (1-foot rise in stillwater elevation) conditions with estimated interior levels also shown in the following table.

TABLE 2-17

FUTURE SEA LEVEL CONDITIONS
ROUGHANS POINT
FLOOD STAGE FREQUENCIES

Return Period (years)	Existing Condition Elevation (ft, NGVD)	1-Foot Rise Future (100 Years) Elevation (ft, NGVD)
1.1	3.6	7.8
1.5	4.4	8.2
2	5.2	9.0
5	7.2	10.7
10	8.6	11.7
50	11.5	12.4
100	12.0	12.6
500	12.5	12.8

As can be seen, an interior level of 9.0 feet NGVD would represent a 2-year frequency flood under future sea level conditions. Elevation 9.0, for existing conditions, is between a 10- and 20-year flood event. In addition, an elevation of 8.0 feet NGVD would occur on an annual basis. This would lead to intense pressures for flood control improvements or result in abandonment.

(4) Effects on Project Modified Stage-Frequencies. To address effects of sea level rise on the project, WES data was again analyzed. Again, WES analyzed 150 storm events with various wind, wave, and stillwater conditions to screen and refine various protection schemes and lead to the finally adopted wide berm and 2-foot cap on the seawall in reaches E and F. Modified flood stage-frequencies (existing sea level conditions) for reduced overtopping alone are shown in the following table.

Analyzing WES data and considering a 1-foot rise in stillwater stage-frequencies, interior elevation frequencies were also estimated for overtopping alone. No coincident rainfall runoff was added because the purpose of this exercise was to determine how effective the project would be under a future sea level condition. If the intent were to determine economic benefits, then coincident rainfall runoff would have to be considered.

TABLE 2-18

FUTURE SEA LEVEL CONDITIONS
ROUGHANS POINT
INTERIOR ELEVATION FREQUENCIES
WIDE BERM WITH 2-FOOT CAP

Return Period (years)	Existing Sea Level Interior Elevations (ft, NGVD)	1-Foot Rise In Sea Level Interior Elevation (ft, NGVD)
1.1	3.6	3.7
1.5	3.6	3.7
2.0	3.6	3.7
5	3.7	3.9
10	3.7	4.9
50	4.4	8.4
100	5.9	9.6
500	9.3	12.8

As can be seen, for a 1-foot sea level rise, future interior levels for a 1 percent chance flood (considering overtopping alone) would be almost 10 feet NGVD as compared to 1 percent chance levels of about 6.0 feet NGVD under present sea level conditions. Again, it is noted that coincident rainfall runoff has not been considered.

(5) Three-Foot Sea Level Rise. A 3-foot rise in sea level would totally inundate Roughans Point annually if flood protective works were not constructed. High annual tide levels would be about 11 feet NGVD and free flow of tide water would enter Roughans Point from the north.

With project conditions (wide berm and 2-foot cap) and a 3-foot sea level rise, the interior area would be flooded frequently and additional pressures for increased flood reduction measures would arise.

g. Perspective. In the preceding sections, historical sea level rise and National Research Council scenarios of potential increased future sea level rise have been discussed. Possible increases in flood frequency, waves, and coastal erosion have been explained. Flood protection measures constructed today may be affected by large sea level rise. This may increase operation and maintenance costs in years to come and may necessitate additional future studies to increase project effectiveness.

It is important to realize that large sea level rise would be a worldwide problem with many major urban centers being faced with potential significant flooding and other problems. Although discussion has focused on the project area, the effect on a national level would be huge. Major economic resources would be required throughout the country to deal with this problem if it materializes.

The best course of action at present is to stay aware of and closely monitor the situation and be prepared to act when increased rise can be predicted with high confidence.

10. REFERENCES*

Meade, Robert H., The Coastal Environment of New England, U.S. Geological Survey, Woods Hole, Massachusetts, 19__.

Shepard, F. P., Submarine Geology, New York, Harper and Brothers, 1963.

Hicks, S.D., H.A. Debaugh, Jr., and L.E. Hickman, Jr., Sea Level Variations for the United States, 1955-1980, Rockville, MD, National Oceanic and Atmospheric Administration, 1983.

Revelle, R., "Probable Future Changes in Sea Level Resulting from Increasing Atmospheric Carbon Dioxide," Changing Climate, Washington, D.C., National Academy Press, 1983.

Hoffman, J.S., D. Keyes, and J.G. Titus, Projecting Future Sea Level Rise; Methodology, Estimates to the Year 2100, and Research Needs, Washington, D.C., U.S. Environmental Protection Agency, 1983.

Hoffman, J.S., J.B. Wells, and J.G. Titus, "Future Global Warning and Sea Level Rise," Iceland Coastal and River Symposium '85, G. Sigbjarnarson, ed., Reykujavik: National Energy Authority, 1986.

National Research Council, Committee on Engineering Implications of Changes in Relative Mean Sea Level, Responding to Changes in Sea Level, National Academy Press, 1987.

Dean, R.G. and R.A. Dalrymple, Water Wave-Mechanics for Engineers and Scientists, Englewood Cliffs, NJ, Prentice-Hall, Inc., 1984.

O'Brien, M.P., Equilibrium Flow Areas of Inlets on Sandy Coasts, J. Waterways and Harbors Div, ASCE, 95 (WW1), 1969.

U.S. Army Corps of Engineers, Shore Protection Manual, Vicksburg, MS, Waterways Experiment Station, 1984.

Swift, D.S.P., J.W. Kofoed, F.P. Saulsbury and P. Sears, Holocene Evolution of the Shelf Surface Central and Southern Atlantic Shelf of North America, Pp. 499-57 in Shelf Sediment Transport, D.J.P. Swift, D.B. Duane and O.H. Pilkey, eds, Stroudsburg, PA, Dowler, Hutchinson and Ross, 1972.

Bruun, P., Sea Level Rise as a Cause of Shore Erosion, Journal of Waterways and Harbors Div, ASCE 88: 117-130, 1962.

Geise, G.S. D.G. Aubrey and P. Zeeb, Passive Retreat of Massachusetts Coastal Upland Due to Relative Sea Level Rise, Woods Hole Oceanographic Institution, 1987.

* Includes references not specifically spelled out in report

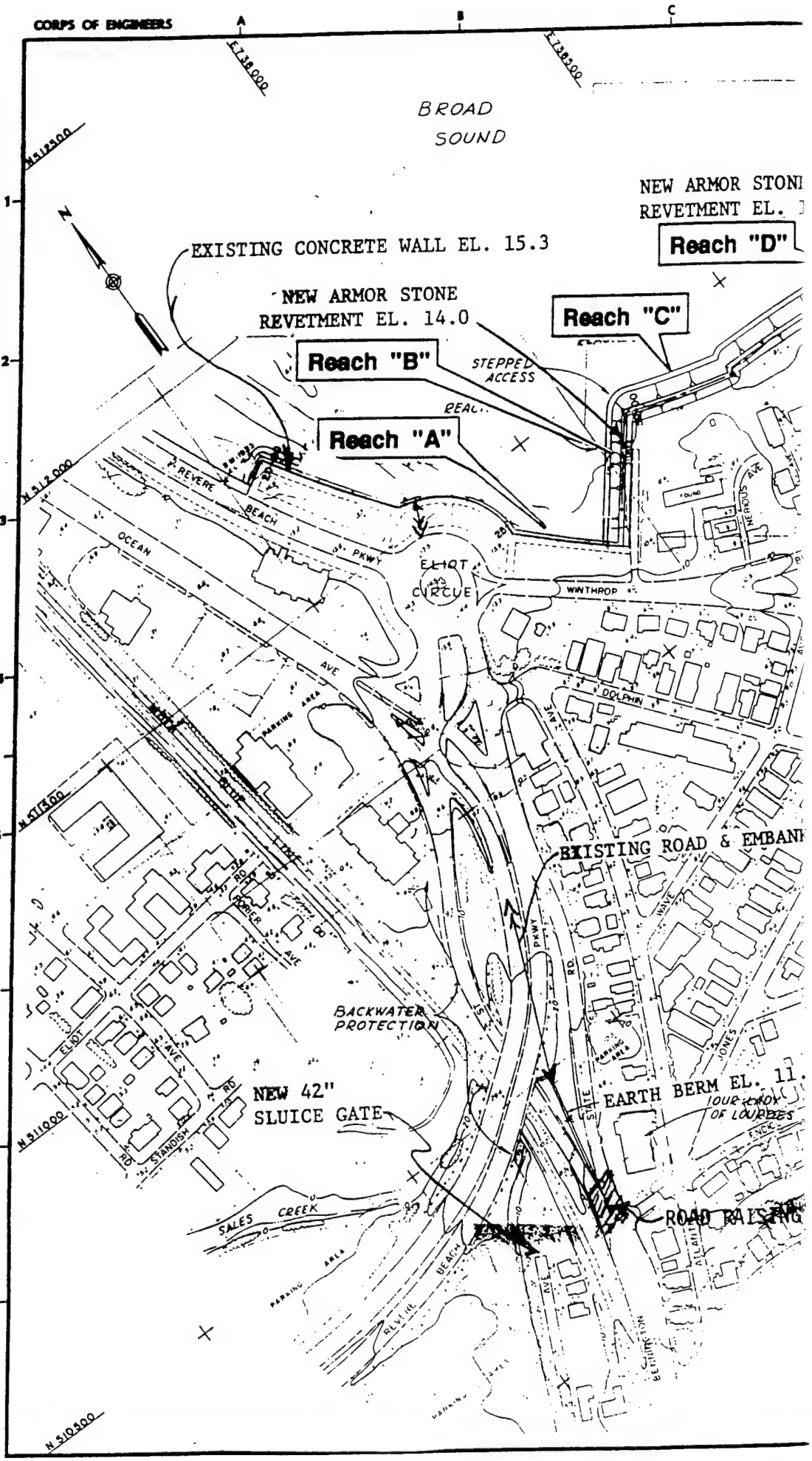
CORPS OF ENGINEERS
A
B
C
E 738000
E 738500
BROAD
SOUND
N 512500
N 512000
N 511500
N 511000
N 510500
NEW ARMOR STONE
REVETMENT EL.
Reach "D"
EXISTING CONCRETE WALL EL. 15.3
NEW ARMOR STONE
REVETMENT EL. 14.0
Reach "C"
Reach "B"
STEPPED
ACCESS
Reach "A"
REVERE
BEACH
PKWY
OCEAN
ELIOT
CIRCLE
WINTHROP
AVE
DOLPHIN
PARKING AREA
EXISTING ROAD & EMBANK
BACKWATER
PROTECTION
NEW 42"
SLUICE GATE
EARTH BERM EL. 11.
SALES
CREEK
ROAD RAISING

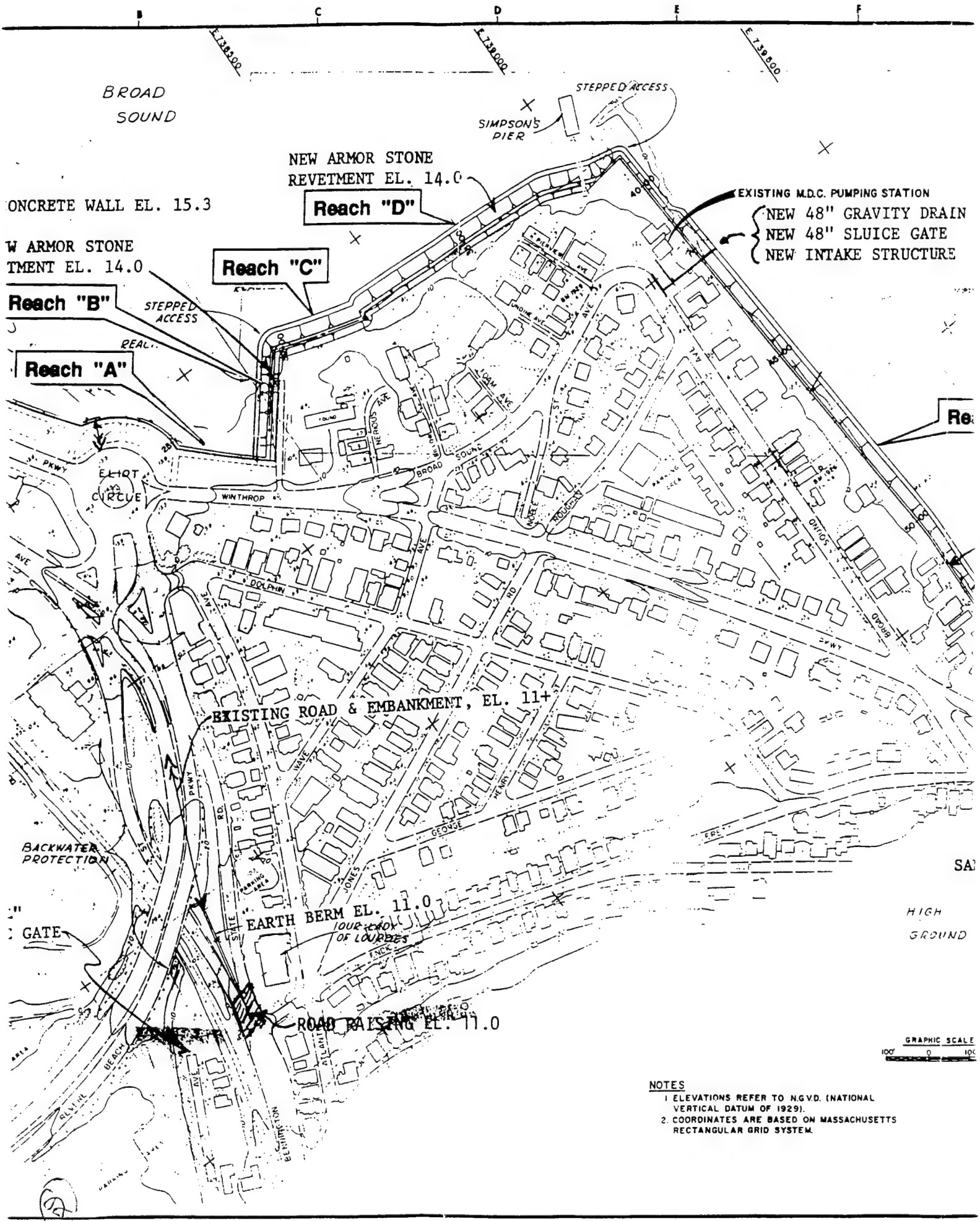
B
C
D
E
F
E 738300
E 739000
E 739800
BROAD SOUND
STEPPED ACCESS
SIMPSON'S PIER
NEW ARMOR STONE REVETMENT EL. 14.0
Reach "D"
EXISTING M.D.C. PUMPING STATION
NEW 48" GRAVITY DRAIN
NEW 48" SLUICE GATE
NEW INTAKE STRUCTURE
ONCRETE WALL EL. 15.3
W ARMOR STONE
TMENT EL. 14.0
Reach "C"
Reach "B"
STEPPED ACCESS
Reach "A"
ELIOT CIRCLE
WINTHROP
BROAD
EXISTING ROAD & EMBANKMENT, EL. 11+
BACKWATER PROTECTION
EARTH BERM EL. 11.0
GATE
ROAD RAISING EL. 11.0
HIGH GROUND
GRAPHIC SCALE
100' 0 100
NOTES
1 ELEVATIONS REFER TO N.G.V.D. (NATIONAL VERTICAL DATUM OF 1929).
2. COORDINATES ARE BASED ON MASSACHUSETTS RECTANGULAR GRID SYSTEM.

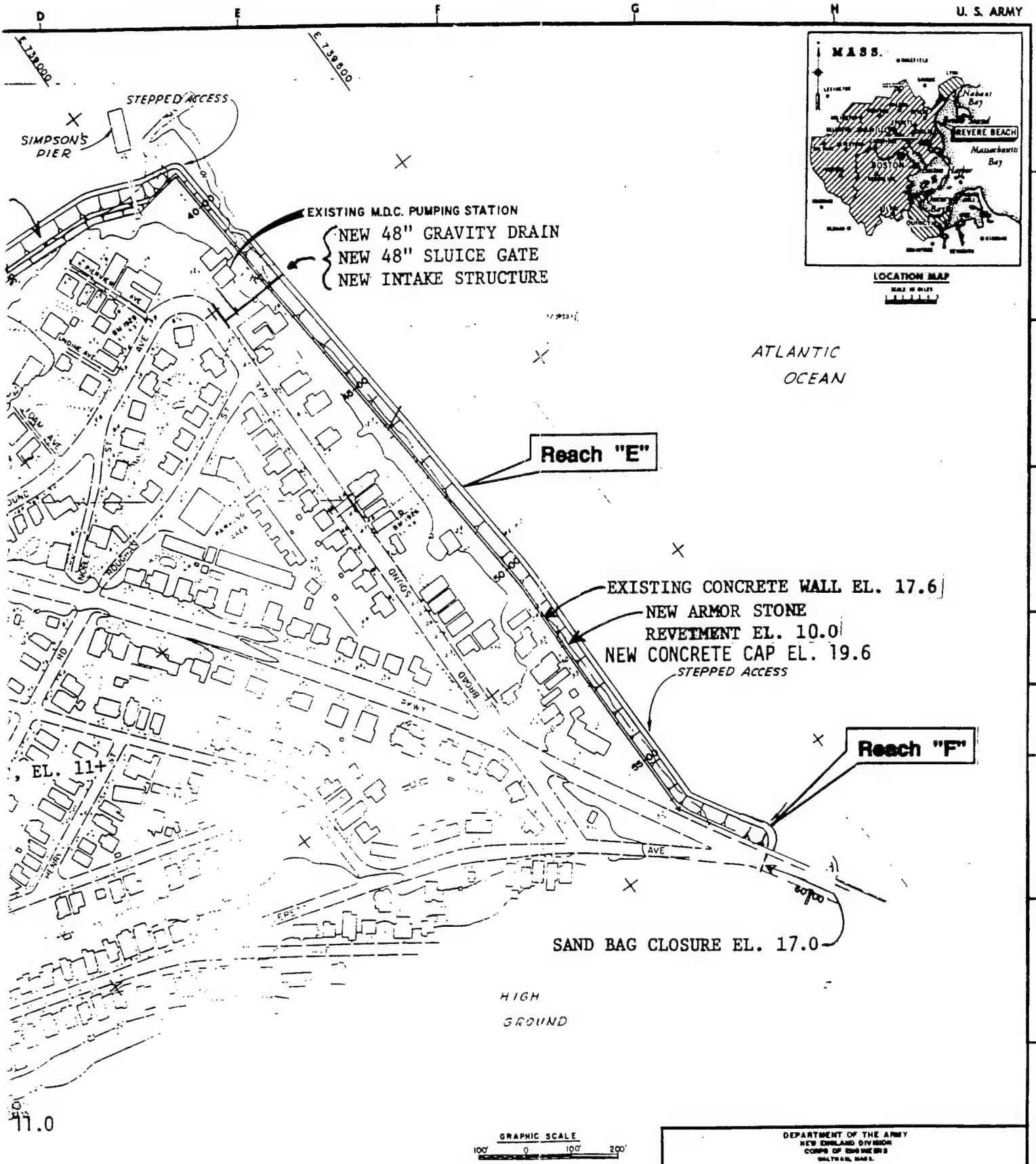
D
E
F
G
H
U. S. ARMY
E 739000
E 739500
STEPPED ACCESS
SIMPSON'S PIER
EXISTING M.D.C. PUMPING STATION
NEW 48" GRAVITY DRAIN
NEW 48" SLUICE GATE
NEW INTAKE STRUCTURE
MASS.
REVERE BEACH
Massachusetts Bay
BOSTON
LOCATION MAP
ATLANTIC OCEAN
Reach "E"
EXISTING CONCRETE WALL EL. 17.6
NEW ARMOR STONE REVETMENT EL. 10.0
NEW CONCRETE CAP EL. 19.6
STEPPED ACCESS
Reach "F"
EL. 11+
SAND BAG CLOSURE EL. 17.0
HIGH GROUND
11.0
GRAPHIC SCALE
100' 0 100' 200'
NOTES
1 ELEVATIONS REFER TO N.G.V.D. (NATIONAL VERTICAL DATUM OF 1929).
2. COORDINATES ARE BASED ON MASSACHUSETTS RECTANGULAR GRID SYSTEM.
DEPARTMENT OF THE ARMY
NEW ENGLAND DIVISION
CORPS OF ENGINEERS
WALTHAM, MASS.
REVERE COASTAL
FLOOD PROTECTION STUDY
MASSACHUSETTS
ROUGHANS POINT
GENERAL PLAN

Plate 2-1

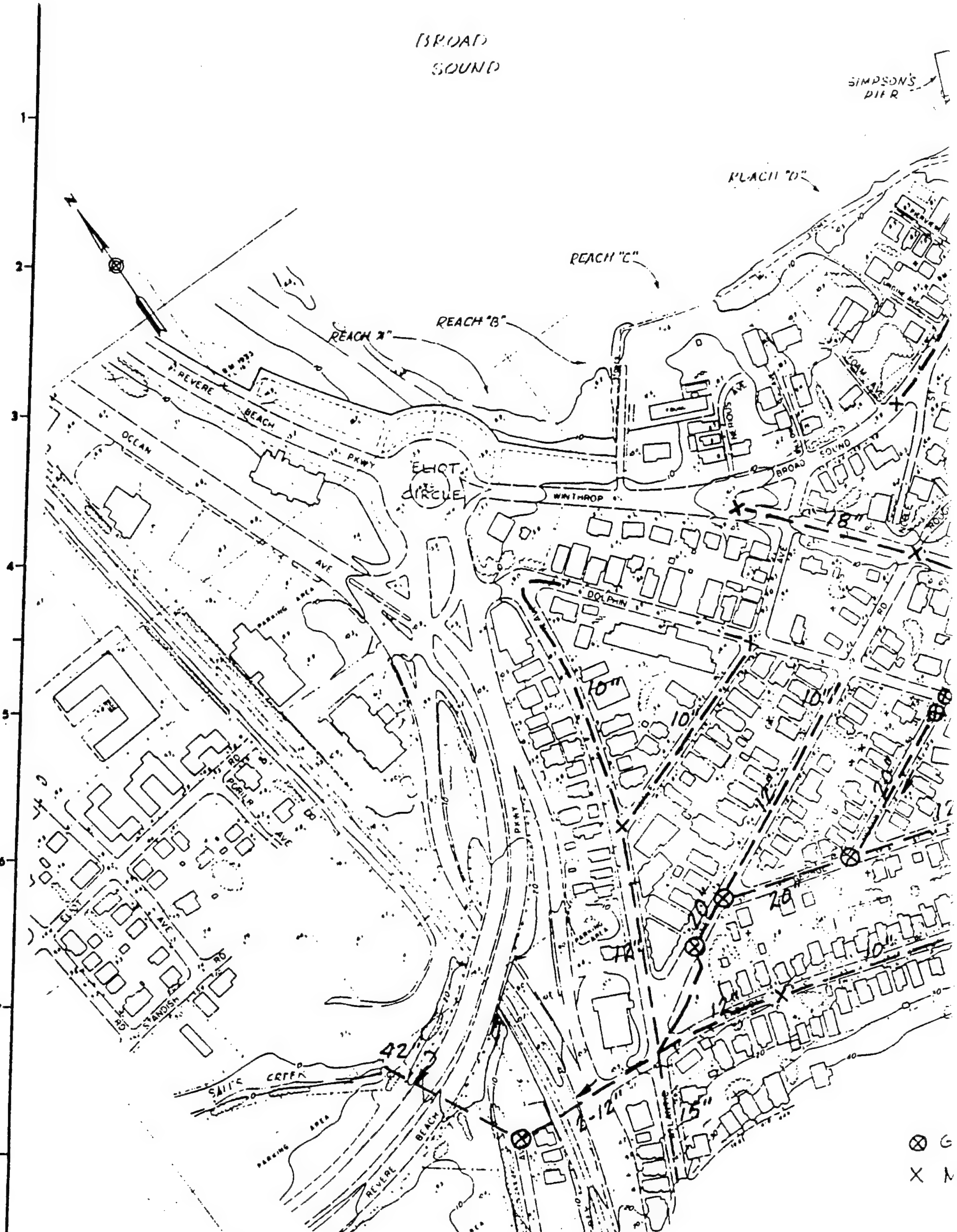
BROAD
SOUND
SIMPSON'S
PIER
REACH "D"
REACH "C"
REACH "B"
REACH "A"
REVERE BEACH PKWY
OCEAN AVE
ELIOT CIRCLE
WINTHROP
BROAD SOUND
DOLPHIN
STANDISH RD
SALT CREEK
REVERE BEACH
PARKING AREA
18"
10"
20"
12"
15"
42"
1
2
3
4
5
6
7
8

R 10/83


SIMPSON'S DIKE
REACH "D"
REACH "C"
EXISTING M.D.C. PUMPING STATION
30"
12"
42"
STREET SURFACE GRATED INLET
ATLA
REACH "E"
18"
12"
8"
54"
STEPPED ACCESS
REACH "F"
EXIST. TIDE GATE
HIGH GROUND
LEGEND
⊗ GRATED TOP MANHOLE
X MANHOLE
DATE OF PHOTOGRAPHY 2-7-84 CONTOUR INTERVAL 2FT
ROUG
EXISTING

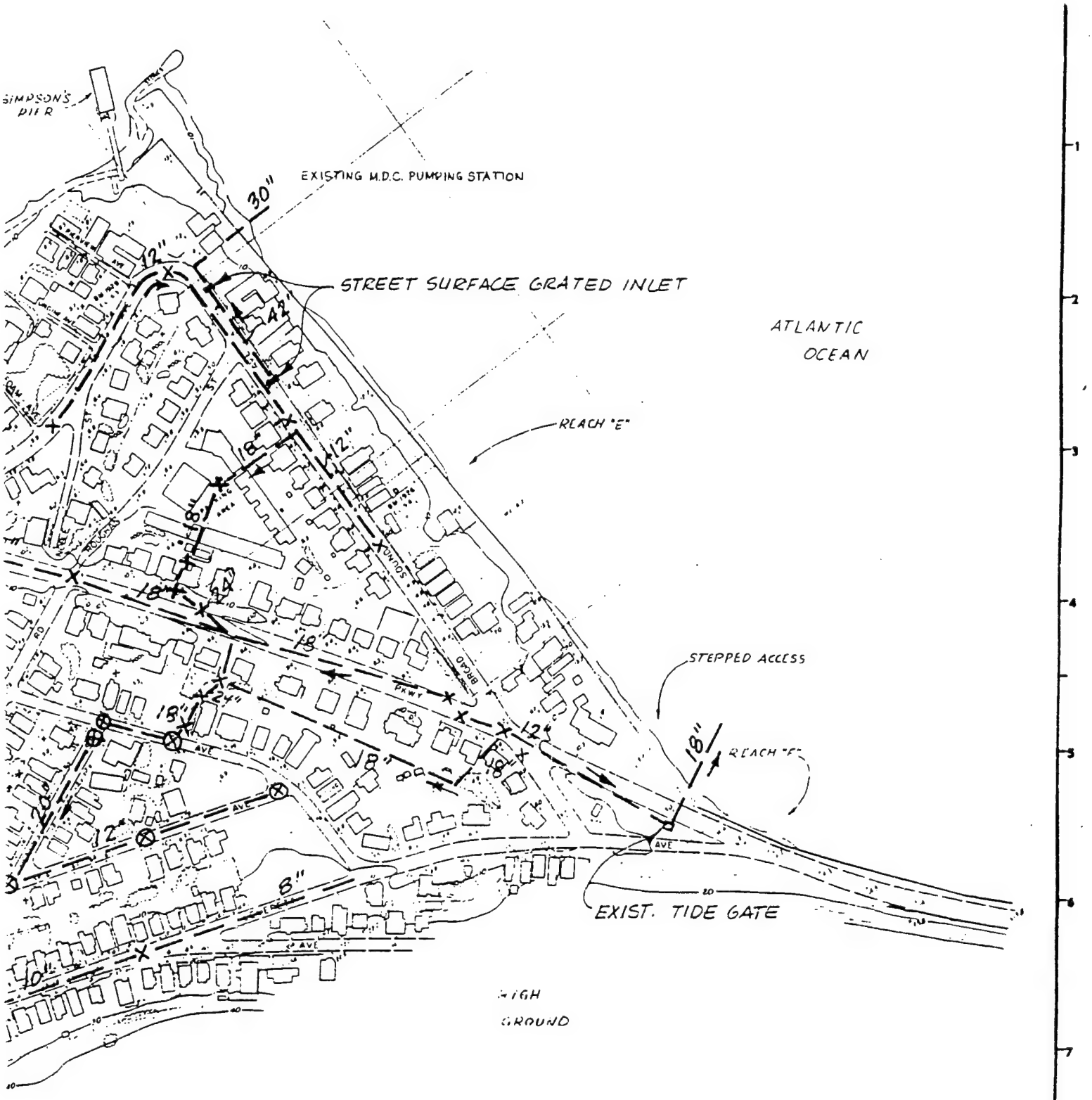

DEPARTMENT OF THE ARMY
NEW ENGLAND DIVISION
CORPS OF ENGINEERS
WALTHAM, MASS

REVERE COASTAL
FLOOD PROTECTION STUDY
MASSACHUSETTS

ROUGHAN'S POINT

EXISTING DRAINAGE SYSTEM

PLATE 2-2

3

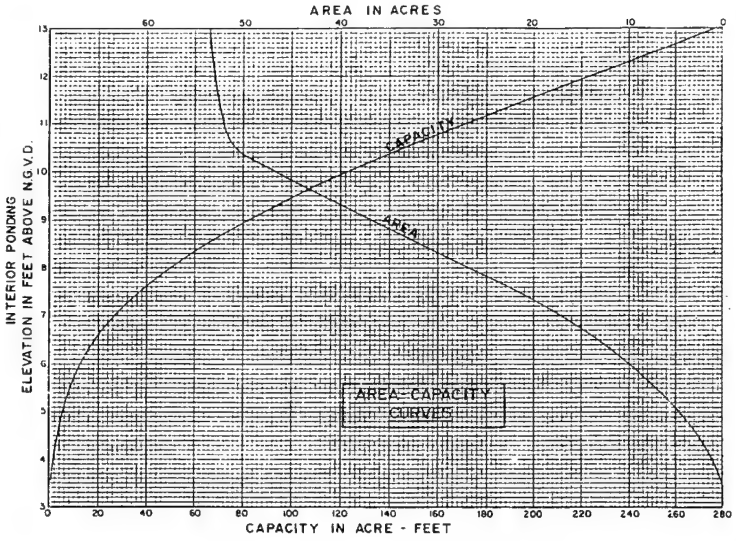

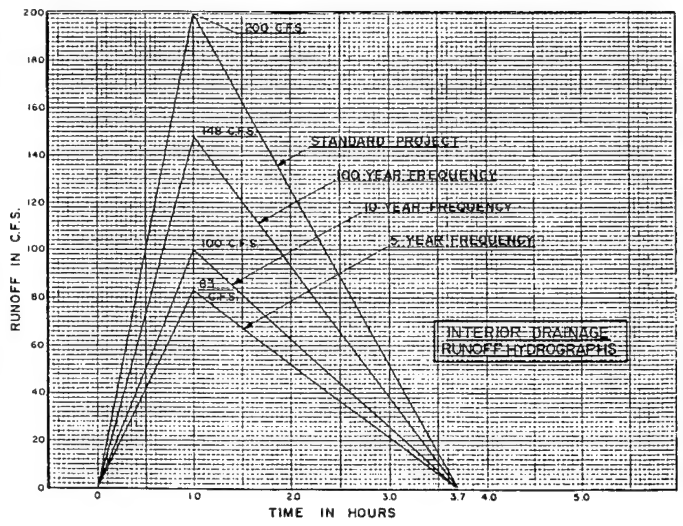

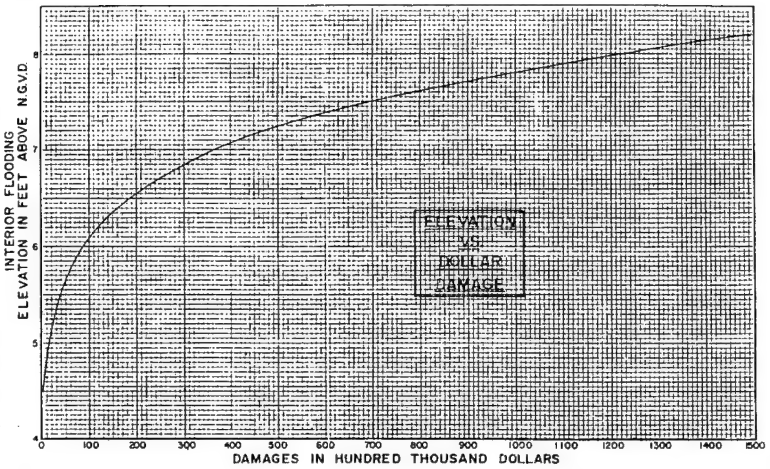

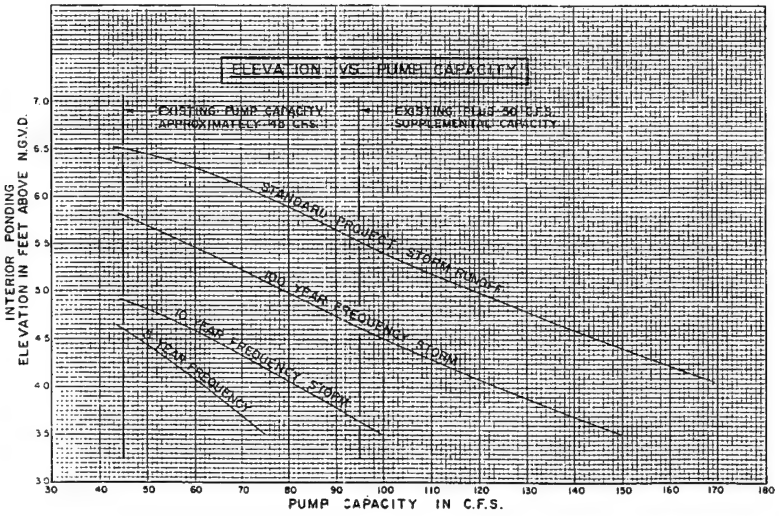

DEPARTMENT OF THE ARMY
NEW ENGLAND DIVISION
CORPS OF ENGINEERS
WALTHAM, MASS.

REVERE COASTAL
FLOOD PROTECTION STUDY
MASSACHUSETTS

ROUGHANS POINT

INTERIOR RUNOFF ANALYSIS

PLATE 2-3

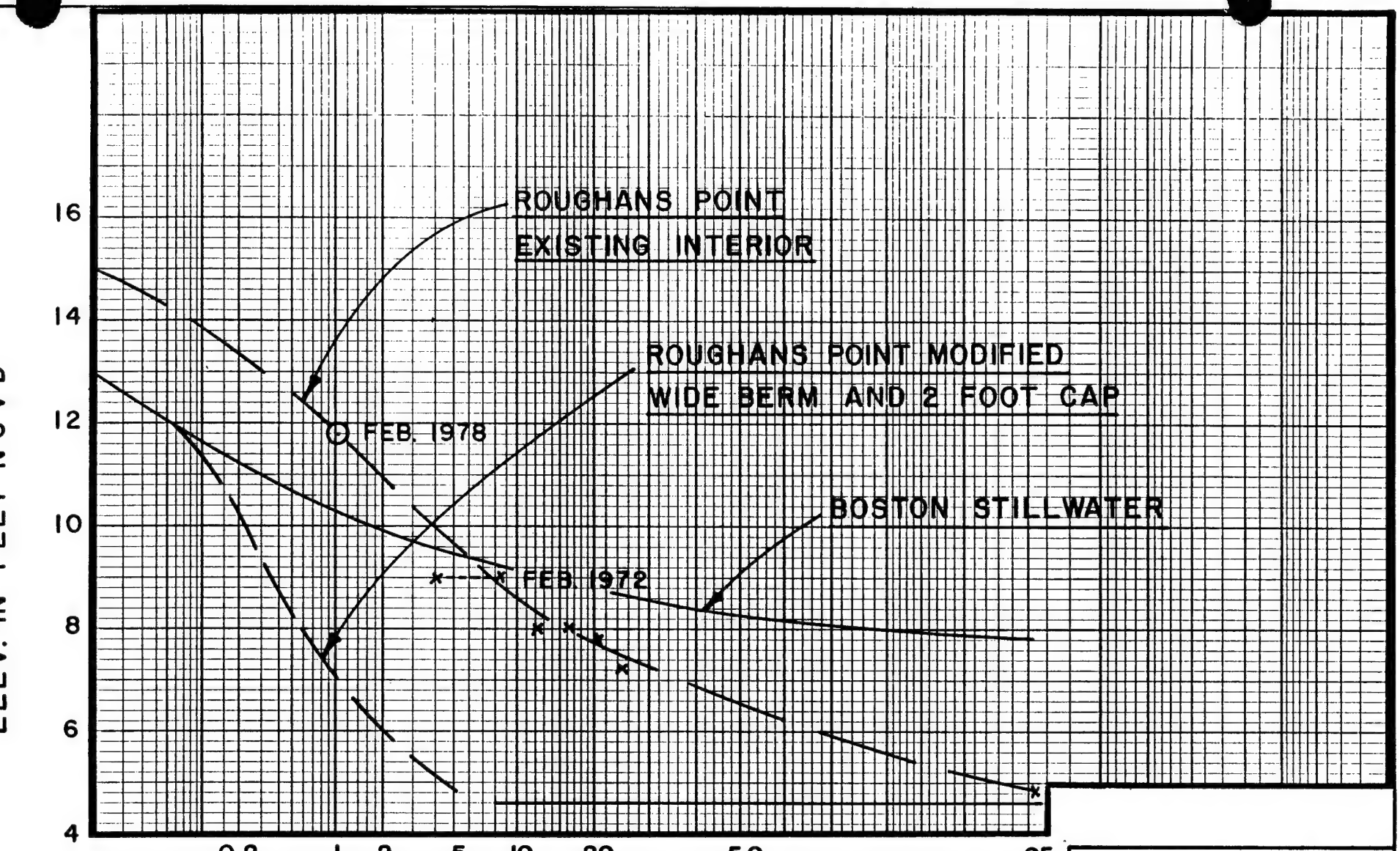

ROUGHANS POINT
REVERE, MASS.

STAGE FREQUENCY CURVES

HEB APR. 1991

PLATE 2-4

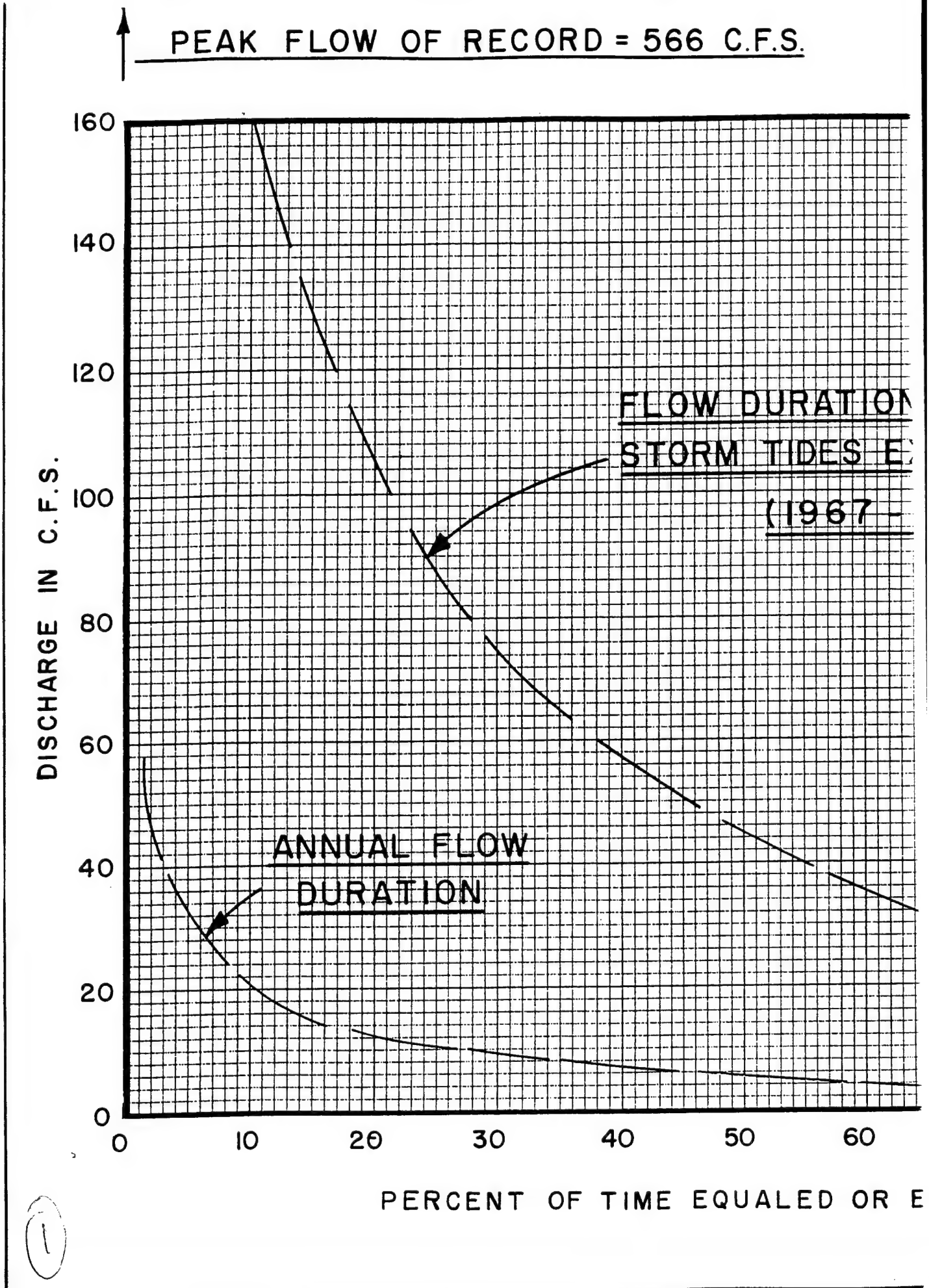
PEAK FLOW OF RECORD = 566 C.F.S.
160
140
120
100
80
60
40
20
0
DISCHARGE IN C.F.S.
FLOW DURATION
STORM TIDES E
(1967 -
ANNUAL FLOW
DURATION
0
10
20
30
40
50
60
PERCENT OF TIME EQUALED OR E

ECORD = 566 C.F.S.

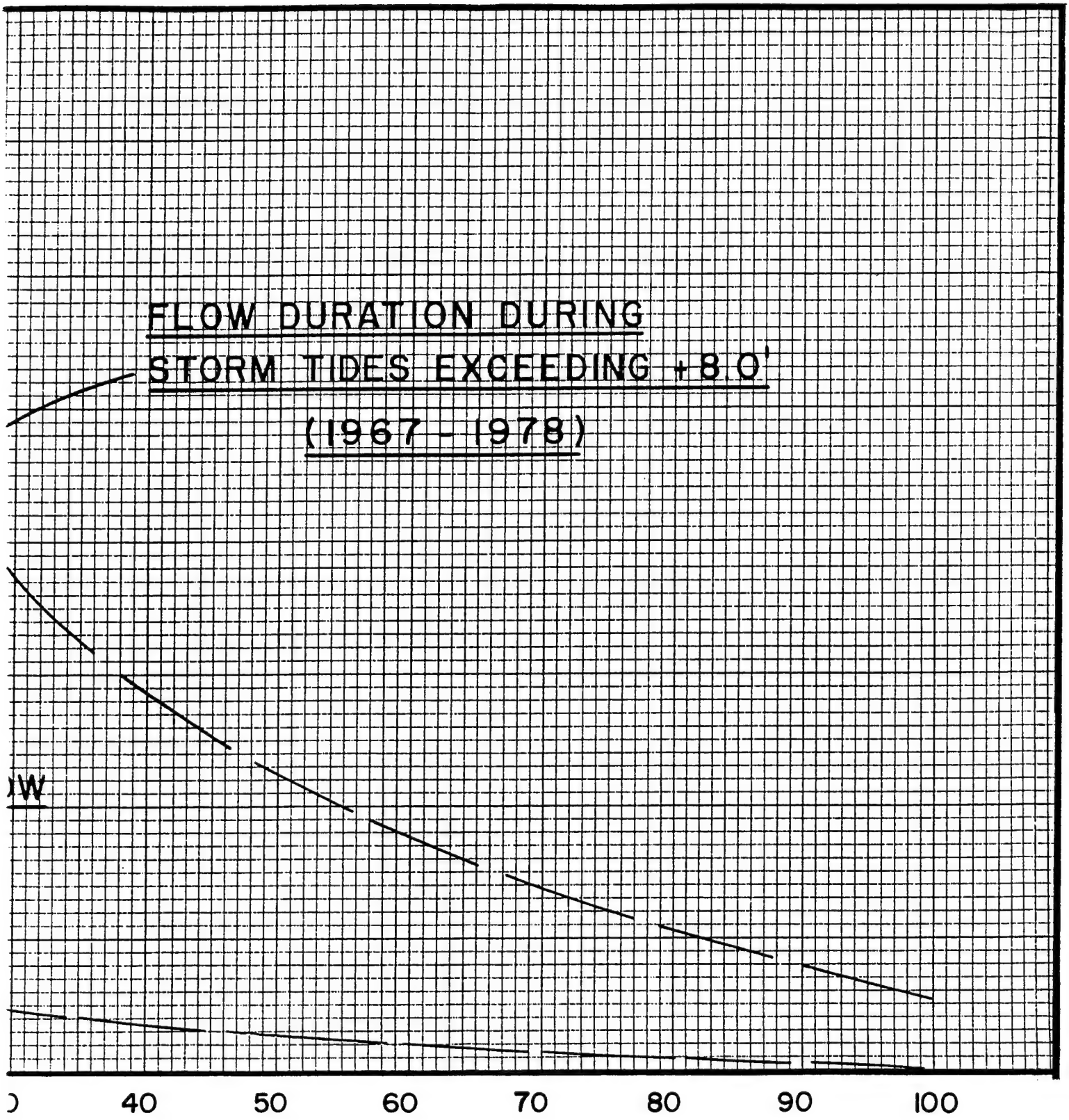

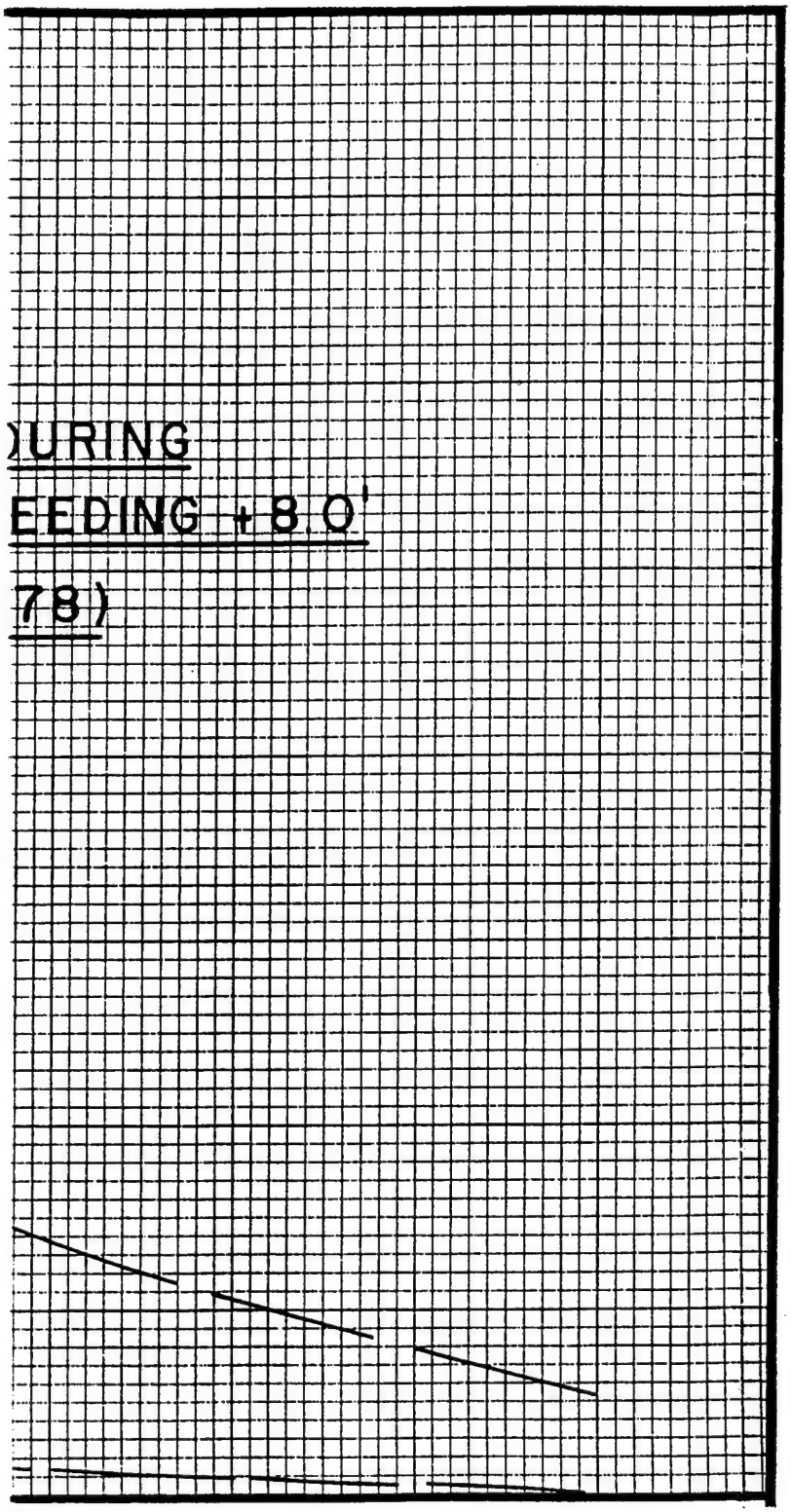

OLD SWAMP RIVER NR.
SO. WEYMOUTH, MASS.
D.A. = 4.5 SQ. MI.

NORMAL & HIGH TIDE FLOW DURATIONS

HYDRO. ENGR. APRIL 1991

PLATE 2-5

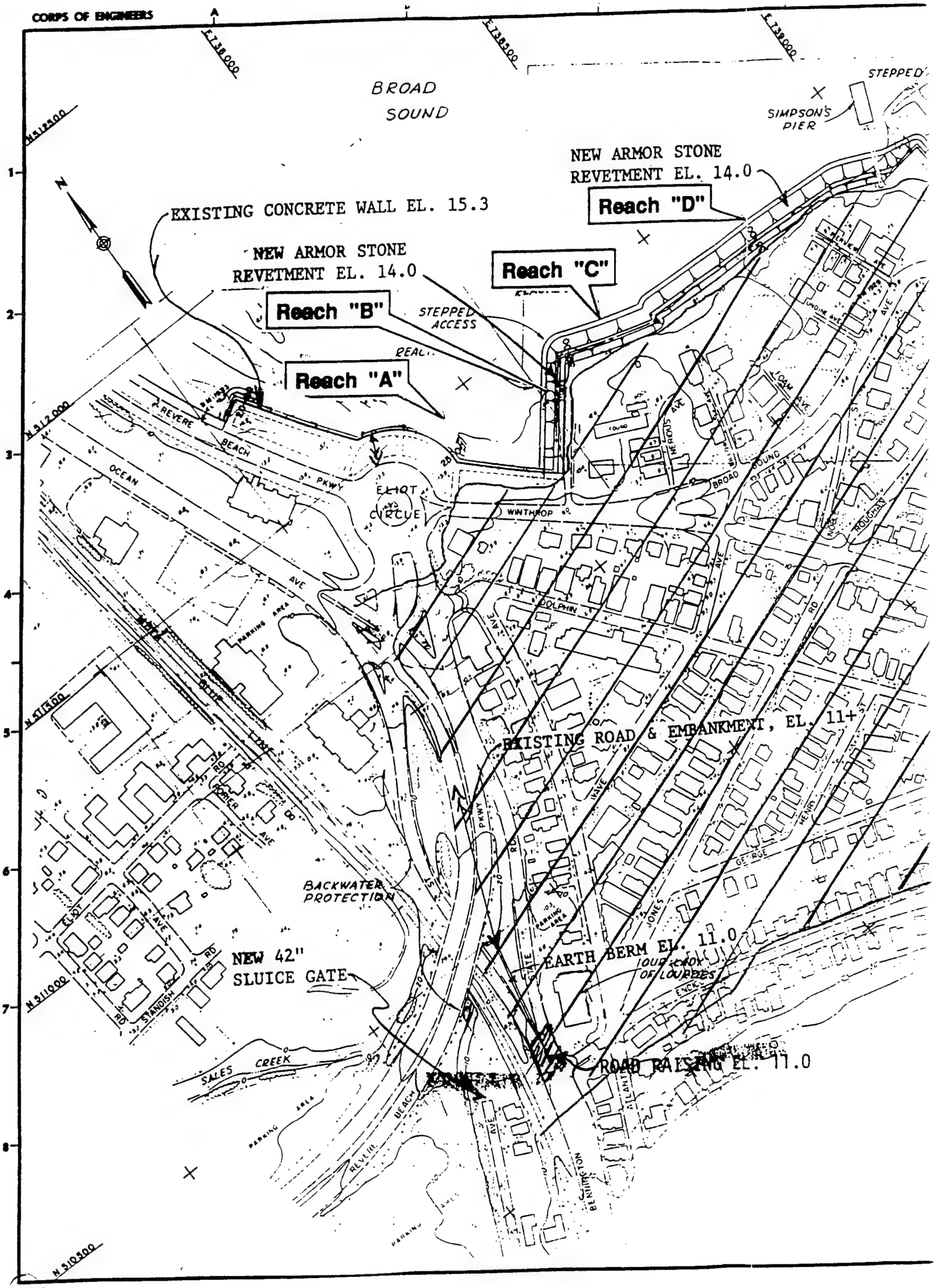
BROAD
SOUND
SIMPSON'S
PIER
STEPPED
NEW ARMOR STONE
REVETMENT EL. 14.0
Reach "D"
EXISTING CONCRETE WALL EL. 15.3
NEW ARMOR STONE
REVETMENT EL. 14.0
Reach "C"
Reach "B"
STEPPED
ACCESS
Reach "A"
REVERE
BEACH
PKWY
OCEAN
ELIOT
CIRCLE
WINTHROP
BROAD SOUND
DOLPHIN
PARKING AREA
EXISTING ROAD & EMBANKMENT, EL. 11+
BACKWATER
PROTECTION
NEW 42"
SLUICE GATE
EARTH BERM EL. 11.0
OUR LADY
OF LOURDES
ROAD RAISING EL. 11.0
SALES
CREEK
STANDISH
JONES
GEORGE
HENRY
BENNINGTON
REVERE
BEACH
PARKING AREA
N 512,000
N 511,500
N 511,000
N 510,500
E 738,000
E 738,500
E 739,000

1

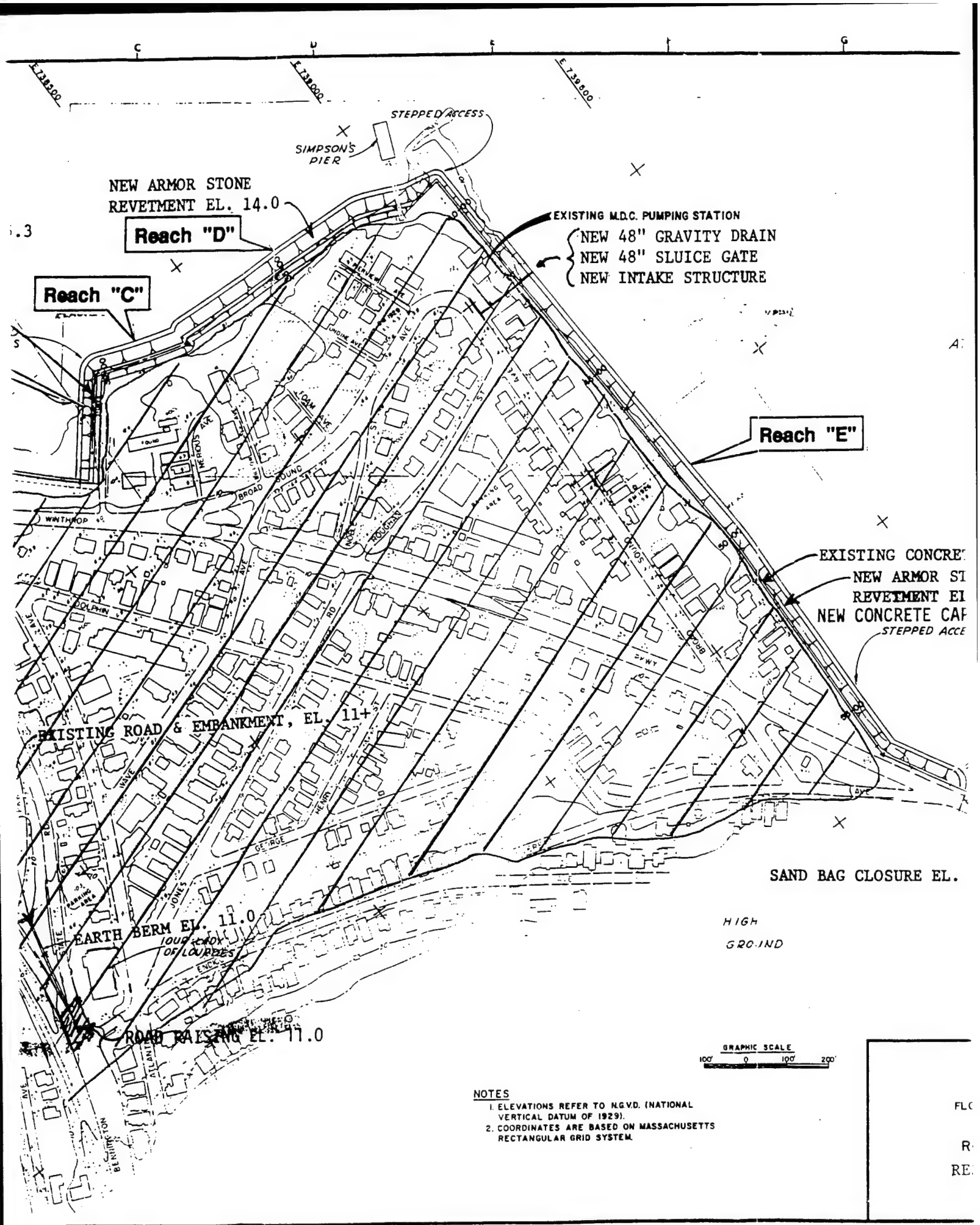
E 738000
E 739000
E 739000
STEPPED ACCESS
SIMPSON'S PIER
NEW ARMOR STONE REVETMENT EL. 14.0
Reach "D"
Reach "C"
EXISTING M.D.C. PUMPING STATION
NEW 48" GRAVITY DRAIN
NEW 48" SLUICE GATE
NEW INTAKE STRUCTURE
Reach "E"
EXISTING CONCRE
NEW ARMOR ST
REVETMENT EI
NEW CONCRETE CAI
STEPPED ACCE
EXISTING ROAD & EMBANKMENT, EL. 11+
SAND BAG CLOSURE EL.
HIGH GROUND
EARTH BERM EL. 11.0
ROAD RAISING EL. 11.0
GRAPHIC SCALE
100' 0 100' 200'
NOTES
1. ELEVATIONS REFER TO N.G.V.D. (NATIONAL VERTICAL DATUM OF 1929).
2. COORDINATES ARE BASED ON MASSACHUSETTS RECTANGULAR GRID SYSTEM.

U. S. ARMY

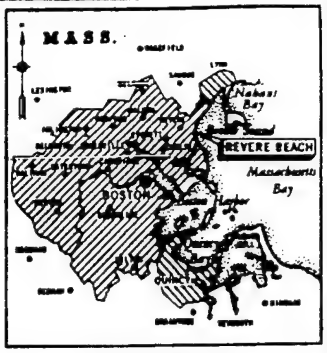

LOCATION MAP

STEPPED ACCESS

SIMPSON'S PIER

EXISTING M.D.C. PUMPING STATION
NEW 48" GRAVITY DRAIN
NEW 48" SLUICE GATE
NEW INTAKE STRUCTURE

ATLANTIC OCEAN

Reach "E"

EXISTING CONCRETE WALL EL. 17.6
NEW ARMOR STONE REVETMENT EL. 10.0
NEW CONCRETE CAP EL. 19.6

STEPPED ACCESS

Reach "F"

SAND BAG CLOSURE EL. 17.0

HIGH GROUND

GRAPHIC SCALE
100' 0 100' 200'

NOTES
1. ELEVATIONS REFER TO N.G.V.D. (NATIONAL VERTICAL DATUM OF 1929).
2. COORDINATES ARE BASED ON MASSACHUSETTS RECTANGULAR GRID SYSTEM.

DEPARTMENT OF THE ARMY
NEW ENGLAND DIVISION
CORPS OF ENGINEERS
WALTHAM, MASS.

REVERE COASTAL
FLOOD PROTECTION STUDY
MASSACHUSETTS

ROUGHANS POINT
RESIDUAL FLOODING
SPN

Plate 2-6

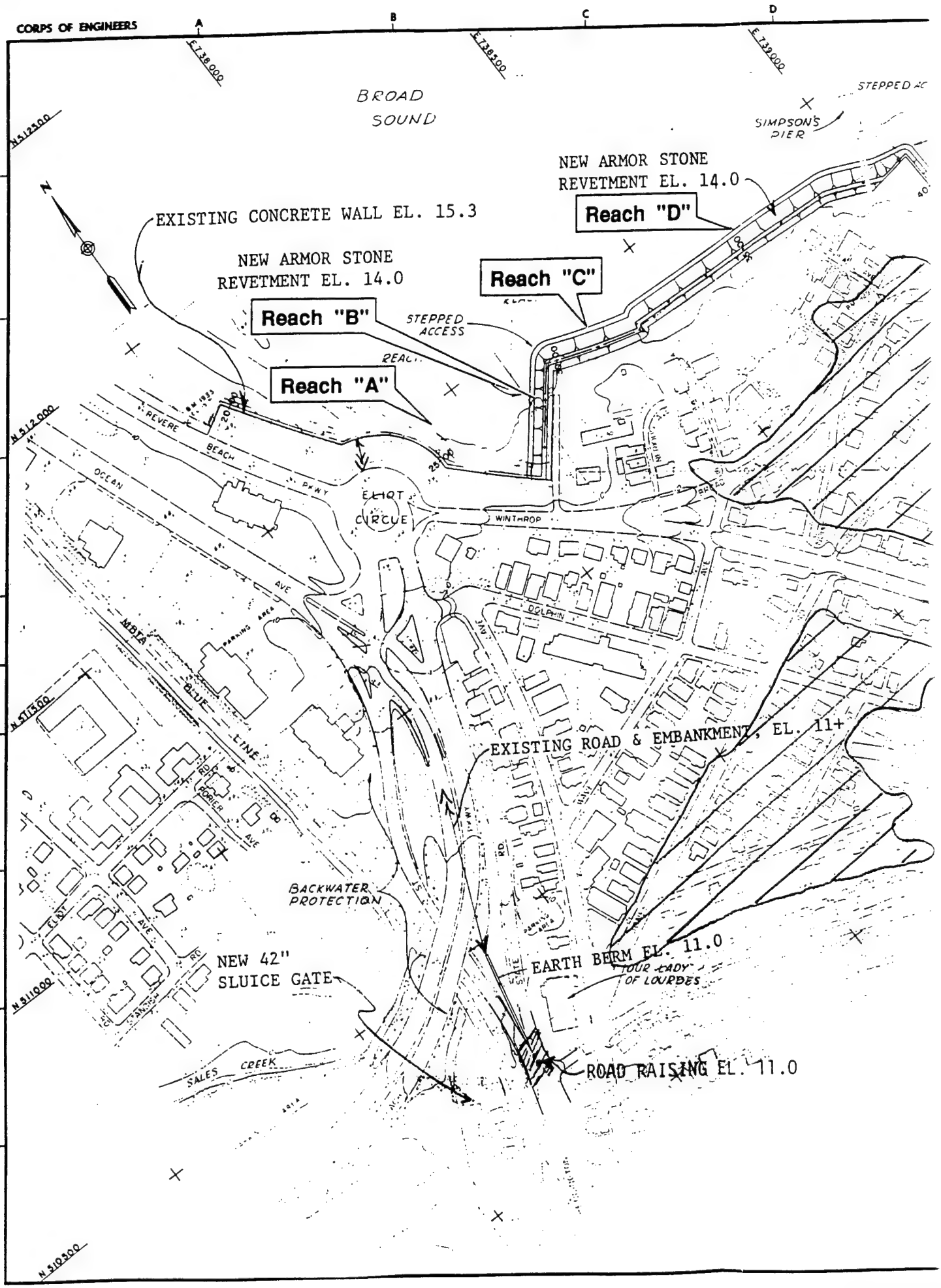
CORPS OF ENGINEERS
A
B
C
D
E 738,000
E 738,500
E 739,000
BROAD SOUND
STEPPED AC
SIMPSON'S PIER
N 512,500
N 512,000
N 511,500
N 511,000
N 510,500
NEW ARMOR STONE REVETMENT EL. 14.0
Reach "D"
EXISTING CONCRETE WALL EL. 15.3
NEW ARMOR STONE REVETMENT EL. 14.0
Reach "C"
Reach "B"
STEPPED ACCESS
Reach "A"
REVERE BEACH PKWY
OCEAN AVE
ELIOT CIRCLE
WINTHROP
DOLPHIN
MBTA
BLUE LINE
PARKING AREA
FORTER AVE
ELIOT AVE
EXISTING ROAD & EMBANKMENT, EL. 11+
BACKWATER PROTECTION
NEW 42" SLUICE GATE
EARTH BERM EL. 11.0
OUR LADY OF LOURDES
SALES CREEK
ROAD RAISING EL. 11.0

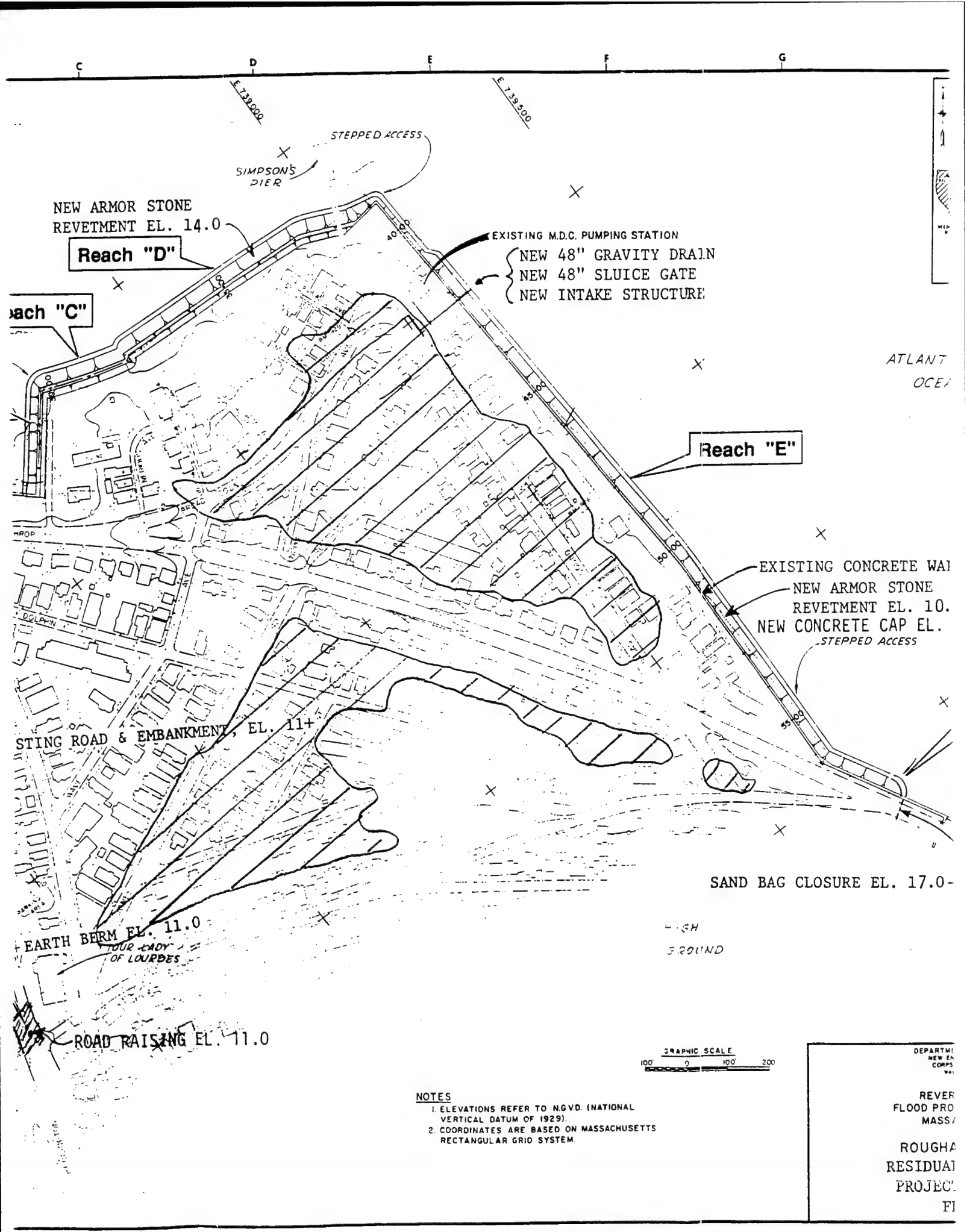
C
D
E
F
G
E 739000
E 739500
STEPPED ACCESS
SIMPSON'S PIER
NEW ARMOR STONE REVETMENT EL. 14.0
Reach "D"
EXISTING M.D.C. PUMPING STATION
NEW 48" GRAVITY DRAIN
NEW 48" SLUICE GATE
NEW INTAKE STRUCTURE
ach "C"
ATLANT
OCE
Reach "E"
EXISTING CONCRETE WAI
NEW ARMOR STONE REVETMENT EL. 10.
NEW CONCRETE CAP EL.
STEPPED ACCESS
STING ROAD & EMBANKMENT, EL. 11+
SAND BAG CLOSURE EL. 17.0-
EARTH BERM EL. 11.0
OUR LADY OF LOURDES
ROAD RAISING EL. 11.0
GRAPHIC SCALE
100' 0 100' 200
NOTES
1. ELEVATIONS REFER TO N.G.V.D. (NATIONAL VERTICAL DATUM OF 1929).
2. COORDINATES ARE BASED ON MASSACHUSETTS RECTANGULAR GRID SYSTEM.
REVER
FLOOD PRO
MASS
ROUGHA
RESIDUAI
PROJEC
FI

U. S. ARMY

D E F G H

E 739000

E 739500

STEPPED ACCESS

SIMPSON'S PIER

EXISTING M.D.C. PUMPING STATION

NEW 48" GRAVITY DRAIN

NEW 48" SLUICE GATE

NEW INTAKE STRUCTURE

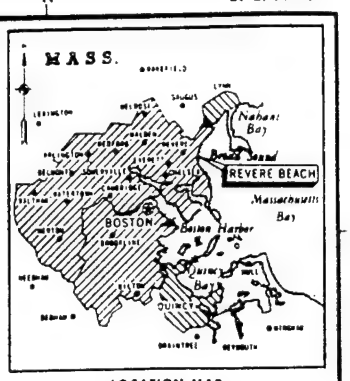

LOCATION MAP

ATLANTIC OCEAN

Reach "E"

EXISTING CONCRETE WALL EL. 17.6

NEW ARMOR STONE REVETMENT EL. 10.0

NEW CONCRETE CAP EL. 19.6

STEPPED ACCESS

Reach "F"

SAND BAG CLOSURE EL. 17.0

EL. 11.0

GRAPHIC SCALE

100' 0 100' 200'

NOTES

1. ELEVATIONS REFER TO N.G.V.D. (NATIONAL VERTICAL DATUM OF 1929).
2. COORDINATES ARE BASED ON MASSACHUSETTS RECTANGULAR GRID SYSTEM.

DEPARTMENT OF THE ARMY
NEW ENGLAND DIVISION
CORPS OF ENGINEERS
WALTHAM, MASS

REVERE COASTAL FLOOD PROTECTION STUDY
MASSACHUSETTS

ROUGHANS POINT
RESIDUAL FLOODING
PROJECT DESIGN
FLOOD

Plate 2-7

APPENDIX A

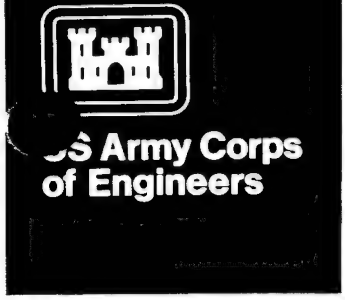

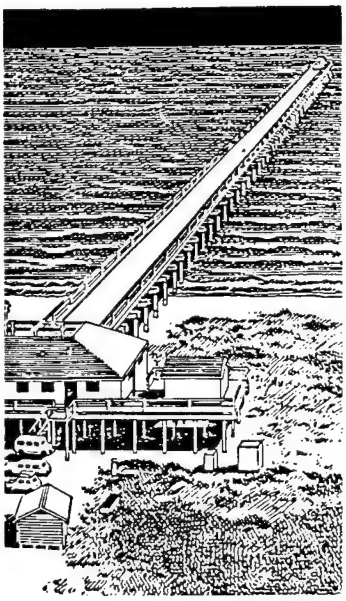

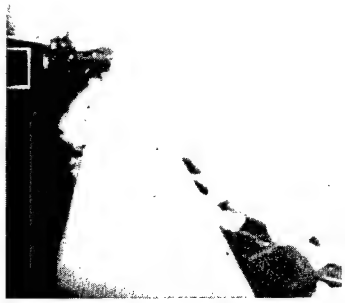

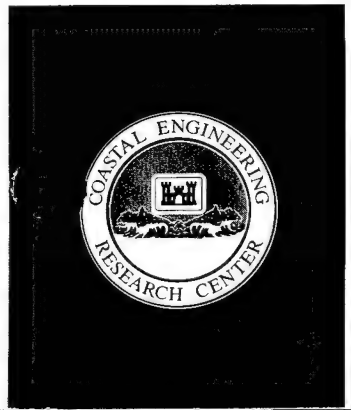

TECHNICAL REPORT CERC-86-7

IRREGULAR WAVE OVERTOPPING OF SEAWALL/REVETMENT CONFIGURATIONS, ROUGHANS POINT, MASSACHUSETTS

Experimental Model Investigation

by

John P. Ahrens, Martha S. Heimbaugh, D. D. Davidson

Coastal Engineering Research Center

DEPARTMENT OF THE ARMY
Waterways Experiment Station, Corps of Engineers
PO Box 631, Vicksburg, Mississippi 39180-0631

September 1986
Final Report

Prepared for

US Army Engineer Division, New England
Waltham, Massachusetts 02254-9149

10. PROJECT NO. (Continued)

Intra-Army Order No. 84-C-0031.

PREFACE

The US Army Engineer Division, New England (NED), requested the US Army Engineer Waterways Experiment Station (WES) Coastal Engineering Research Center (CERC) to conduct numerical and physical model studies to determine flood levels at Roughans Point, Massachusetts. Funding authorizations by NED were granted in Intra-Army Order No. 84-C-0031, dated 1 May 1984.

Physical model tests were conducted at CERC under general direction of Dr. R. W. Whalin, former Chief, CERC; Mr. C. E. Chatham, Chief, Wave Dynamics Division; and Mr. D. D. Davidson, Chief, Wave Research Branch. Tests were conducted by Messrs. Cornelius Lewis, Sr., Engineering Technician, and John Heggins, Computer Technician, under the supervision of Mr. John P. Ahrens, Oceanographer. This report was prepared by Mr. Ahrens, Mr. Davidson, and Ms. Martha S. Heimbaugh, Civil Engineer. Dr. James R. Houston was Chief and Mr. Charles C. Calhoun, Jr., was Assistant Chief, CERC, during the preparation and publication of this report. This report was edited by Ms. Shirley A. J. Hanshaw, Information Products Division, Information Technology Laboratory, WES.

Liaison was maintained with Mr. Charles Wener, Chief of NED's Hydraulics and Water Quality Section (HWQS), during the course of this study by means of conferences, progress reports, and telephone conversations. Mr. Donald Wood of the HWQS staff was sent to WES to assist in model testing and data analysis for a temporary assignment.

COL Allen F. Grum, USA, was the previous Director of WES. COL Dwayne G. Lee, CE, is the present Commander and Director. Dr. Robert W. Whalin is Technical Director.

CONTENTS

LIST OF FIGURES

CONVERSION FACTORS, NON-SI TO SI (METRIC)
UNITS OF MEASUREMENT

Non-SI units of measurement used in this report can be converted to SI (metric) units as follows:

Multiply	By	To Obtain
acres	4046.873	square meters
cubic feet per second per foot	0.929	cubic meters per second per meter
feet	0.3048	meters
inches	2.54	centimeters
miles (US statute)	1.609347	kilometers
pounds (mass)	0.4535924	kilograms
pounds (mass) per cubic foot	16.01846	kilograms per cubic meter
square feet	0.09290304	square meters
tons (2,000 lb, mass)	907.1847	kilograms

IRREGULAR WAVE OVERTOPPING OF SEAWALL/REVETMENT CONFIGURATIONS, ROUGHANS POINT, MASSACHUSETTS

Experimental Model Investigation

PART I: INTRODUCTION

Background

1. This report discusses laboratory model tests of irregular wave overtopping for seawall and revetment configurations being considered for use at Roughans Point, Massachusetts (Figure 1). The tests were initiated by US Army Engineer Division, New England (NED), because of a lack of confidence in their wave overtopping estimates made by using the Shore Protection Manual (SPM) (1984). Roughans Point is a 55-acre* residential area which is partially protected from coastal flooding by seawalls on both its northern and eastern boundaries. The Roughans Point interior suffers damage from frequent flooding caused by the overtopping of seawalls. Laboratory tests discussed in this report were part of a more comprehensive study which included extensive use of computer models to calculate the frequency of occurrence of flood water levels for the interior of Roughans Point, along the open coast to the north, and for estuarine areas along the Saugus-Pines River system. The physical model tests provided wave overtopping coefficients only for the various seawall/revetment configurations used in the numerical flood routing model for the interior of Roughans Point. Water level calculations for the coastline north of Roughans Point and the estuarine areas did not include consideration of wave overtopping. For further information about the computer models and the organization of the entire study see Hardy and Crawford (in preparation). The model tests described in this report were conducted primarily to develop methods to reduce wave overtopping of the eastern seawall (Figure 2, Reach E), to determine objective criteria for judging the effectiveness of the methods to reduce overtopping, and to provide wave overtopping coefficients to the numerical flood routing model.

---

* A table of factors for converting non-SI to SI (metric) units is presented on page 3.

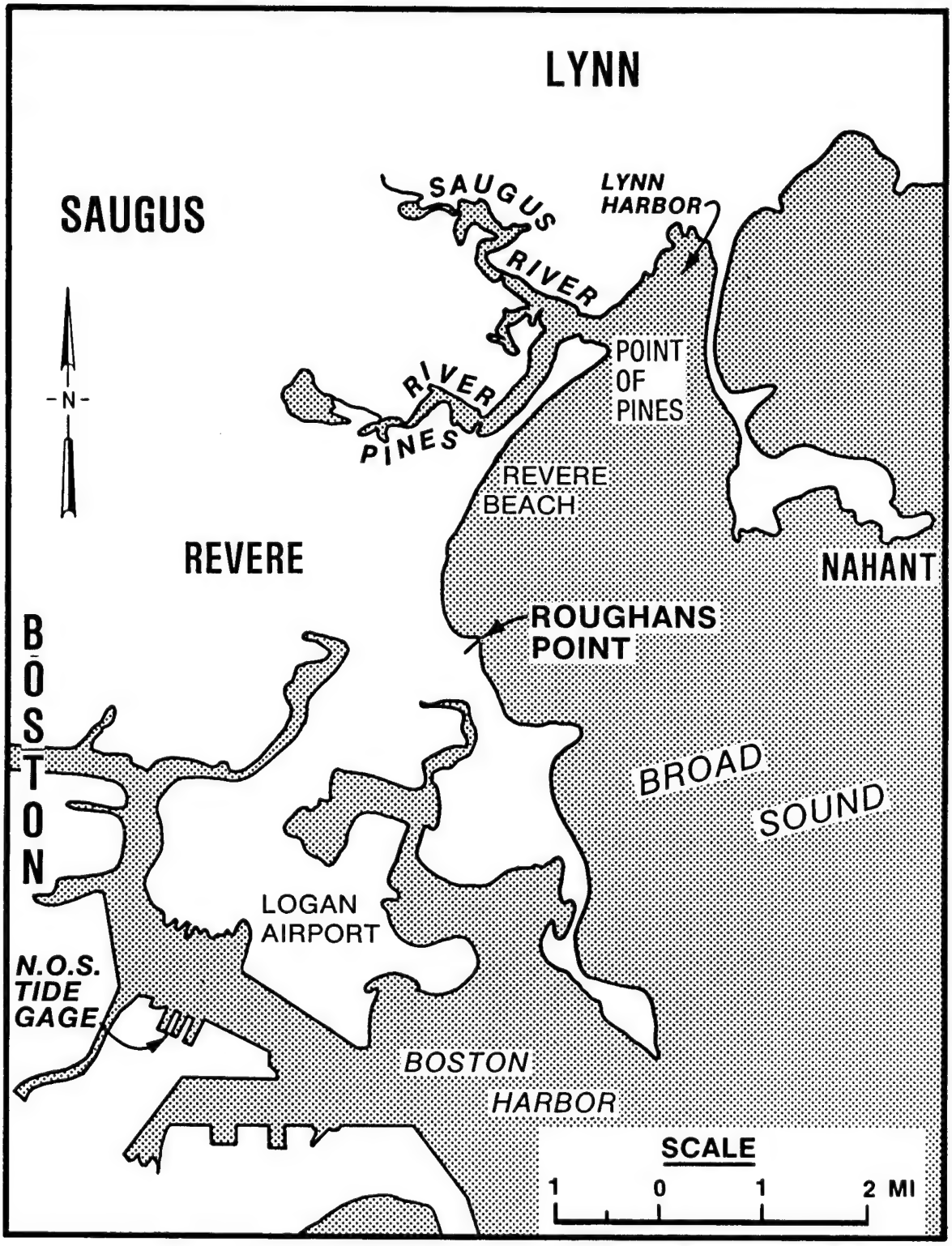

Figure 1. Location and vicinity map

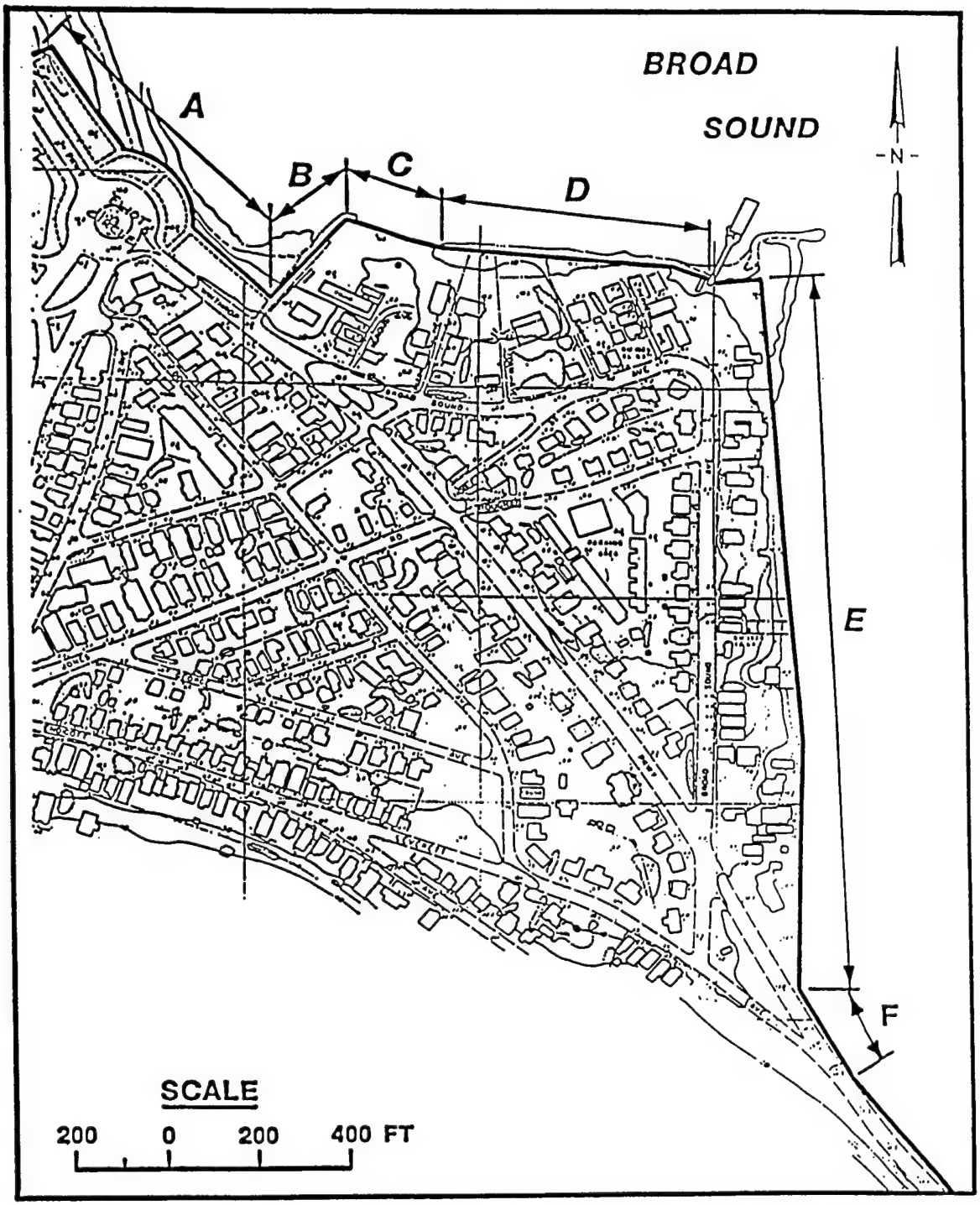

Figure 2. Location of Reaches A through F at Roughans Point

2. A number of different revetment configurations were constructed in front of the Roughans Point seawall, and the wall crest elevation was varied to determine their ability to reduce wave overtopping of the wall. Results of this effort have yielded specific information to help solve the Roughans Point site-specific problem and general information which will help to improve current techniques for calculating irregular wave overtopping rates given in the SPM (1984). A simple way to quantify the overtopping potential of the various seawall/revetment configurations is presented.

Purpose

3. The purposes of this two-dimensional (2-D) wave overtopping study were to:

a. Evaluate the effectiveness of 10 proposed seawall/revetment configurations at reducing wave overtopping of the Roughans Point seawall.

b. Determine a simple method to predict wave overtopping of the Roughans Point seawall.

PART II: THE MODEL

Model Design

4. Model tests were conducted in a wave tank 3 by 3 by 150 ft long. This tank had a hydraulically actuated piston wave blade which was controlled by an Automatic Data Aquisition Control System (ADACS) computer. In order to reduce scale effects, the largest scale consistent with the available facilities was used. The undistorted Froude scale used was 1:16 (model:prototype). Although this study was primarily concerned with overtopping rates for various seawall/revetment configurations, armor stone size distributions for the model revetments were carefully determined to correspond with prototype sizes designed by NED in their planning studies (NED 1982). Based on Froude's Model law (Stevens 1942) and the linear scale of 1:16, the following model-to-prototype relations were derived (dimensions are in terms of length (L) and time (T)):

Characteristic	Dimension	Model-to-Prototype Scale Relations
Length	L	L_r = 1:16
Area	L^2	A_r^2 = 1:256
Volume	L^3	$V_r = L_r^3$ = 1:4,096
Time	T	$T_r = L_r^{1/2}$ = 1:4

5. The specific weight of fresh water used in the model was assumed to be 62.4 pcf and that of seawater 64.0 pcf. The specific weight of armor stone used in the model and that proposed for the prototype was 165 pcf. These variables are related using the following transference equation:

$$\frac{(W_a)_m}{(W_a)_p} = \frac{(\gamma_a)_m}{(\gamma_a)_p} \left(\frac{L_m}{L_p}\right)^3 \left[\frac{(S_a)_p - 1}{(S_a)_m - 1}\right]^3$$

where

W_a = weight of an individual armor stone, lb

m, p = model-to-prototype quantities, respectively

γ_a = specific weight of an individual armor stone, pcf

L_m/L_p = linear scale of model

S_a = specific gravity of an individual armor stone relative to the water in which the breakwater is constructed, i.e., $S_a = \gamma_a/\gamma_w$

γ_w = specific weight of water, pcf

Model armor stone sizes ranged from 0.38 to 0.70 lb with a median weight of 0.55 lb for all configurations tested except one, Configuration 9, which used armor stone ranging from 0.593 to 1.431 lb with a median weight of 1.0185 lb. Applying the above transference equation, the equivalent range of weights tested was from 1,745 to 3,255 lb in the prototype, with a median weight of 2,551 lb prototype, and from 2,747 to 6,629 lb in the prototype, with a median weight of 4,718 lb, respectively.

Model Conditions and Testing Procedures

Wave tank calibration

6. A 1V on 100H slope was selected as representative of the Roughans Point bathymetry seaward of the eastern seawall. Using this bathymetry, wave conditions in the wave tank were measured at various locations using parallel wire resistance wave gages but without any seawall/revetment plan in place. Figure 3 shows the location of the gages. This setup allowed calibration of the wave tank apparatus without significant wave reflections, which is analogous to wave forecast by hindcast procedures.

7. During the initial tests of Configuration 1 (vertical seawall with no fronting revetment) severe wave reflections were created in the tank because of the vertical wall. To eliminate this reflection, the tank was divided into two sections, one containing the test structure and the other containing a wave absorber to reduce the unnatural wave tank reflections. Figures 4 and 5 show plan and profile views of the partitioned sections of the wave tank for the final tests conducted on Configuration 1. Dividing of the tank significantly reduced the wave tank reflections for all test conditions; thus, it was decided Gage 7 in the wave absorber channel could be used to measure the incident wave conditions rather than depend on the original calibration data. Gage 7 was used to measure the incident zero-moment wave height H_{mo}, but the period of peak energy density T_p was assummed on the basis of

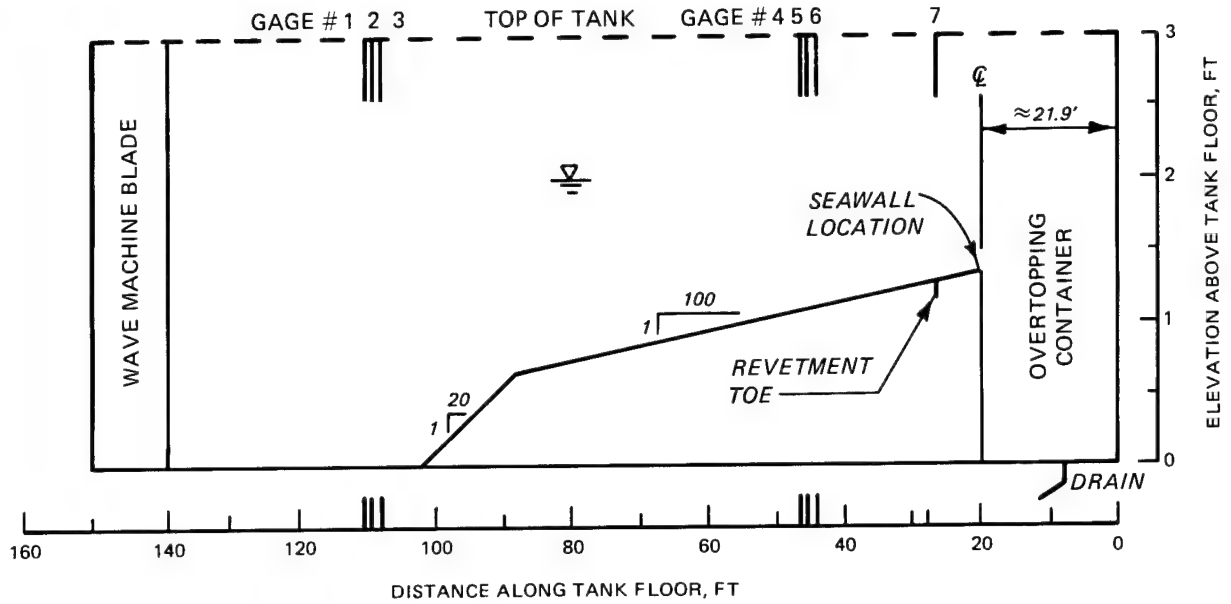

Figure 3. Wave gage location in 3- by 3- by 150-ft-long wave tank

conservation of wave period to be the period that was programmed to be generated by the wave machine and therefore will be referred to as the nominal T_p .

Test conditions

8. A wide range of wave conditions was represented in these tests. The periods of peak energy density T_p tested were 5, 7, 8, 9, 10, and 12 sec in the prototype. The still-water levels (swl) tested ranged between about +8.58 and +10.80 ft National Geodetic Vertical Datum (NGVD). The tests produced local zero-moment wave heights ranging from about 2.5 to 9.0 ft with most heights in the 5- to 8-ft range. Tabulated test conditions and data results are given in Appendix A.

Test procedures

9. During a single test run, irregular waves were generated continuously for 33 min. The ADACS was programmed to produce a modified Joint North Sea Wave Program (JONSWAP) wave spectrum for the water depth at the wave blade. Water depths at the wave blade ranged from about 32.0 to 35.0 ft. JONSWAP spectra tend to be rather narrow (Hasselmann et al. 1973), in that a large portion of the total energy is concentrated near the frequency associated with the period of peak energy density T_p . Since wave shoaling and breaking were very conspicuous between the wave blade and structure for most

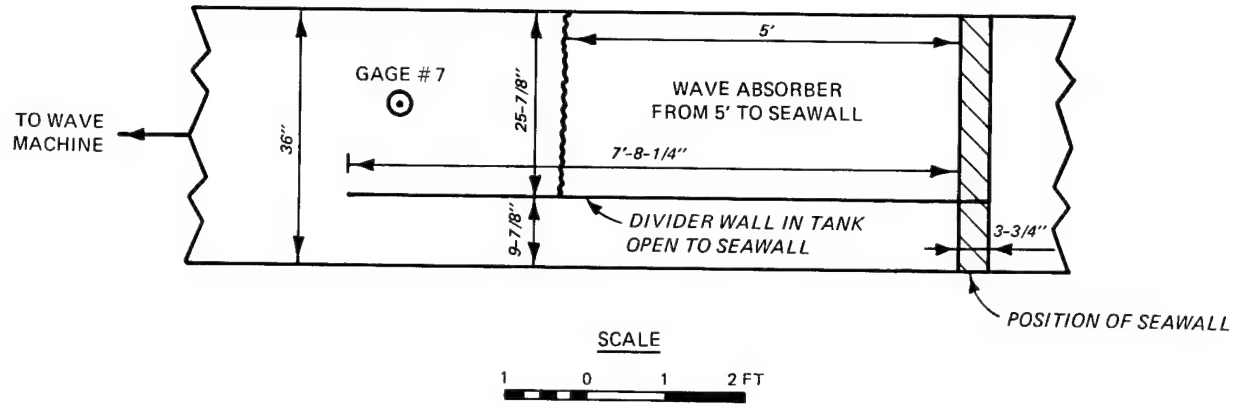

Figure 4. Plan view of Configuration 1, seawall with no fronting revetment

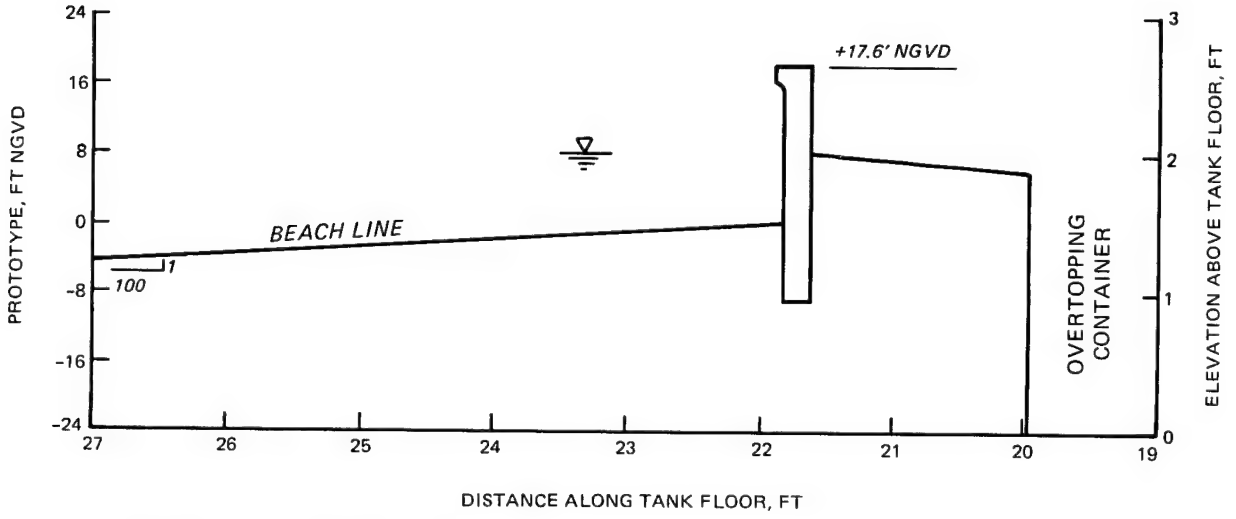

Figure 5. Configuration 1, seawall with no riprap revetment

of the tests, the wave conditions in front of the seawall do not have a JONSWAP spectrum but represent a wider type of spectrum.

10. Overtopping rates were determined by measuring the change in water level in the overtopping container behind the seawall during a test run. If overtopping rates were high, water was added to the seaside portion of the flume during the test run to compensate for the water lost over the wall and to maintain an approximately constant water level seaward of the seawall. Water levels were measured to the closest one thousandth of a foot before and after a test run, both in the overtopping container and the offshore portion of the wave tank, using point gages.

11. Information data presented in all the data tables are given in prototype dimensions. Table 1 is a list of the various seawall/revetment configurations tested during this study with figure and plate numbers that correspond to their descriptions and data plots, respectively. Also note that the underlayer sizes shown in the cross-sectional figures are oversized in order to compensate for scale effects present in the model.

Table 1

List of Various Seawall/Revetment Configurations, Figure Numbers, and Overtopping Coefficients

Configuration Designation Number	Description of Seawall/Revetment Configuration	Figures Showing Configuration	Plates Showing Data	Overtopping Coefficients: Regression Q_o / C_1	Overtopping Coefficients: Nonregression Q_o / C_1	Configuration Overtopping Rating Coefficient, A^q: Regression	Configuration Overtopping Rating Coefficient, A^q: Nonregression
1	Existing Roughans Point seawall with no riprap revetment	5	1	76.554 -14.078		0.0797	
2*	Roughans Point seawall with standard riprap revetment	6,7	2	30.539 -13.431		0.0404	
3	Roughans Point seawall with a wave absorber riprap revetment	10	3	485.413 -20.845		0.0448	
4	Roughans Point seawall with riprap revetment having a wide berm at +8 ft NGVD	11	4	1,157.479 -25.461	439.220 -21.621	0.0219	0.0310
5	Roughans Point seawall with riprap revetment having a double berm at +6 and +10 ft NGVD	13	5	758.240 -25.226		0.0155	
6	Roughans Point seawall with riprap revetment having a berm at +10 ft NGVD and 1.0-ft cap on seawall	14	6	353.541 -23.943		0.0112	
7	Roughans Point seawall with riprap revetment having a wide berm at +8 ft NGVD and a 1.0-ft cap on seawall	15	7	57.628 -19.569	305.821 -23.073	0.0083	0.0131
8	Roughans Point seawall with riprap revetment having a wide berm at +8 ft NGVD and a 2.0-ft cap on seawall	16	8	93.037 -22.154		0.0055	
9	Roughans Point seawall with beach breakwater	18	9	15.226 -14.410	109.508 -18.654	0.0140	0.0218
10	Sheet-pile seawall with standard riprap revetment, designed for less severe wave conditions	20	10	75.189 -17.783		0.0204	

* Plan recommended by NED in planning investigations (NED 1982).

PART III: PRESENTATION OF RESULTS

Development of Overtopping Parameters

12. One of the most important findings of this study was the development of a dimensionless relative freeboard parameter F' which consolidated all of the data for one structure configuration into a single trend. The term, F' is defined

$$F' = \frac{F}{\left(H_{mo}^2 \quad L_p\right)^{1/3}} \tag{1}$$

where F is the freeboard, i.e., the difference between the crest height of the seawall and the local SWL, and L_p is the Airy wave length calculated using the water depth at Gage 7 and the nominal T_p. Equation 1 can be thought of as the ratio of the freeboard and the severity of the local wave action. The term F' combines a large amount of information into one parameter which contains the seawall crest elevation, the local water depth or water level, the zero-moment wave height, and the period of peak energy density of the spectrum through the use of L_p. This parameter, F', seems to consolidate the data into a single trend better than other variables, including the parameter F/H_{mo} suggested by the work of Goda (1969) and Seelig (1980) or the dimensionless freeboard parameter $F/(T_z g H_s)$ used by Owen (1982), where T_z is the zero-crossing wave period, H_s is the significant wave height, and g is the acceleration of gravity. Using L_p in the F' parameter seems to be a very effective way to account for wave period effects which are conspicuous when observing the laboratory tests. After a short time of model observation, it was obvious (other factors being equal) that the larger the T_p of the spectra the greater the overtopping.

13. Following the rationale given above, the overtopping rate Q is plotted versus F' (Plates 1-10) for all of the seawall/revetment configurations given in Table 1. The overtopping rate Q is defined as the volume of water overtopping the seawall per unit length of seawall per unit time. For this study, Q is given in units of cubic feet per foot per second. Also shown in Plates 1 through 10 is a regression curve which has been fit to the

data shown in the respective plate. On some plates a second curve (nonregression) has been added. The second curve has been added where the data scatter suggests that for design purposes a trend more conservative than the regression curve should be used. The second curves are not regression curves but are curves that have been fit by eye on the basis of the judgment of the principal investigators. Where both curves are present the nonregression curve is the one that is recommended for use for design purposes. It should be noted that various vertical scales have been used in Plates 1-10. The vertical scales were chosen to help portray the observed data effectively, but the scales make direct comparisons between these plates difficult. Comparisons between various configurations are made later in the text.

14. All of the curves shown in Plates 1-10 have been fit to an equation of the general form

$$Q = Q_o e^{C_1 F'} \tag{2}$$

where C_1 is a dimensionless coefficient, and Q_o is a coefficient with the same units as Q (ft^2/sec). The coefficients have been determined either by regression analysis or "fit by eye" as mentioned above. Equation 2 seems to have the proper form to fit all of the data sets rather well and is the same form as the overtopping equation developed by Owen (1982) in his laboratory study of irregular wave overtopping of sea dikes. Coefficients Q_o and C_1, for both regression and nonregression curves, are given in Table 1.

15. Although the parameter F' given by Equation 1 and used as the independent variable for Plates 1-10 may seem a bit abstract at first, it is effective in consolidating the data into well defined trends that can be readily identified. Generally, there is a large change in Q in the range of F' between 0.3 and 0.5. For F' greater than 0.5 there is little wave overtopping, while for F' less than 0.3 there is considerable overtopping regardless of the seawall/revetment configuration.

16. These large amounts of wave overtopping result from the effect of large waves hitting the seawall or seawall/revetment at high water levels. The term high waves means those with crest elevations probably in the range of 70 to 80 percent of the freeboard. For these conditions it is difficult to envision a strategy which would be effective. The wave just surges up at the wall and inundates the recurve then spills over the crest of the seawall in

large masses of "green" water. It is hard to imagine any surface feature of the wall or fine tuning of the fronting revetment being particularly effective for this extreme situation. For the tests conducted in this study, the inundation mode of overtopping occurred primarily when F' was less than about 0.3. Because changes in the geometry of the various seawall/revetment configurations is not very important when overtopping is in the inundation mode, it was not deemed necessary to make comparisons of data trends for F' less than 0.3.

17. One simple way to evaluate the effectiveness of a seawall/revetment configuration is to use the area under the data trend curve. The less area under the curve the more effective the configuration. Because of the discussion given above, a logical lower limit for integration is 0.3, although other limits could be used. The overtopping ranking coefficient A_q is defined

$$A_q = Q_o \int_{F'_{min}}^{\infty} e^{C_1 F'} \, dF' = - \frac{Q_o}{C_1} \, e^{C_1 F'_{min}} \qquad (3)$$

A_q is shown in Table 1 using $F'_{min} = 0.3$. As with any complex phenomenon no single parameter can be used to evaluate performance without considerable care; but because this parameter seems to be such a logical extension of the method of computing overtopping rates developed in this report, it is presented here. When evaluating structures, the smaller the value of A_q the more effective the seawall configuration.

18. At the request of NED, overtopping coefficients and overtopping ranking coefficients were calculated for a previous monochromatic wave overtopping study conducted by Saville (1955). Discussion of this effort and tabulation of the coefficients are given in Appendix B.

Stability of Armor Stone

19. All configurations tested used the 2,551-lb median stone weight, except Configuration 9 which used 4,718-lb medium stone weight (as described in paragraph 5). Occasionally during testing, one or two armor stones would be dislodged, but this movement was not significant; and the armor stone for all configurations, except the double berm in Configuration 5 was observed to

be stable for all swl/wave conditions tested. The double berm in Configuration 5 merged into a single slope and then stabilized. The armor slope for Configuration 6 was purposely constructed similiar to the stabilized slope in Configuration 5 and proved to be stable throughout the testing of Configuration 6. With the exception of Configuration 5, armor stone movement for all configurations was not significant, with only one or two stones being dislodged after long periods of wave attack. Thus the stone size represented in the model should be satisfactory for any storms within the conditions tested.

PART IV: DISCUSSION

20. It was found that a standard riprap revetment (Configuration 2) in front of the seawall (Figures 6 and 7 and Plate 2) reduced wave overtopping rates in the range of 40 to 50 percent over what was expected to overtop in the absence of the revetment (Configuration 1, Plate 1). A comparison of the data trends for Configuration 1 and 2 is given in Figure 8. In general, the standard revetment did not reduce overtopping rates very effectively. Two problems, which were not detected prior to the test, can be identified with the standard revetment:

a. If the top of the revetment is too high, it interferes with the recurve causing the recurve not to function effectively.

b. If the revetment acts as a ramp, which it often does, it causes the waves to ride up and over the wall without a major discontinuity in the flow. This "ramp effect" is pictured in Figure 9.

21. The wave absorber revetment (Configuration 3, Table 1, and Figure 10) was an attempt to make the revetment a better wave absorber by adding armor stone. Configuration 3's performance (Plate 3) was poor because it was not recognized at that point how important it was to maintain discontinuities in the configuration, such as the recurve and the wall itself, to disrupt the wave action and runup flow. In designing Configuration 3, the main goal was to try to dissipate as much wave energy as possible within the spatial constraints.

22. The revetment with a wide berm at +8 ft NGVD (Configuration 4, Table 1, and Figure 11) was designed to provide a discontinuity to wave action and runup flow, to allow the recurve to function effectively, and to still be a good dissipator of wave energy. Configuration 4 results (Plate 4) show it to be a very effective design in reducing overtopping, and its performance is better compared to the standard revetment (Configuration 2 in Figure 12).

23. Configuration 5 (Table 1 and Figure 13), with a double berm, was an attempt to fine tune the idea developed in Configuration 4. The slope connecting the two berms was 1V on 2H and was not stable with the more severe wave conditions. As a consequence, the two berms had merged into a single, somewhat sloped, berm by the end of the tests. Configuration 5's performance (Plate 5) indicates it was effective in terms of reducing overtopping, but the need for two berms is probably not worth the added design and construction complexity. A single rather flat slope between +6 and +10 ft NGVD probably

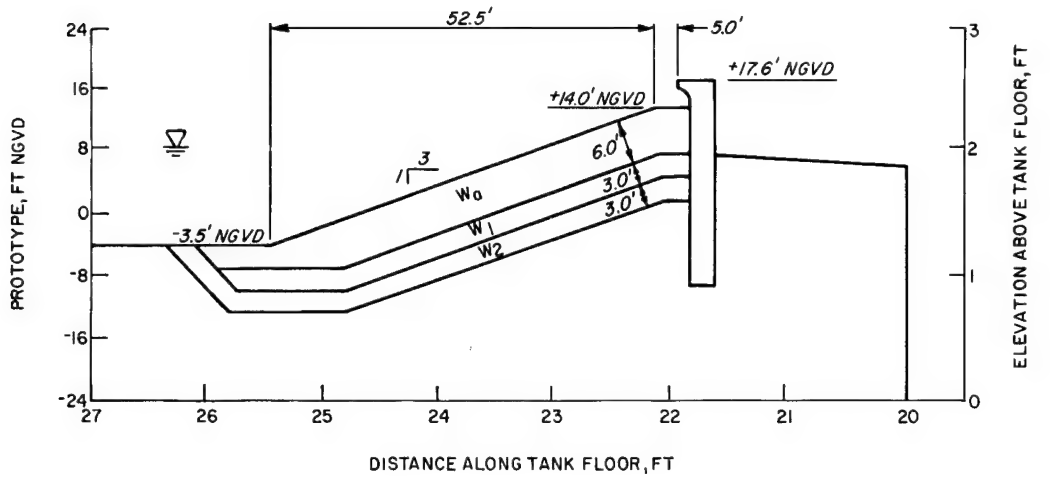

LEGEND

SYMBOL	STONE WEIGHT, W_{50}
W_a	2551 LB
W_1	347 LB
W_2	45 LB

Figure 6. Configuration 2, seawall with standard riprap revetment

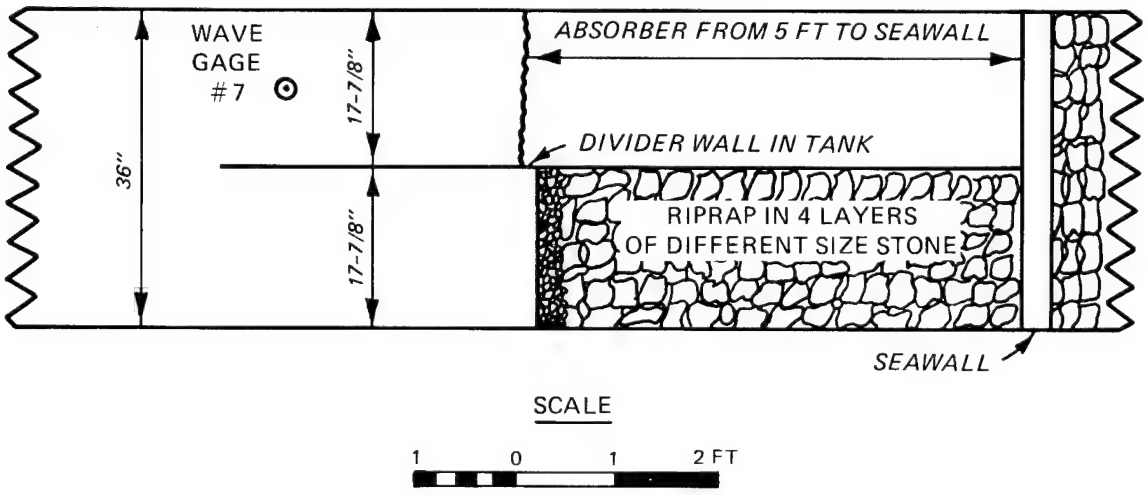

Figure 7. Plan view of Configuration 2 in wave tank

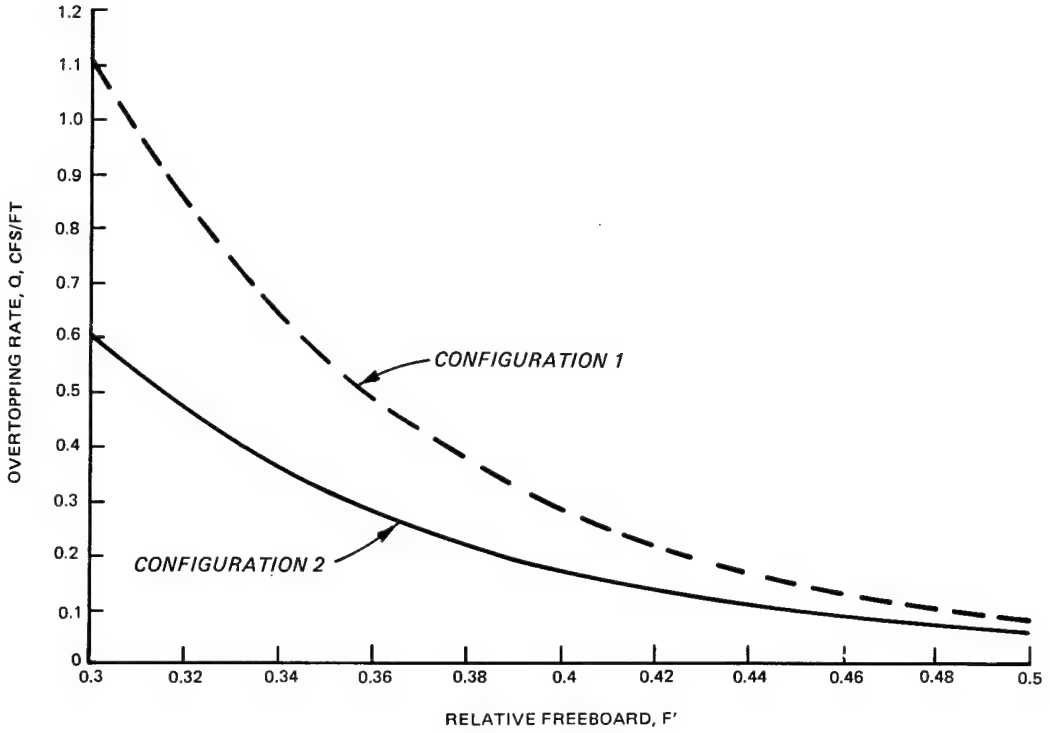

Figure 8. Comparison of data trends for Configurations 1 and 2

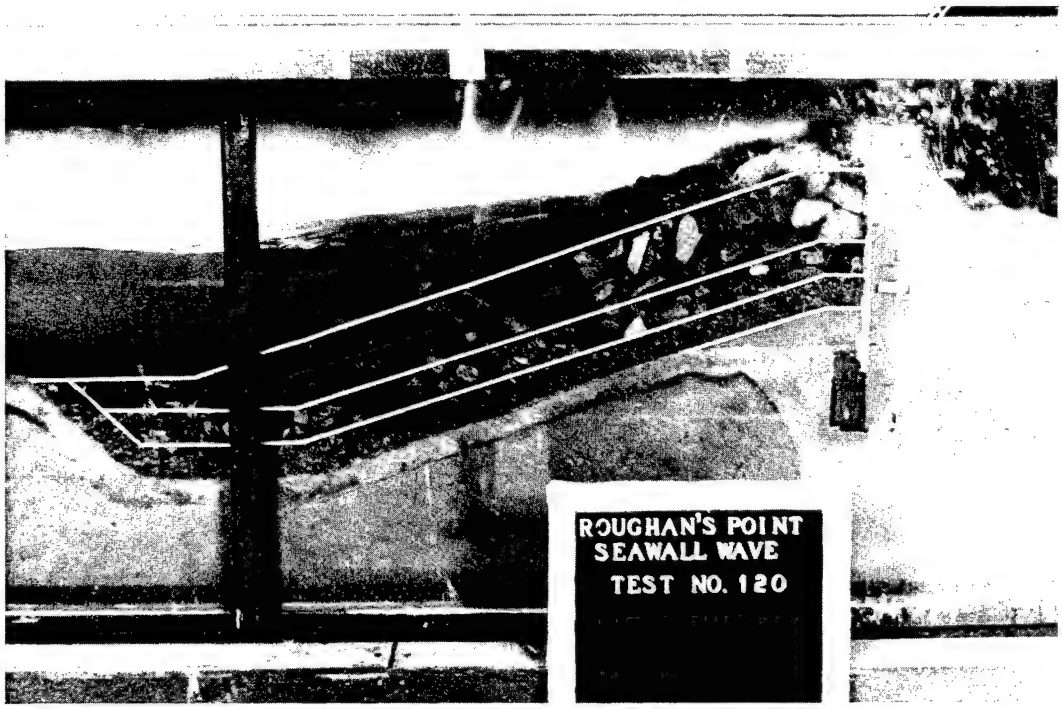

Figure 9. Configuration 2, seawall with standard riprap revetment as it appeared in the model study

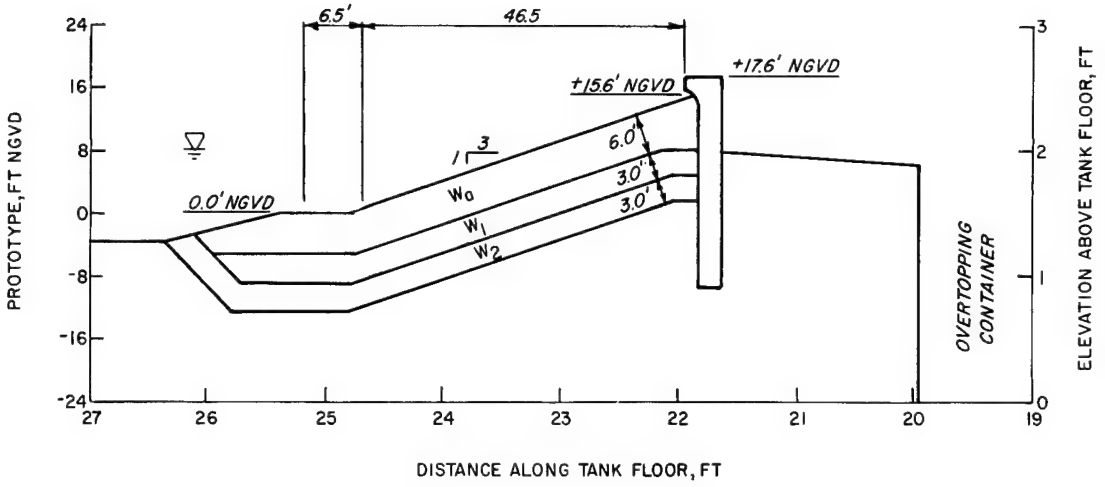

LEGEND

SYMBOL	STONE WEIGHT, W_{50}
W_a	2551 LB
W_1	347 LB
W_2	45 LB

Figure 10. Configuration 3, seawall with a wave absorber riprap revetment

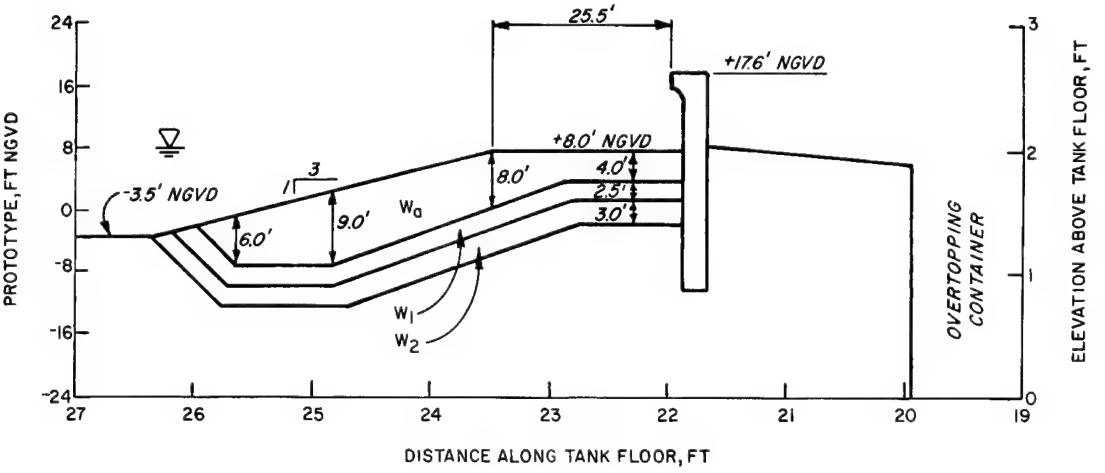

LEGEND

SYMBOL	STONE WEIGHT, W_{50}
W_a	2551 LB
W_1	347 LB
W_2	45 LB

Figure 11. Configuration 4, seawall with riprap revetment having a wide berm at +8 ft NGVD

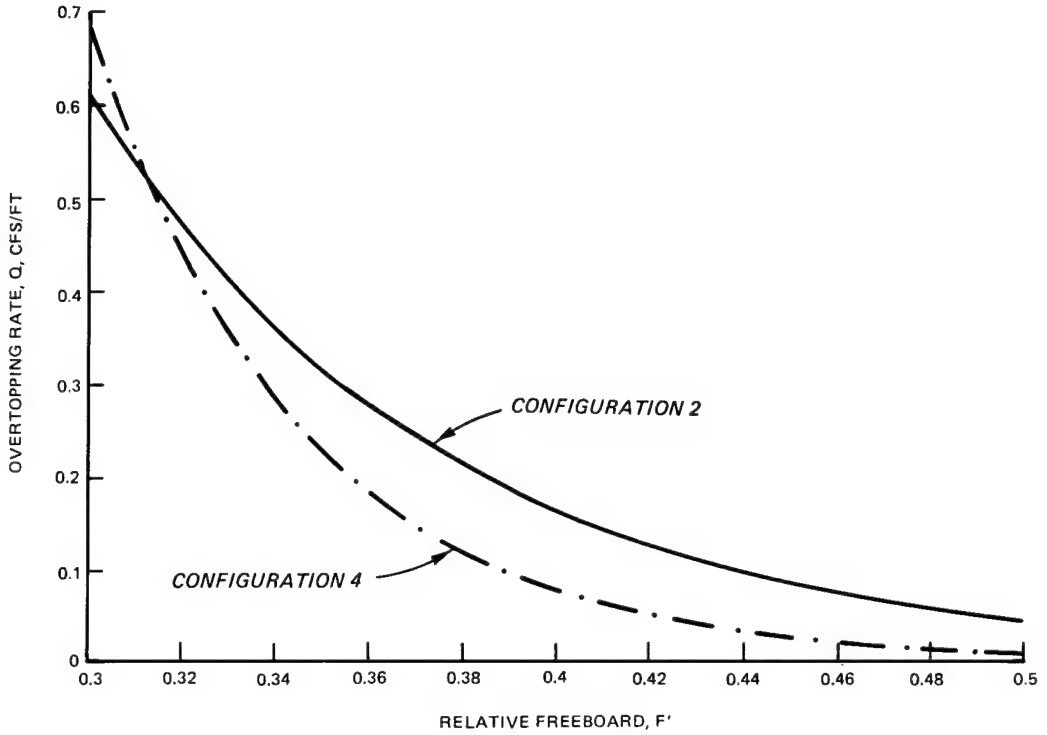

Figure 12. Comparison of data trends for Configurations 2 and 4

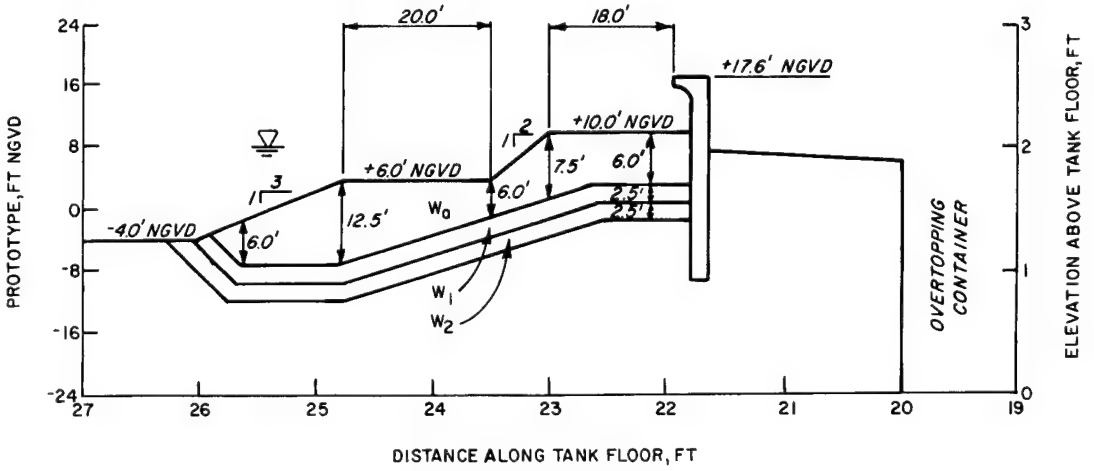

LEGEND

SYMBOL	STONE WEIGHT, W_{50}
W_a	2551 LBS
W_1	347 LBS
W_2	45 LBS

Figure 13. Configuration 5, seawall with riprap revetment having a double berm at +6 and +10 ft NGVD

would have been just as effective as the double berm. Problems with armor stability would not have been encountered, and construction would be easier.

24. Configurations 6, 7, and 8 (Table 1 and Figures 14, 15, and 16) use a combination of fronting revetment and a cap on the seawall in an effort to further reduce overtopping rates. Data plots of Q versus F' for each of these configurations are given in Plates 6, 7, and 8, respectively. Since all the data trends indicate that there is an approximately exponential relation between the freeboard and overtopping rates, adding a cap (vertical height) to the seawall would be an effective means of reducing wave overtopping. Figure 17 shows a comparison of data trends for Configurations 1, 4, 7, and 8 in which Configuration 1 is a seawall with no revetment and Configurations 4, 7, and 8 represent a revetment having a wide berm at +8 ft NGVD and a seawall with no cap, a 1.0-ft cap, and a 2.0-ft cap, respectively. These data show that a wide berm revetment (Configuration 4) is better than no revetment (Configuration 1), but Configuration 4 can be made more effective by adding height to the wall (Configurations 7 and 8). One way to think about the effectiveness of added wall height is to consider the amount of stone that would have to be placed in front of the seawall to obtain a similar amount of reduction in overtopping as a 1.0-foot cap on the seawall. Although Figure 17 does not answer this question quantitatively, it suggests that a 1.0-ft cap is equivalent to a significant amount of stone in front of the seawall. The coefficients given in Table 1 and the curves drawn using the coefficients were computed using a seawall crest height of 17.6 ft NGVD in all cases. This approach is rather like treating the cap as just additional stone to dissipate wave energy and is necessary to compare the effectiveness of various configurations with various seawall crest elevations. In principle, the performance of a cap (added wall height) can be anticipated using Equations 1 and 2 and test data for a configuration without a cap, but this approach was not tried because of lack of confidence in the ability to extrapolate results using such a new method of predicting overtopping rates.

25. Configuration 9 (Table 1 and Figure 18) is an attempt to evaluate the ability of an offshore breakwater to reduce wave overtopping without going very far offshore. Since the breakwater was so close to the seawall, it is referred to as a beach breakwater in Table 1. The beach breakwater was relatively effective at reducing overtopping (Plate 9) but even so, its performance seemed to be something of a disappointment. The appearance of the

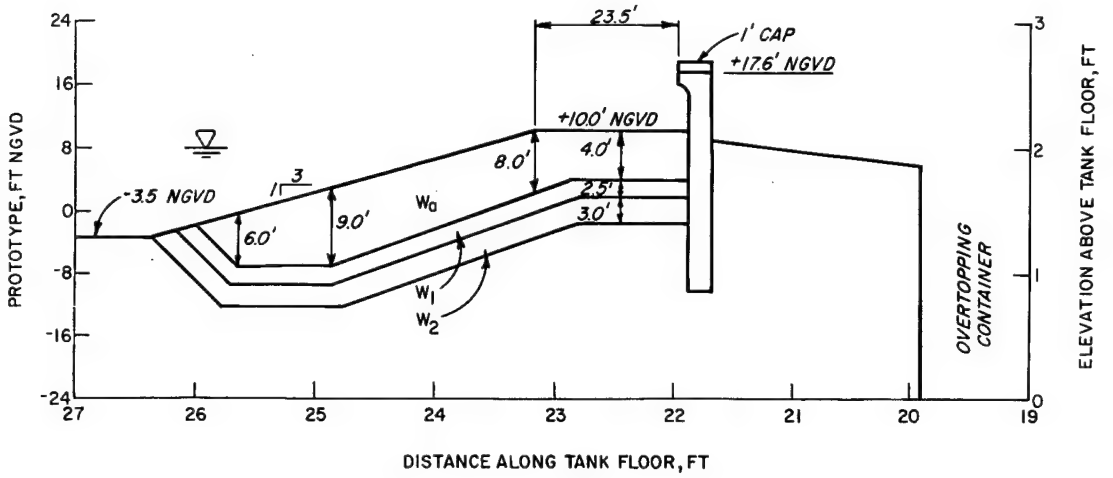

LEGEND

SYMBOL	STONE WEIGHT, W_{50}
W_a	2551 LB
W_1	347 LB
W_2	45 LB

Figure 14. Configuration 6, seawall with riprap revetment having a berm at +10 ft NGVD and 1.0-ft cap on seawall

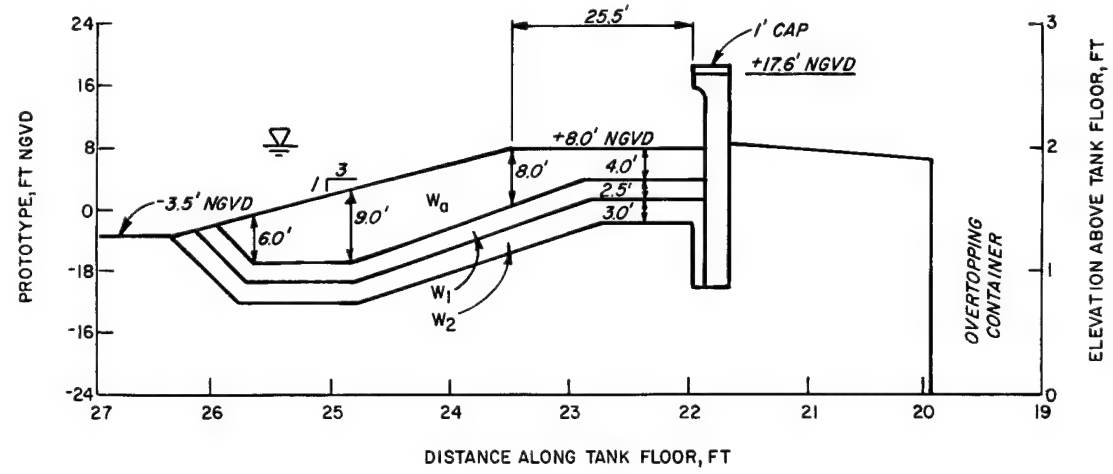

LEGEND

SYMBOL	STONE WEIGHT, W_{50}
W_a	2551 LB
W_1	347 LB
W_2	45 LB

Figure 15. Configuration 7, seawall with riprap revetment having a wide berm at +8 ft NGVD and a 1.0-ft cap on seawall

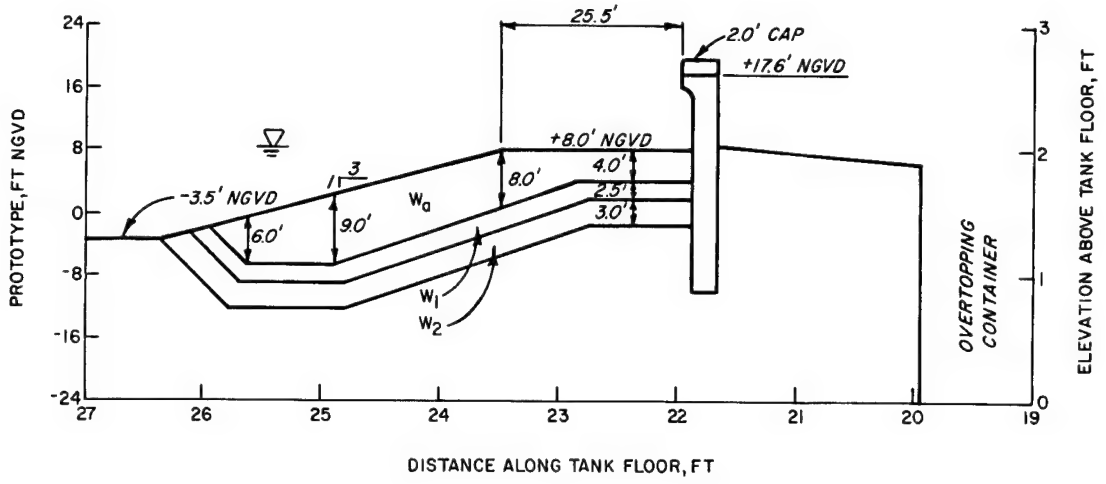

LEGEND

SYMBOL	STONE WEIGHT, W_{50}
W_a	2551 LB
W_1	347 LB
W_2	45 LB

Figure 16. Configuration 8, seawall with riprap revetment having a wide berm at +8 ft NGVD and a 2.0-ft cap on seawall

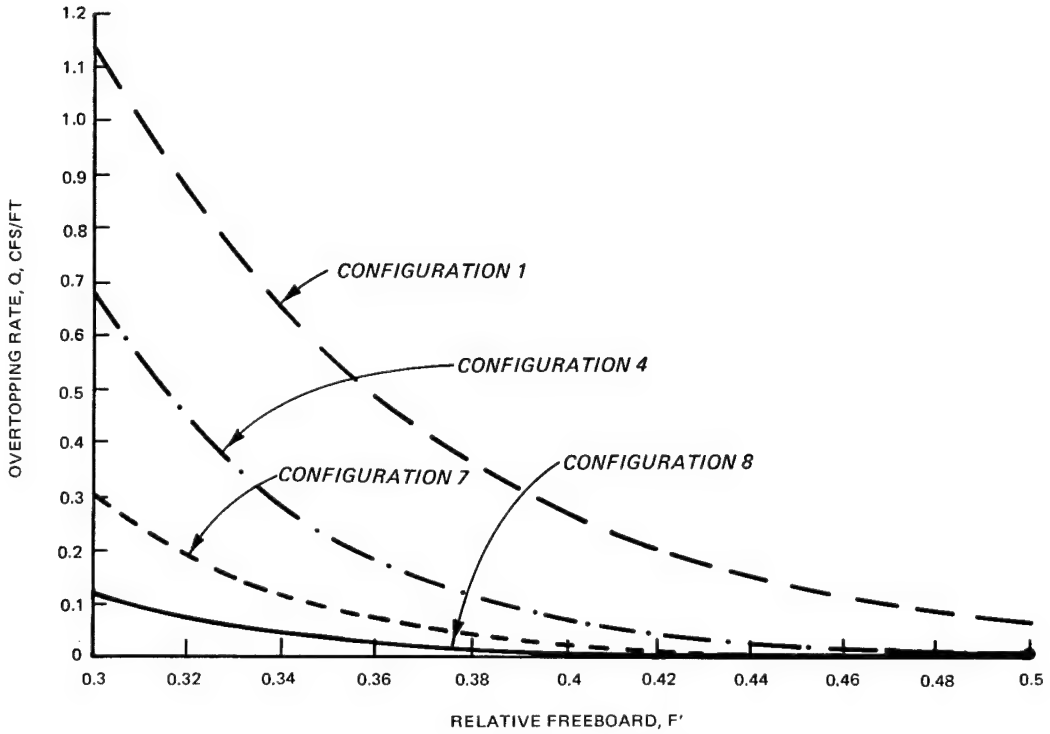

Figure 17. Comparison of data trends for Configurations 1, 4, 7, and 8

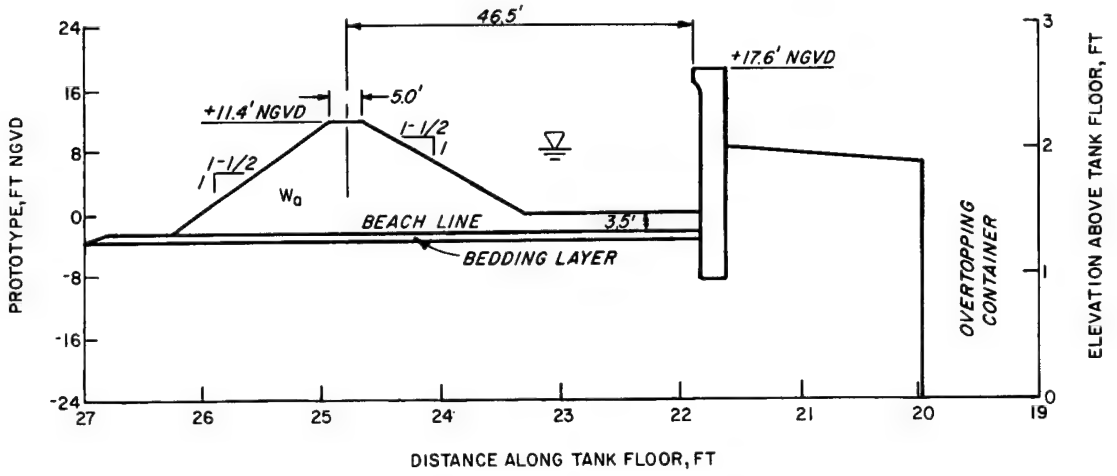

LEGEND

SYMBOL	STONE WEIGHT, W_{50}
W_a	4718 LB

Figure 18. Configuration 9, seawall with beach breakwater

beach breakwater and the seawall inspired considerable confidence since both represent formidable discontinuities to waves and runup flow and a considerable amount of armor stone was used to dissipate wave energy. Figure 19 shows how the beach breakwater appeared in the model study. It appears that one problem with the beach breakwater was the lack of distance between the breakwater and the seawall to dissipate as much wave energy as could potentially be achieved from all the turbulence that was introduced by the breakwater. However, if the breakwater were moved farther offshore it would be in deeper water and therefore require a larger structure making construction more difficult. There is also the problem that the breakwater requires larger armor stone because it has to be built with steeper side slopes than the revetment in order to fit into the allocated space. In addition, the beach between the breakwater and the seawall needs to be armored to prevent scour. Probably because of the roughness and high porosity of all the armor stone there was no tendency for wave resonance to be observed in the pond formed between the breakwater and seawall. The added complexity of building a beach breakwater compared to a revetment against the seawall suggests that the breakwater would not be cost effective.

26. Configuration 10 (Table 1 and Figure 20) is a sheet-pile seawall with a standard riprap revetment fronting it. A plot of Q versus F' for

Figure 19. Configuration 9, seawall with beach breakwater as it appeared in the model study

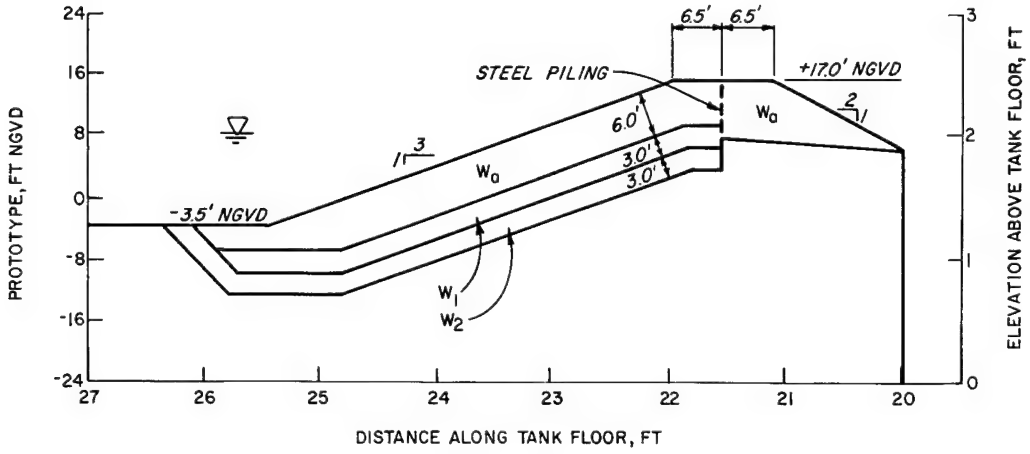

LEGEND

SYMBOL	STONE WEIGHT, W_{50}
W_a	2551 LB
W_1	347 LB
W_2	45 LB

Figure 20. Configuration 10, sheet-pile seawall with standard riprap revetment designed for less severe wave conditions

Configuration 10 is presented in Plate 10. This configuration has offshore water depths somewhat shallower than those for the other configurations. It was being considered for sheltered areas along Broad Sound (Reaches A through D, Figure 2) and was not intended for use on the open coast (see Hardy and Crawford (in preparation) for details related to the strategy for reducing flooding at Roughans Point). In the model the shallower offshore depths were achieved by lowering the reference water level 1.6 ft. As a result there is greater truncation of the large waves in the wave height distribution for this configuration than for the other configurations, and the results cannot be compared. Attempting to compare the results leads to the conclusion that a standard revetment fronting a sheet-pile seawall is unusually effective in reducing wave overtopping when contrasted to a standard revetment fronting the recurved seawall. The reason for the anomaly appears to be that overtopping rates are unusually sensitive to a few large waves, and there are not many of these large waves because of the shallow offshore water depths used for Configuration 10.

PART V: SUMMARY AND CONCLUSIONS

27. A number of revetment configurations were tested for effectiveness in reducing irregular wave overtopping of the Roughans Point seawall. Results of the study are summarized in Figures 21 and 22. The tests indicate that a standard riprap revetment in front of the wall with the top of the riprap close to the top of the wall (Configuration 2, as recommended by NED) is not the most effective configuration for reducing overtopping. Configuration 4, a riprap revetment with a relatively wide berm at +8 ft NGVD and a wall crest elevation of +17.6 ft NGVD proved to be the most effective overall revetment configuration unless a cap is added to the seawall. This berm configuration appeared to be high enough and wide enough to dissipate wave energy well but still low enough so that the seawall provided an effective discontinuity to the wave and runup flow and allowed the recurve to function efficiently. To obtain the maximum effectiveness, the berm should have an elevation equal to the average annual high water event, be as wide as possible, and intersect the seawall low enough so that a major discontinuity to wave action and runup flow is maintained. By higher expected water levels a recurrence interval in the range of 1 to 5 years is implied. These findings appear to be consistent with recent research conducted at H.R.S. Wallingford on irregular wave overtopping of sea dikes (see Owen (1982) and Allsop*).

28. Increasing the height of the seawall is also a very effective method to reduce wave overtopping, although for many situations this option is not acceptable.

29. A new method to compute overtopping rates caused by irregular wave conditions has been presented which seems to have several advantages over the current method of computing irregular wave overtopping rates given in the SPM (1984). The method's advantages are that it:

a. Is simple.

b. Does not use the runup or potential runup to compute overtopping rates.

c. Is naturally well adapted for use with irregular wave conditions.

d. Provides a simple way to compare and rank the effectiveness of various structural configurations in reducing wave overtopping.

---

* Personal communication with N. W. H. Allsop, Hydraulics Research Limited, Wallingford, Oxfordshire, England, 1985.

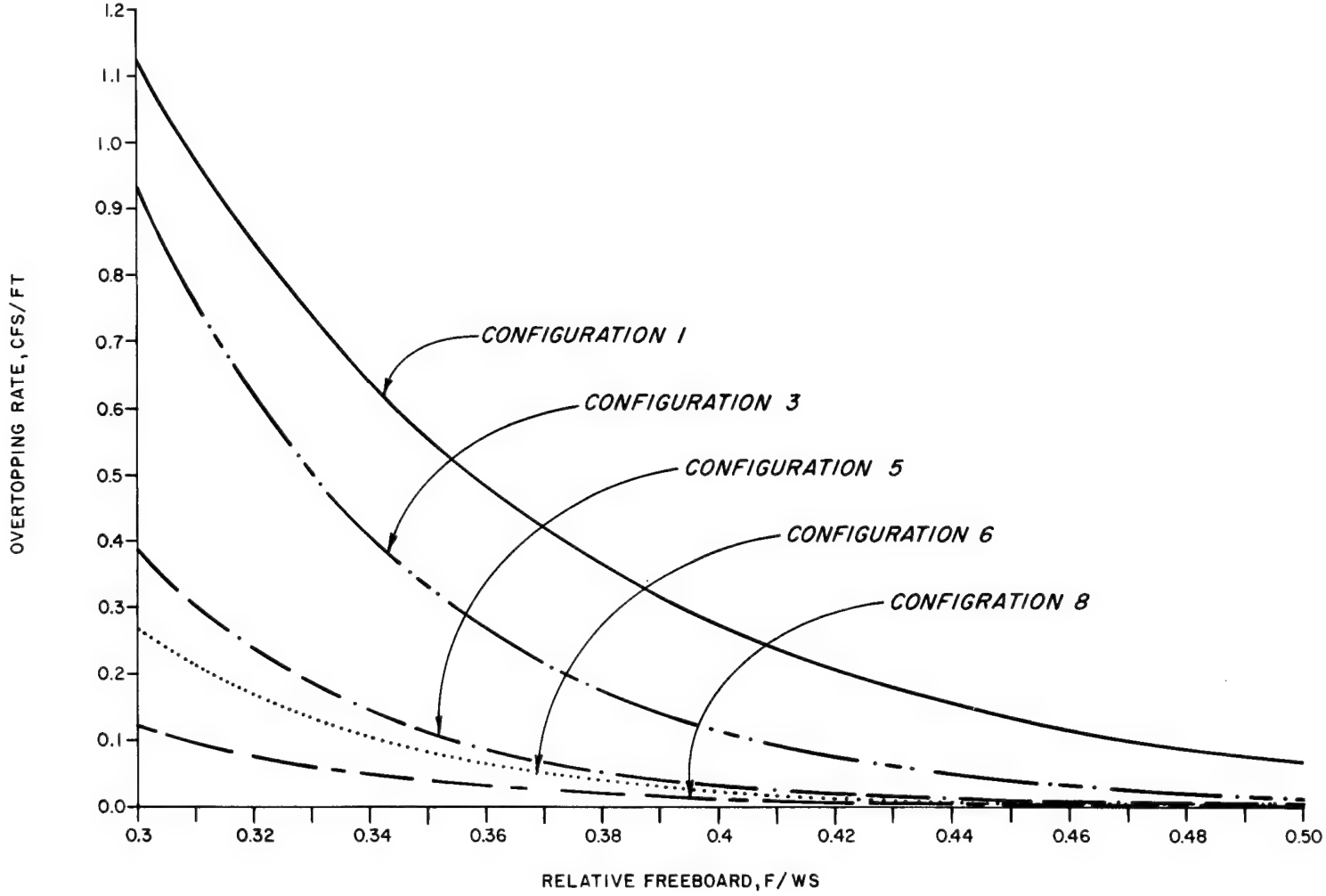

Figure 21. Comparison summary of data trends for Configurations 1, 3, 5, 6, and 8

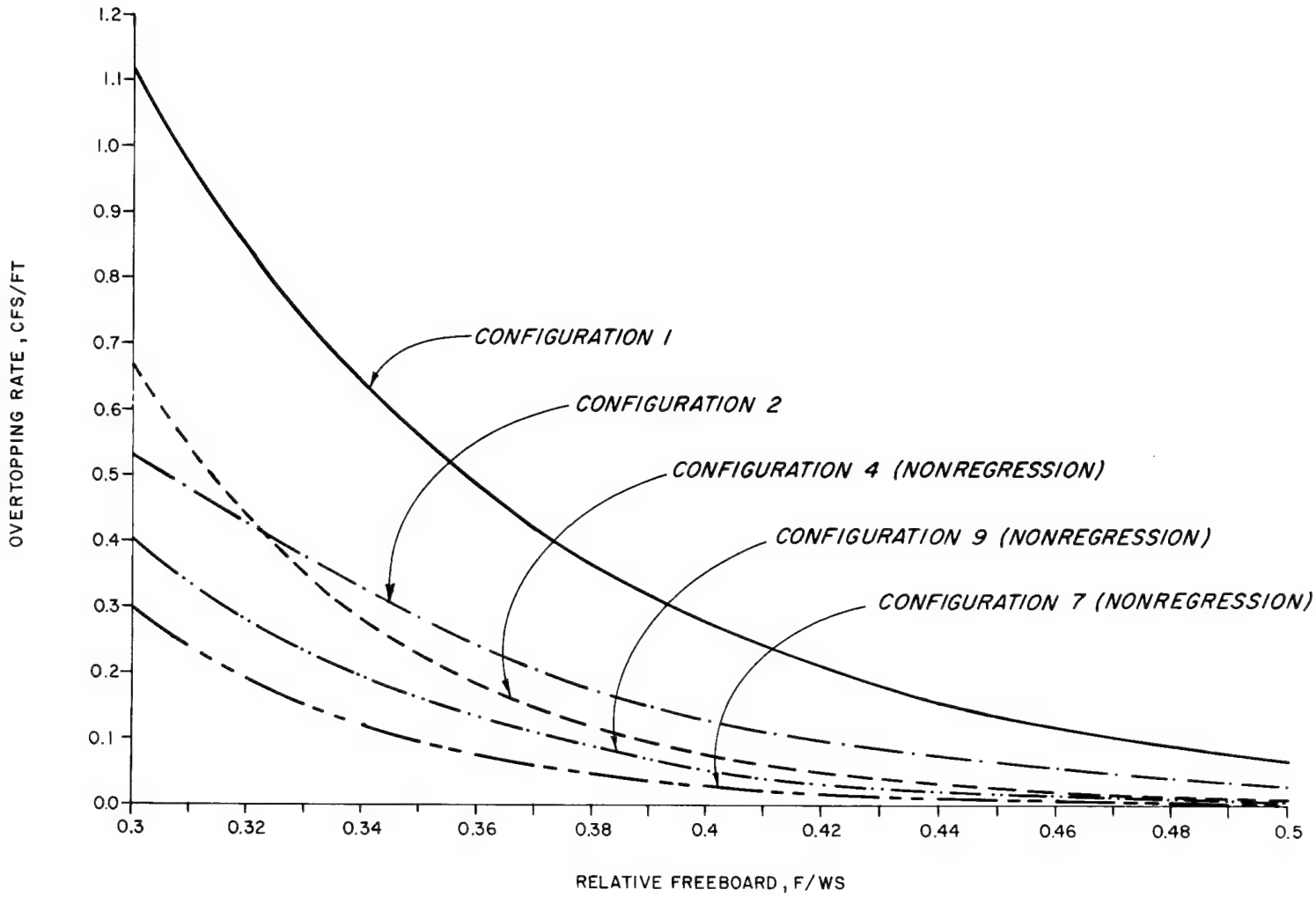

Figure 22. Comparison summary of data trends for Configurations 1, 2, 4, 7, and 9

It is also believed that this new method is more accurate than the SPM method because it was developed directly from irregular wave conditions rather than being adapted from monochromatic wave overtopping tests.

30. The new method of computing overtopping rates and overtopping data presented herein was used by Hardy and Crawford (in preparation) to compute the stage frequency curves for interior flooding at Roughans Point.

REFERENCES

Goda, Y. 1969. "Reanalysis of Laboratory Data on Wave Transmission over Breakwaters," Report of the Port and Harbor Research Institute, Vol 18, No. 3, Yokosuka, Japan.

Hardy, T. A., and Crawford, P. L. In preparation. "Frequency of Coastal Flooding at Roughans Point, Broad Sound, Lynn Harbor, and the Saugus-Pines River System," CERC Technical Report, US Army Engineer Waterways Experiment Station, Vicksburg, Miss.

Hasselmann, L., et al. 1973. "Measurements of Wind-Wave Growth and Swell Decay During the Joint North Sea Wave Project (JONSWAP)," Deutsches Hydrogrephisches Institute, Hamburg, Germany.

Hughes, S. A. 1984 (Dec). "The TMA Shallow-Water Spectrum Description and Applications," Technical Report CERC-84-7, US Army Engineer Waterways Experiment Station, Vicksburg, Miss.

Owen, M. W. 1982 (Sep). "Overtopping of Sea Defenses," Proceedings of the International Conference on Hydraulic Modelling of Civil Engineering Structures, Paper #3, Coventry, England, pp. 469-480.

Saville, T., Jr. 1955 (Oct). "Laboratory Data on Wave Runup and Overtopping on Shore Structures," Technical Manual-64, US Government Printing Office, Washington, DC.

Seelig, W. N. 1980 (Jun). "Two-Dimensional Tests of Wave Transmission and Reflection Characteristics of Laboratory Breakwaters," CERC Technical Report 80-1, US Army Engineer Waterways Experiment Station, Vicksburg, Miss.

Shore Protection Manual. 1984, 4th ed. 2 vols, US Army Engineer Waterways Experiment Station, Coastal Engineering Research Center, US Government Printing Office, Washington, DC.

Stevens, J. C., et al. 1942. "Hydraulic Models," Manual on Engineering Practices No. 25, American Society of Civil Engineers, New York.

US Army Engineer Division, New England. 1982. "Roughans Point, Revere, Massachusetts, Coastal Flood Protection Study," Waltham, Mass.

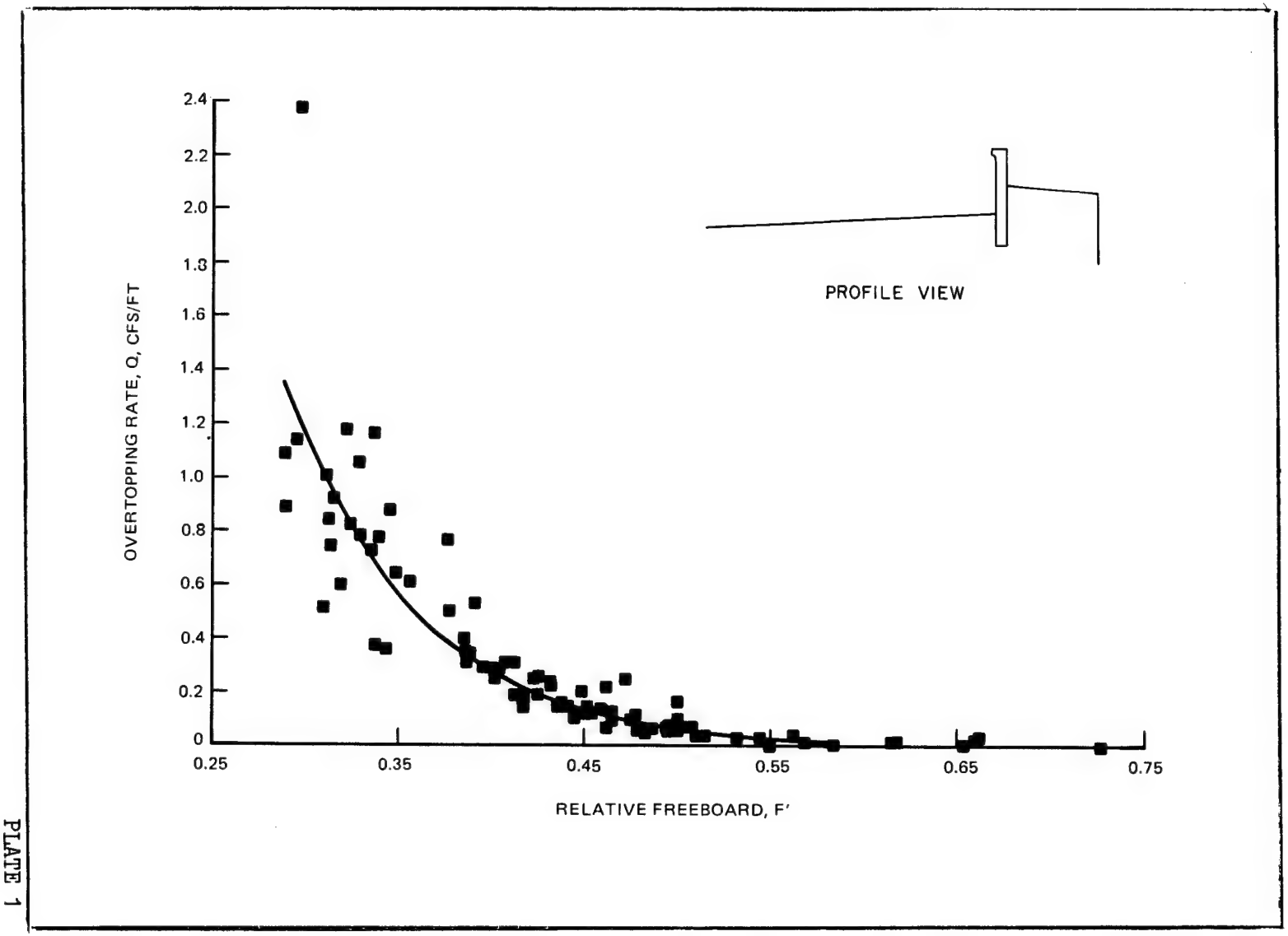
2.4
2.2
2.0
1.8
1.6
1.4
1.2
1.0
0.8
0.6
0.4
0.2
0
OVERTOPPING RATE, Q, CFS/FT
PROFILE VIEW
0.25
0.35
0.45
0.55
0.65
0.75
RELATIVE FREEBOARD, F'

PLATE 1

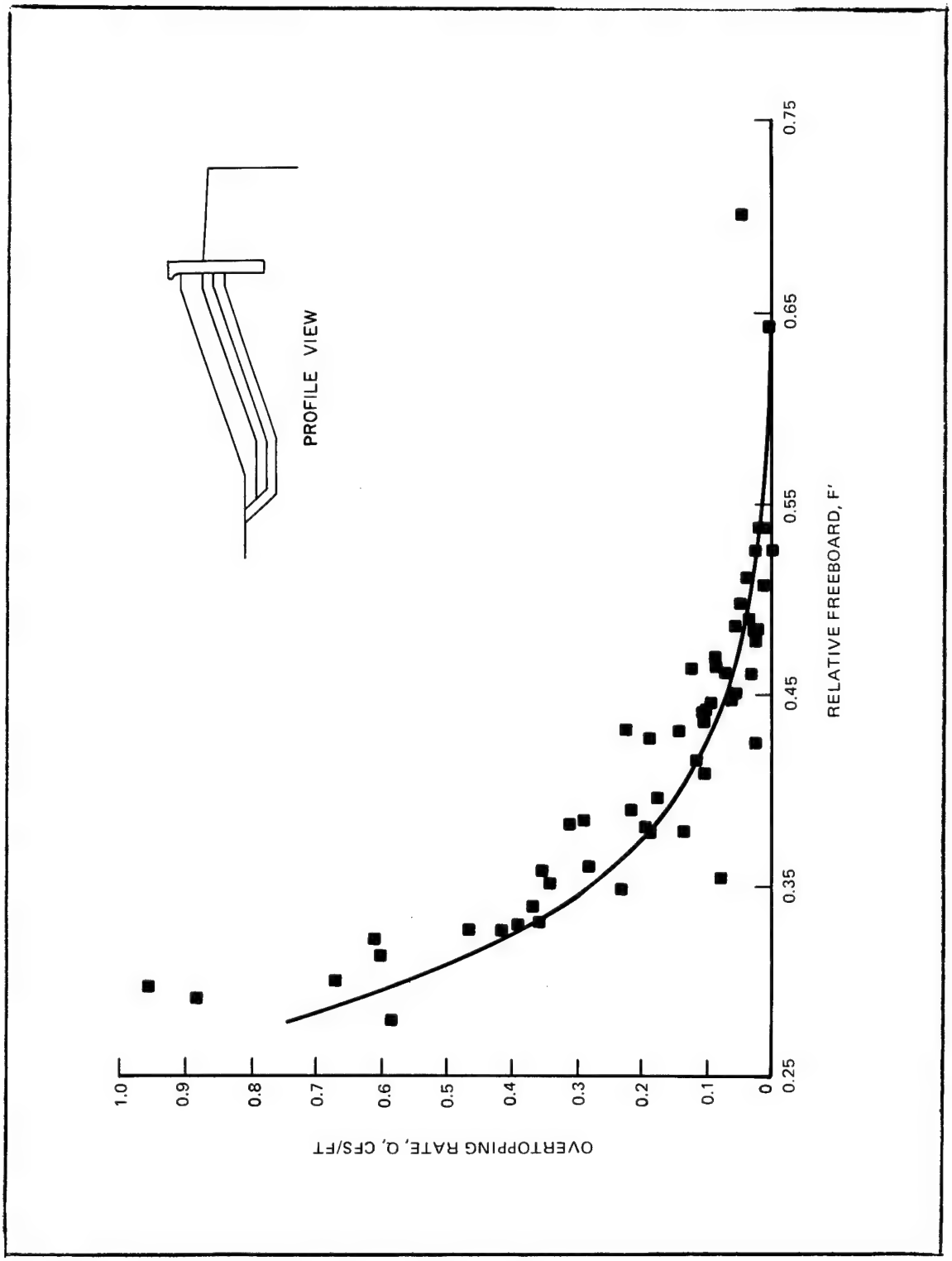
PROFILE VIEW
OVERTOPPING RATE, Q, CFS/FT
1.0
0.9
0.8
0.7
0.6
0.5
0.4
0.3
0.2
0.1
0
0.25
0.35
0.45
0.55
0.65
0.75
RELATIVE FREEBOARD, F'

PLATE 2

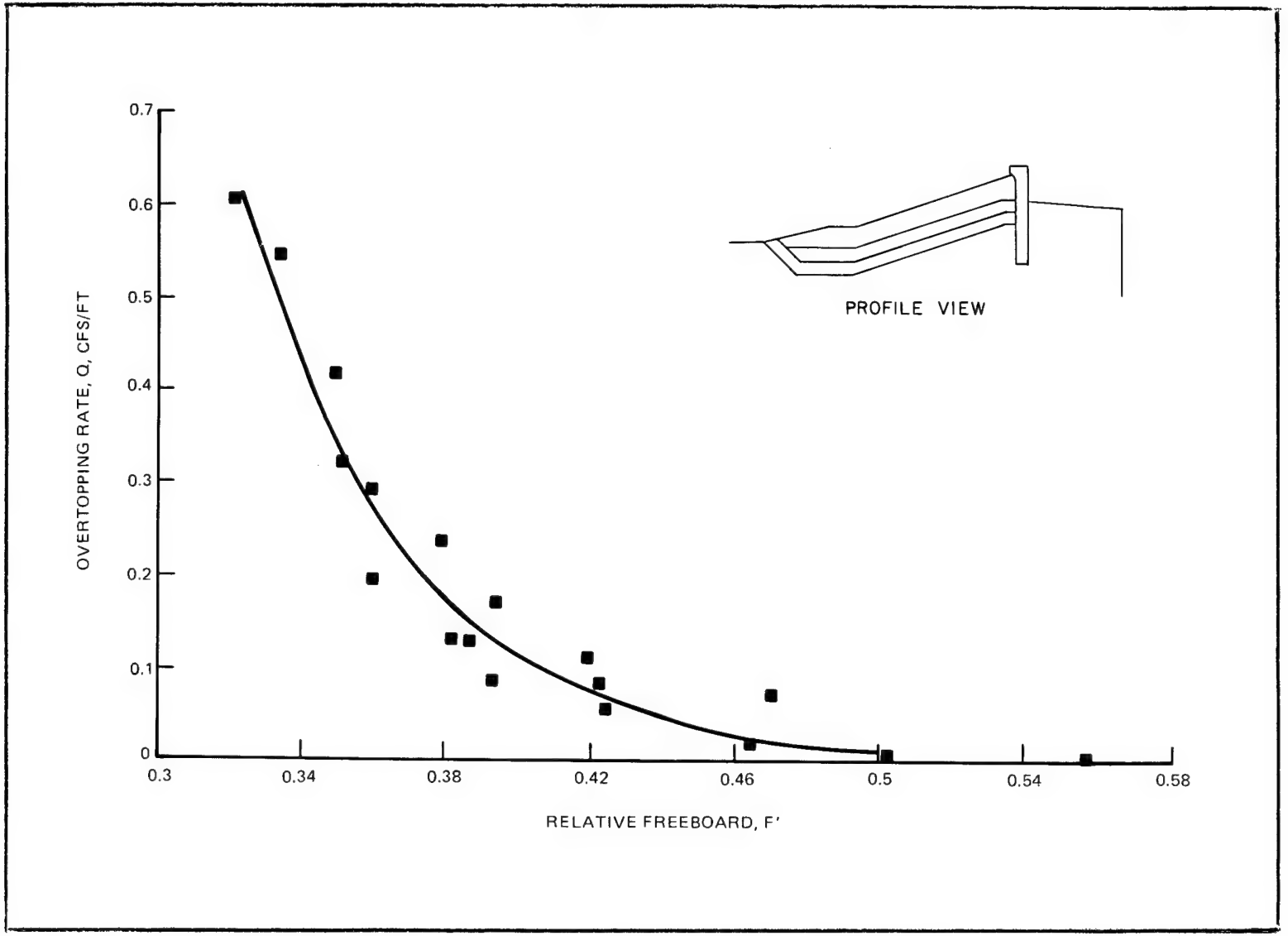
0.7
0.6
0.5
0.4
0.3
0.2
0.1
0
OVERTOPPING RATE, Q, CFS/FT
0.3
0.34
0.38
0.42
0.46
0.5
0.54
0.58
RELATIVE FREEBOARD, F'
PROFILE VIEW

PLATE 3

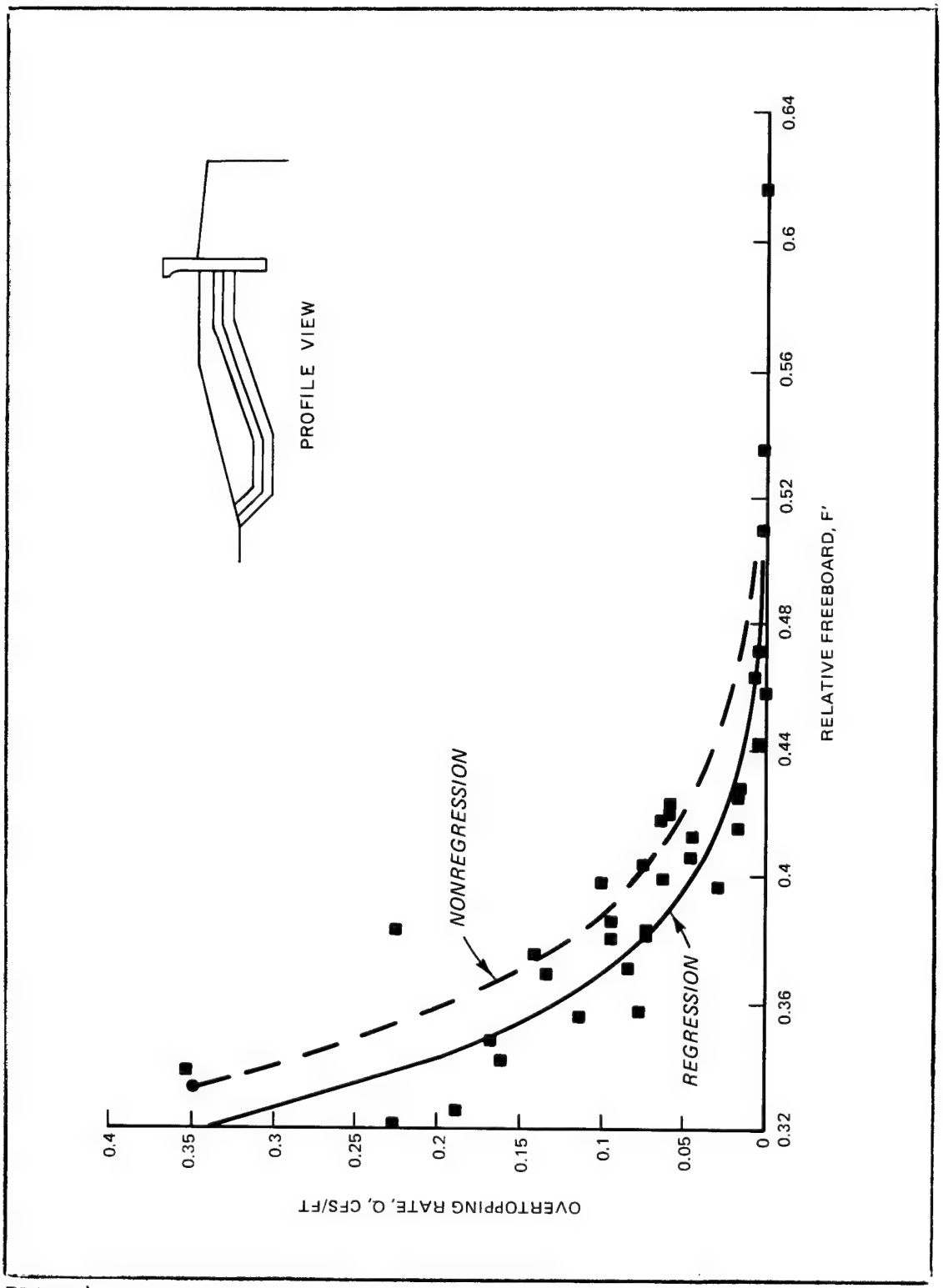
PROFILE VIEW
NONREGRESSION
REGRESSION
OVERTOPPING RATE, Q, CFS/FT
RELATIVE FREEBOARD, F'
0.4
0.35
0.3
0.25
0.2
0.15
0.1
0.05
0
0.32
0.36
0.4
0.44
0.48
0.52
0.56
0.6
0.64

PLATE 4

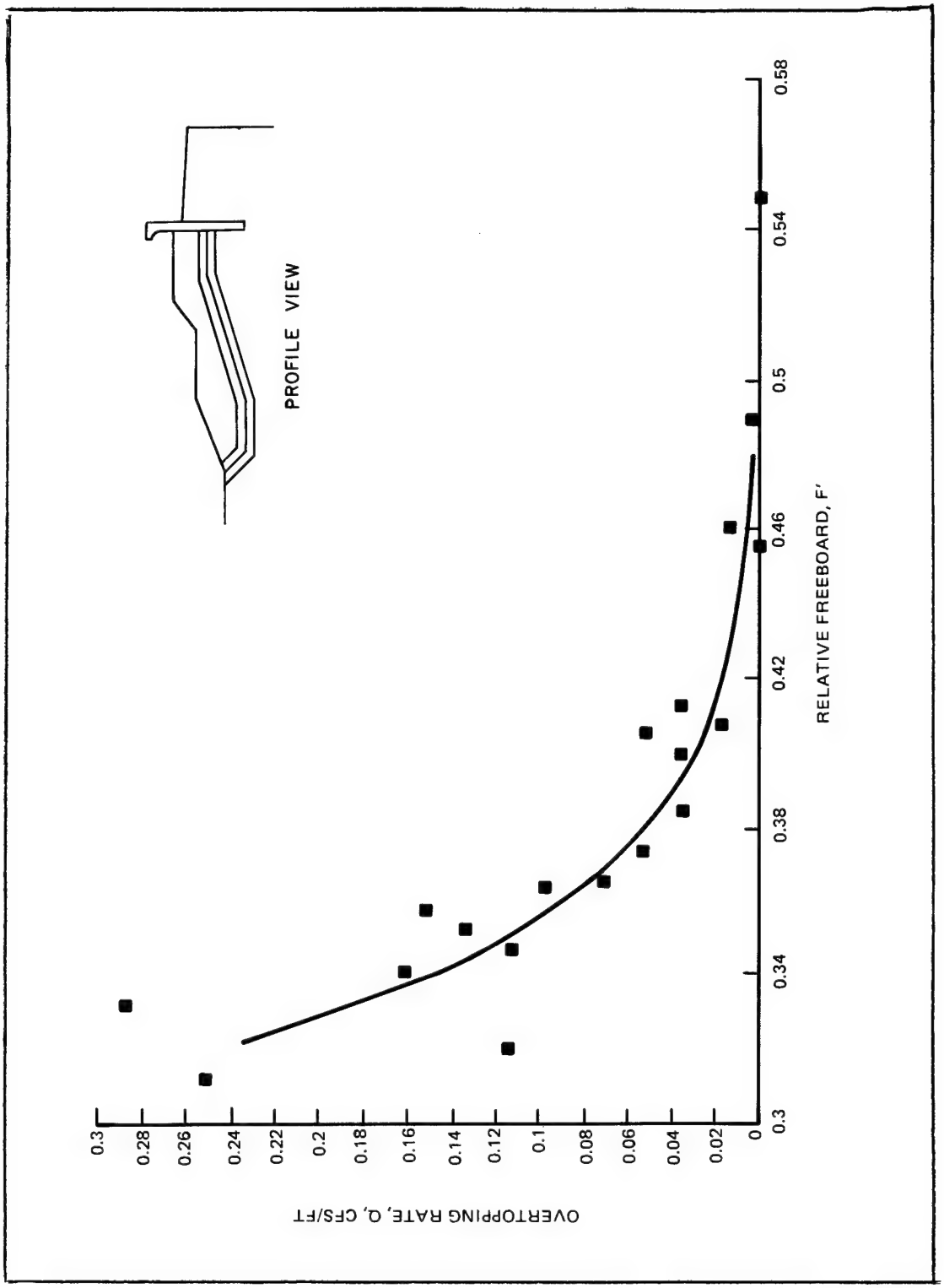
PROFILE VIEW
OVERTOPPING RATE, Q, CFS/FT
0.3
0.28
0.26
0.24
0.22
0.2
0.18
0.16
0.14
0.12
0.1
0.08
0.06
0.04
0.02
0
0.3
0.34
0.38
0.42
0.46
0.5
0.54
0.58
RELATIVE FREEBOARD, F'

PLATE 5

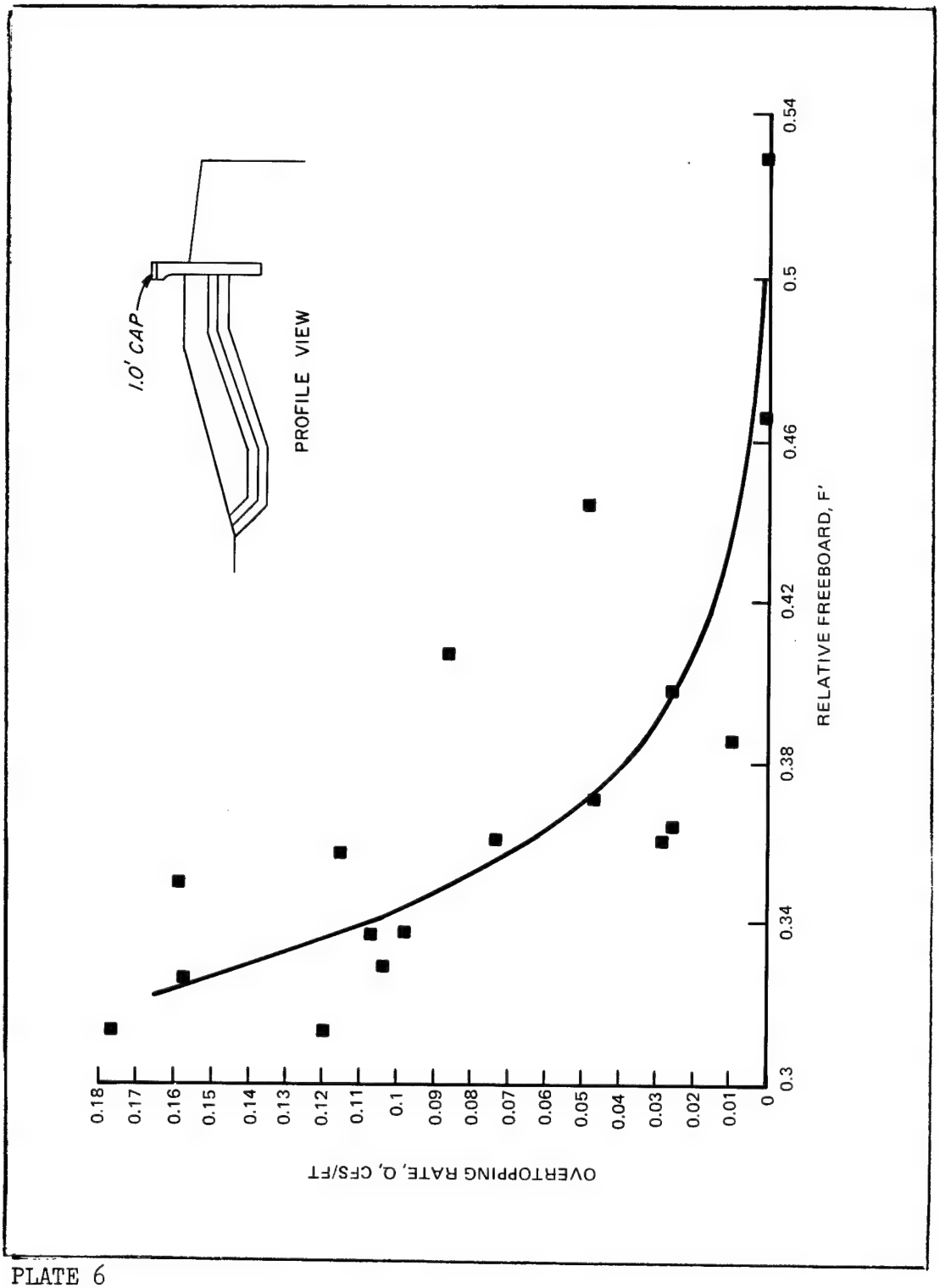
1.0' CAP
PROFILE VIEW
OVERTOPPING RATE, Q, CFS/FT
0.18
0.17
0.16
0.15
0.14
0.13
0.12
0.11
0.1
0.09
0.08
0.07
0.06
0.05
0.04
0.03
0.02
0.01
0
0.3
0.34
0.38
0.42
0.46
0.5
0.54
RELATIVE FREEBOARD, F'

PLATE 6

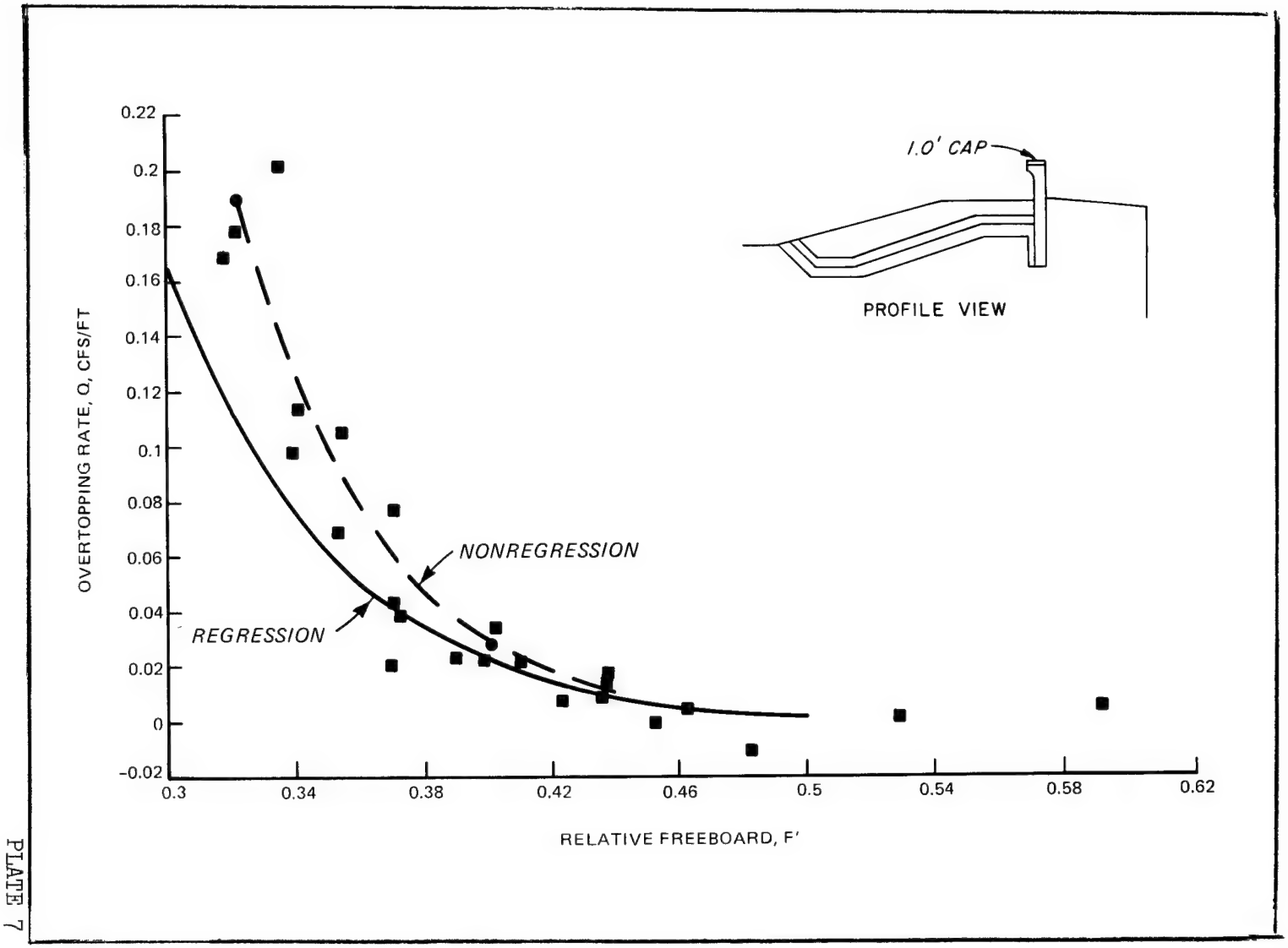
0.22
0.2
0.18
0.16
0.14
0.12
0.1
0.08
0.06
0.04
0.02
0
-0.02
OVERTOPPING RATE, Q, CFS/FT
0.3
0.34
0.38
0.42
0.46
0.5
0.54
0.58
0.62
RELATIVE FREEBOARD, F'
NONREGRESSION
REGRESSION
1.0' CAP
PROFILE VIEW

PLATE 7

PLATE 8

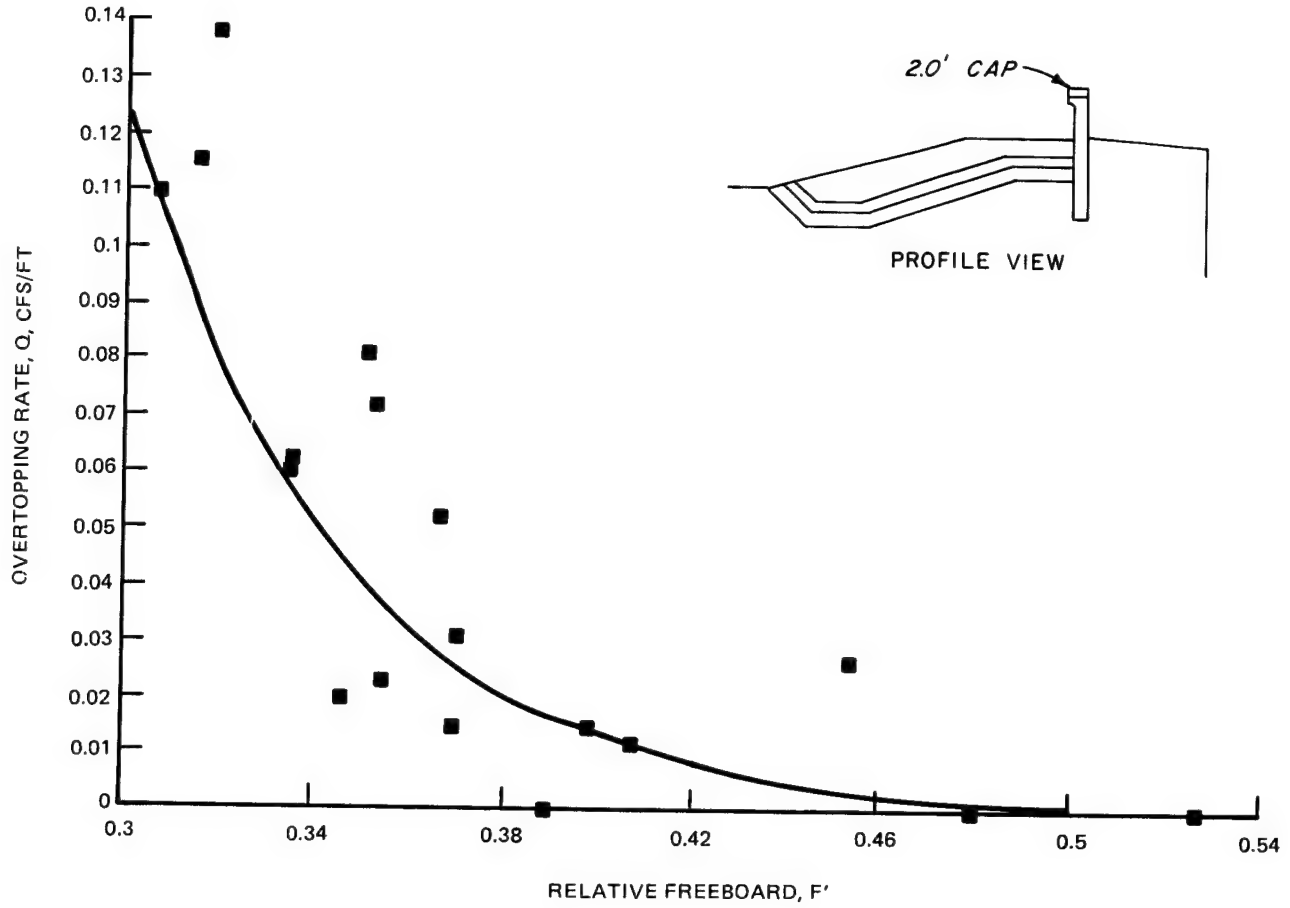
2.0' CAP
PROFILE VIEW
OVERTOPPING RATE, Q, CFS/FT
0.14
0.13
0.12
0.11
0.1
0.09
0.08
0.07
0.06
0.05
0.04
0.03
0.02
0.01
0
0.3
0.34
0.38
0.42
0.46
0.5
0.54
RELATIVE FREEBOARD, F'

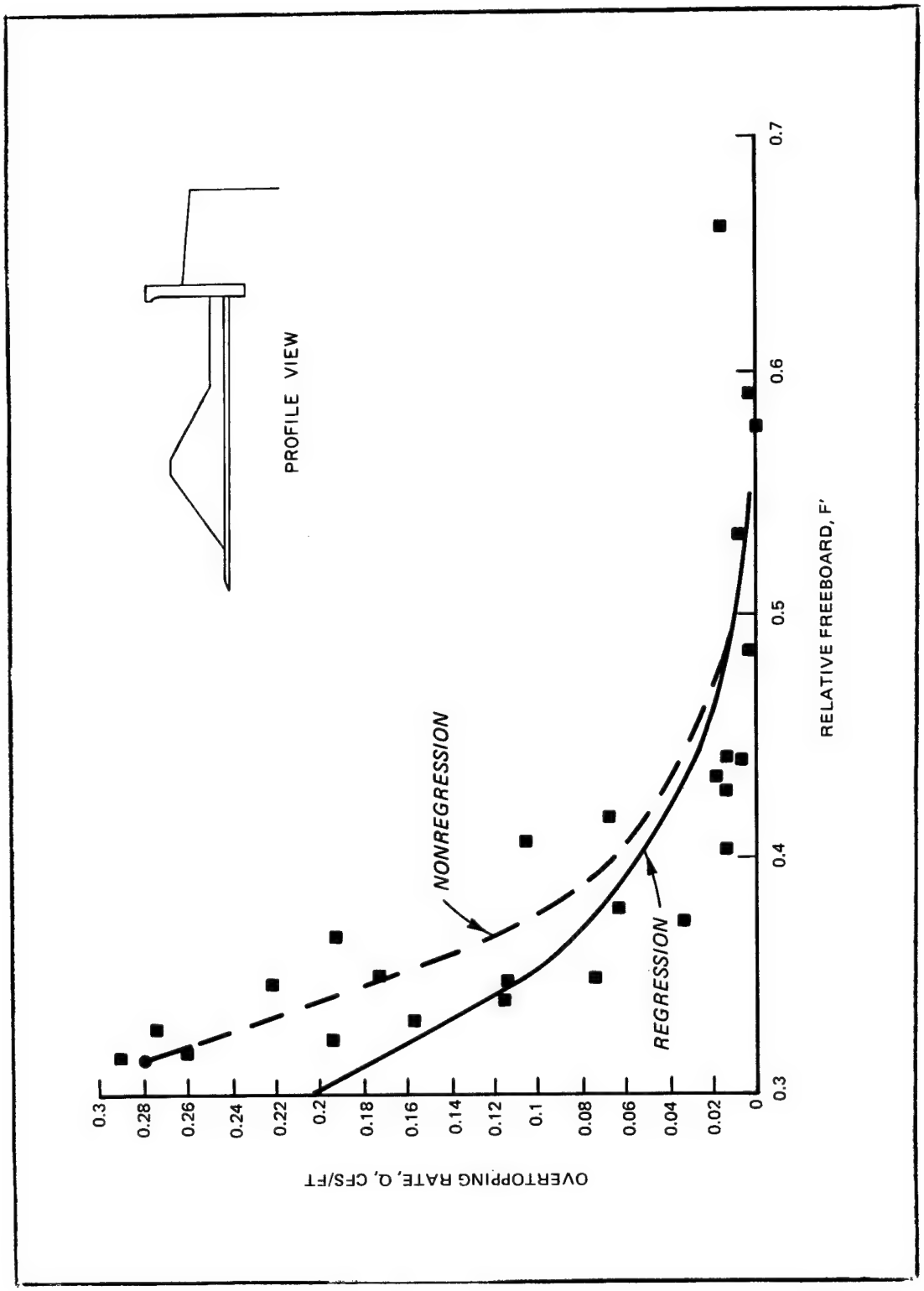
PROFILE VIEW
NONREGRESSION
REGRESSION
OVERTOPPING RATE, Q, CFS/FT
RELATIVE FREEBOARD, F'
0.3
0.28
0.26
0.24
0.22
0.2
0.18
0.16
0.14
0.12
0.1
0.08
0.06
0.04
0.02
0
0.3
0.4
0.5
0.6
0.7

PLATE 9

PLATE 10

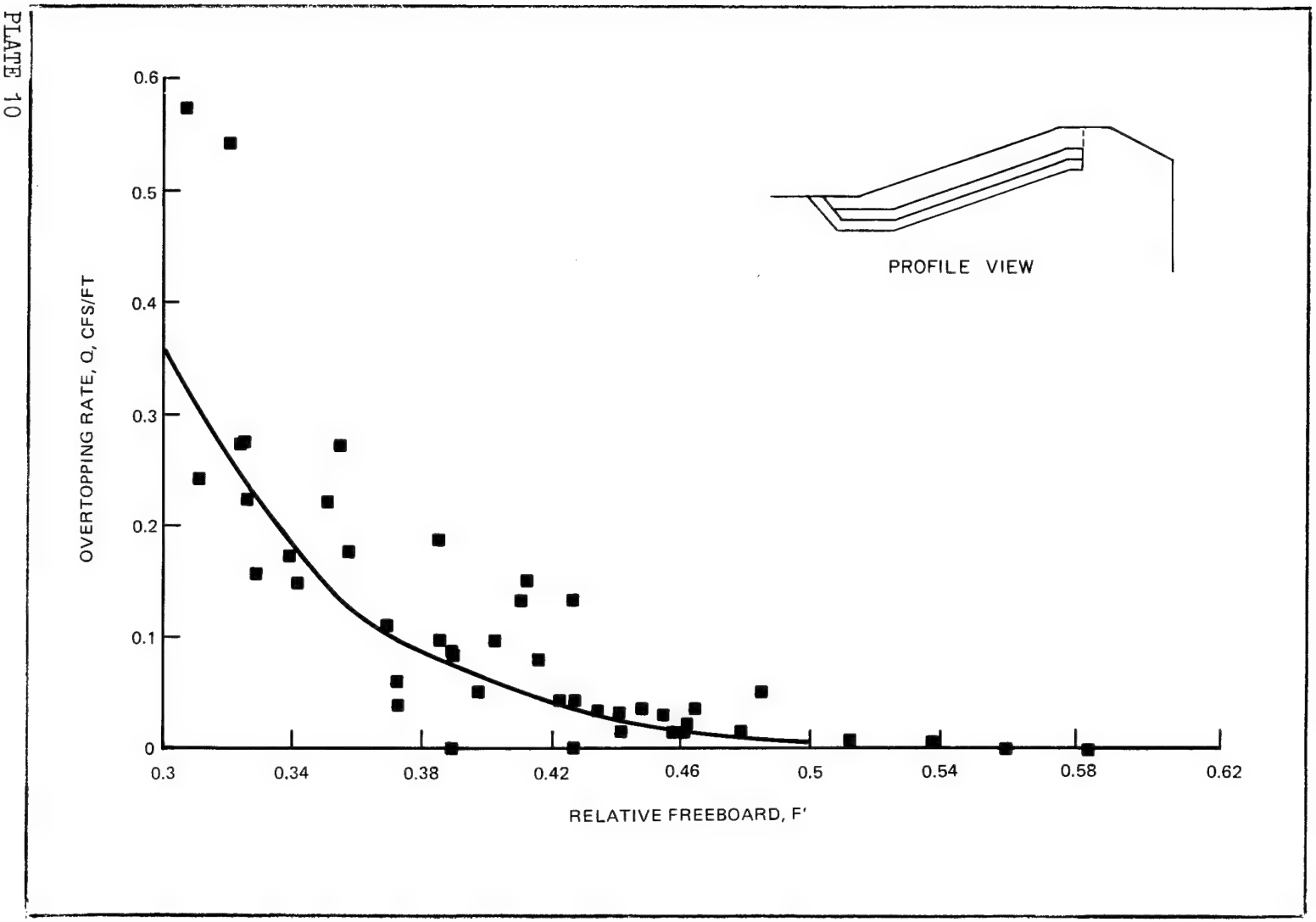
0.6
0.5
0.4
0.3
0.2
0.1
0
OVERTOPPING RATE, Q, CFS/FT
0.3
0.34
0.38
0.42
0.46
0.5
0.54
0.58
0.62
RELATIVE FREEBOARD, F'
PROFILE VIEW

APPENDIX A: DATA TABLES

Table A1

Seawall With No Revetment Data, Configuration 1

Test No.	Gage Seven Hmo ft.	Nom. Tp sec.	Gage Seven depth ft.	Nom. L ft.	SWL1 ft.	SWL2 ft.	Ave. FRBD ft.	Toe depth ft.	Ovtp. level1 ft.	Ovtp. level2 ft.	Ovtp. rate cfs/ft	Rel. Frbd. F/ws
1	5.55	8	12.464	154	2.031	2.027	9.136	8.944	0.327	0.341	0.033420	0.543734
2	6.8	8	12.456	154	2.031	2.026	9.144	8.936	0.341	0.383	0.100287	0.475287
3	6.97	8	12.52	154	2.031	2.034	9.08	9	0.383	0.431	0.114664	0.464255
4	7.15	8	12.472	154	2.034	2.025	9.128	8.952	0.431	0.486	0.131452	0.458843
5	5.79	9	12.472	175	2.031	2.028	9.128	8.952	0.486	0.514	0.066948	0.506108
6	6.79	9	12.44	175	2.031	2.024	9.16	8.92	0.514	0.573	0.141129	0.456705
7	7.22	9	12.464	175	2.031	2.027	9.136	8.944	0.573	0.64	0.160364	0.437238
8	7.82	9	12.424	175	2.031	2.022	9.176	8.904	0.64	0.72	0.191616	0.416392
9	4.09	10	12.496	195	2.031	2.031	9.104	8.976	0.729	0.734	0.011982	0.613863
10	4.08	10	12.488	195	2.031	2.03	9.112	8.968	0.734	0.74	0.014379	0.615406
11	5.76	10	12.408	195	2.031	2.02	9.192	8.888	0.74	0.77	0.071908	0.493306
12	6.76	10	12.448	195	2.031	2.025	9.152	8.928	0.77	0.83	0.143879	0.441441
13	7.21	10	12.416	195	2.031	2.021	9.184	8.896	0.83	0.91	0.191970	0.424355
14	7.44	10	12.4	195	2.031	2.019	9.2	8.88	0.91	0.97	0.144075	0.416288
15	5.88	7	12.472	133	2.031	2.028	9.128	8.952	0.97	0.971	0.002401	0.548917
16	6.58	7	12.448	133	2.031	2.025	9.152	8.928	0.97	0.987	0.040836	0.510600
17	6.92	7	12.416	133	2.031	2.021	9.184	8.896	0.987	1.01	0.055260	0.495462
18	7.29	7	12.408	133	2.031	2.02	9.192	8.888	1.01	1.033	0.055272	0.478969
19	6.21	7	12.424	133	2.031	2.022	9.176	8.904	1.033	1.047	0.033650	0.532077
20	6.31	8	12.448	154	2.031	2.025	9.152	8.928	1.06	1.085	0.060108	0.500022
21	6.35	9	12.448	175	2.031	2.025	9.152	8.928	1.081	1.131	0.120255	0.477149
22	6.51	10	12.432	195	2.031	2.023	9.168	8.912	1.131	1.18	0.117907	0.453463
23	7.93	9	12.424	175	2.031	2.022	9.176	8.904	1.179	1.257	0.187802	0.412532
24	4.84	7	13.224	137	2.078	2.075	8.376	9.704	0.102	0.109	0.016672	0.567849
25	6.24	7	13.176	137	2.078	2.069	8.424	9.656	0.109	0.129	0.047642	0.482119
26	6.6	7	13.168	137	2.078	2.068	8.432	9.648	0.129	0.168	0.092930	0.464886
27	6.76	7	13.152	137	2.078	2.066	8.448	9.632	0.168	0.228	0.143039	0.458369
28	4.56	8	13.248	158	2.078	2.078	8.352	9.728	0.228	0.244	0.038157	0.561817
29	6.05	8	13.144	158	2.078	2.065	8.456	9.624	0.244	0.348	0.248171	0.471095
30	6.49	8	13.176	158	2.078	2.069	8.424	9.656	0.348	0.396	0.114625	0.447853
31	6.87	8	13.16	158	2.078	2.067	8.44	9.64	0.396	0.489	0.222239	0.432001
32	4.95	9	13.168	180	2.078	2.068	8.432	9.648	0.489	0.505	0.038255	0.514165
33	6.08	9	13.16	180	2.078	2.067	8.44	9.64	0.505	0.591	0.205723	0.448727
34	7.16	9	13.072	180	2.078	2.056	8.528	9.552	0.591	0.723	0.316096	0.406581
35	7.4	9	13.096	180	2.078	2.059	8.504	9.576	0.739	0.863	0.297354	0.396623
36	4.96	10	13.152	201	2.078	2.066	8.448	9.632	0.863	0.896	0.079194	0.495869
37	6.23	10	13.176	201	2.078	2.069	8.424	9.656	0.896	0.989	0.223322	0.424744
38	7.13	10	13.024	201	2.078	-2.05	8.576	9.504	0.989	1.109	0.288435	0.395208
39	7.33	10	13.088	201	2.078	2.058	8.512	9.568	1.109	1.256	0.353814	0.385091
40	6.91	10	13.072	201	2.078	2.056	8.528	9.552	1.256	1.359	0.248210	0.401294
41	6.54	9	13.088	180	2.078	2.058	8.512	9.568	1.359	1.458	0.238803	0.431077
42	6.44	8	13.16	158	2.078	2.067	8.44	9.64	1.458	1.519	0.147255	0.451023
43	7.03	8	13.176	158	2.078	2.069	8.424	9.656	1.519	1.625	0.256092	0.424615
44	7.68	9	13.08	180	2.078	2.057	8.52	9.56	1.625	1.767	0.343476	0.387651
45	6.15	12	13.16	243	2.078	2.067	8.44	9.64	0.012	0.135	0.292873	0.402924
46	6.56	12	13.16	243	2.078	2.067	8.44	9.64	0.135	0.267	0.314695	0.385955
47	4.82	7	13.728	140	2.125	2.091	7.872	10.208	0.267	0.281	0.033400	0.531305
48	6.22	7	13.792	140	2.125	2.099	7.808	10.272	0.281	0.323	0.100229	0.444600
49	6.73	7	13.792	140	2.125	2.099	7.808	10.272	0.323	0.429	0.253141	0.421845
50	7.5	7	14.112	140	2.125	2.139	7.488	10.592	0.429	0.638	0.499885	0.376370

(Continued)

Table A1 (Concluded)

Test No.	Gage Seven Hmo ft.	Nom. Tp sec.	Gage Seven depth ft.	Nom. L ft.	SWL1 ft.	SWL2 ft.	Ave. FRBD ft.	Toe depth ft.	Ovtp. level1 ft.	Ovtp. level2 ft.	Ovtp. rate cfs/ft	Rel. Frbd. F/ws
51	4.74	8	13.912	162	2.139	2.1	7.688	10.392	0.638	0.679	0.098182	0.499792
52	6.24	8	13.992	162	2.125	2.124	7.608	10.472	0.679	0.809	0.311570	0.411758
53	7.85	8	14.4	162	2.125	2.175	7.2	10.89	0.809	1.294	1.165867	0.334385
54	7.55	8	14.296	162	2.175	2.112	7.304	10.776	1.294	1.56	0.641749	0.348143
55	5.1	9	13.832	184	2.125	2.104	7.768	10.312	1.56	1.649	0.215088	0.460952
56	6.47	9	14.2	184	2.125	2.15	7.4	10.68	0.029	0.35	0.765196	0.374705
57	7.69	9	14.36	184	2.15	2.145	7.24	10.84	0.35	0.791	1.055161	0.326724
58	7.95	9	14.36	184	2.145	2.15	7.24	10.84	0.791	1.28	1.175301	0.319561
59	5.01	10	14.392	206	2.15	2.149	7.208	10.872	0.21	0.28	0.166955	0.416837
60	6.55	10	14.264	206	2.149	2.134	7.336	10.744	0.28	0.535	0.609160	0.354821
61	7.4	10	14.096	206	2.134	2.128	7.504	10.576	0.535	0.84	0.730590	0.334592
62	8.21	10	13.952	206	2.125	2.119	7.648	10.432	0.039	0.289	0.595798	0.318197
63	6.97	12	13.728	250	2.125	2.091	7.872	10.208	0.289	0.44	0.360567	0.342465
64	6.98	12	14.176	250	2.125	2.147	7.424	10.656	0.44	0.784	0.823406	0.322666
65	3.84	7	14.176	140	2.147	2.125	7.424	10.656	0.784	0.787	0.007192	0.583052
66	2.68	8	13.96	162	2.125	2.12	7.64	10.44	0.787	0.788	0.002397	0.726382
67	6.84	8	13.928	162	2.125	2.116	7.672	10.408	0.788	1.011	0.535269	0.390570
68	2.86	9	14.016	184	2.125	2.127	7.584	10.496	1.011	1.025	0.033643	0.661782
69	NA	9	14.04	184	2.127	2.128	7.56	10.52	1.025	1.337	0.750941	NA
70	2.7	10	14.04	206	2.128	2.127	7.56	10.52	0.448	0.457	0.021509	0.660171
71	7.6	10	13.896	206	2.125	2.112	7.704	10.376	0.457	0.78	0.773188	0.337456
72	2.51	12	14	250	2.125	2.125	7.6	10.48	0.78	0.78	0	0.653207
73	8.05	9	13.744	184	2.125	2.093	7.856	10.224	0.78	1.146	0.879055	0.343873
74	4.44	7	14.736	143	2.172	2.17	6.864	11.216	0.011	0.039	0.066638	0.485895
75	8.11	7	14.496	143	2.172	2.14	7.104	10.976	0.039	0.197	0.376375	0.336545
76	7.57	8	14.648	166	2.172	2.159	6.952	11.128	0.197	0.526	0.785583	0.328102
77	8.55	8	14.496	166	2.172	2.14	7.104	10.976	0.526	0.946	1.006533	0.309140
78	8.82	7	15.056	143	2.172	2.21	6.544	11.536	0.946	1.931	2.376665	0.293147
79	4.01	8	14.672	166	2.172	2.162	6.928	11.152	0.441	0.51	0.164940	0.499431
80	4.55	9	14.744	189	2.172	2.171	6.856	11.224	0.51	0.568	0.138731	0.435086
81	7.83	9	14.504	189	2.172	2.141	7.096	10.984	0.025	0.411	0.920398	0.313582
82	9.05	9	14.288	189	2.172	2.114	7.312	10.768	0.411	0.886	1.137374	0.293393
83	4.23	10	14.416	211	2.172	2.13	7.184	10.896	0.886	0.913	0.064808	0.461365
84	7.86	10	14.248	211	2.172	2.109	7.352	10.728	0.016	0.328	0.743615	0.312389
85	8.59	10	14.424	211	2.172	2.131	7.176	10.904	0.328	0.783	1.088499	0.287381
86	7	12	14.416	256	2.172	2.13	7.184	10.896	0.571	0.786	0.514961	0.309186
87	7.83	12	14.392	256	2.172	2.127	7.208	10.872	0.206	0.578	0.888522	0.287890
88	3.93	5	14.56	96	2.172	2.148	7.04	11.04	0.578	0.583	0.011964	0.617381
89	6.9	5	15.224	96	2.172	2.231	6.376	11.704	0.583	0.75	0.399946	0.384201
90	8.38	7	14.883	143	2.231	2.13	6.712	11.368	0.176	0.529	0.842816	0.311107

Table A2

Standard Revetment Seawall Data, Configuration 2

Test No.	Gage Seven Hmo ft.	Nom. Tp sec.	Gage Seven Depth ft.	Mon. Lp Gage Seven ft.	SWL1 ft.	SWL2 ft.	Ave. FRBD ft.	Toe Depth ft.	Ovtp. level1 ft.	Ovtp. level2 ft.	Ovtp. rate cfs/ft	Relative Frbd. F/ws
92	3.78	8	12.488	154	2.021	2.04	9.112	8.968	0.064	0.099	0.046302	0.700666
93	7.53	8	12.408	153	2.04	2.011	9.192	8.888	0.099	0.146	0.062202	0.446888
94	7.81	8	12.336	153	2.021	2.021	9.264	8.816	0.146	0.227	0.107267	0.439950
95	6.43	7	12.336	132	2.021	2.021	9.264	8.816	0.227	0.227	0	0.525824
96	7.55	7	12.248	132	2.021	2.01	9.352	8.728	0.227	0.246	0.025173	0.477439
97	7.35	7	12.264	132	2.021	2.012	9.336	8.744	0.246	0.288	0.055663	0.485135
98	6.01	9	12.184	173	2.012	2.011	9.416	8.664	0.288	0.318	0.039773	0.511551
99	6.96	9	12.168	173	2.021	2	9.432	8.648	0.318	0.381	0.083562	0.464757
100	8.12	9	12.256	173	2.021	2.011	9.344	8.736	0.381	0.468	0.115480	0.414987
101	6.01	10	12.336	194	2.021	2.021	9.264	8.816	0.468	0.486	0.023904	0.484014
102	6.52	10	12.288	194	2.021	2.015	9.312	8.768	0.517	0.571	0.071761	0.461093
103	7.29	10	12.248	193	2.021	2.01	9.352	8.728	0.571	0.679	0.143635	0.430085
104	5.78	5	12.336	90	2.021	2.021	9.264	8.816	0.679	0.682	0.003992	0.643019
105	4.74	12	12.256	234	2.021	2.011	9.344	8.736	0.682	0.697	0.019961	0.537347
106	5.8	12	12.256	234	2.021	2.011	9.344	8.736	0.697	0.762	0.086535	0.469701
107	6.5	12	12.336	235	2.021	2.021	9.264	8.816	0.762	0.93	0.223913	0.431164
108	7.3	8	12.328	153	2.021	2.02	9.272	8.808	0.035	0.059	0.031739	0.460653
109	6.14	7	12.408	133	2.031	2.02	9.192	8.888	0.251	0.255	0.005300	0.537573
110	7.21	7	12.408	133	2.031	2.02	9.192	8.888	0.255	0.278	0.030482	0.482977
111	6.21	8	12.416	154	2.031	2.021	9.184	8.896	0.279	0.288	0.013255	0.507669
112	7.56	8	12.408	153	2.031	2.02	9.192	8.888	0.288	0.359	0.094150	0.445705
113	6.11	9	12.48	175	2.031	2.029	9.12	8.96	0.359	0.387	0.037147	0.488216
114	8.21	9	12.336	174	2.031	2.011	9.264	8.816	0.387	0.466	0.104863	0.408007
115	5.5	7	13.176	136	2.078	2.069	8.424	9.656	0.466	0.486	0.026560	0.525482
116	7.09	7	13.208	136	2.078	2.073	8.392	9.688	0.486	0.56	0.098319	0.441801
117	5.57	8	13.152	158	2.078	2.066	8.448	9.632	0.56	0.597	0.049185	0.497709
118	7.12	8	13.08	157	2.078	2.057	8.52	9.56	0.597	0.738	0.187601	0.426521
119	5.82	9	13.16	179	2.078	2.067	8.44	9.64	0.738	0.832	0.125210	0.462862
120	7.86	9	13.096	179	2.078	2.059	8.504	9.576	0.832	1.064	0.309519	0.381998
121	6.03	10	13.16	200	2.078	2.067	8.44	9.64	0.624	0.702	0.103775	0.435519
122	7.45	10	13.056	199	2.078	2.054	8.544	9.536	0.702	0.917	0.286453	0.383392
123	6.05	7	13.848	139	2.125	2.106	7.752	10.328	0.21	0.252	0.055644	0.450491
124	7.61	7	13.808	139	2.125	2.101	7.792	10.288	0.252	0.414	0.214841	0.388764
125	5.71	8	13.928	162	2.125	2.116	7.672	10.408	0.414	0.49	0.100906	0.440722
126	8.54	8	13.896	162	2.125	2.112	7.704	10.376	0.49	0.765	0.365747	0.338513
127	6.42	9	13.84	183	2.125	2.105	7.76	10.32	0.749	0.881	0.175878	0.395521
128	8.43	9	13.872	183	2.125	2.109	7.728	10.352	0.881	1.172	0.388528	0.328366
129	6.4	10	13.92	206	2.125	2.115	7.68	10.4	0.507	0.647	0.186107	0.377527
130	8.11	10	13.96	206	2.125	2.12	7.64	10.44	0.647	1.104	0.609271	0.320571
131	6.53	7	14.688	143	2.172	2.164	6.912	11.168	1.121	1.22	0.132364	0.378484
132	7.68	7	14.536	142	2.172	2.145	7.064	11.016	0.619	0.791	0.228930	0.347684
133	8.11	7	14.24	141	2.172	2.108	7.36	10.72	0.791	1.046	0.340107	0.350379
134	5.06	8	14.672	166	2.172	2.162	6.928	11.152	1.046	1.191	0.193769	0.379516
135	7.63	8	14.672	166	2.172	2.162	6.928	11.152	0.131	0.444	0.414911	0.325483
136	8.31	8	14.208	163	2.172	2.104	7.392	10.688	0.444	0.712	0.356265	0.329661
137	6.89	9	14.184	185	2.172	2.101	7.416	10.664	0.712	0.922	0.279812	0.359230
138	7.81	9	14.288	186	2.172	2.114	7.312	10.768	0.922	1.272	0.467621	0.325433
139	9.17	9	14.256	186	2.172	2.11	7.344	10.736	0.581	1.298	0.956495	0.293785
140	6.29	10	NA	NA	2.172	NA	NA	NA	0.797	NA	NA	NA
141	7.76	10	14.36	209	2.172	2.123	7.24	10.84	0.065	0.518	0.600517	0.311471

(Continued)

Table A2 (Concluded)

Test No.	Gage Seven Hmo ft.	Nom. Tp sec.	Gage Seven Depth ft.	Mon. Lp Gage Seven ft.	SWL1 ft.	SWL2 ft.	Ave. FRBD ft.	Toe Depth ft.	Ovtp. level1 ft.	Ovtp. level2 ft.	Ovtp. rate cfs/ft	Relative Frbd. F/ws
142	9.09	10	14.176	207	2.172	2.1	7.424	10.656	0.518	1.181	0.883686	0.288001
143	5.35	12	14.664	255	2.172	2.161	6.936	11.144	0.13	0.397	0.353850	0.357518
144	6.9	12	14.752	256	2.174	2.17	6.848	11.232	0.397	0.9	0.669121	0.297628
145	7.71	12	14.744	256	2.172	2.171	6.856	11.224	0.607	1.046	0.584995	0.276746
146	6.98	5	14.52	95	2.172	2.143	7.08	11	0.247	0.266	0.025178	0.424612
147	6.49	10	14.296	208	2.172	2.115	7.304	10.776	0.266	0.325	0.078216	0.354233

Table A3

Absorber/Revetment Seawall

Data, Configuration 3

Test No.	Gage Seven Hmo ft.	Nom. Tp sec.	Gage Seven depth ft.	Nom. Lp ft.	SWL1 ft.	SWL2 ft.	Ave. FRBD ft.	Toe depth ft.	Ovtp. level1 ft.	Ovtp. level2 ft.	Ovtp. rate cfs/ft	Rel. Frbd. F/ws
1	5.55	8	14.36	164.05	2.15	2.145	7.24	10.84	0.061	0.125	0.085	0.422
2	6.59	8	14.32	163.84	2.15	2.14	7.28	10.8	0.125	0.304	0.237	0.379
3	7.32	8	14.2	163.22	2.15	2.125	7.4	10.68	0.304	0.524	0.292	0.359
4	4.81	5	14.36	94.77	2.15	2.145	7.24	10.84	0.524	0.528	0.005	0.557
5	5.61	5	14.368	94.79	2.15	2.146	7.232	10.848	0.528	0.533	0.007	0.502
6	6.39	5	14.312	94.65	2.15	2.139	7.288	10.792	0.533	0.549	0.021	0.464
7	6.09	7	14.24	140.92	2.15	2.13	7.36	10.72	0.549	0.591	0.056	0.424
8	6.96	7	14.264	141.03	2.15	2.133	7.336	10.744	0.591	0.688	0.129	0.387
9	7.68	7	14.312	141.23	2.15	2.139	7.288	10.792	0.688	0.835	0.196	0.360
10	6.05	9	14.16	185.19	2.15	2.12	7.44	10.64	0.855	0.984	0.172	0.393
11	7.2	9	14.16	185.19	2.15	2.12	7.44	10.64	0.984	1.225	0.322	0.350
12	8.03	9	14.32	186.15	2.15	2.14	7.28	10.8	1.225	1.678	0.607	0.318
13	5.97	10	14.168	207.25	2.15	2.121	7.432	10.648	0.045	0.35	0.404	0.382
14	6.82	10	14.2	207.47	2.15	2.125	7.4	10.68	0.35	0.665	0.418	0.348
15	7.39	10	14.16	207.19	2.15	2.12	7.44	10.64	0.665	1.075	0.547	0.331
16	5.72	8	13.456	159.28	2.1	2.082	8.144	9.936	1.075	1.13	0.073	0.470
17	6.86	8	13.408	159.02	2.1	2.076	8.192	9.888	1.13	1.214	0.112	0.419
18	6.71	8	13.984	162.09	2.1	2.148	7.616	10.464	1.214	2.179	1.297	0.393

Table A4

Riprap with Wide Berm Data, Configuration 4

Test No.	Gage Seven Hmo ft.	Nom. Tp sec.	Gage Seven depth ft.	Nom. L ft.	SWL1 ft.	SWL2 ft.	Ave. FRBD ft.	Toe depth ft.	Ovtp. level1 ft.	Ovtp. level2 ft.	Ovtp. rate cfs/ft	Rel. Frbd. F/ws
19	6.000	8	14.160	163.01	2.15	2.120	7.440	10.640	0.587	0.620	0.044	0.412
20	5.840	8	14.160	163.01	2.15	2.120	7.440	10.640	0.620	0.664	0.059	0.420
21	6.013	8	14.296	163.72	2.15	2.137	7.304	10.776	0.664	0.720	0.075	0.404
22	5.079	5	14.392	94.84	2.15	2.149	7.208	10.872	0.720	0.721	0.001	0.535
23	6.048	5	14.456	95.00	2.15	2.157	7.144	10.936	0.721	0.724	0.004	0.472
24	6.752	5	14.392	94.84	2.15	2.149	7.208	10.872	0.724	0.727	0.004	0.442
25	6.630	7	14.312	141.23	2.15	2.139	7.288	10.792	0.727	0.749	0.029	0.397
26	7.244	7	14.376	141.51	2.15	2.147	7.224	10.856	0.749	0.812	0.084	0.370
27	7.856	7	14.296	141.16	2.15	2.137	7.304	10.776	0.812	0.897	0.113	0.355
28	6.233	9	14.240	185.67	2.15	2.130	7.360	10.720	0.980	1.149	0.226	0.381
29	6.999	9	14.160	185.19	2.15	2.120	7.440	10.640	1.149	1.207	0.078	0.357
30	8.128	9	14.200	185.43	2.15	2.125	7.400	10.680	0.289	0.460	0.227	0.321
31	5.927	10	14.240	207.74	2.15	2.130	7.360	10.720	0.460	0.531	0.094	0.379
32	6.989	10	14.240	207.74	2.15	2.130	7.360	10.720	0.531	0.652	0.161	0.340
33	7.732	10	14.104	206.81	2.15	2.113	7.496	10.584	0.652	0.793	0.188	0.324
34	4.769	12	14.176	251.00	2.15	2.122	7.424	10.656	0.793	0.806	0.017	0.415
35	6.070	12	14.320	252.22	2.15	2.140	7.280	10.800	0.806	0.931	0.167	0.346
36	6.759	12	14.048	249.91	2.15	2.106	7.552	10.528	0.931	1.196	0.354	0.335
37	6.521	8	13.576	159.92	2.10	2.097	8.024	10.056	0.235	0.279	0.058	0.424
39	7.191	8	13.568	159.88	2.10	2.096	8.032	10.048	0.323	0.399	0.101	0.397
40	4.873	5	13.576	92.82	2.10	2.097	8.024	10.056	0.399	0.400	0.001	0.617
41	5.989	5	13.600	92.88	2.10	2.100	8.000	10.080	0.400	0.401	0.001	0.536
42	6.456	5	13.600	92.88	2.10	2.100	8.000	10.080	0.401	0.402	0.001	0.509
43	6.106	7	13.600	138.11	2.10	2.100	8.000	10.080	0.402	0.407	0.007	0.483
44	6.939	7	13.600	138.11	2.10	2.100	8.000	10.080	0.407	0.420	0.017	0.425
45	7.460	7	13.584	138.04	2.10	2.098	8.016	10.064	0.420	0.454	0.045	0.406
46	6.315	9	13.528	181.30	2.10	2.091	8.072	10.008	0.454	0.502	0.064	0.417
47	7.116	9	13.544	181.40	2.10	2.093	8.056	10.024	0.502	0.573	0.094	0.385
48	7.764	9	13.448	180.80	2.10	2.081	8.152	9.928	0.573	0.673	0.133	0.368
49	5.713	10	13.560	203.01	2.10	2.095	8.040	10.040	0.673	0.685	0.016	0.428
50	6.800	10	13.528	202.78	2.10	2.091	8.072	10.008	0.685	0.740	0.073	0.383
51	6.819	10	13.552	202.95	2.10	2.094	8.048	10.032	0.740	0.795	0.073	0.381
52	4.660	12	13.599	246.05	2.10	2.100	8.001	10.079	0.795	0.795	.000	0.458
53	5.764	12	13.560	245.71	2.10	2.095	8.040	10.040	0.795	0.842	0.063	0.399
54	6.316	12	13.592	245.99	2.10	2.099	8.008	10.072	0.842	0.948	0.141	0.374

Table A5

Riprap with Two Berms Data, Configuration 5

Test No.	Gage Seven Hmo ft.	Nom. Tp sec.	Gage Seven depth ft.	Nom. L ft.	SWL1 ft.	SWL2 ft.	Ave. FRBD ft.	Toe depth ft.	Ovtp. level1 ft.	Ovtp. level2 ft.	Ovtp. rate cfs/ft	Rel. Frbd. F/ws
55	5.964	8	14.399	164.25	2.15	2.150	7.201	10.879	0.200	0.227	0.036	0.400
56	6.985	8	14.328	163.88	2.15	2.141	7.272	10.808	0.227	0.300	0.097	0.364
57	7.368	8	14.208	163.26	2.15	2.126	7.392	10.688	0.300	0.414	0.151	0.357
58	4.880	5	14.399	94.86	2.15	2.150	7.201	10.879	0.414	0.414	.000	0.549
59	5.806	5	14.392	94.84	2.15	2.149	7.208	10.872	0.414	0.417	0.004	0.489
60	6.456	5	14.399	94.86	2.15	2.150	7.201	10.879	0.417	0.417	.000	0.455
61	6.273	7	14.376	141.51	2.15	2.147	7.224	10.856	0.417	0.430	0.017	0.408
62	7.160	7	14.368	141.47	2.15	2.146	7.232	10.848	0.430	0.470	0.053	0.374
63	7.973	7	14.392	141.58	2.15	2.149	7.208	10.872	0.596	0.680	0.112	0.347
64	6.414	9	14.392	186.59	2.15	2.149	7.208	10.872	0.680	0.733	0.071	0.365
65	7.280	9	14.304	186.06	2.15	2.138	7.296	10.784	0.733	0.854	0.161	0.340
66	8.006	9	14.080	184.70	2.15	2.110	7.520	10.560	0.854	1.069	0.287	0.330
67	5.703	10	14.320	208.29	2.15	2.140	7.280	10.800	1.069	1.095	0.035	0.385
68	6.816	10	14.360	208.56	2.15	2.145	7.240	10.840	1.095	1.215	0.160	0.340
69	7.672	10	14.240	207.74	2.15	2.130	7.360	10.720	1.215	1.300	0.114	0.319
70	4.709	12	14.400	252.90	2.15	2.150	7.200	10.880	0.720	0.759	0.052	0.405
71	5.972	12	14.280	251.89	2.15	2.135	7.320	10.760	0.759	0.859	0.133	0.352
72	7.278	12	14.240	251.55	2.15	2.130	7.360	10.720	0.859	1.047	0.251	0.310
73	5.726	8	13.600	160.05	2.10	2.100	8.000	10.080	0.010	0.020	0.013	0.460
74	6.882	8	13.504	159.53	2.10	2.088	8.096	9.984	0.020	0.047	0.036	0.413

Table A6

Capped Seawall with Berm Data, Configuration 6

Test No.	Gage Seven Hmo ft.	Nom. Tp sec.	Gage Seven depth ft.	Nom. L ft.	SWL1 ft.	SWL2 ft.	Ave. FRBD ft.	Toe depth ft.	Ovtp. level1 ft.	Ovtp. level2 ft.	Ovtp. rate cfs/ft	Rel. Frbd. F/ws
76	5.828	8	14.399	164.25	2.15	2.150	7.201	10.879	0.030	0.096	0.087	0.406
77	7.040	8	14.360	164.05	2.15	2.145	7.240	10.840	0.096	0.152	0.074	0.360
78	7.809	8	14.352	164.01	2.15	2.144	7.248	10.832	0.152	0.226	0.098	0.336
79	5.157	5	14.400	94.86	2.15	2.150	7.200	10.880	0.226	0.227	0.001	0.529
80	6.241	5	14.400	94.86	2.15	2.150	7.200	10.880	0.227	0.228	0.001	0.466
81	6.945	5	14.240	94.48	2.15	2.130	7.360	10.720	0.245	0.282	0.049	0.444
82	6.780	7	14.400	141.61	2.15	2.150	7.200	10.880	0.290	0.298	0.011	0.386
83	7.514	7	14.400	141.61	2.15	2.150	7.200	10.880	0.298	0.320	0.029	0.360
84	8.250	7	14.208	140.78	2.15	2.126	7.392	10.688	0.320	0.440	0.159	0.348
85	6.467	9	14.256	185.77	2.15	2.132	7.344	10.736	0.440	0.476	0.048	0.371
86	7.549	9	14.232	185.62	2.15	2.129	7.368	10.712	0.476	0.557	0.108	0.336
87	8.445	9	14.240	185.67	2.15	2.130	7.360	10.720	0.557	0.690	0.177	0.311
88	6.201	10	14.320	208.29	2.15	2.140	7.280	10.800	0.690	0.710	0.027	0.364
89	7.239	10	14.328	208.34	2.15	2.141	7.272	10.808	0.710	0.788	0.104	0.328
90	7.946	10	14.248	207.80	2.15	2.131	7.352	10.728	0.788	0.878	0.120	0.312
91	4.952	12	14.304	252.09	2.15	2.138	7.296	10.784	0.878	0.898	0.027	0.398
92	5.918	12	14.240	251.55	2.15	2.130	7.360	10.720	0.898	0.985	0.116	0.356
93	6.786	12	14.264	251.75	2.15	2.133	7.336	10.744	0.985	1.103	0.158	0.324

Table A7

Capped Seawall with Wide Berm Data, Configuration 7

Test No.	Gage Seven Hmo ft.	Nom. Tp sec.	Gage Seven depth ft.	Nom. L ft.	SWL1 ft.	SWL2 ft.	Ave. FRBD ft.	Toe depth ft.	Ovtp. level1 ft.	Ovtp. level2 ft.	Ovtp. rate cfs/ft	Rel. Frbd. F/ws
121	8.102	9	12.792	176.64	2.05	2.049	8.808	9.272	0.201	0.219	0.024	0.389
122	7.258	7	12.720	134.08	2.05	2.040	8.880	9.200	0.219	0.223	0.005	0.463
123	6.047	5	12.784	90.74	2.05	2.048	8.816	9.264	0.223	0.227	0.005	0.591
124	7.296	8	12.760	155.46	2.05	2.045	8.840	9.240	0.227	0.238	0.015	0.437
125	5.877	12	12.800	238.98	2.05	2.050	8.800	9.280	0.238	0.245	0.009	0.435
126	6.451	10	12.776	197.37	2.05	2.047	8.824	9.256	0.245	0.259	0.019	0.437
127	7.181	9	12.768	176.48	2.05	2.046	8.832	9.248	0.259	0.265	0.008	0.423
128	7.727	8	14.360	164.05	2.15	2.145	7.240	10.840	0.321	0.395	0.098	0.338
129	6.841	8	14.312	163.80	2.15	2.139	7.288	10.792	0.395	0.453	0.077	0.370
130	5.886	8	14.424	164.38	2.15	2.153	7.176	10.904	0.453	0.479	0.035	0.402
131	6.460	5	14.440	94.96	2.15	2.152	7.160	10.920	0.479	0.479	0.000	0.452
132	5.932	5	14.384	94.83	2.15	2.146	7.216	10.864	0.479	0.471	-0.011	0.483
133	5.196	5	14.376	94.81	2.15	2.145	7.224	10.856	0.471	0.472	0.001	0.528
134	7.840	7	14.360	141.44	2.15	2.145	7.240	10.840	0.472	0.524	0.069	0.352
135	7.312	7	14.304	141.20	2.15	2.138	7.296	10.784	0.524	0.553	0.039	0.372
136	6.308	7	14.320	141.27	2.15	2.140	7.280	10.800	0.130	0.147	0.023	0.409
137	6.286	9	14.400	186.63	2.15	2.150	7.200	10.880	0.147	0.180	0.044	0.370
138	7.390	9	14.240	185.67	2.15	2.130	7.360	10.720	0.180	0.266	0.114	0.340
139	8.140	9	14.288	185.96	2.15	2.136	7.312	10.768	0.410	0.537	0.169	0.317
140	7.658	10	14.272	207.96	2.15	2.134	7.328	10.752	0.537	0.562	0.033	0.318
141	7.088	10	14.312	208.24	2.15	2.139	7.288	10.792	0.562	0.714	0.202	0.333
142	6.008	10	14.368	208.62	2.15	2.146	7.232	10.848	0.714	0.730	0.021	0.369
143	6.895	12	14.280	251.89	2.15	2.135	7.320	10.760	0.730	0.864	0.179	0.320
144	5.901	12	14.304	252.09	2.15	2.138	7.296	10.784	0.864	0.943	0.105	0.354
145	4.880	12	14.352	252.49	2.15	2.144	7.248	10.832	0.943	0.960	0.023	0.399

Table A8

Double Capped Seawall with Wide Berm Data, Configuration 8

Test No.	Gage Seven Hmo ft.	Nom. Tp sec.	Gage Seven depth ft.	Nom. Lp ft.	SWL1 ft.	SWL2 ft.	Ave. FRBD ft.	Toe depth ft.	Ovtp. level1 ft.	Ovtp. level2 ft.	Ovtp. rate cfs/ft	Rel. Frbd. F/ws
146	6.481	5	14.408	94.883	2.152	2.149	7.192	10.888	0.100	0.120	0.026	0.454
147	8.041	7	14.360	141.439	2.150	2.145	7.240	10.840	0.120	0.135	0.020	0.346
148	7.963	8	14.288	163.675	2.150	2.136	7.312	10.768	0.135	0.182	0.062	0.335
149	8.604	9	14.280	185.912	2.150	2.135	7.320	10.760	0.182	0.265	0.110	0.305
150	7.749	10	14.304	208.180	2.150	2.138	7.296	10.784	0.265	0.352	0.115	0.314
151	6.869	12	14.344	252.426	2.150	2.143	7.256	10.824	0.352	0.456	0.138	0.318
152	5.878	12	14.336	252.359	2.150	2.142	7.264	10.816	0.456	0.510	0.072	0.353
153	7.070	10	14.288	208.071	2.150	2.136	7.312	10.768	0.510	0.555	0.060	0.335
154	7.091	9	14.216	185.526	2.150	2.127	7.384	10.696	0.555	0.616	0.081	0.351
155	6.920	8	14.320	163.841	2.150	2.140	7.280	10.800	0.616	0.655	0.052	0.366
156	7.767	7	14.352	141.404	2.150	2.144	7.248	10.832	0.708	0.725	0.023	0.355
157	5.981	5	14.400	94.864	2.150	2.150	7.200	10.880	0.725	0.725	.000	0.479
158	4.864	12	14.384	252.763	2.150	2.148	7.216	10.864	0.725	0.736	0.015	0.398
159	6.018	10	14.352	208.509	2.150	2.144	7.248	10.832	0.736	0.747	0.015	0.369
160	6.453	9	14.280	185.912	2.150	2.135	7.320	10.760	0.747	0.770	0.031	0.370
161	5.914	8	14.320	163.841	2.150	2.140	7.280	10.800	0.770	0.779	0.012	0.407
162	6.703	7	14.400	141.610	2.150	2.150	7.200	10.880	0.779	0.779	.000	0.359
163	5.194	5	14.400	94.864	2.150	2.150	7.200	10.880	0.779	0.779	.000	0.526

Table A9

Seawall with Beach Breakwater Data, Configuration 9

Test No.	Gage Seven Hmo ft.	Nom. Tp sec.	Gage Seven depth ft.	Nom. L ft.	SWL1 ft.	SWL2 ft.	Ave. FRBD ft.	Toe depth ft.	Ovtp. level1 ft.	Ovtp. level2 ft.	Ovtp. rate cfs/ft	Rel. Frbd. F/ws
94	7.648	8	14.280	163.63	2.15	2.135	7.320	10.760	0.133	0.300	0.221	0.345
95	6.016	8	14.280	163.63	2.15	2.135	7.320	10.760	0.300	0.380	0.106	0.405
96	7.035	8	14.264	163.55	2.15	2.133	7.336	10.744	0.380	0.525	0.193	0.365
97	5.162	5	14.344	94.73	2.15	2.143	7.256	10.824	0.525	0.531	0.008	0.533
98	6.042	5	14.272	94.55	2.15	2.134	7.328	10.752	0.531	0.533	0.003	0.485
106	6.809	5	14.400	94.86	2.15	2.150	7.200	10.880	0.041	0.046	0.007	0.439
107	7.175	7	14.368	141.47	2.15	2.146	7.232	10.848	0.046	0.071	0.033	0.373
108	8.011	7	14.320	141.27	2.15	2.140	7.280	10.800	0.071	0.127	0.074	0.349
109	8.481	7	14.280	141.09	2.15	2.135	7.320	10.760	0.127	0.214	0.115	0.338
110	6.998	9	14.344	186.30	2.15	2.143	7.256	10.824	0.214	0.300	0.114	0.347
111	8.106	9	14.200	185.43	2.15	2.125	7.400	10.680	0.300	0.446	0.194	0.322
112	8.403	9	14.208	185.48	2.15	2.126	7.392	10.688	0.470	0.689	0.291	0.314
113	5.750	10	14.400	208.84	2.15	2.150	7.200	10.880	0.689	0.737	0.064	0.378
114	7.330	10	14.240	207.74	2.15	2.130	7.360	10.720	0.737	0.855	0.157	0.329
115	7.856	10	14.216	207.58	2.15	2.127	7.384	10.696	0.855	1.050	0.260	0.316
116	4.658	12	14.280	251.89	2.15	2.135	7.320	10.760	1.050	1.101	0.068	0.416
117	6.026	12	14.312	252.16	2.15	2.139	7.288	10.792	1.101	1.230	0.172	0.348
118	6.733	12	14.272	251.82	2.15	2.134	7.328	10.752	1.230	1.435	0.275	0.325
101	7.168	8	12.792	155.64	2.05	2.049	8.808	9.272	0.580	0.590	0.013	0.440
102	7.516	8	12.792	155.64	2.05	2.049	8.808	9.272	0.590	0.600	0.013	0.427
103	5.106	5	12.776	90.72	2.05	2.047	8.824	9.256	0.600	0.612	0.016	0.662
104	6.047	5	12.784	90.74	2.05	2.048	8.816	9.264	0.612	0.614	0.003	0.591
105	6.254	5	12.792	90.76	2.05	2.049	8.808	9.272	0.614	0.614	.000	0.577
119	5.988	12	12.760	238.62	2.05	2.045	8.840	9.240	0.276	0.290	0.019	0.432
120	7.278	10	12.792	197.49	2.05	2.049	8.808	9.272	0.290	0.300	0.013	0.403

Table A10

Sheet-Pile Seawall with Standard Revetment

Data, Configuration 10

TEST NO.	Gage Seven Hmo ft.	Nom. Tp sec.	Gage Seven Depth ft.	Nom. Lp Gage Seven ft.	SWL1 ft.	SWL2 ft.	Ave. FRBD ft.	Toe Depth ft.	Ovtp. level1 ft.	Ovtp. level2 ft.	Ovtp. rate cfs/ft	Relative Frbd. F/ws
148	5.860	5	13.152	91.724	2.072	2.072	6.256	9.632	0.015	0.015	0.000	0.427
149	7.000	7	13.040	135.570	2.072	2.058	6.368	9.520	0.015	0.145	0.172	0.339
150	7.075	8	13.056	157.098	2.072	2.060	6.352	9.536	0.015	0.425	0.543	0.319
151	7.539	9	12.976	177.817	2.072	2.050	6.432	9.456	0.425	0.919	0.524	0.297
152	7.132	10	12.976	198.828	2.072	2.050	6.432	9.456	0.201	0.550	0.463	0.297
153	6.028	12	13.104	241.699	2.072	2.066	6.304	9.584	0.550	0.982	0.575	0.306
154	6.895	7	13.056	135.643	2.072	2.060	6.352	9.536	0.106	0.218	0.148	0.341
155	6.987	8	12.992	156.745	2.072	2.052	6.416	9.472	0.218	0.387	0.224	0.326
156	7.141	9	12.664	175.808	2.072	2.011	6.744	9.144	0.387	0.595	0.276	0.325
157	6.705	10	12.968	198.770	2.072	2.049	6.440	9.448	0.595	0.777	0.242	0.310
158	7.279	7	12.280	131.999	2.025	2.010	7.128	8.760	0.068	0.114	0.061	0.373
159	7.519	8	12.216	152.380	2.025	2.002	7.192	8.696	0.114	0.281	0.221	0.351
160	7.868	9	12.280	173.292	2.025	2.010	7.128	8.760	0.281	0.487	0.273	0.323
161	7.324	10	12.248	193.462	2.025	2.006	7.160	8.728	0.487	0.605	0.157	0.328
162	6.628	7	12.400	132.573	2.025	2.025	7.008	8.880	0.645	0.645	0.000	0.390
163	6.902	8	12.256	152.610	2.025	2.007	7.152	8.736	0.645	0.728	0.110	0.369
164	6.776	9	12.272	173.240	2.025	2.009	7.136	8.752	0.728	0.860	0.176	0.357
165	6.540	10	12.240	193.402	2.025	2.005	7.168	8.720	0.860	1.064	0.272	0.354
166	6.758	7	12.592	133.483	1.978	2.096	6.816	9.072	0.010	0.039	0.038	0.373
167	NA	8	11.088	145.712	1.978	1.908	8.320	7.568	0.039	0.190	0.200	NA
168	7.351	9	10.624	161.871	1.978	1.850	8.784	7.104	0.190	0.291	0.134	0.426
169	7.045	10	10.856	182.662	1.978	1.879	8.552	7.336	0.291	0.392	0.134	0.410
170	6.451	7	11.424	127.791	1.978	1.950	7.984	7.904	0.392	0.402	0.013	0.457
171	6.566	8	11.480	148.075	1.978	1.957	7.928	7.960	0.402	0.435	0.044	0.427
172	7.035	9	11.520	168.172	1.978	1.962	7.888	8.000	0.435	0.501	0.088	0.389
173	6.796	10	11.488	187.658	1.978	1.958	7.920	7.968	0.501	0.575	0.098	0.386
174	7.026	8	11.584	148.694	1.978	1.970	7.824	8.064	0.575	0.648	0.097	0.403
175	5.523	5	11.648	87.531	1.978	1.978	7.760	8.128	0.040	0.040	0.000	0.559
176	6.602	7	11.576	128.554	1.978	1.969	7.832	8.056	0.040	0.063	0.030	0.441
177	6.724	8	11.568	148.599	1.978	1.968	7.840	8.048	0.063	0.124	0.081	0.415
178	7.190	9	11.400	167.345	1.978	1.947	8.008	7.880	0.124	0.188	0.085	0.390
179	6.782	10	11.008	183.879	1.978	1.898	8.400	7.488	0.188	0.302	0.151	0.412
180	6.158	12	11.512	227.061	1.978	1.961	7.896	7.992	0.302	0.443	0.187	0.385
181	5.183	5	11.648	87.531	1.978	1.978	7.760	8.128	0.428	0.428	0.000	0.584
182	6.194	7	11.560	128.474	1.978	1.967	7.848	8.040	0.428	0.439	0.015	0.461
183	6.546	8	11.576	148.646	1.978	1.969	7.832	8.056	0.439	0.471	0.042	0.423
184	6.627	9	11.656	169.103	1.978	1.979	7.752	8.136	0.471	0.509	0.050	0.397
185	5.411	5	10.888	85.219	1.931	1.930	8.520	7.368	0.045	0.045	0.000	0.628
186	6.065	7	10.896	125.089	1.931	1.931	8.512	7.376	0.045	0.050	0.007	0.512
187	6.656	8	10.832	144.140	1.931	1.923	8.576	7.312	0.050	0.066	0.021	0.462
188	6.925	9	10.784	163.018	1.931	1.917	8.624	7.264	0.066	0.091	0.033	0.435
189	6.823	10	10.336	178.426	1.931	1.861	9.072	6.816	0.091	0.118	0.036	0.448
190	5.297	12	10.872	220.862	1.931	1.928	8.536	7.352	0.118	0.144	0.034	0.465
191	4.824	5	10.896	85.244	1.931	1.931	8.512	7.376	0.144	0.144	0.000	0.677
192	5.637	7	10.896	125.089	1.931	1.931	8.512	7.376	0.163	0.167	0.005	0.537
193	6.243	8	10.888	144.486	1.931	1.930	8.520	7.368	0.167	0.177	0.013	0.479
194	6.436	9	10.816	163.246	1.931	1.921	8.592	7.296	0.177	0.199	0.029	0.454
195	6.268	10	10.888	182.919	1.931	1.930	8.520	7.368	0.199	0.210	0.015	0.442
196	5.189	12	10.656	218.725	1.931	1.901	8.752	7.136	0.210	0.249	0.052	0.485

APPENDIX B: ANALYSIS OF SAVILLE'S DATA

1. In addition to determining overtopping coefficients from the Roughans Point laboratory tests, some additional coefficients were derived from a previous study for use in estimated overtopping rates for the existing north wall at Roughans Point. The previous study was conducted by Saville (1955)* using monochromatic wave conditions on a variety of seawall configurations. While the degree of comparability between monochromatic and irregular wave overtopping tests is not fully understood, the coefficients determined from the earlier monochromatic tests were applied to existing seawall configurations for sheltered locations on Broad Sound (Reaches A through D, Figure 2, main text). Note that the monochromatic coefficients should not be used for locations exposed to the open coast. Monochromatic data trends were also similar to the irregular wave overtopping data trends, and the monochromatic coefficients exhibited logical tendencies. A_q for example, as shown in Table B1, is a measure of the amount of overtopping and tends to increase with increasing water depth, which is what logically should happen.

Table B1

Overtopping Coefficients for Saville's Monochromatic Data

Structure Configuration	Water Depth d_s, ft	Overtopping Coefficients $Q = Qe^{C_1F'}$ *		Configuration Overtopping Rating A_q**
		Q_o, ft^2/sec	C_1	
Vertical wall	0.0	3.47	-10.074	0.0168
	4.5	3.82	-5.762	0.1177
	9.5	10.58	-6.776	0.2045
Riprap 1 on 1.5	0.0	6.88	-11.434	0.0195
	4.5	8.66	-9.751	0.0476
	9.0	18.86	-9.762	0.1033

* The range of F' is from 0.094 to 1.277.
** See paragraph 17.

* References cited in this appendix are included in the References at the end of the main text.

2. The monochromatic wave conditions considered included two seawall configurations at three different water levels. Because of the wide range in water levels, the data were analyzed as six distinct subsets. The structure configurations were a vertical wall and a riprap armored seawall with a slope of 1 on 1.5. Both structures had 1 on 10 fronting slopes, and the water depths tested were deep at the toes of the structures.

3. In Saville's test report (Saville 1955), the local wave height near the structure is not given. Therefore, the local wave height had to be calculated in order to develop coefficients as consistent as possible with those determined from the irregular wave tests. Using the deepwater height and period, the wave height and wave length in a depth of 13.5 ft was calculated using linear wave theory. A depth of 13.5 ft represents a water depth within the range used to develop the overtopping coefficients for the irregular wave tests. The estimated wave height and wave length in 13.5 ft of water was used to calculate the dimensionless freeboard F' (see Equation 1). The range of wave heights was from 2.75 to 13.32 ft, and the range of wave periods was from 2.96 to 15.00 sec. The overtopping coefficients from Saville's tests are given in Table B1. These monochromatic wave coefficients cannot be compared directly to the coefficients given in Table 1 (in main text) for irregular waves; however, they can be used to evaluate the relative effectiveness of the six structure configurations/swl permutations.

APPENDIX B

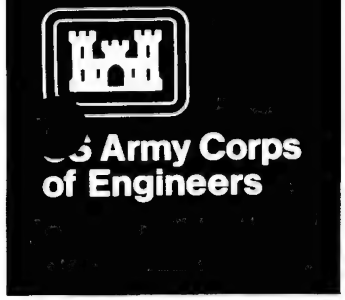

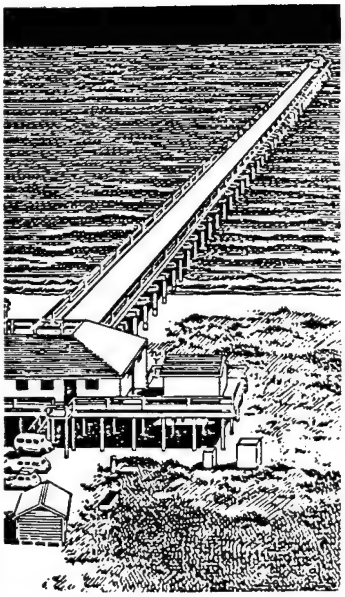

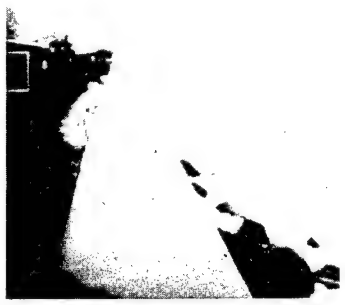

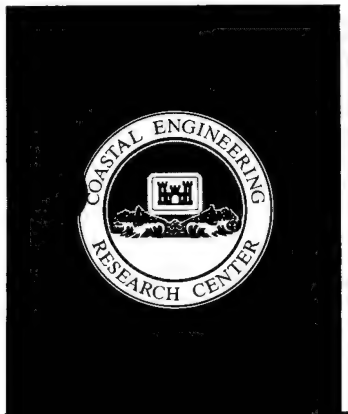

TECHNICAL REPORT CERC-86-8

FREQUENCY OF COASTAL FLOODING AT ROUGHANS POINT, BROAD SOUND, LYNN HARBOR, AND THE SAUGUS-PINES RIVER SYSTEM

by

Thomas A. Hardy, Peter L. Crawford

Coastal Engineering Research Center

DEPARTMENT OF THE ARMY
Waterways Experiment Station, Corps of Engineers
PO Box 631, Vicksburg, Mississippi 39180-0631

September 1986
Final Report

Approved For Public Release; Distribution Unlimited

Prepared for

US Army Engineer Division, New England
Waltham, Massachusetts 02254-9149

20. ABSTRACT (Continued)

Northeaster all structure combinations tested would be ineffective at protecting the interior of Roughans Point. Tests were conducted to determine a structure height for the north wall. These tests indicated that significant overtopping did not begin until the north wall structure was lowered below 13 ft National Geodetic Vertical Datum (NGVD). Since the existing height of the north wall is above this level at several sections, it is recommended that the revetment height be set at 13 ft NGVD with the wall height set so that there is a transition between the existing wall heights.

For areas where stage-frequency curves are presented for the still-water level resulting from the combination of storm surge and astronomical tide, only the storm surge and probability models were necessary. These areas include both open coast and estuarine locations. For areas flooded by the still-water level, results of the modeling indicated that the whole study area floods to approximately the same level. Flood levels are efficiently conveyed through the inlet and throughout the flood plain of the Saugus-Pines River system. Inside the inlet, there is a small gradient in the still-water level, rising from north to south, which results from local setup caused by north to northeast wind directions which predominate during storm conditions. This local wind setup results in flood levels inside the inlet which differ by one-half to three-fourths of a foot during the more severe storm events. Outside the river system in Broad Sound a smaller north-south gradient exists with differences of only a few tenths of a foot resulting. Data collected by the US Army Engineer Division, New England, after completion of the modeling indicated that losses do occur as flood levels propagate upstream of the Fox Hill Drawbridge on the Saugus River and upstream of the Highway embankment on the Pines River. Stage-frequency curves for these areas were adjusted to accommodate these additional data. The curves were lowered 0.3 and 0.5 ft at the lower return periods for upstream Saugus River and Pines River locations, respectively. Reductions were reduced for higher return periods because higher flood levels would provide greater access of floodwaters to these areas.

The setup and operation of all models, except the physical model, are described. The method of constructing stage-frequency curves is explained, and estimates of the error involved in each of the processes are discussed. The final products are curves which relate flood stage to frequency of occurrence for several possible structures at Roughans Point as well as for several coastal and river areas.

PREFACE

The US Army Engineer Division, New England (NED) requested the US Army Engineer Waterways Experiment Station (WES) Coastal Engineering Research Center (CERC) to conduct numerical and physical model studies to determine the frequency of flood levels at Roughans Point and at other coastal areas in Revere, Saugus, and Lynn, Massachusetts. The studies were conducted principally to provide greater confidence in the flood protection plan for Roughans Point as presented in the planning report (NED 1983) and were part of a larger study, "Continuing Planning and Engineering Studies for Roughans Point," provided for under the 12 September 1969 Southeastern New England authorization of the US Senate Committee on Public Works. A small funding contribution came from Revere Backshore planning studies conducted under the same authority.

This report contains the results of the numerical investigations conducted between May 1984 and December 1985. Close consultation and cooperation were maintained between CERC and NED throughout the study, and the efforts of Mr. Charles Wener, NED, were particularly important in its successful completion.

Work was performed by personnel of the Research Division (CR), CERC, under the direction of Dr. James R. Houston, former Chief, CR. Mr. Thomas A. Hardy, Coastal Processes Branch (CR-P), was the Principal Investigator for this study under the direction of Mr. H. Lee Butler, former Chief, CR-P, and current Chief, CR. Mr. Hardy was responsible for the probability modeling, storm surge modeling, flood routing, and synthesis of the total modeling effort. Mr. Peter L. Crawford, Coastal Oceanography Branch (CR-O), was responsible for the wave modeling. Mr. Crawford worked under the direction of Dr. E. F. Thompson, Chief, CR-O. Upon completion of the study, Chief and Assistant Chief, CERC, were Dr. Houston and Mr. Charles C. Calhoun, Jr., respectively. This report was edited by Ms. Shirley A. J. Hanshaw, Information Products Division, Information Technology Laboratory, WES.

COL Allen F. Grum, USA, was the previous Director of WES. COL Dwayne G. Lee, CE, is the present Commander and Director. Dr. Robert W. Whalin is Technical Director.

CONTENTS

CONVERSION FACTORS, NON-SI TO SI (METRIC)
UNITS OF MEASUREMENT

Non-SI units of measurement used in this report can be converted to SI (metric) units as follows:

Multiply	By	To Obtain
acres	4,046.873	square meters
cubic feet per second	0.02831685	cubic meters per second
feet	0.3048	meters
knots (international)	1.8532	kilometers per hour
miles (US statute)	1.609344	kilometers
square miles (US statute)	2.589988	square kilometers

FREQUENCY OF COASTAL FLOODING AT ROUGHANS POINT, BROAD SOUND, LYNN HARBOR, AND THE SAUGUS-PINES RIVER SYSTEM

PART I: INTRODUCTION

1. The study area was located in the cities of Revere, Lynn, and Saugus, Massachusetts, which are immediately north of Boston. Roughans Point (Figure 1) is a 55-acre* residential area which is below the elevation of a spring tide at many locations. Seawalls along both the northern and eastern boundaries offer some protection against coastal flooding. However, damage resulting from flooding caused when waves overtop the seawalls is a frequent occurrence. The Saugus and Pines Rivers join just before passing under the General Edwards Bridge and out into Broad Sound. The lower 2,500 acres of the drainage area just behind Revere Beach are mostly river channel and marsh. This area borders residential, commercial, and industrial areas, many of which are at an elevation only a few feet greater than the elevation of the maximum astronomical tide. Flooding is caused by the inundation of low lying areas by the combination of astronomical tide and storm surge. The Revere Beach-Point of Pines-Lynn Harbor region is made up of recreational beaches, residential and industrial land protected by seawalls, and harbor areas. Flooding results from overtopping of seawalls and dunes by storm waves. Figure 2 is a map of the study area vicinity showing the above locations.

2. The desired products of this project are stage-frequency curves which relate the elevation of floodwaters to the average waiting time between floods of equal or greater severity. The ordinate of these curves is stage, measured in feet above the National Geodetic Vertical Datum (NGVD), and the abscissa is return period expressed in years. The primary goal of this study initially was to provide flood frequencies at Roughans Point where flooding is caused by the overtopping of seawalls by storm waves. The numerical model efforts needed to predict waves and water levels at Roughans Point could also predict these quantities at nearby locations. Therefore, the scope of the project was expanded to provide flood frequencies for the Saugus-Pines River

---

* A table of factors for converting non-SI units of measurement to SI (metric) units is presented on page 3.

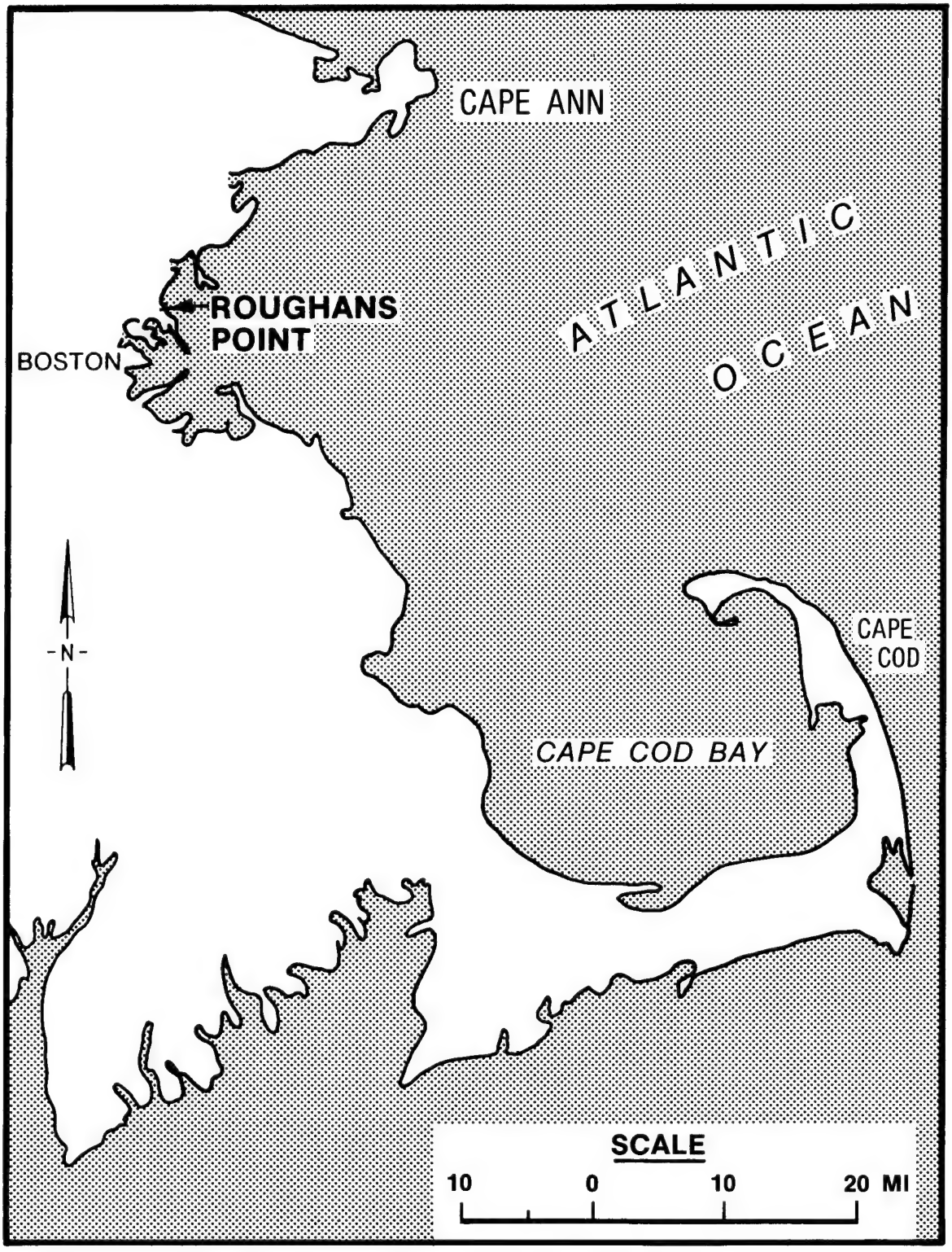

Figure 1. Location of study area

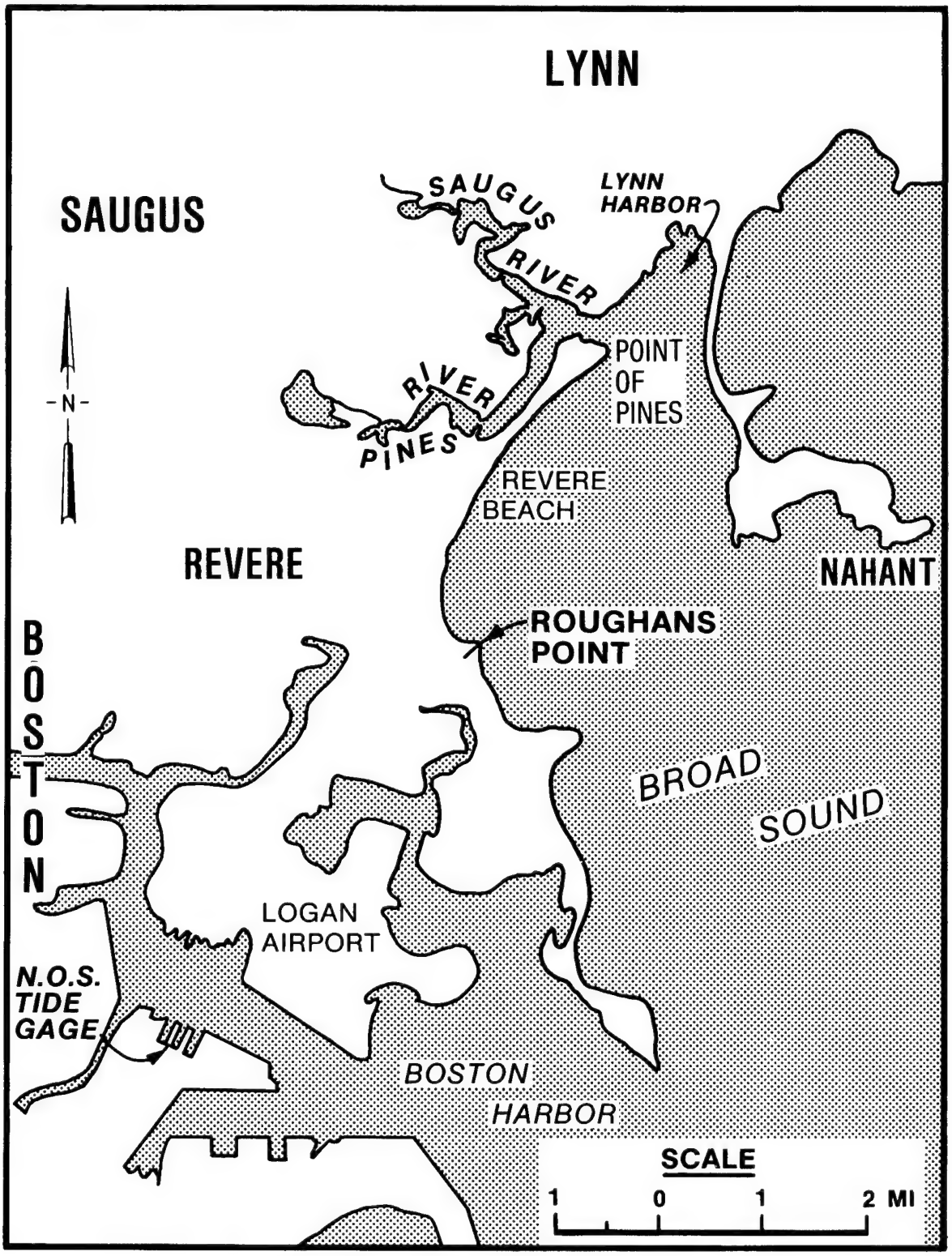

Figure 2. Study area vicinity

System, as well as wave and water level information, and techniques which could be used for future overtopping studies at Point of Pines and Lynn Harbor. The study was then divided into two main sections, determined by whether the cause of the water levels was due to wave overtopping or combined surge and tide. Roughans Point was the only location where stage-frequency curves were generated for flooding resulting from wave overtopping. For the Saugus-Pines River System, flooding results from the inundation of low lying areas by the combination of storm surge and astronomical tide. Even though flooding at Revere Beach, Point of Pines, and Lynn Harbor is caused mostly by wave overtopping, only the still-water level frequency will be reported because the present study did not include investigation of overtopping for these areas. Wave overtopping for these areas will be estimated by US Army Engineer Division, New England (NED), in other studies using techniques and data developed by US Army Engineer Waterways Experiment Station (WES) Coastal Engineering Research Center (CERC) for the present study. Areas where the stage-frequency curves are based upon combined surge and tide levels, but include no wave effects, will be referred to as still-water level locations.

Terminology

3. To avoid excessive repetition and to provide greater clarity, the following terms are defined for use throughout this report.

Event	Storm plus tide
MSL	Mean sea level
NGVD	National Geodetic Vertical Datum (formerly called mean sea level datum of 1929)
Northeaster	Extra-tropical storm
Stage	Elevation of the still-water level above NGVD
Still-water Level	Elevation of surge plus tide water surface
Storm	The historical meteorology (wind, waves, and surge) independent of the tide with which it actually occurred
Surge	Storm-induced component of still-water level
Tide	Astronomical tide

Overview of Project Technique

4. The establishment of frequency curves required the conjunctive use of several modeling components. At Roughans Point the combined use of probability, numerical storm surge, numerical wave, physical, and flood routing models was required to produce the stage-frequency curves. Whereas, for the still-water locations (Saugus-Pines River and Revere Beach-Lynn Harbor areas) only the probability and numerical storm surge models were required. The following is a brief description of each model.

5. The probability model was designed to complete four tasks: select events for simulation by the other models, assign probabilities to these events, create stage-frequency curves, and determine a measure of confidence in the final results. The numerical storm surge model simulated the storm plus tide events producing a time-history of still-water levels at specific locations throughout the study area. A numerical, spectral wave model simulated the wave field which accompanied each of the events simulated by the storm surge model. Also, a monochromatic wave model estimated the locally generated waves which were not considered in the spectral model. The wave parameters of height, period, and direction were calculated at selected sites throughout the study area. The physical model determined coefficients for an overtopping rate equation by testing multiple combinations of water level and spectral wave characteristics for several existing and proposed structures at Roughans Point. The physical modeling is not fully described in this report. (For complete details of the physical modeling see Ahrens and Heimbaugh (in preparation). The flood routing model calculated the maximum stage in the interior of Roughans Point caused by each event. Maximum stage was determined after outflows from drainage, pumping, seepage, and weir flow over low lying boundaries were considered.

6. Figure 3 is a flow chart which depicts the conjunctive use of the above models for the establishment of stage-frequency curves. Basically, the probability model selected and assigned probability to the surge-tide-wave events simulated. Then, the surge model simulated the still-water level. At this point stage-frequency curves were generated for the still-water locations. To develop the flood levels caused by wave overtopping at Roughans Point, the wave, physical, and flood routing models were necessary. The wave model simulated the parameters, height, period, and direction. The output of

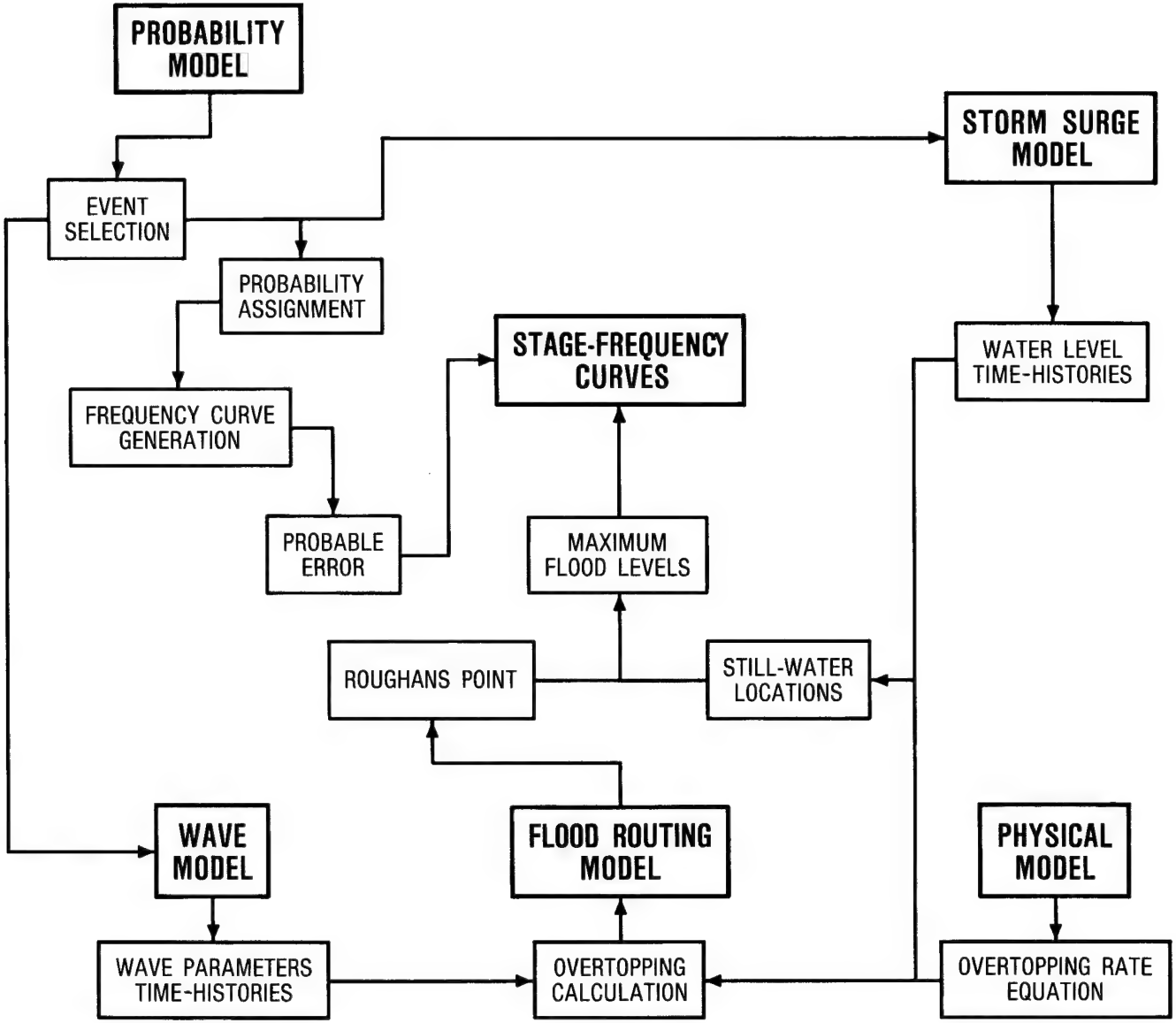

Figure 3. Flow chart of project technique

the two numerical models (surge and wave) were the main inputs to the physical model's overtopping rate equation which produced the overtopping rate for each required time-step. The water volume due to overtopping was then routed through the Roughans Point area, and a maximum stage was calculated for each event. Finally, a stage-frequency curve was created for flood levels induced by wave overtopping.

Organization of Report

7. This report is structured as follows. Part II is a description of the probability model. Modeling of the surge plus tide events is discussed in Part III, including calibration and verification of the storm surge model. Part IV is a description of the numerical wave modeling. The methods for calculating the overtopping rate time-histories and routing the flood through Roughans Point are discussed in Part V. The construction of stage-frequency curves is explained in Part VI. Part VII contains discussion of the results, including an estimate of the error in the stage-frequency curves. Because of the large volume of results generated by the numerical models, time-histories of ocean water levels, waves, winds, overtopping rates, and Roughans Point interior flood levels are not provided in this report but were given to NED on computer tape.

PART II: PROBABILITY MODEL

8. Unlike the physical model which simulates a physical process with physical operations and the numerical models which simulate physical processes with mathematical operations, the probability model does not simulate a physically realizable entity. The title 'model' is used for symmetry with the other components of this project. The probability model is essentially an assemblage with four specific tasks: select events for simulation by the other three models, assign probabilities to these events, create stage-frequency curves, and determine a measure of confidence in these curves.

9. Ideally, there would be a long historical data record of the desired quantity at the desired location (for example, 100 years of overtopping data at Roughans Point). For this ideal case modeling would not be necessary. An overtopping rate frequency curve could be created using well-established statistical techniques which can be found in any hydrology text. However, as is usually the case, sufficient data records for the quantities of interest were not available. Therefore, three separate modeling efforts, a physical overtopping model, a numerical storm surge model, and a numerical wave model were implemented to overcome the lack of data.

10. There are several possible approaches in establishing frequency curves where the scarcity of data in the immediate study area requires a modeling approach. The two most common are called the historical method and the joint probability method (JPM). In the historical method, a series of historical events is recreated with the pertinent data being saved in the necessary locations. In effect, it is like operating a time machine with the hindsight to know what data to collect and where to collect it. Probability is assigned to each event by a standard ranking method. For the JPM, the storm type is parameterized. For example, hurricane wind fields can be defined by three parameters, central pressure deficit, radius to maximum winds, and forward speed. Then, an ensemble of synthetic events is simulated representing those events which are possible in the study area. Probability is assigned to individual events by assigning probabilities to parameter values which determine that event. If the parameters are independent, then the probability of the event would be the product of the probabilities of the component parameters. Several studies have been conducted using the above two methods, including Meyers (1970) and Prater, Hardy, and Butler (in preparation). For the present

study, since hurricanes do not significantly contribute to stage-frequencies in the project area, and since northeasters are difficult to parameterize, a modification of the historical approach was used. Historical storm surge time-histories were combined randomly with tide time-histories to produce synthetic event water level time-histories. Probabilities were assigned using data from a nearby tide gage. This process is explained in detail in the following paragraphs.

Choosing Storm Surge Time-Histories

11. Regardless of the approach selected, data in the vicinity of the study area are essential for identifying inputs to the numerical modeling and for assigning probabilities. This project was fortunate in having convenient sources for the necessary data. The National Ocean Service's (NOS's) Boston tide gage has been in continuous service since 1922. This gage is located at Commonwealth Pier in Boston Harbor which is less than 5 miles from the study area. Wave hindcast information was available for deep water adjacent to the study area from the WES Wave Information Study (WIS). Hourly wind data were available from Logan International Airport which is less than 5 miles from the study area. The 20-year period from 1956-1975 was chosen from which to gather data for use in the numerical modeling. This period was selected because information was available from the above mentioned sources in all the necessary data categories: water level, wind, and wave.

12. By defining storm surge as the difference between measured water level and predicted tide, a partial duration series of storm surge time-histories (26 storms) was extracted from the Boston tide gage data. A minimum value of the maximum surge, 2.5 ft, was used to define those storms which had a reasonable probability of causing significant flooding. If surges much below the 2.5-ft level were combined with possible tides, it would be unlikely that any of the resulting events would be selected as one of the relatively small number of events to be modeled (only 150 events with water levels from 7.9 to 11.2-ft NGVD were selected). The value of 2.5 ft was chosen using the following guidance: with this surge level, only 5 percent (Harris 1981) of the hourly tide heights are high enough so that the combined surge plus tide would be greater than 7.9 ft NGVD. The combination of surge and tide and the selection of the events to be modeled are explained later in this report.

13. Two additional storms from outside the 1956-1975 period were included in the storm ensemble: 29 November 1945 and 6 February 1978. All the necessary data were obtainable for these storms which caused the first and second highest surges recorded at Boston. Furthermore, the February 1978 event caused the highest still-water level (10.3 ft NGVD) on record in Boston. Adding these two storms helped ensure the top end of the storm ensemble was representative of what could occur at Boston. Therefore, a total of 28 storms was chosen to represent the surge time-histories which are possible at Boston. Table 1 contains a list of these storms and their maximum surges. The maximum surges listed in Table 1 might differ slightly from maximum surges derived elsewhere. There are two reasons for these small discrepancies. First, great care was taken to use a set of tidal prediction constituents which best fits the tidal signal at Boston. With the large tidal range at Boston, slight errors in phase could cause significant errors in the calculated surge. Five separate sets of constituents received from NOS were tested, and the set of constituents with the best fit was used for these calculations. Second, often the maximum surge in historical storms occurs at low water because of the increase in surge with decreasing water level given constant wind speed and direction. Since the surges needed to be independent of their historic tide, the surge time-histories were edited by eye to remove 12-hour oscillations caused by this shallow-water effect.

Table 1

Historical Storms Chosen to Represent Possible Surges at Boston

Storm No.	Date	Maximum Surge ft	Storm No.	Date	Maximum Surge ft
1	11-30-45	4.8	15	4-13-61	4.4
2	1-9-56	3.3	16	3-7-62	2.5
3	3-16-56	3.3	17	12-6-62	2.7
4	4-8-56	2.6	18	2-19-64	2.7
5	1-8-58	2.9	19	1-23-66	3.1
6	1-15-58	2.7	20	1-30-66	3.6
7	2-16-58	3.6	21	12-25-66	2.9
8	3-15-58	2.8	22	2-9-69	3.4
9	3-21-58	3.2	23	12-27-69	3.2
10	4-2-58	2.7	24	2-4-72	2.9
11	12-29-59	2.6	25	2-19-72	4.0
12	2-19-60	2.5	26	11-9-72	2.8
13	3-4-60	3.7	27	12-16-72	3.2
14	1-20-61	3.4	28	2-6-78	4.7

Creating Synthetic Surge Plus Tide Events

14. Since the tidal range at Boston (mean range--9.5 ft and maximum range--14.6 ft) is much larger than the largest recorded surge (approximately 5 ft), the tide is a very important component of the total water level. Rather than numerically model the relatively small sample of historical events (surge plus tide), synthetic events were created by combining the historical storm surge time-histories with possible tide time-histories. The basic assumption behind this technique is that the surge time-history (edited to remove the shallow-water effect) of any storm is independent of the tide with which it occurs. In other words, the phenomena which cause tides are not related to the phenomena which cause storms. Therefore, a storm may occur with any tide that is possible during storm season.

15. Using tidal constituents from NOS analyses of the Boston tide gage, hourly tide heights for the winter season were predicted. The period from 15 October to 30 April was chosen as winter season, and 19 years of this seasonal record were generated to simulate a tidal epoch. Combining the 28 surge time-histories with every possible tide time-history during this tide series would result in more than 2.5 million combinations. Obviously, it would be economically impossible to simulate all these possibilities. Furthermore, it is not necessary to simulate a large percentage of the possibilities in order to adequately represent the population. In order to form a representative sample of the total ensemble, a random selection process was devised.

16. The 28 surge time-histories were combined with a large number of tide time-histories. Each of these synthetic surge plus tide time-histories was created from storm and tide time-histories by randomly choosing a starting point in the tide series, matching this point to the start of a storm, and adding the tide and surge levels at each hour for the length of the storm. The resulting large number of possible event time-histories served as the data set from which events were randomly selected for simulation by the numerical models. Each of the 26 storms, in the 20-year partial duration series of surge, was combined with 500 tide time-histories chosen at random from the 19-year tide series. Each of these storms was considered to have an equal likelihood of occurrence (each storm did, in fact, occur during the 20 years). The two additional storms (1945 and 1978) were not part of the 20-year partial

duration series and, therefore, did not have the same likelihood of occurrence as the other 26 members in the ensemble. Therefore, these two extra storms were combined with a fewer number of tides. To determine the number of events which should be formed using these two storms, the following simplified analysis was used. The 1945 and 1978 storms had the first and second largest surges in a 58-year annual series (the length of available data). Assuming a Weibull plotting position formula, $p = m/N+1$, where m is the rank and $N = 58$, the 1945 and the 1978 surges would have frequencies of 1/59 and 2/59, respectively. Assuming the other 26 members of the storm ensemble to have frequencies of 1/20, and using the ratios of these frequencies, the 1945 storm was combined with 170 tides and the 1978 storm with 340 tides. For example, $(1/59) / (1/20) \times 500 = 170$. This analysis is not rigorous from a statistical standpoint and was done primarily to prevent the two storms with the strongest winds and largest waves from being overrepresented at low and medium water levels. Approximately 13,500 possible surge plus tide time-histories resulted from this process ($26 \times 500 + 340 + 170$). Events to be simulated were selected from this file of possible surge plus tide time-histories.

Selecting Events to Model

17. A flood-causing event is multidimensional. The severity of the damage caused by the event is determined by several factors, among which are the magnitude and duration of winds, waves, and water levels. Because of the difficulty of ranking multidimensional entities, as well as the lack of available data for doing so, it is necessary to reduce the dimensionality. Therefore, only one dimension, maximum still-water level, was used to measure the severity of an event. This criterion was chosen for two main reasons. First, it was deemed the most important; and, second, there was a large volume of available data. NED has established a stage-frequency curve (Figure 4) at (NED 1983) relating maximum still-water level with its frequency of occurrence the Boston NOS tide gage. This stage-frequency curve was used as the basis for both event selection and the assignment of probability to simulated events.

18. Based upon previous experience (Prater, Hardy, and Butler, in preparation) it was estimated that by simulating 50 events the frequency of still-water level would be accurately represented throughout the study area.

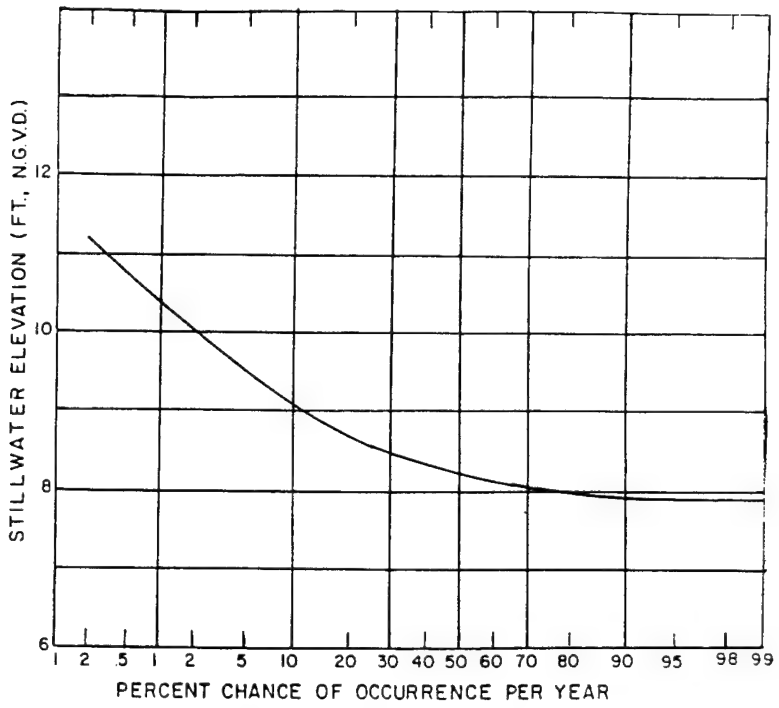

Figure 4. NED stage-frequency curve for Boston

still-water level would be accurately represented throughout the study area. However, the extra variables involved in simulating waves and wave overtopping volumes would cause added uncertainty in the final frequency curves at Roughans Point. Therefore, it was decided to simulate 150 events in order to increase the confidence that the frequency curves based upon overtopping calculations were accurate. The 150 events were selected and simulated, and then frequencies were calculated in three separate sets, each containing 50 events. This was done to establish a measure of confidence in the selection procedure. This confidence calculation will be explained in Part VI.

19. The selection process involved four steps. First, the stage increments, for which simulations were to be performed, were chosen. As previously mentioned, the highest still-water level on record for the Boston area is 10.3 ft NGVD, which occurred during the February 1978 northeaster. As predicted by the NED curve, the 500-year level is 11.2 ft NGVD, and the annual level is 7.9 ft NGVD. Events were selected to duplicate the NED stage-frequency curve below the 500-year level at the Boston gage. Therefore, given the small range in elevation and choosing three sets of 50 events, selections were made every 0.1 ft from 7.9 to 10.4 ft and every 0.2 ft from 10.4 to 11.2 ft. Next, the number of events to be selected at each stage increment

was decided. The results of these first two processes are shown in Table 2. Examining Table 2, it can be seen that more events were selected for the lower range of water levels (≈8 ft NGVD) than were selected for the higher water levels (above 10.5 ft NGVD). This was done for two reasons. First, the probability mass representing the lower part of the NED curve will be much larger than the probability mass representing the higher portion of the curve. This is caused by the logarithmic nature of the frequency of water levels. Experience has shown that frequency curves are more easily constructed when the probability masses assigned to simulated events vary as little as possible. For example, the probability mass per year associated with a 0.1-ft increment located at 8.0 ft on the NED curve is 0.14; whereas, the probability mass per year for a 0.2-ft increment at 11.2 ft is 0.00035. Therefore, more events were selected at the lower return periods to divide this large probability mass into smaller segments. Secondly, especially when considering overtopping, events formed from many more combinations are possible at the lower stages (large surge plus low tide plus medium waves, small surge plus medium tide plus large waves, etc). At the higher stages fewer combinations are possible (large surge plus large tide plus large waves). Consequently, the higher end of the curve can be represented by fewer events than can the lower end.

20. Choosing the stage increment sizes and the number of events selected for simulation from each increment is a subjective decision. This decision is based on the range of stages to be represented, the largest differences in probability tolerable for accurate curve generation, and the financial constraints on the number of events that can be simulated. Unfortunately, the only sure way to determine if the decisions are correct is to view the results. Therefore selections are made, and the goodness of these decisions is reflected in the error bands presented in Part VIII.

21. The third part of the selection process is the actual selection of events. The 13,500 possible events, created by combining the storm surge with tide, were ranked by the maximum water level that occurred during the surge plus tide time-history. At each of the stage increments shown in Table 2, events were randomly selected from the portion of the 13,500 events with maximum water level equal to that height increment. This was done independently for each of the three sets of 50 events. Although these maximum water levels are for the Boston NOS tide gage, events selected for simulation in the study

Center of Height Increment ft, NGVD	Number Selected	Center of Height Increment ft, NGVD	Number Selected
7.9	5	9.4	1
8.0	4	9.5	1
8.1	4	9.6	1
8.2	3	9.7	1
8.3	3	9.8	1
8.4	3	9.9	1
8.5	2	10.0	1
8.6	2	10.1	1
8.7	2	10.2	1
8.8	2	10.3	1
8.9	1	10.4	1
9.0	1	10.6	1
9.1	1	10.8	1
9.2	1	11.0	1
9.3	1	11.2	1

NOTE: These are the numbers of events selected for each set of 50 events. Total events selected at each height increment would be three times the numbers found in this table.

area were chosen from this ranked set. This method of transferring these surge plus tide time-histories to the study area was determined during calibration of the storm surge model (see Part III).

22. Figure 5 shows the fourth and final part of the selection process, the assignment of probability to the selected events. The probability p, represented by each stage increment, is calculated by taking the difference of the exceedance probabilities P of the end points of the increment. If more than one event was selected to represent that stage increment, then the probability assigned to that increment is divided equally among the chosen events. Table 3 contains the maximum water levels (predicted at the Boston gage) and the probabilities assigned to the three sets of selected events. The column in Table 3 labeled "Storm" refers to the numbering of the storms in Table 1. Note that since the selection process is random, not all the storms are represented in each of the three sets of 50 events (denoted as A, B, and C in Table 3), and the number of times a storm is chosen varies from set to set. In conclusion, the essence of the selection process is to choose events for simulation so that the stage-frequency curve, for a known location is

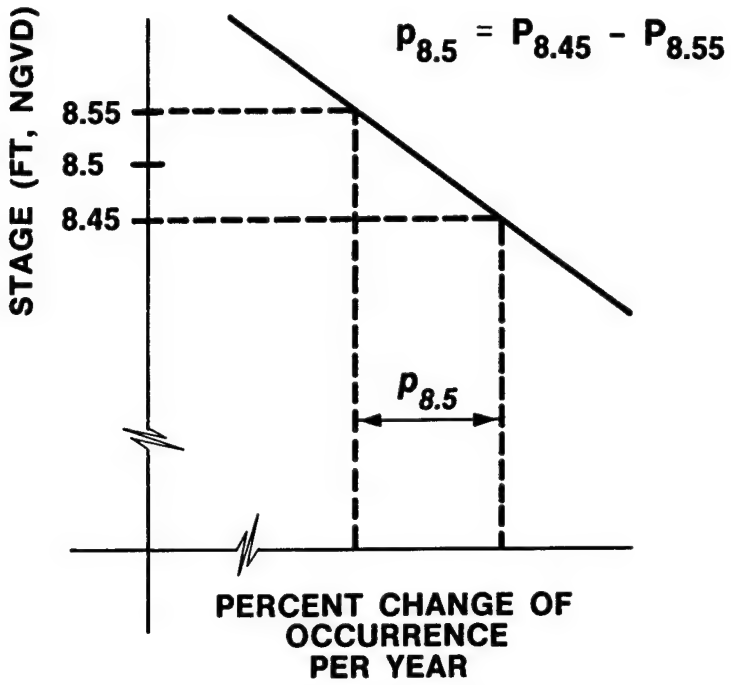

Figure 5. Assigning probabilities to events selected for simulation

duplicated by a limited number of events. When these events are simulated, the probability masses assigned to the events are used to construct stage-frequency curves throughout the modeled area.

Table 3

Events Selected for Modeling

Storm	Set A Max. Level ft, NGVD	Set A Prob.	Set B Max. Level ft, NGVD	Set B Prob.	Set C Max. Level ft, NGVD	Set C Prob.
1	8.3	0.0223	9.9	0.0031	9.3	0.0115
	10.0	0.00375	10.3	0.0018	9.5	0.0093
	10.3	0.0018	10.6	0.0021	10.9	0.00115
	10.4	0.0022	10.7	0.0016	--	--
2	8.0	0.0350	--	--	8.1	0.0250
	8.3	0.0223	--	--	--	--
3	7.9	0.0420	8.1	0.0250	8.3	0.0223
	8.7	0.0160	9.6	0.0082	8.4	0.0183
	9.8	0.0045	10.1	0.0025	8.7	0.0160
	10.1	0.0025	--	--	--	--
4	8.2	0.0293	--	--	7.9	0.0420
5	8.4	0.0183	7.9	0.0420	8.1	0.0250
6	9.4	0.0090	8.1	0.0250	8.0	0.0350
	--	--	8.6	0.0190	8.6	0.0190
	--	--	--	--	9.8	0.0045
7	8.8	0.0145	7.9	0.0420	8.2	0.0293
	9.3	0.0115	--	--	8.3	0.0223
	--	--	--	--	9.7	0.0045
8	--	--	--	--	8.1	0.0250
	--	--	--	--	8.5	0.0250
	--	--	--	--	8.5	0.0250
9	8.1	0.0250	8.2	0.0293	9.6	0.0082
	8.9	0.0220	--	--	--	--
10	7.9	0.0420	8.1	0.0250	8.0	0.0350
	9.2	0.0135	8.4	0.0183	--	--
11	8.4	0.0183	8.8	0.0145	--	--
	8.8	0.0145	--	--	--	--
12	8.0	0.0350	7.9	0.0420	--	--
	8.7	0.0160	8.8	0.0145	--	--
13	8.2	0.0293	9.5	0.0093	8.1	0.0250
	10.2	0.0026	--	--	--	--

(Continued)

Table 3 (Continued)

Storm	Set A Max. Level ft, NGVD	Set A Prob.	Set B Max. Level ft, NGVD	Set B Prob.	Set C Max. Level ft, NGVD	Set C Prob.
14	8.6	0.0190	7.9	0.0420	8.4	0.0183
	8.6	0.0190	--	--	8.6	0.0190
15	8.0	0.0350	8.1	0.0250	--	--
	10.7	0.0016	9.3	0.0115	--	--
	--	--	9.7	0.0045	--	--
16	7.9	0.0420	--	--	--	--
	8.1	0.0250	--	--	--	--
17	--	--	8.4	0.0183	8.8	0.0145
	--	--	--	--	8.9	0.0220
18	--	--	--	--	8.0	0.0350
	--	--	--	--	9.0	0.0190
19	8.3	0.0223	8.2	0.0293	7.9	0.0420
	9.9	0.0031	8.7	0.0160	8.2	0.0293
	--	--	8.9	0.0220	--	--
20	--	--	8.2	0.0293	10.1	0.0025
	--	--	9.1	0.0165	10.5	0.0021
21	8.0	0.0350	8.0	0.0350	--	--
	8.1	0.0250	8.0	0.0350	--	--
	8.5	0.0250	8.7	0.0160	--	--
22	7.9	0.0420	8.6	0.0190	7.9	0.0420
	7.9	0.0420	9.0	0.0190	7.9	0.0420
	--	--	--	--	8.8	0.0145
	--	--	--	--	9.2	0.0135
23	--	--	8.3	0.0223	9.4	0.0090
	--	--	8.3	0.0223	--	--
24	--	--	--	--	8.2	0.0293
	--	--	--	--	8.7	0.0160
25	8.2	0.0293	7.9	0.0420	8.3	0.0223
	8.5	0.0250	10.2	0.0026	10.2	0.0026
	9.0	0.0190	10.4	0.0022	10.3	0.0018
	9.1	0.0165	10.9	0.00115	10.4	0.0022
	9.5	0.0093	--	--	--	--
26	--	--	8.0	0.0350	9.1	0.0165
	--	--	8.4	0.0183	--	--

(Continued)

Table 3 (Concluded)

Storm	Set A Max. Level ft, NGVD	Set A Prob.	Set B Max. Level ft, NGVD	Set B Prob.	Set C Max. Level ft, NGVD	Set C Prob.
27	8.1	0.0250	8.0	0.0350	7.9	0.0420
	8.4	0.0183	8.5	0.0250	8.0	0.0350
	9.7	0.0045	9.8	0.0045	9.9	0.0031
	--	--	--	--	10.0	0.00275
28	9.6	0.0082	8.3	0.0223	8.4	0.0183
	10.5	0.0021	8.4	0.0250	10.7	0.0016
	11.0	0.00035	9.2	0.0135	11.1	0.00035
	11.1	0.00035	9.4	0.0090	--	--
	--	--	10.0	0.00375	--	--
	--	--	11.1	0.00035	--	--

PART III: STORM SURGE PLUS TIDE SIMULATION

23. The WES Implicit Flooding Model (WIFM) was used as the hydrodynamic storm surge model. A detailed description will not be given in this report. The numerical and hydrodynamic features of WIFM are discussed in Butler (1978) and the application of WIFM to coastal studies is demonstrated in numerous reports (including Butler 1983). WIFM solves the vertically integrated, time-dependent, shallow-water wave equations of fluid motion using an alternating direction, implicit, finite-difference algorithm. The model allows subgrid barriers which can be non-overtoppable, overtoppable, or submerged. An important feature of WIFM is the capability for using an exponentially stretched numerical grid which permits a concentration of grid resolution in areas of interest. Also included in the code is the capability to flood or dry individual cells during a simulation.

Grid Development

24. In order to model storm surge, it is usually necessary to extend the computational grid past the edge of the continental shelf and into deep water. Since it also is desirable to have small cell sizes in areas of interest, a very large number of grid cells may be necessary to model a study area using one grid. Consequently, in locations with a wide continental shelf, as in the present study, a two-grid system is usually developed. A global grid with coarse resolution extends throughout the study area and out past the edge of the continental shelf. A nearshore grid which extends only over the immediate study area but with much finer resolution is also developed. A surge plus tide event is first simulated on the global grid. Then, using boundary conditions saved during the global run, the event is simulated on the nearshore grid.

25. The present study does not use this two-grid system. Because of the project's proximity to the NOS tidal gage in Boston Harbor, a method was devised to use the Boston tide gage in place of a global grid. Use of the single grid resulted in considerable savings avoiding both simulation on an outer grid and stage-frequency curve generation at a connection point between two grids. This process involved setting up a single grid (Figure 6) and then calibrating the model to produce correct water levels throughout the study

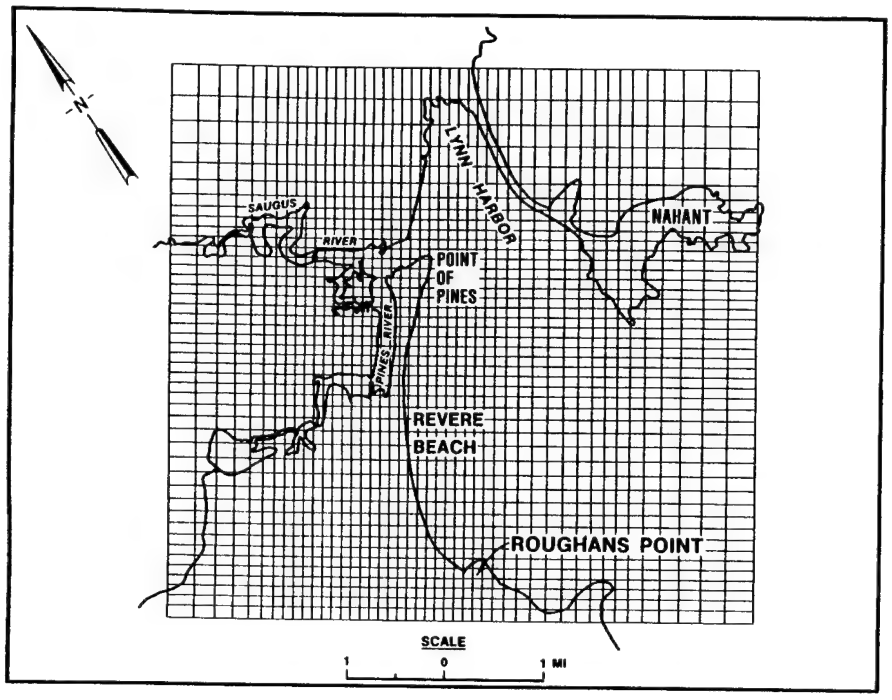

Figure 6. Numerical grid for storm surge model

area using altered Boston water levels to drive the boundary. The procedure used to alter the Boston water levels to produce the desired results is described in the section on model calibration.

26. The final grid configuration has 2,025 cells arranged in 45 rows and 45 columns. The cells with the finest resolution are 500 ft square and cover most of the areas of interest: Roughans Point, Point of Pines, the Saugus-Pines Inlet, and the initial reaches of both rivers. The cells with the coarsest resolution, located near the boundary, are approximately 1,500 by 700 ft. The grid is orientated to match the predominant direction of the river system, since the initial reaches of the rivers form nearly 90-deg angles.

Wind Forcing

27. Wind speed and direction are required inputs to WIFM for the modeling of storm surge. For this study a spatially constant but temporally varying wind forcing was used. The wind data were supplied by NED using raw data from Logan International Airport and a wind data analysis computer program

developed by NED. The wind data were 1-min averages of both wind speed and direction reported hourly and corrected to a 33-ft elevation. The hourly wind data were interpolated to 60-sec time-steps and applied without spatial variation to the entire study area. Two factors allowed this simplified treatment of wind forcing. First, the small geographic area of the modeled area was close to the source of the wind data. Second, the use of Boston tide gage data for boundary conditions already included the effect of the wind over the continental shelf, so the local winds were needed only to locally redistribute the surge. For the 28 northeasters chosen for this study, the average maximum hourly wind speed was 33 knots and varied from 25 knots to 48 knots. The wind directions for these maximum winds varied from 0 to 292 deg (all but three were between 0 and 90 deg) The average direction of the maximum hourly values was 73 deg. Wind directions are referenced clockwise from North.

Data Collection

28. During the summer of 1984, NED supervised the placement and operation of five tide gages in the study area. Figure 7 shows the location of these gages. Two of the gages, Simpson's Pier and Bay Marine Lobster, were located outside the river system at Roughans Point and in Lynn Harbor, respectively. The other three gages (Fox Hill Drawbridge, Broad Sound Tuna, and Atlantic Lobster) are located in the Saugus-Pines River system. All of these gages were in operation from June to October 1984. No other data collection efforts were commissioned solely for numerical modeling. Bathymetric and elevation data for Revere Beach and throughout most of the river system were obtained from previous surveys conducted for beach and channel improvement projects and for highway projects. Excellent data were generally available for the area east of the Salem Turnpike and for the area immediately adjacent to the abandoned highway embankment. Bathymetric data for Lynn Harbor and Broad Sound were obtained from NOS nautical charts.

Model Calibration

29. Since all five study area gages were not operational during any storm and the two gages left in operation during the winter of 1985 did not experience any significant storm induced high water, the model could not be

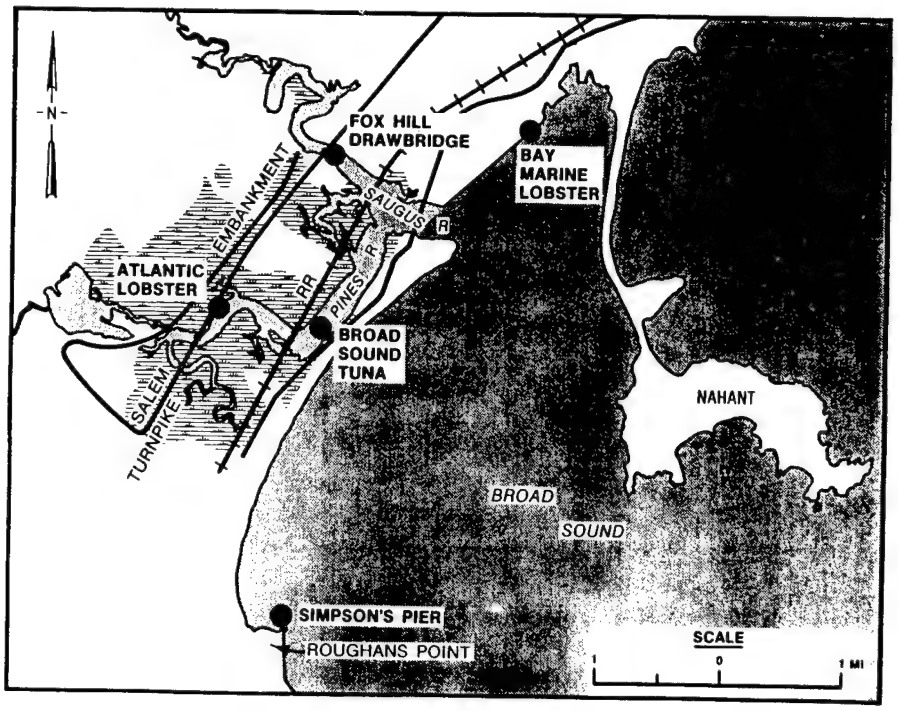

Figure 7. Location of study area tide gages

calibrated or verified to a surge plus tide event. Consequently, two periods during the summer of 1985, one at spring tide and the other at neap tide, were chosen for calibration and verification of the model.

30. A 29-hour period from 0800 29 July to 1300 30 July 1984 was chosen for calibration. During this period data were available from all five study area tide gages, and both the highest tide and the largest range of the month occurred (6.7 and 13.0 ft NGVD, respectively, at Boston). Data from each gage are plotted against data from the NOS gage at Boston (Figures 8-12). The gage at Simpson's Pier went dry at -4.2 ft NGVD resulting in the horizontal lines at low tide in Figure 8. Several facts can be immediately seen from these figures. The range, phase, and MSL of the study area gages are very close to those of the Boston gage. The water levels at high tide are all within several tenths of a foot, and the phases at high tide are all within several minutes. It is interesting that Broad Sound Tuna, a river gage, has the highest tides resulting from a small upward shift in MSL. The largest differences occur at low water where the river gages show a distinctly higher and later low tide, relative to Boston. During the calibration process, adjustments were made in the following items so that the numerical results would

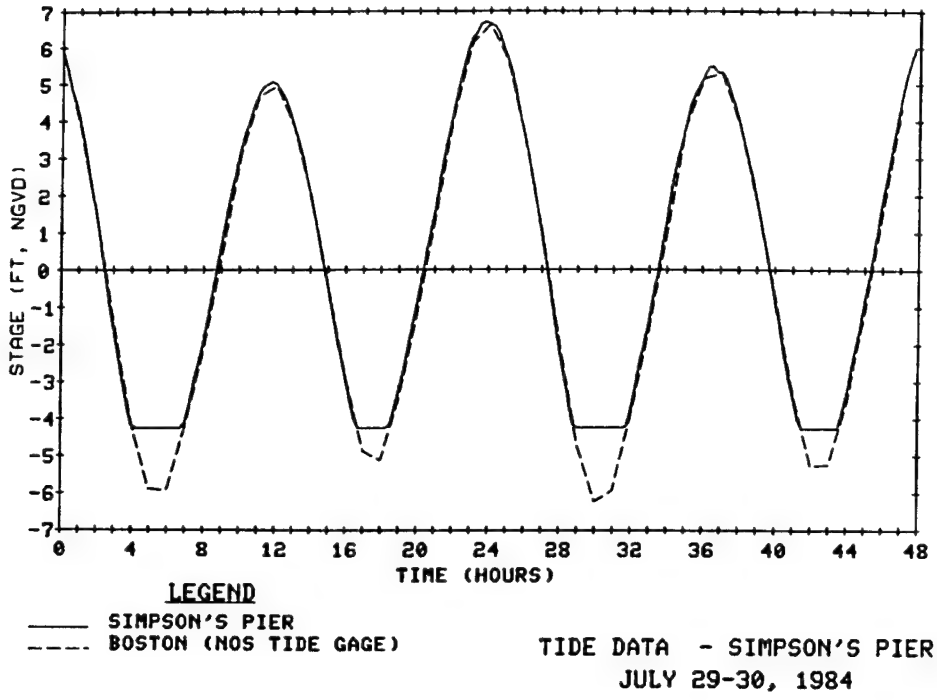

Figure 8. Tidal calibration data, Simpson's Pier

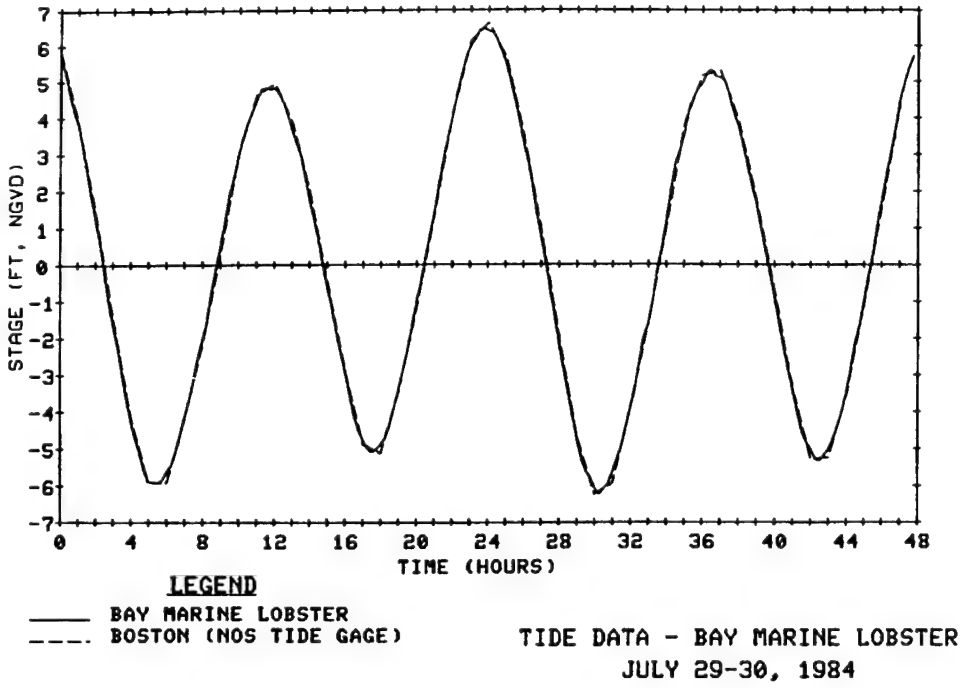

Figure 9. Tidal calibration data, Bay Marine Lobster

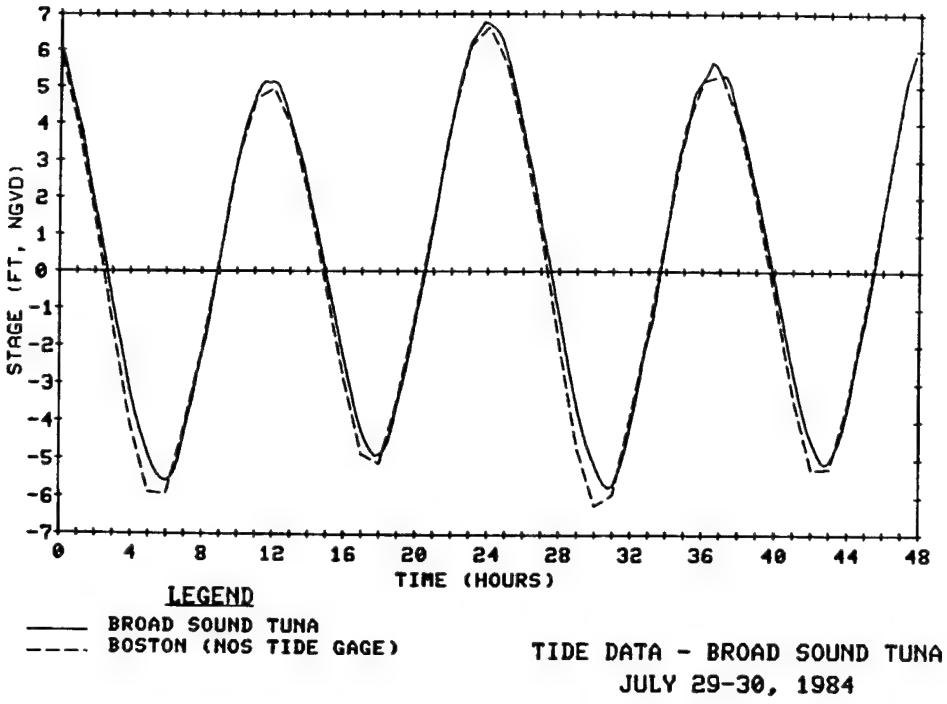

Figure 10. Tidal calibration data, Broad Sound Tuna

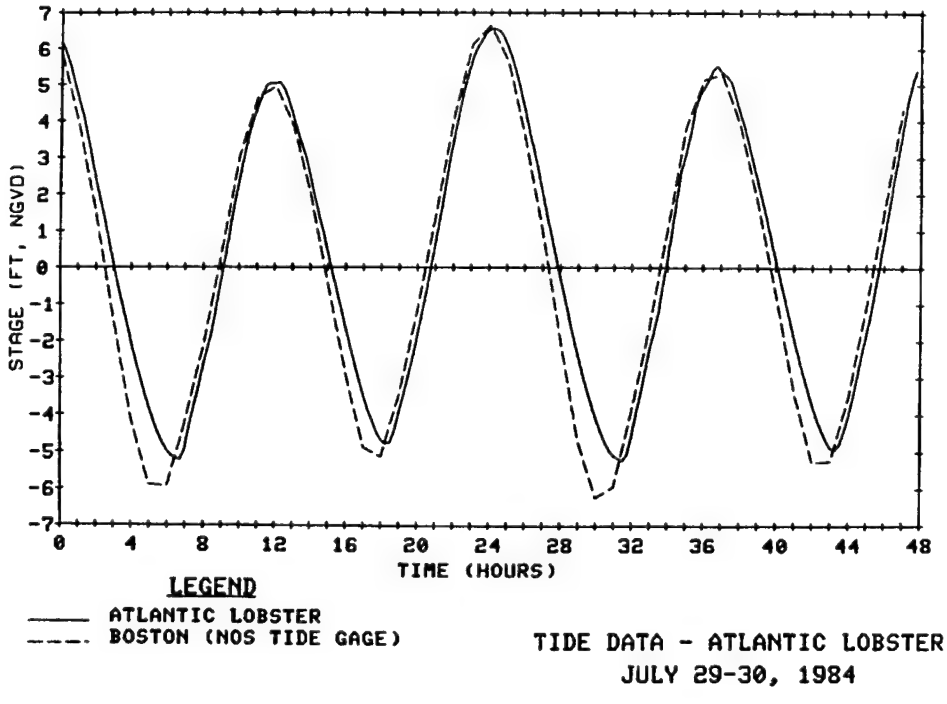

Figure 11. Tidal calibration data, Atlantic Lobster

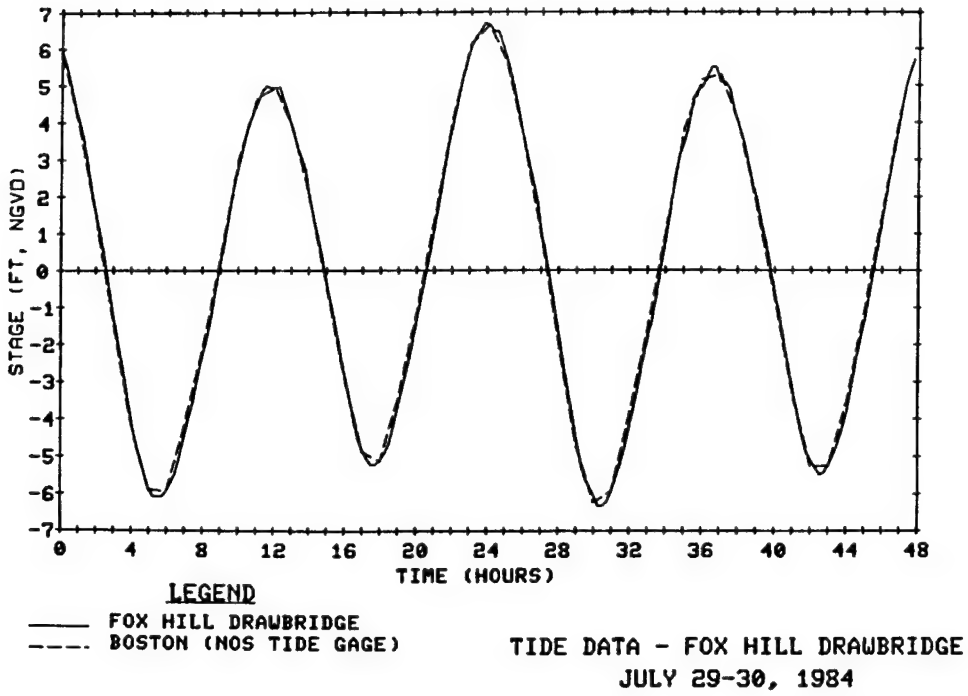

Figure 12. Tidal calibration data, Fox Hill Drawbridge

closely match the tide gage data for the 29-hour period specified above. These adjustments are explained below.

a. Cross-sectional areas and frictional characteristics of both channels and the bridge openings were adjusted. The minimum cell size of 500 ft was much larger than the channel width at many of the constrictions. A smaller cell size would have greatly increased modeling costs; therefore, using the 500-ft cell size necessitated that the flow be adjusted through these oversized areas by alterations in depth and friction. It would have been convenient if the depth could have been adjusted on the oversized cells so that cross-sectional areas would match between model and prototype. However, due to the large tidal range in the study area, matching cross-sectional areas would have caused the channels to dry up well above low water. Consequently, it was necessary to make these cells deeper than the area represented in the prototype would justify. Higher water levels would cause excessive flow through these oversized channels. A compromise depth was selected so that the channel would remain flowing at low water levels. At low water the opposite problem would occur. Since the depth of the channels in the study area is much greater than the compromise depth used in the model cells, the flow restriction is higher in the model than in the prototype. This causes a reduction in flow in the model at low water. Therefore, in addition to the compromise depth, frictional characteristics were made dependent upon depth to produce smaller Manning's n values at low

water and greater n values at higher water. With these adjustments, the model was able to duplicate the calibration data in the Saugus-Pines river system.

b. Storage in both channel and ponds in upper reaches of both rivers was adjusted in order to match elevations, particularly those measured at Atlantic Lobster and Broad Sound Tuna. Very little bathymetric data and no tidal data were available for these areas. Therefore, storage was at first estimated from USGS topographic maps and then changed during the calibration process. The final storage areas selected remained reasonable based upon the available data.

c. As was mentioned previously, data from the Boston gage were adapted for use as boundary conditions for the model. Since the tide in the study area conforms so closely with that measured at Boston, only minor alterations to the Boston tide were necessary. The calibration process found that Boston data should be multiplied by 0.984 and shifted forward in time by 5 min before being used as boundary values.

31. The results of the calibration process are depicted in Figures 13-17. These figures show excellent agreement between numerical and measured water levels during a period of large tidal range.

Model Verification

32. A 32-hour period from 1000 15 August to 1800 16 August 1984 was chosen to verify the hydrodynamic model. This time period was chosen because good data were available from the five study area tide gages as well as from the NOS gage at Boston. Also, since the calibration was preformed for a spring tide, a neap tide with a lower high tide and a small range (4.8 and 8.2 ft NGVD, respectively) was chosen to verify the model. The results for the five study area gages are shown in Figures 18-22. These results show excellent agreement between numerical and measured water levels for all five locations.

Simulation of Event Ensemble by the Hydrodynamic Model

33. The 150 selected events were simulated on a CYBER 205 computer in three sets of 50 by the calibrated and verified storm surge model. The simulations of the individual events varied from 13 to 75 hours prototype time depending upon the number of high tides that needed to be modeled. For each of the 150 surge plus tide time-histories, all highs with still-water levels

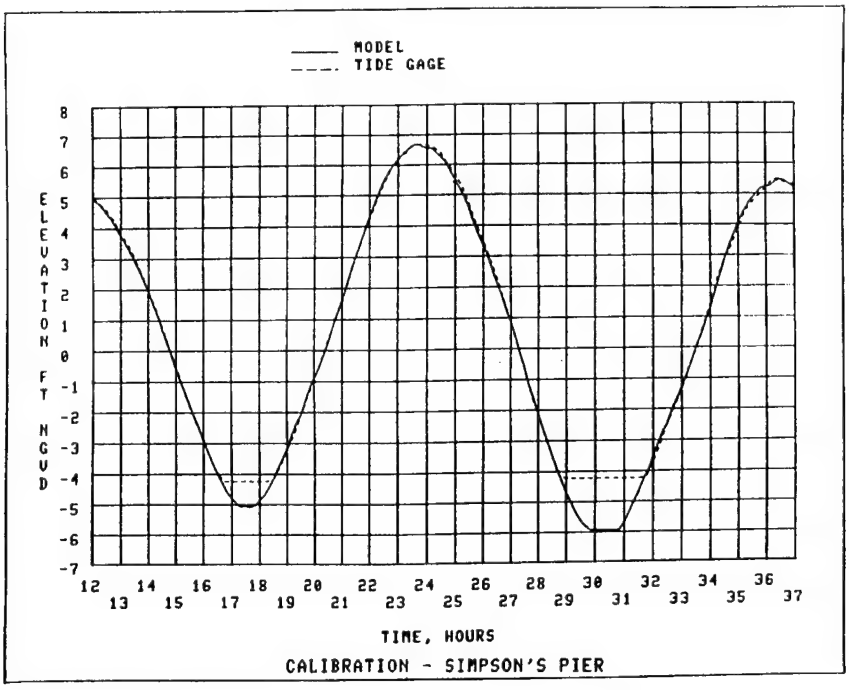

Figure 13. Surge model calibration results, Simpson's Pier

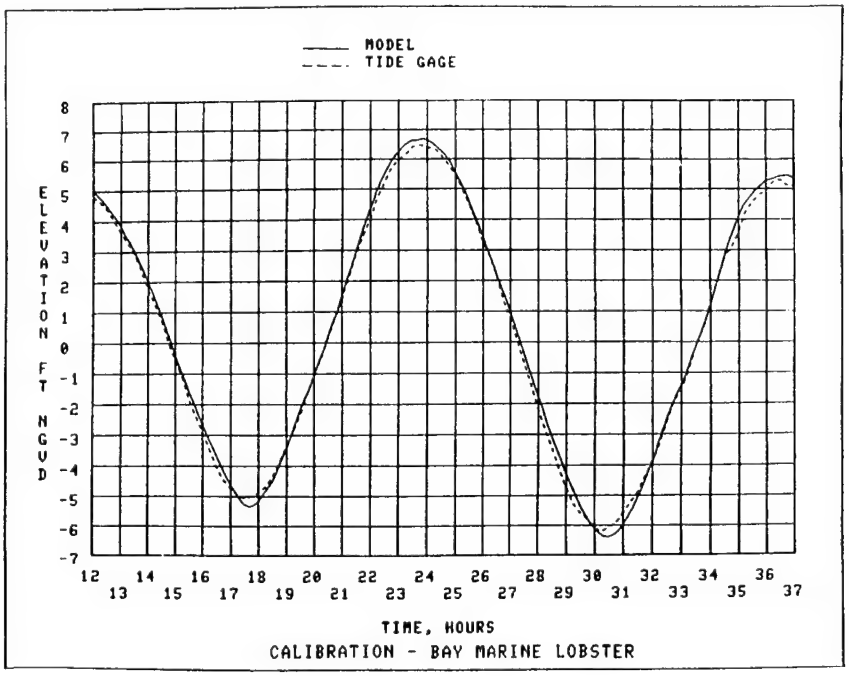

Figure 14. Surge model calibration results, Bay Marine Lobster

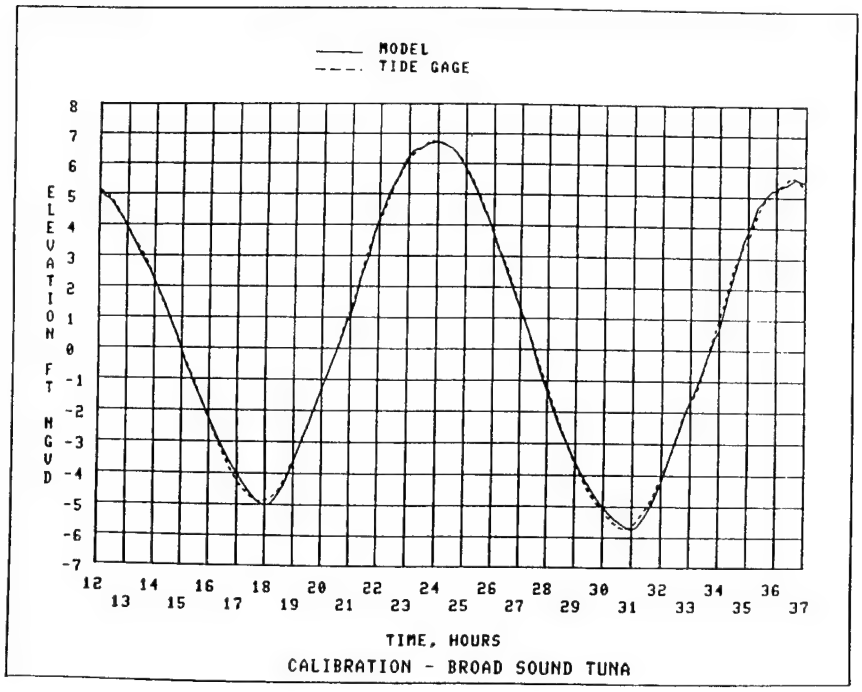

Figure 15. Surge model calibration results, Broad Sound Tuna

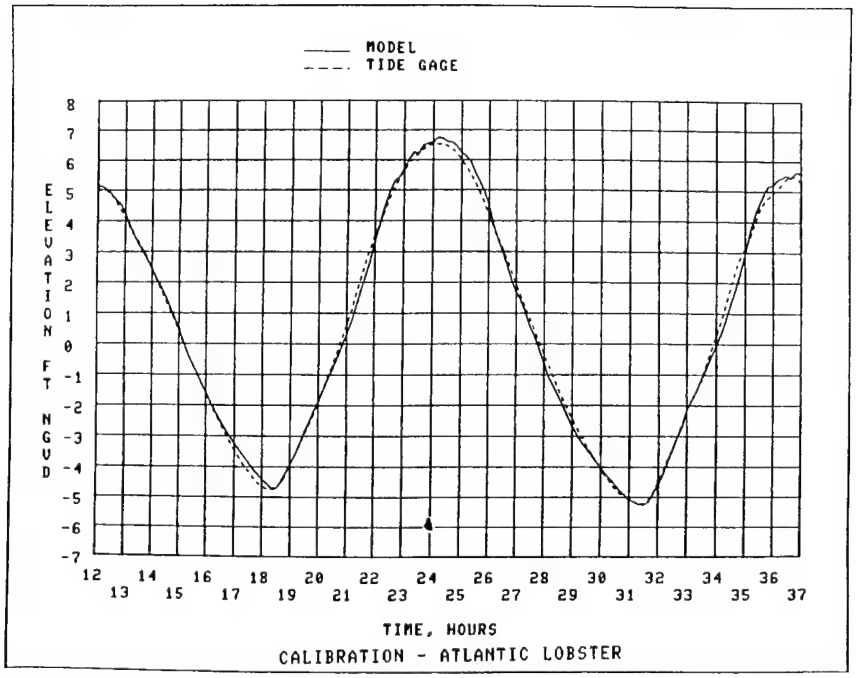

Figure 16. Surge model calibration results, Atlantic Lobster

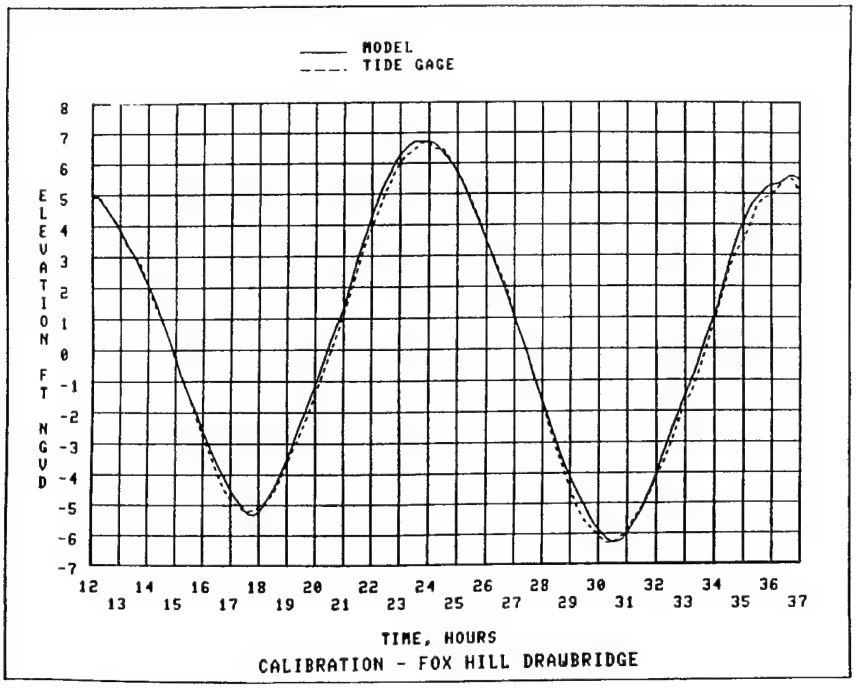

Figure 17. Surge model calibration results, Fox Hill Drawbridge

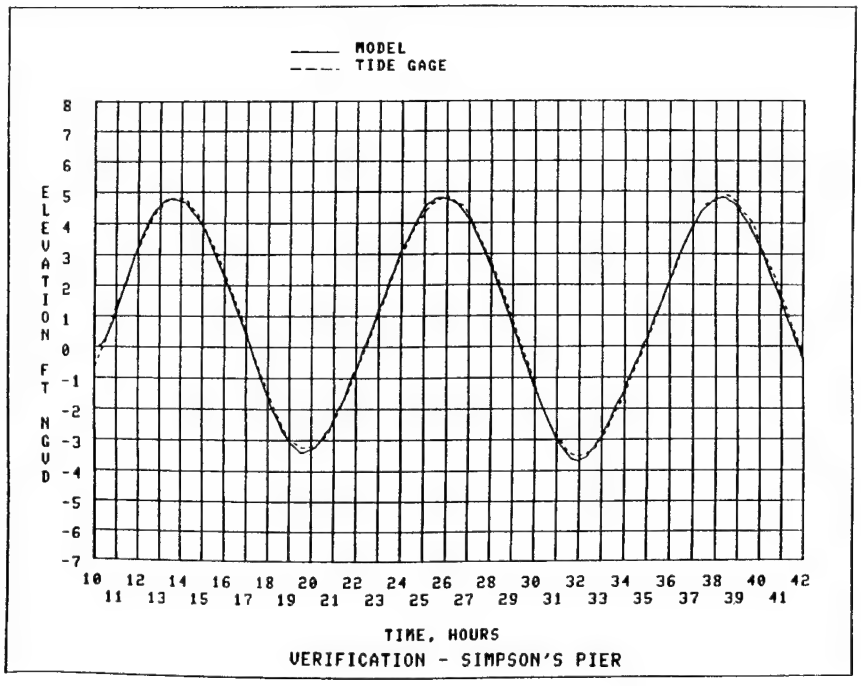

Figure 18. Surge model verification results, Simpson's Pier

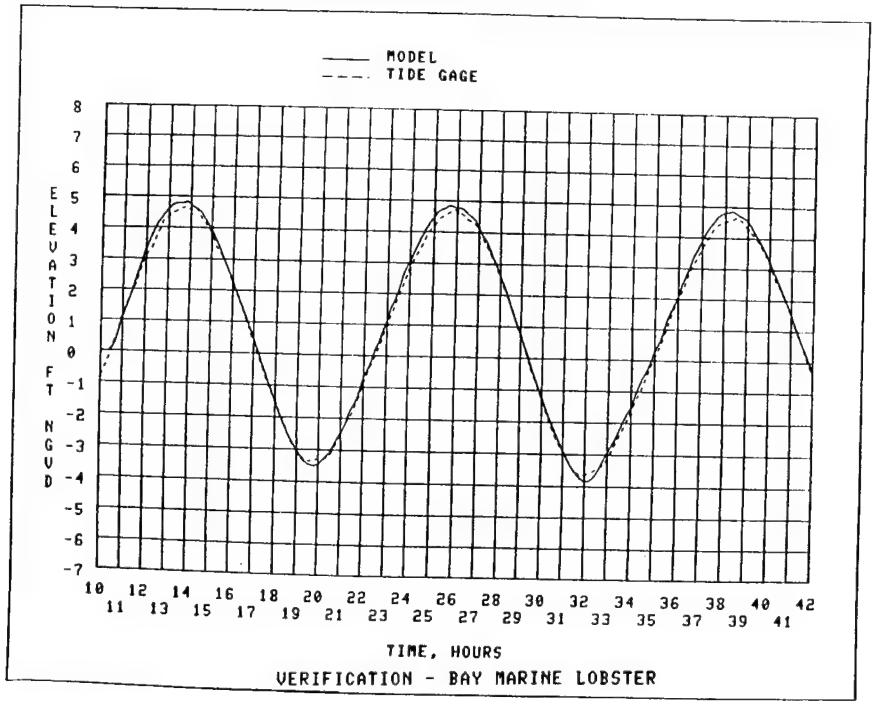

Figure 19. Surge model verification results, Bay Marine Lobster

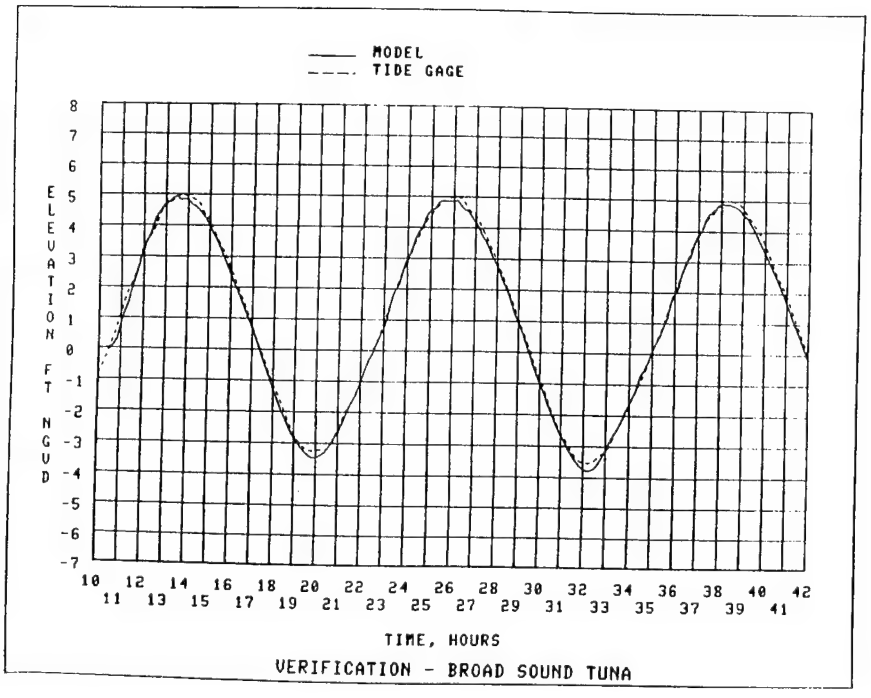

Figure 20. Surge model verification results, Broad Sound Tuna

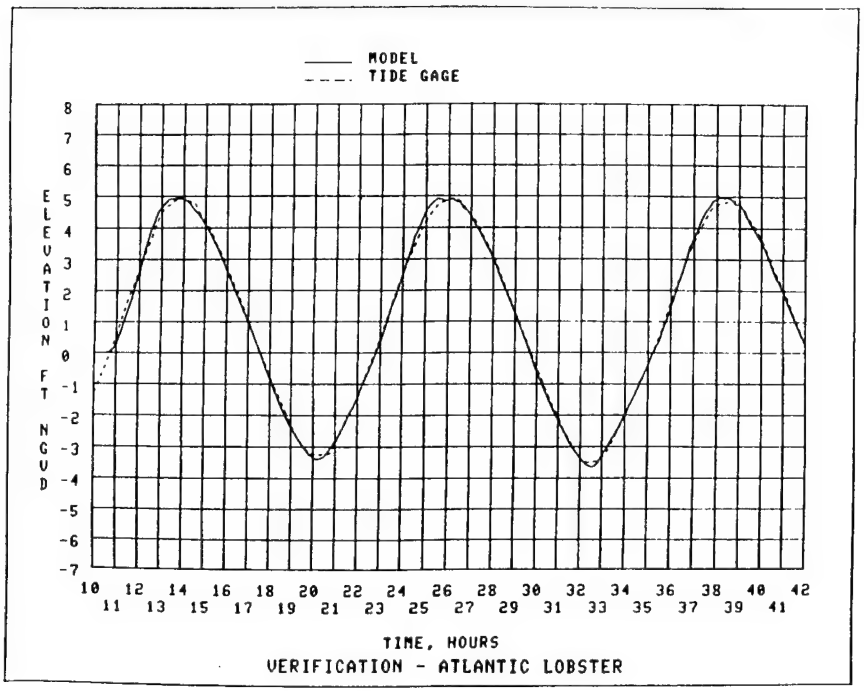

Figure 21. Surge model verification results, Atlantic Lobster

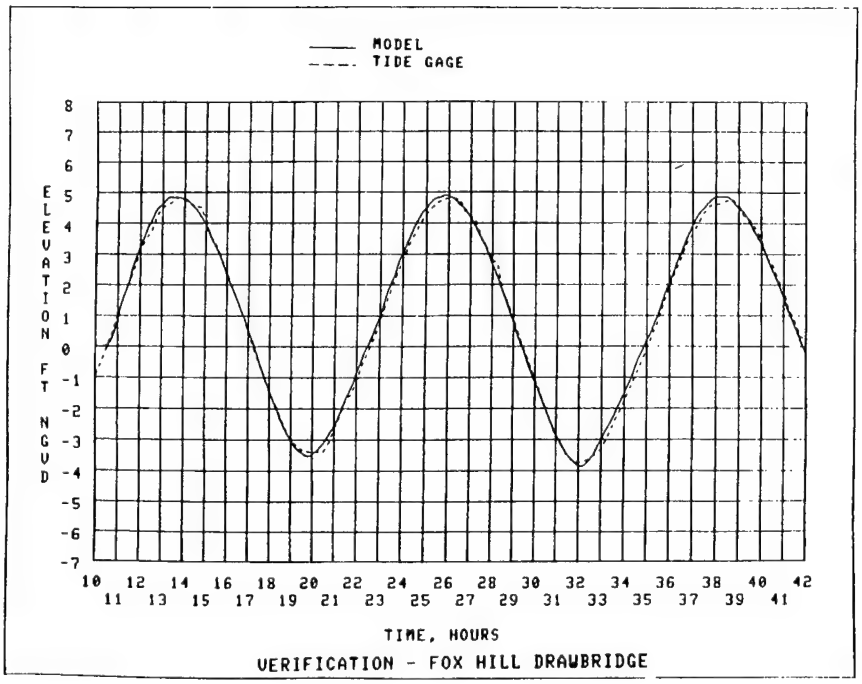

Figure 22. Surge model verification results, Fox Hill Drawbridge

greater than 7.0 ft NGVD were included in the simulation. A constant time-step of 60 sec was used for all events. Two computer files, saving information at each of the numerical gage locations shown in Figure 23, were the main result of each simulation. The first file was a time-history of water levels at 15-min increments. This file was used both to plot the water level time-histories at each numerical gage and to provide information to the computer codes which calculated wave overtopping rates and interior volumes at Roughans Point. The second file listed the maximum elevation experienced at each of the numerical gages during each event. This file was used to construct the stage-frequency curves for the still-water locations. Both of these computer files were given to NED on magnetic tape.

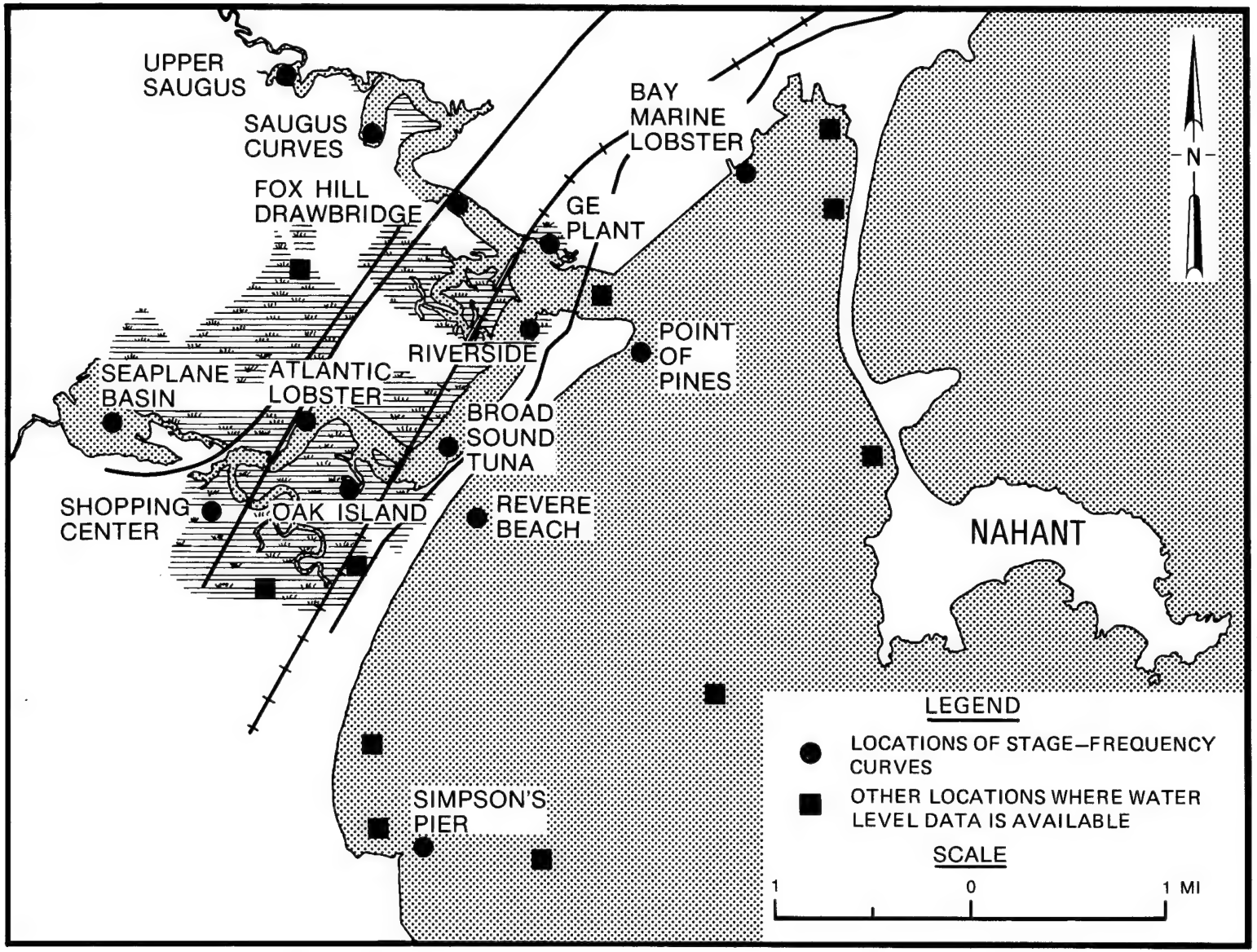

Figure 23. Location of surge model numerical gages

PART IV: WAVE MODELING

34. For each event (surge plus tide), the wave climate in a 25.9-square mile area of Broad Sound was simulated for each hour when the still-water level was above 7.0 ft NGVD. The area considered is shown in Figure 24. Depths, at mean low water, range from 0 ft at the beaches to approximately 82 ft along the eastern boundary of the grid. The shallow depths in the area required the use of a shallow-water wave model.

35. A steady-state, shallow-water, directional-spectral wave model (ESCUBED) was used to perform the simulations. The required simulations actually called for the use of a time-dependent model, but the cost of using such a model was prohibitive. In lieu of a truly transient simulation, ESCUBED was run once for each hour of each event, and the resulting wave climate was taken to be representative of the conditions existing for the entire hour.

36. For each run of ESCUBED it was necessary to specify a directional spectrum at points along the eastern boundary of the grid shown in Figure 24. To do this, wave train characteristics (e.g. significant wave heights and peak spectral wave periods) were used to define the TMA spectral shape (Hughes 1984), and the resulting one-dimensional spectrum was then distributed directionally. The wave train characteristics represented both sea and swell and were derived using the methods and data of WIS.

37. A total of 848 hr of simulation was made. Resulting wave heights in the lee of Nahant peninsula indicated that local wave generation in this area was inadequately simulated by ESCUBED. Hence, an additional analysis was required when winds were from the northeast.

38. Shallow-water wave growth equations were used to estimate locally generated wave heights and periods off the north seawall at Roughans Point as well as at Point of Pines and in Lynn Harbor. The total wave climate in these regions was then assumed to be a combination of these locally generated waves and the ESCUBED results.

39. It is important to note that no wave data from Broad Sound were available. Hence, it was not possible to calibrate ESCUBED or to verify its results.

40. The following sections discuss the WIS methods and data, the ESCUBED wave model, and the analysis of local wave generation in the lee of Nahant Peninsula.

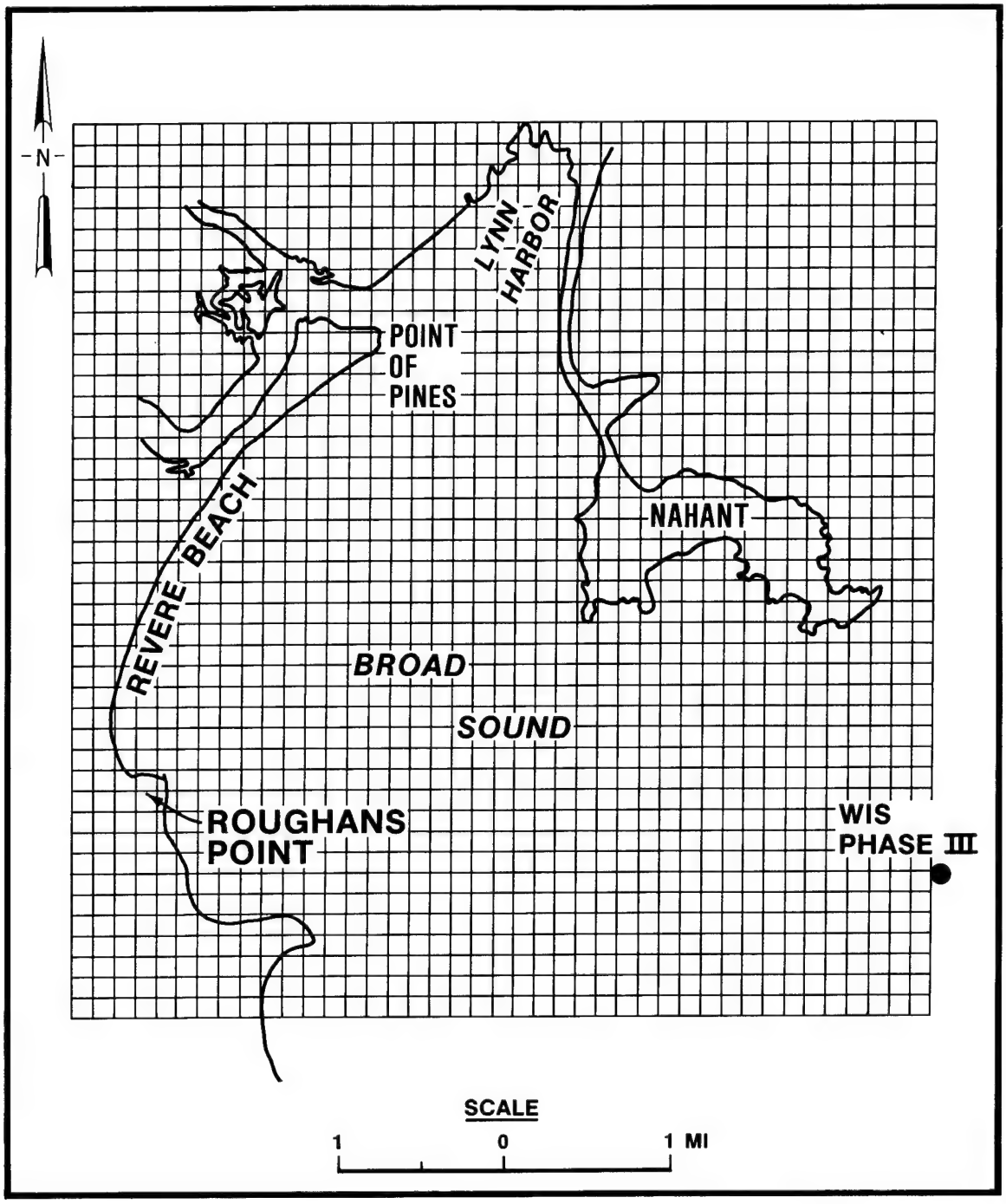

Figure 24. Numerical grid for spectral wave model

WIS Methods and Data

41. In late 1976 a study to produce a wave climate for US coastal waters was initiated at WES. This ongoing study, WIS, consists of three phases. Phase I (Corson et al. 1981) and Phase II (Corson et al. 1982) wave characteristics were generated by a numerical model which simultaneously propagated and transformed the waves over a discrete grid representing segments of the Atlantic Ocean. Phase I acted in the deep ocean. Phase II acted over the continental shelf where, for the purpose of classifying waves, depths may be either intermediate or deep. Phase III draws upon the Phase II data to provide nearshore wave characteristics in depths as shallow as 30 ft. For all three phases, data are available at selected points referred to as stations.

42. WIS methods and data were to be used to establish the boundary conditions for ESCUBED. Theoretically, the ESCUBED grid could have been extended seaward as far as the nearest Phase II station (Phase II stations are approximately 34 miles offshore and 34 miles apart), and the data available at this station could then have been used in the boundary conditions. The costs of computing over such a large grid would have been prohibitive. The Phase III methodology provided an inexpensive bridge between the Phase II station and the much smaller grid actually used.

Phase III Methodology

43. The reader is referred to Jensen (1983) for a complete description of the Phase III methodology. A summary is given here. The Phase II results comprise directional spectra. The Phase III methodology first takes these spectra and separates them into two wave trains, swell and sea. The two are assumed to behave independently. The swell is characterized by the height H, frequency f, and propagation direction θ of a unidirectional, monochromatic wave. The energy of the sea will be distributed in frequency-direction space. A one-dimensional spectrum $E_1(f)$ can be defined in terms of the directional or two-dimensional spectrum $E_2(f,\theta)$ which is expressed as

$$E_1(f) = \int_0^{2\pi} E_2(f,\theta)\, d\theta \qquad (1)$$

44. The Phase III methodology assumes that, at the Phase II station, $E_1(f)$ can be represented parametrically using only two parameters: the energy based significant wave height H_{m_o} and the frequency of the spectral peak f_m. This one-dimensional spectrum is then given a directional distribution using the following equation:

$$E_2(f,\theta) = E_1(f) \frac{8}{3\pi} \cos^4 (\theta - \theta_m) \tag{2}$$

Here, θ_m is the central angle of the spectrum. $E_2(f,\theta)$ is discretized so that each component can be propagated from the Phase II station to the Phase III station in accordance with linear wave theory.

45. The Phase III methodology assumes straight and parallel bottom contours so that refraction and shoaling of swell and of the discrete elements of $E_2(f,\theta)$ may be determined analytically. The sea is further transformed by wave-wave interactions. Depth-controlled criteria limit both H and H_{m_o}. Sheltering by capes or peninsulas is included in the Phase III methodology.

46. Refraction, shoaling, and depth limitation acting on the swell transform H, f, and θ at the Phase II station into new values in shallow water at the Phase III station. If the Phase III station were sheltered from the swell, then H is zero. Refraction, shoaling, wave-wave interactions, and sheltering acting on individual components of the sea result in a new spectrum for sea at the Phase III station. H_{m_o}, f_m, and θ_m are extracted from this spectrum.

47. The final Phase III result comprises six wave characteristics: H, f, and θ of the swell and H_{m_o}, f_m, and θ_m of the sea. The wave climate at the Phase III station is taken to be completely defined by these six parameters.

Use of Phase III Methodology for Broad Sound Wave Climate Simulations

48. WIS Phase II, sta 13, directional spectra were used as deepwater input. This station is located at latitude 42° 32.5' N and longitude 70° 14' W. The Phase III station was positioned at latitude 42° 23.5' N and longitude

70° 53.5' W (Figure 24). This puts the Phase III station approximately 4.6 mi due east of Roughans Point in 75 ft of water. Cape Ann, to the northeast, and Cape Cod, to the southeast, provided some shelter for the Phase III station. The sheltering was such that only those waves approaching from between N40° E and S60° E could reach the Phase III station.

49. Phase III results were produced at 3-hour intervals. Linear interpolation was used to calculate H, f, θ, H_{m_o}, f_m, and θ_m for every hour.

Wave Climate Simulations for Broad Sound

Summary of ESCUBED

50. The reader is referred to Hubertz (1985) for a detailed discussion of ESCUBED. Relevant aspects of the model are presented here.

51. Essentially, ESCUBED propagates components of discrete directional spectra over a user specified bathymetry. Calculations proceed to propagate individual components of these spectra across a rectangular, uniformly spaced finite difference grid.

52. The grid used for the wave climate simulations at Broad Sound is shown in Figure 24. The grid spacing in both the x and y directions is 656 ft (200 m). At each grid point, the energy of the individual components of a spectrum is limited by the finite depth water equilibrium range proposed by Kitaigorodskii, Krasitskii, and Zaslavakii (1975). The range, which applies for frequencies greater than the peak, is a function of depth and frequency. This limitation could be thought of as an energy sink where the energy loss is through turbulent and viscous processes associated with white capping and large scale breaking.

Determination of a spectrum for the ESCUBED boundary condition

53. The Phase III wave characteristics for sea, H_{m_o}, and f_m were used to generate a TMA spectrum $E_{TMA}(f,h)$ (Hughes 1984). The TMA spectrum is representative of fully developed wind seas in finite depth water.

54. The TMA spectrum was evaluated using the depth at the Phase III station, i.e. $h = 75$ ft. Let $E_{TMA}(f,75\text{ ft}) = E_{TMA}(f)$. The one-dimensional spectrum $E_{TMA}(f)$ was distributed directionally using a $\cos^4(\theta - \theta_m)$ spreading. No energy was allowed to have a direction outside

the WIS Phase III sheltering angles. The total energy of the one-dimensional and directional spectra must be equal. This requirement is expressed as

$$\int_0^{\infty} E_{TMA}(f)df = \int_0^{\infty} \int_0^{2\pi} E_{sea}(f,\theta)\, d\theta\, df \qquad (3)$$

where $E_{sea}(f,\theta)$ is the directional spectrum of the sea along the eastern boundary of the ESCUBED grid.

55. Assuming the relationship shown in Equation 4, Equation 5 can be derived from Equation 3. The κ in Equation 5 is a constant which is determined by Equation 6. The limits of integration in Equation 6 match the Phase II sheltering angles since the energy density outside these angles is zero, as indicated below.

$$E_{sea}(f,\theta) = \kappa \cos^4 (\theta - \theta_m)\, E_{TMA}(f) \qquad (4)$$

$$\int_0^{\infty} E_{TMA}(f)\, df = \int_0^{2\pi} \kappa \cos^4 (\theta - \theta_m)\, d\theta \int_0^{\infty} E_{TMA}(f)\, df \qquad (5)$$

$$\kappa = \left[\int_{(-1/6)\pi}^{(5/18)\pi} \cos^4 (\theta - \theta_m)\, d\theta \right]^{-1} \qquad (6)$$

The continuous spectrum, $E_{sea}(f,\theta)$ is discretized using a frequency increment $\Delta f = 0.01$ Hz and a direction increment $\Delta\theta = 20$ deg . Let $E_{sea}(f_i,\theta_i)$ be this discrete spectrum.

56. The final step in determining a directional spectrum representing both sea and swell for the boundary condition at the eastern side of the grid is to add the swell to $E_{sea}(f_i,\theta_i)$. The swell can also be represented by a discrete spectrum, $E_{swell}(f_i,\theta_i)$. If the energy of the swell is uniformly distributed over one frequency-direction band of the spectrum, then a discrete directional spectrum $E_{swell}(f_i,\theta_i)$ can be written as follows:

$$E_{swell}(f_i,\theta_i) = \begin{cases} \frac{H^2}{8\Delta f \Delta\theta} & \text{and} \quad f_i - \frac{1}{2}\Delta f \leq f < f_i + \frac{1}{2}\Delta f \\ & \quad \theta_i - \frac{1}{2}\Delta\theta \leq \theta < \theta_i + \frac{1}{2}\Delta\theta \\ 0 & \text{otherwise} \end{cases} \qquad (7)$$

Finally, the discrete directional spectrum used as a boundary condition for ESCUBED is the sum of $E_{sea}(f_i,\theta_i)$ and $E_{swell}(f_i,\theta_i)$.

ESCUBED Results

57. ESCUBED output contains the following information from the wave climate simulations:

a. H_{m_o} , f_m , and θ_m representing the energy based significant wave height, the frequency of the spectral peak, and the direction of the spectral peak at each grid point, respectively.

b. Directional and one-dimensional spectra at selected points in the vicinity of Roughans Point and at points 1.24 miles due east of Roughans Point.

Model results in the lee of Nahant Peninsula indicated that, in this area, ESCUBED inadequately simulated the local wave generation by wind. Although ESCUBED allowed wind energy to be added to the energy of existing waves, ESCUBED did not allow initial growth of waves in the areas sheltered from the WIS input on the boundary. Since these locally generated waves are especially important for waves at the north wall of Roughans Point and for locations along the shore of Broad Sound from Point of Pines into Lynn Harbor, further analysis was required.

Locally Generated Waves in the Lee of Nahant Peninsula

58. The equations for shallow-water wave growth for fetch-limited waves, presented in the Shore Protection Manual (SPM 1984, p. 3-55), were used to obtain an improved determination of the waves attacking the north wall at Roughans Point, at Point of Pines, and at locations in Lynn Harbor.

59. The depth and fetch vary across Broad Sound. At each point where the locally generated analysis was required (see Figure 25 for locations marked A-E), the area was divided into sectors as shown in Figure 26 for the

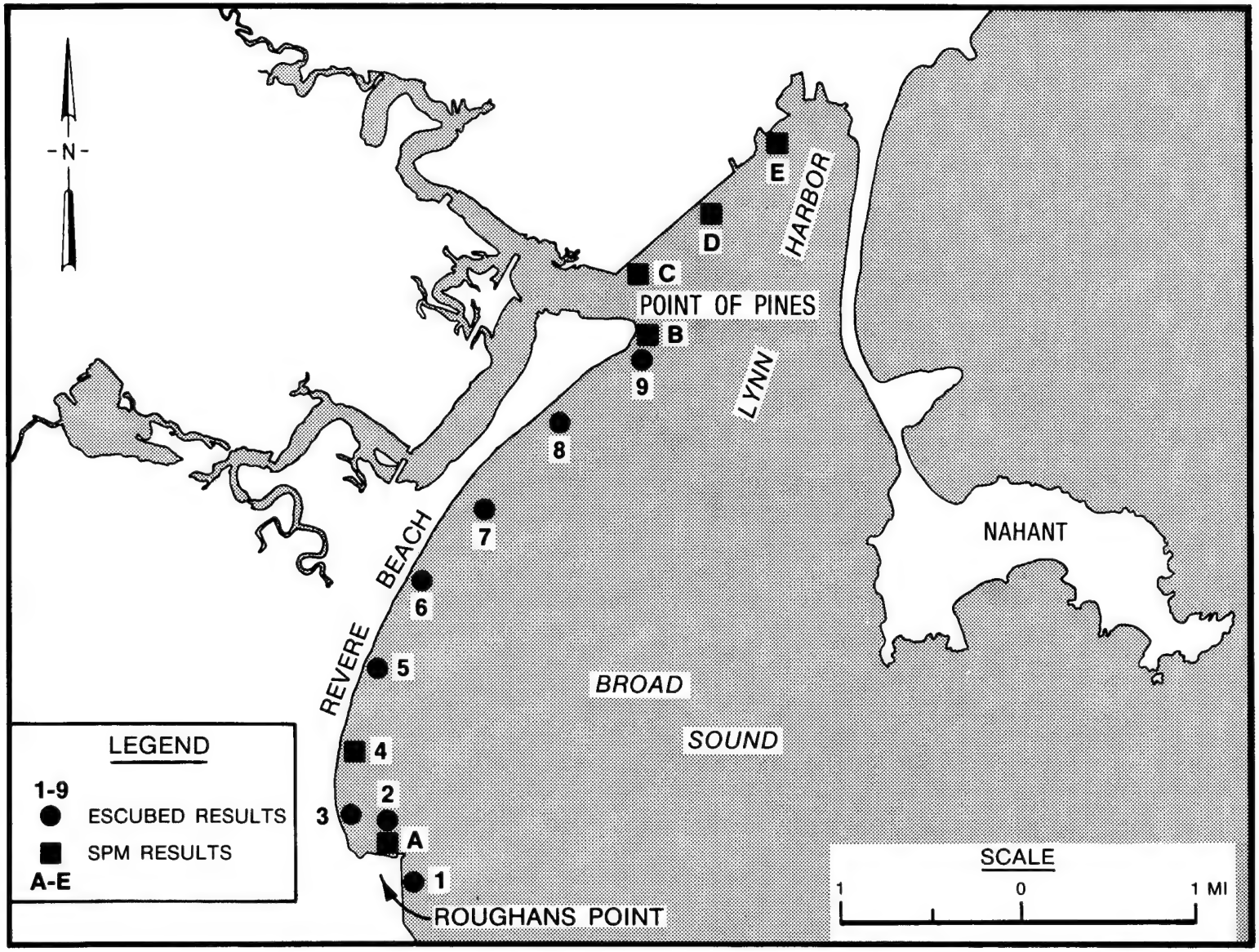

Figure 25. Locations for which locally generated waves were calculated

Roughans Point north wall. A representative fetch and depth were assigned to each sector. For each hour of simulation the appropriate fetch and depth were chosen according to the wind direction. Wave propagation direction was assumed to be the same as wind direction. The sectors, fetch lengths, and depths for the five locations are listed in Table 4. Note that the depth at mean low water (MLW) is listed, but the depth used for the calculations varies with surge and tide. The most important distinction between the ESCUBED and locally generated waves at the Roughans Point north wall is that the ESCUBED

Table 4

Sectors, Fetch Length, and Depths Used for Local Wave Generation

Location	Sector Deg Azimuth		Fetch Length ft	Depth ft, MLW
A	0	25	3,750	2.5
	25	52	5,200	8.0
	52	73	5250	12.0
B	0	34	2,700	7.0
	34	75	6,800	1.0
	65	100	5,600	1.0
	100	117	6,100	1.0
	117	144	8,000	1.0
	144	185	29,600	5.0
	185	216	15,000	1.0
C	51	119	5,300	1.0
	119	131	6,300	1.0
	131	153	8,400	1.0
	153	186	32,000	1.0
	186	231	2,700	7.0
D	51	133	4,300	1.0
	133	145	5,400	1.0
	145	161	9,700	1.0
	161	187	32,800	5.0
	187	205	20,500	5.0
	205	231	3,700	7.0
E	51	95	3,000	20.0
	95	123	3,100	1.0
	123	153	3,600	1.0
	153	167	9,800	1.0
	167	188	33,600	5.0
	188	213	21,300	5.0
	213	231	4,900	7.0

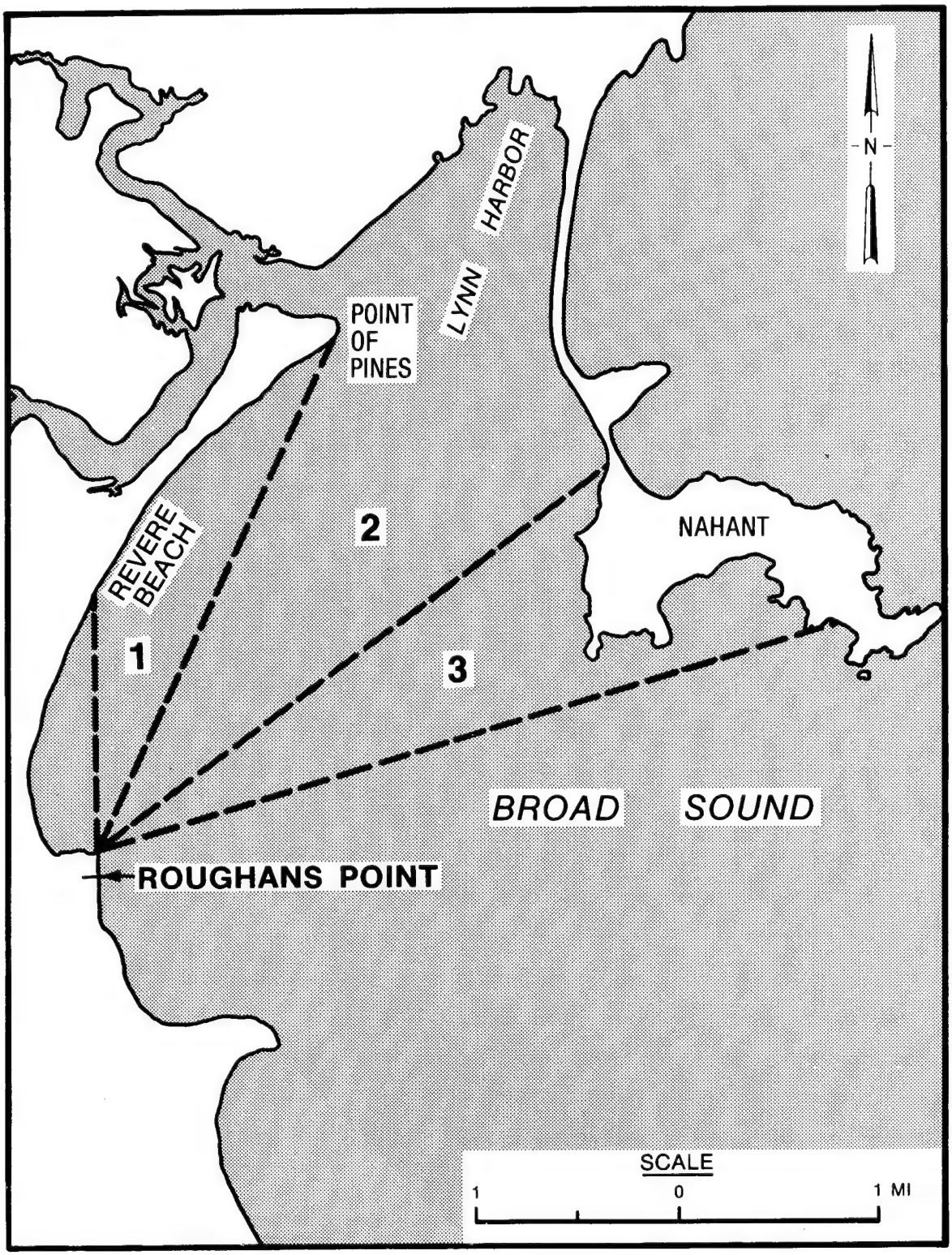

Figure 26. Three sectors used for determining locally generated waves at Roughans Point North Wall

waves attack the wall at oblique angles, whereas the locally generated waves have a more perpendicular angle of attack. For the Lynn Harbor locations the ESCUBED results are essentially negligible, and therefore, the locally generated waves dominate for these locations.

60. Table 5 is a summary of the wave heights, periods, and directions from the ESCUBED modeling for several locations from Roughans Point up along Revere Beach to Point of Pines. These locations are marked 1-9 in Figure 25. Table 6 is a summary of the locally generated waves. These areas are marked A-E in Figure 25. These two tables are provided to demonstrate the range of wave parameters generated by the models. Waves were modeled only during periods of possible overtopping at Roughans Point (water levels above 7.0 ft NGVD) during northeaster conditions. The average values shown do not take into account the varying probabilities of the surge-tide-wave events.

Table 5

Summary of ESCUBED Wave Parameter Results

Location*	Height, ft			Period, sec			Direction, deg True N		
	Min.	Avg.	Max.	Min.	Avg.	Max.	Min.	Avg.	Max.
1	0.5	5.9	9.6	1.9	9.3	14.3	30	92	97
2	0.2	1.9	3.4	1.7	7.9	14.3	**	**	**
3	0.4	5.4	9.5	1.9	8.9	14.3	31	91	103
4	0.2	3.9	8.7	1.7	9.1	14.3	34	109	111
5	0.2	5.1	9.6	2.0	9.1	14.3	100	114	149
6	0.2	4.5	9.1	2.0	9.1	14.3	100	122	149
7	0.2	3.4	8.0	2.0	9.1	14.3	100	130	149
8	0.2	1.8	4.3	2.0	9.1	14.3	100	145	149
9	0.2	0.2	0.3	1.9	3.8	4.3	100	141	150

* Refer to Figure 25 for locations.

** Wave height for the north wall was calculated from the two direction bands (70 and 50 deg) which were the closest to normal to the north wall. No direction was calculated for these waves.

Table 6

Summary of Locally Generated Wave Results

Location*	Height, ft			Period, sec			Direction, deg True N		
	Min.	Avg.	Max.	Min.	Avg.	Max.	Min.	Avg.	Max.
A	0.3	1.8	3.7	1.2	2.3	3.3	0.0	31.4	67.5
B	0.1	1.1	2.4	0.6	1.6	2.9	0.0	41.0	202.5
C	0.4	1.3	2.4	1.2	1.9	3.0	67.5	84.3	225.0
D	0.3	1.2	2.4	1.1	1.8	3.0	67.5	84.6	225.0
E	0.3	1.0	2.4	1.0	1.6	3.0	67.5	84.3	225.0

* Refer to Figure 25 for location.

PART V: FLOOD STAGES FOR THE INTERIOR OF ROUGHANS POINT

61. Once water levels, waves, and probabilities were determined for the simulated events, three processes remained before stage-frequency curves for the interior of Roughans Point could be constructed. These processes were the physical modeling of both existing and proposed Roughans Point structures, calculation of the overtopping rates, and routing of the resulting volumes through the Roughans Point area.

62. A two-dimensional physical model study was conducted to determine a method to calculate the overtopping rates at Roughans Point. Figure 27 is a map of Roughans Point showing the four northern reaches (A, B, C, and D) and the two eastern reaches (E and F). Reach B was not included in the overtopping analysis because its angle of orientation does not allow for direct wave attack. Reach F was not included in the overtopping analysis since water coming over this reach should flow toward the south away from Roughans Point. The structure chosen for reach E will be continued for reach F, both to provide protection for the integrity of the existing wall at reach F and to provide a more suitable termination location for the structure. Model tests were run for one proposed northern structure, the existing eastern structure, and five alternative eastern structures. Analysis of the existing northern structures (A, C, and D) was accomplished using overtopping data from a previous model study. Figures 28-31 contain drawings of the existing and originally proposed structure cross sections (NED 1983). Additional physical model tests, varying the shape of the revetment and the height of the wall, were conducted for the alternative structures for reach E (Figure 32). Only one proposed northern structure was tested, and it was used at all the north reach locations during simulations of the five different reach E alternatives. The pertinent facts for the 10 structures are included in Table 7. For complete details of the physical modeling see Ahrens and Heimbaugh (in preparation).

63. The results of the physical modeling were coefficients (Q_0 and C_1 in Table 6) for an overtopping rate equation (Equation 8). As indicated below, Equation 8 determines overtopping rate per foot of structure length with structure height, water level, wave height, and wave length as the independent variables.

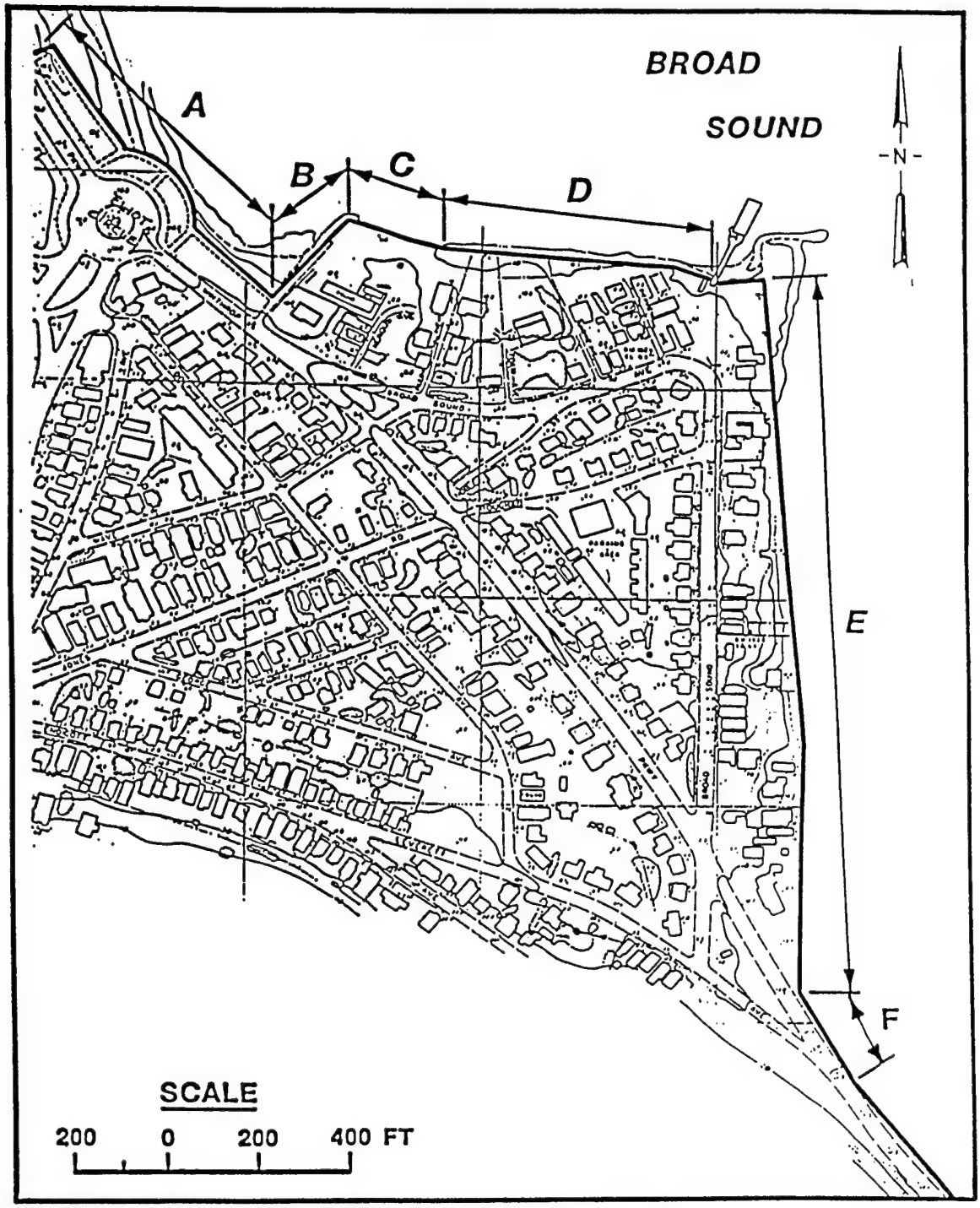

Figure 27. Location of reaches A-F at Roughans Point

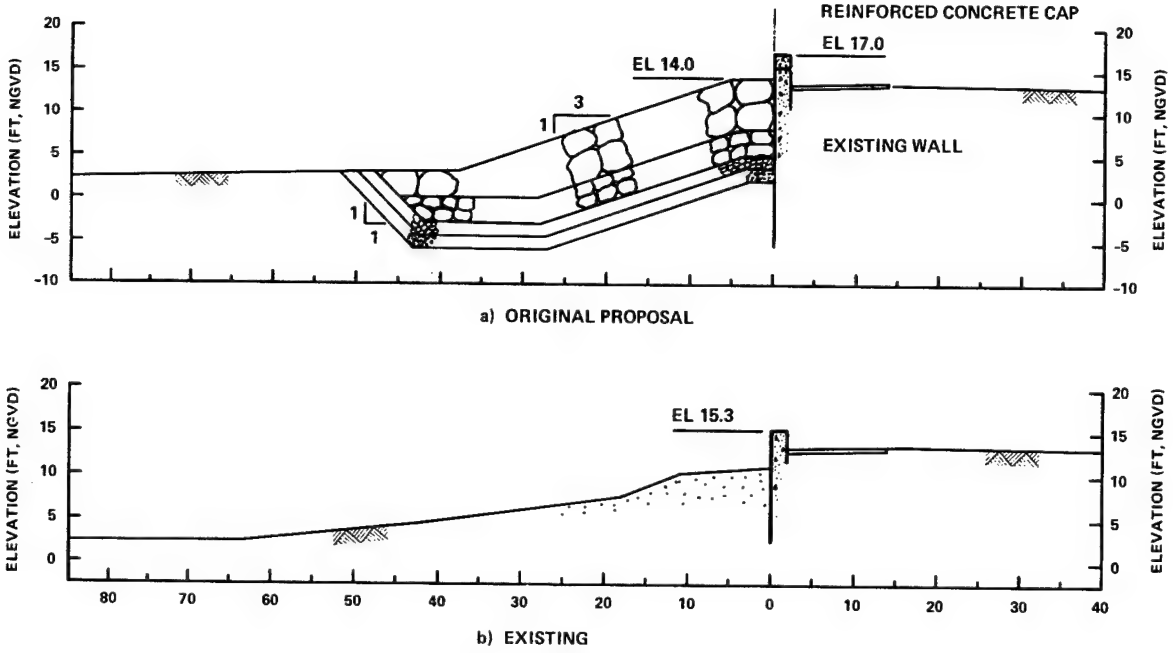

Figure 28. Existing and originally proposed Roughans Point structures for reach A

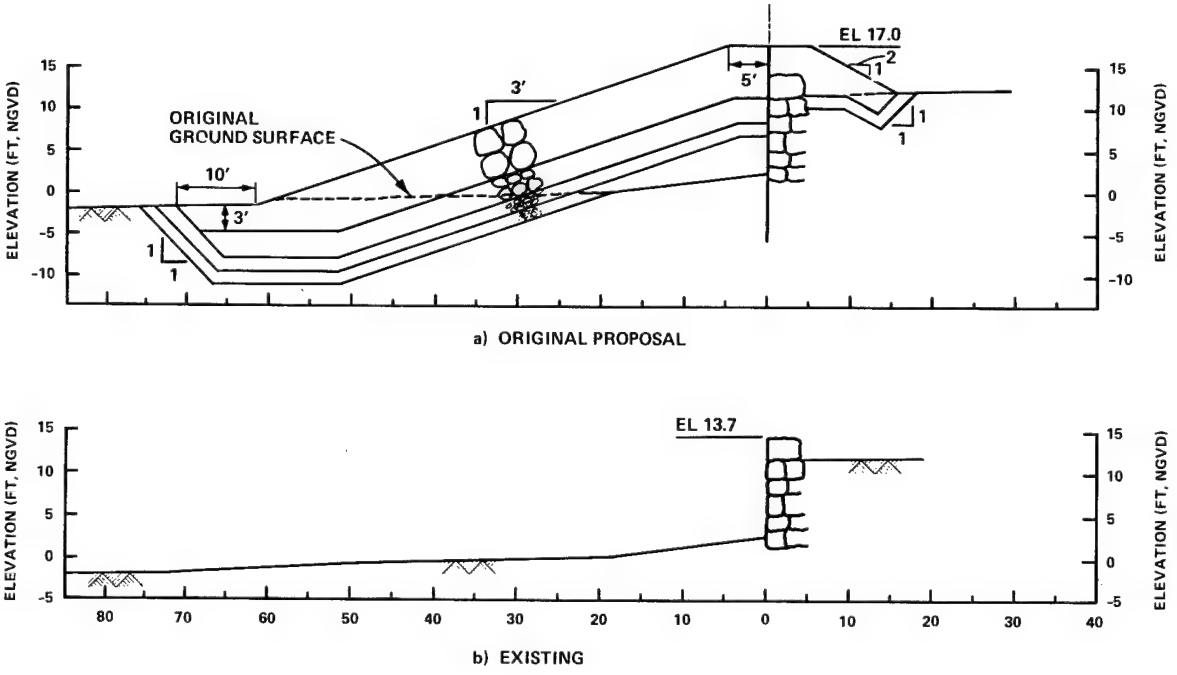

Figure 29. Existing and originally proposed Roughans Point structures for reach C

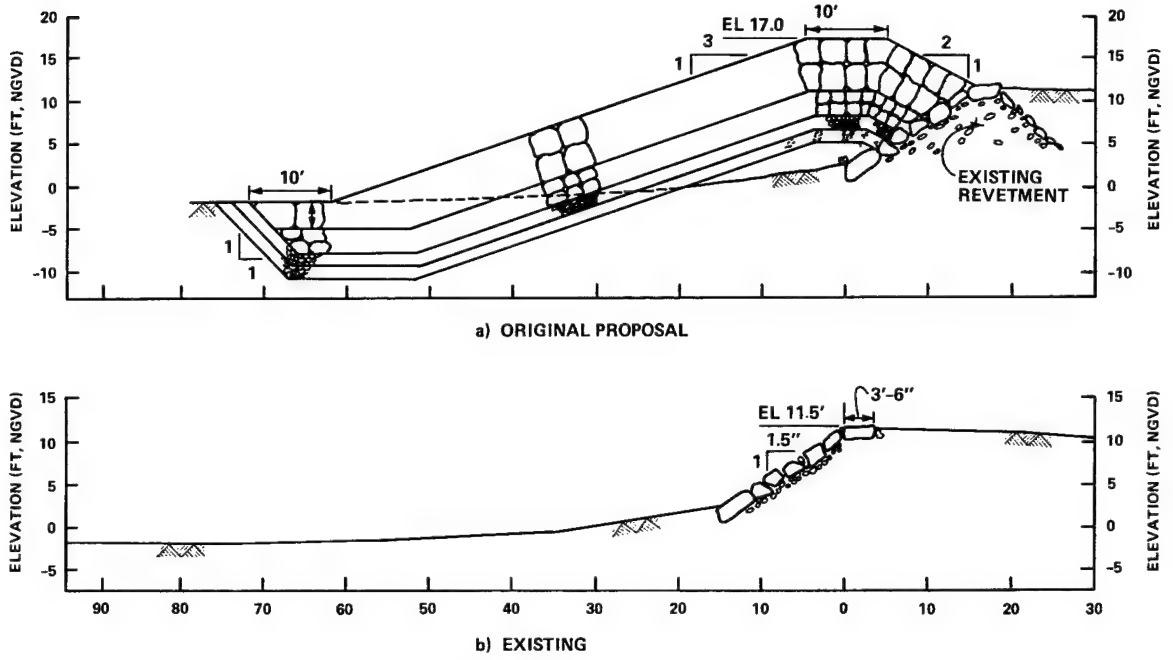

Figure 30. Existing and originally proposed Roughans Point structures for reach D

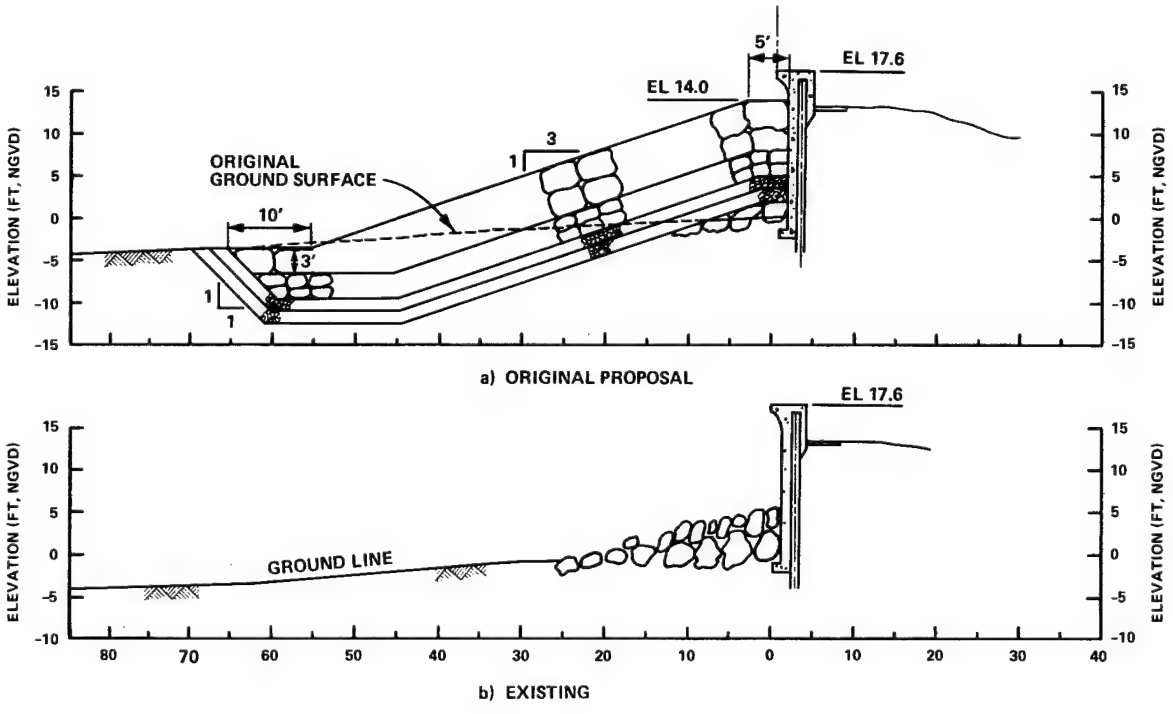

Figure 31. Existing and originally proposed Roughans Point structures for reach E

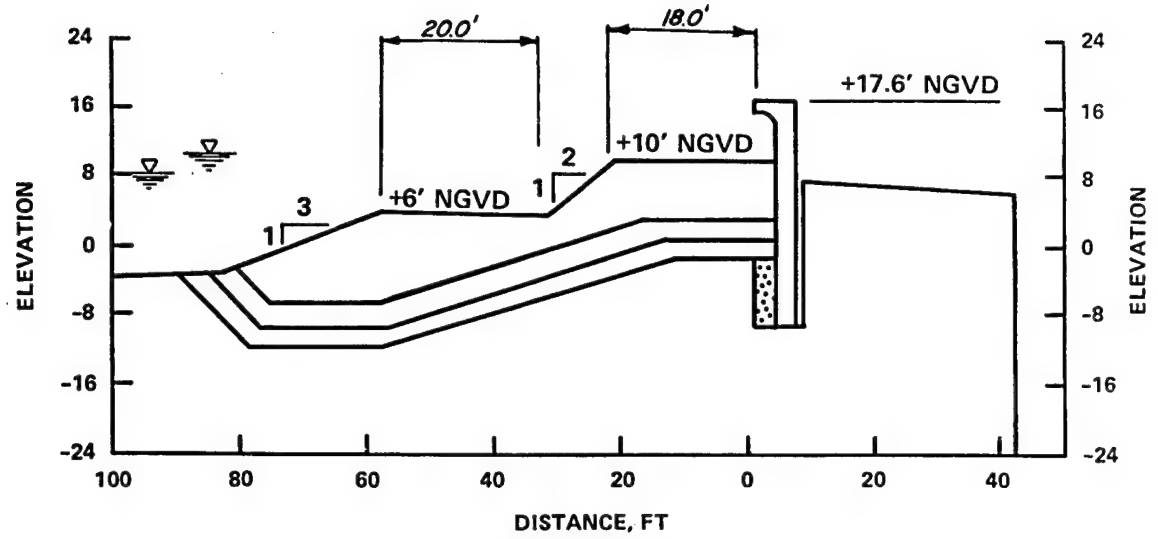

a. Two berms

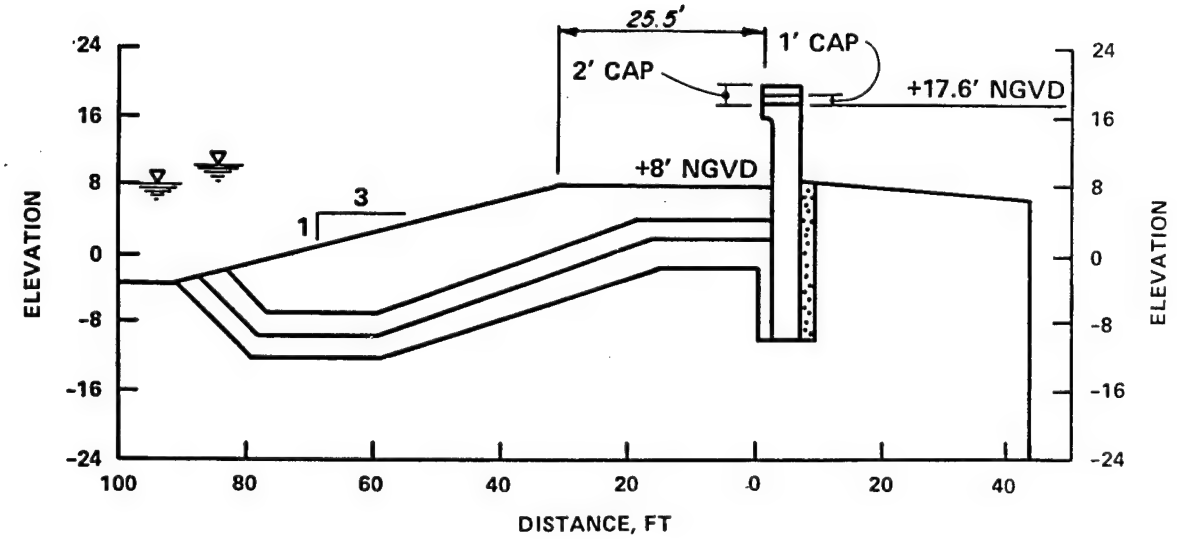

b. Wide berm, wide berm + 1-ft cap, and wide berm + 2-ft cap

Figure 32. Additional reach E structures analyzed

Table 7

Results of Physical Modeling

Test	Wall Height ft, NGVD	Revetment Slope ft/ft	Revetment Height ft, NGVD	Q_0	C_1
North Wall (A,C,D)					
Existing - A	15.3	-	-	3.473	-10.074
- C	13.7	-	-	10.580	-6.776
- D	11.0	1.5	11.0	18.859	-9.762
Original Proposal (A,C,D)	17.0	3.0	17.0	75.189	-17.783
East Wall (E)					
Existing	17.6	-	-	76.554	-14.078
Original Proposal	17.6	3.0	14.0	30.539	-13.431
Two Berms	17.6	3.0*	10.0*	158.240	-25.226
Wide Berm	17.6	3.0	8.0	439.220	-21.621
Wide Berm + 1-ft Cap	18.6	3.0	8.0	305.821	-23.073
Wide Berm + 2-ft Cap	19.6	3.0	8.0	93.037	-22.154

* Two berms (10.0 and 6.0 ft) in this alternative (see Figure 32).

$$Q = Q_0 e^{(C_1 F')}$$

$$F' = \frac{F}{\left(LH_{m_o}^2\right)^{1/3}} \tag{8}$$

where

Q = overtopping rate per foot of structure, cubic feet/sec/ft

Q_0 = coefficient determined from physical modeling, cubic feet/sec/ft

C_1 = coefficient determined from physical modeling

F' = dimensionless freeboard

F = freeboard, difference between still-water level and structure height, ft

L = wave length at structure, ft

Overtopping Rate Calculation

64. A computer code was developed to calculate overtopping rates for both existing and alternative structures for the 150 simulated events. Inputs to this code were time-histories of water level and wave parameters and coefficients from the physical modeling. Output was a time-history (15-min

increments) of overtopping rates at each reach for each event simulated.

65. A check was made to limit the calculated overtopping rates. Assuming that the maximum volume that can overtop a wall (when the freeboard is reduced to zero) is the volume contained between the elevation of the top of the wall and the surface of the wave (Weggel 1976), and assuming linear wave theory with a sinusoidal wave profile, Equation 9 can be derived. The 0.85 factor is included to account for nonlinearity of the real wave form. The condition where Q reached its maximum rate was not common, occurring only at the peak of the most severe events at existing reach D are expressed as

$$Q_{max} = \frac{0.85\ HL}{2\pi T} \tag{9}$$

66. The contribution from wind-aided overtopping was added to the rates calculated from the physical modeling results. This contribution is calculated using Equation 10 (adapted from the SPM (1984, p. 7-44)). Equation 10 is multiplied by 0.30 to account for overprediction.* For wind speeds of 60 mph or greater, $W = 2.0$; for wind speeds equal to 30 mph, $W = 0.5$. When the wind speed is zero, $W = 0.0$. For all other wind speeds W is interpolated from these values. Since wave runup data were not available from the physical modeling, Equation 11 (Ahrens and McCartney 1975) was used to estimate R in Equation 10. Equation 12 shows how the correction for wind aided overtopping is combined with the physical modeling results to produce total overtopping Q_t . Wind aided overtopping was usually less than 10 percent of total overtopping. These equations are written as follows:

$$C_w = 0.3W\left(\frac{F}{R} + 0.1\right)\cos\alpha\cos\beta \tag{10}$$

where

C_w = fraction of overtopping which is wind aided

W = coefficient based upon wind speed

R = wave runup, ft

α = wind angle relative to line normal to structure, degrees

β = structure slope, degrees

* Personal communication with John Ahrens, 1985, Wave Research Branch, Wave Dynamics Division, CERC.

$$R = \frac{Ha\chi}{1 + b\chi} \tag{11}$$

where

a = 0.956, regression coefficient

b = 0.398, regression coefficient

$$\chi = \frac{\tan \beta}{\sqrt{\frac{d}{L_0}}}$$

d = water depth at structure, d

and

$$Q_t = Q\ (1 + C_w) \tag{12}$$

where Q_t is the total overtopping rate per foot of structure in cubic feet per second per foot.

Flood Routing

67. Since the final desired result at Roughans Point is the frequency of the interior water levels, another computer code was developed to route overtopping volumes through the Roughans Point interior. This flood routing code used output from the water level modeling and overtopping rate calculations. Output from the flood routing consisted of the maximum stage calculated for each event. These maximum levels were used for input to generate the stage-frequency curve, for the interior of Roughans Point.

68. For this report the only source of flooding considered was from wave overtopping. Runoff from rainfall was not considered. This will have an effect on the resulting stage-frequency curve, especially at the lower return periods. This contribution will be determined by NED.

69. Outflows from the interior of Roughans Point result from several sources: storm drainage, seepage, pumping, and overflow both into the ocean over low wall sections and into other drainage areas over elevated roadways. Proposed improvements, in addition to providing for reduced rates of overtopping, also include increased storm drainage and pumping. Figure 33 contains a

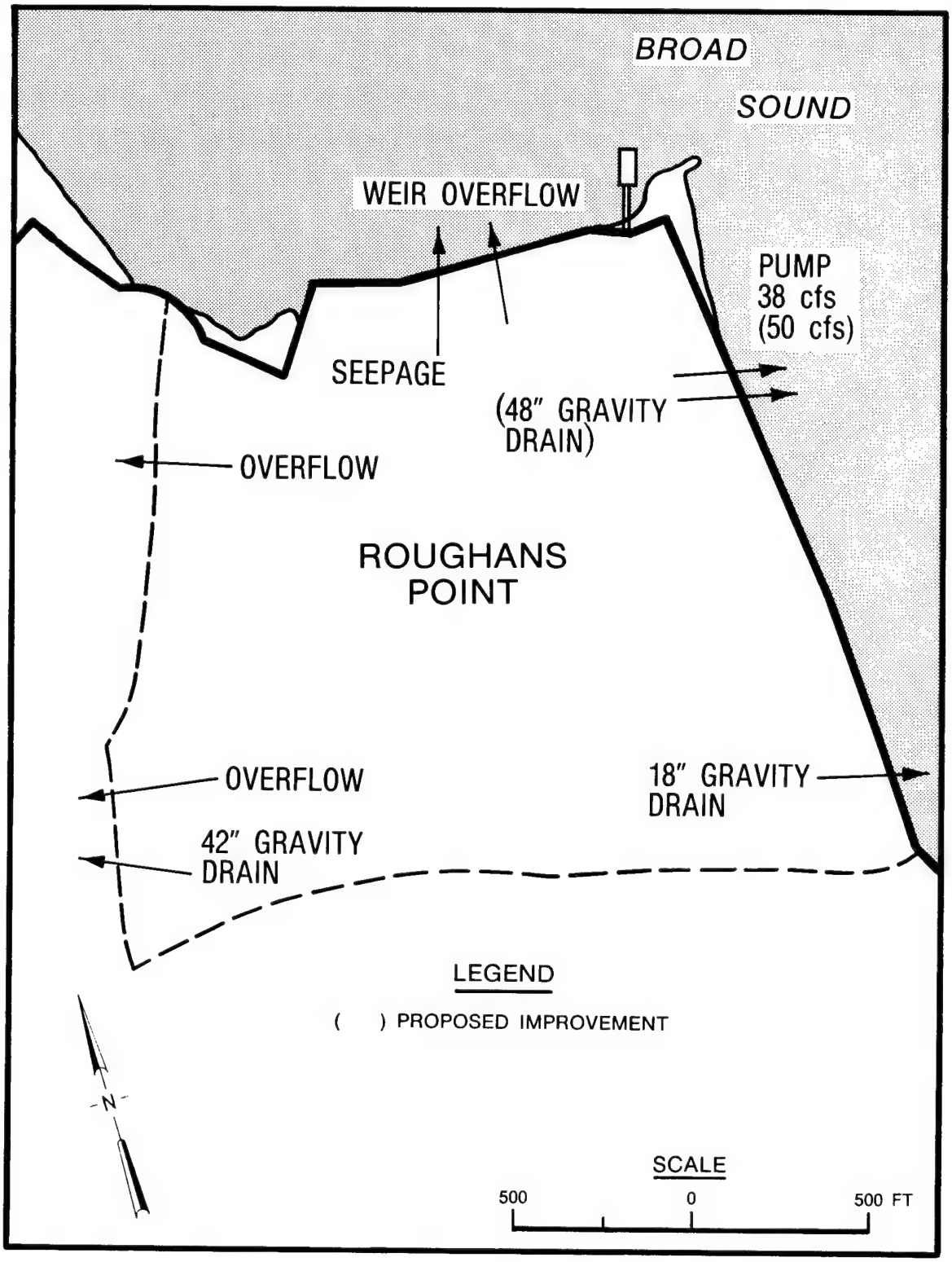

Figure 33. Sources of outflow from the Roughans Point interior

map of the Roughans Point area showing locations of both existing and proposed sources of outflow from the area.

70. There are two existing storm drainage outlets. The largest drain, a 42-in. diam pipe, runs to the west under Revere Beach Parkway at the southwest corner of Roughans Point. The other outlet is an 18-in. diam flat-gated drain which discharges into the ocean at the south end of Broad Sound Avenue. Two proposed improvements, both located at the existing pumping station, are an improved pump intake and a new gravity drain (42 in. diam) into the ocean through reach E.

71. Especially for existing conditions, the water levels inside Roughans Point can reach elevations which are higher than the existing wall at reach D (10.5 ft NGVD). Since the inside water level at these times would be higher than the ocean level, water would flow out over this wall section during peak flooding. This occurs with maximum interior water levels greater than approximately a 40-year return period. Also, at the western edge of the Roughans Point area, there are at least two locations where, at high water levels, water would flow over and under Revere Beach Parkway and into an adjacent drainage area. This outflow was modeled using weir equations.

72. The existing pumping station was built in 1975. The station has three pumps with a combined capacity of 48 cfs. However, with the existing intakes, the capacity is reduced to approximately 38 cfs. As was stated above, proposed improvements to the intakes for the pumping station are planned. The pumping station was inoperative during most of the February 1978 storm because of electric power failure. Also, if a severe storm is forecast the pumping station might not be operational after the evacuation of the area.

73. Loss of water from the interior of Roughans Point will also occur because of infiltration into the ground and seepage through the walls back out into the ocean. The seepage rate should be highest at low tide and when the interior levels are near the top of wall at reach D, where the ground appears especially porous.

74. Four basic equations (13-16) were used in the flood routing calculations. Equations 13-16 and the accompanying coefficients used to calculate the outflows from the interior of Roughans Point during times of overtopping were supplied by NED and were based upon their knowledge of drainage and hydrologic characteristics of the interior of Roughans Point. Drainage and seepage were calculated by Equation 13. Weir outflow was calculated when the

interior water level was higher than a boundary of the Roughans Point area. The weir outflow calculations were accomplished with two separate equations. When the ocean water level is below the height of a boundary, Equation 14 is used. When the ocean level is above the boundary, Equation 15 is used. Equation 16 was used for calculating the outflow due to pumping. Equations 13-16 are expressed as

$$Q_{out} = C_3(S_i - S_b)^{0.5} \tag{13}$$

where

Q_{out} = flow rate in cubic feet per second

C_n = coefficients (3-6)

S_i = interior water level

S_b = the larger of either 4.0 ft NGVD or ocean water level

$$Q_{out} = C_4\ (2.7)(S_i - S_w)^{1.5} \qquad \text{if } S_i > S_w \text{ and } S_o < S_w \tag{14}$$

where

S_w = height of wall section

S_o = ocean water level

$$Q_{out} = C_5(2.7)(S_i - S_w)^{1.5}\left[1 - \left(\frac{S_o - S_w}{S_i - S_w}\right)^{1.5}\right]^{0.385} \qquad \text{if } S_i > S_w \text{ and } S_o > S_w \tag{15}$$

$$Q_{out} = C_6 \tag{16}$$

75. The coefficients which were used in the above equations are shown in Table 8. Coefficients C_4 and C_5 are the length of weir section. Coefficient C_6 is the pumping rate in cubic feet per second. The increase in C_6 for the proposed condition is due to improved inlet design. Coefficient C_3 (see page and drainage) increases for the proposed condition because of the addition of a gravity drain (see Figure 33). Note that two values are listed for coefficients C4 and C5 . For existing conditions, reach D was divided into two sections for this analysis, one section at a height of

Table 8

Coefficients Used in Outflow Equations 13-16

Coefficient	Existing	Proposed
C_3	44	94
C_4	250	--
	575	--
C_5	250	--
	575	--
C_6	38	50

10.5 ft NGVD and the other section at a height of 11.5 ft NGVD (the first and second numbers, respectively). The overflows at the west end of the Roughans Point area are included only in the 11.5-ft coefficient.

76. In the flood routing calculations, the path and time of travel of the water from the time it overtopped the walls until it reached drainage points were not considered. Therefore, all water entering Roughans Point was assumed to be immediately available for drainage. The characteristics of inlets and the capacity of the system were taken into account in the coefficients of Equations 13-16. The flood routing calculations can be summarized as follows. A 1-minute time-step was used. Inflow volumes from wave overtopping from all reaches were combined and then added to the volume remaining from the previous time-step. Outflows were subtracted using the methods outlined in the previous paragraphs. For each time-step the resulting stage was determined from a stage-volume relationship supplied by NED (Figure 34). Finally, the maximum stage during each event was determined for use in stage-frequency generation.

77. Sufficient data were available during two historical events, February 1972 and February 1978, for a rough calibration and verification of the combined overtopping and flood routing process. The maximum interior flood level which occurred during these two events was estimated from water marks and eyewitness accounts. For calibration of the Roughans Point interior calculations, the 1978 event was simulated by the storm surge and wave models. Then the overtopping rates and maximum stage were calculated by the computer codes described above. The first attempt predicted interior stages which were in excess of those observed; therefore, refinements and adjustments, discussed

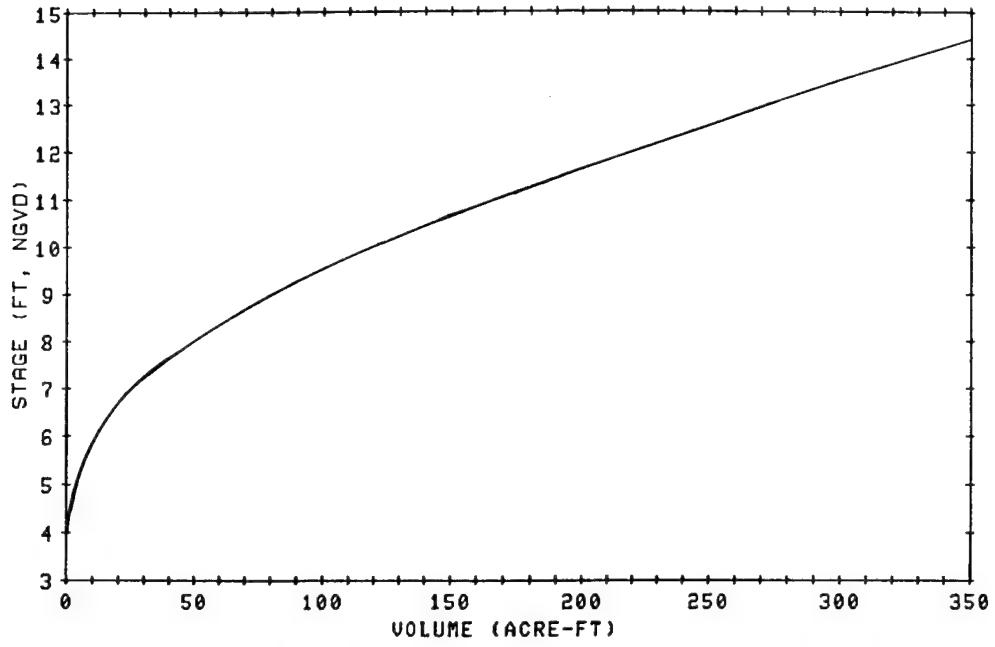

Figure 34. Stage volume versus volume relationship for Roughans Point interior

in the following paragraphs, were made to match the estimated stages.

78. For existing conditions, overtopping at reach D was not allowed during periods of weir outflow at that wall. Since there would be a continuous current flowing outward in this situation, it was reasoned that any overtopping would almost immediately be conveyed back into the ocean. Without this reasoning, reach D would contribute enormous quantities of overtopping at those times when Roughans Point was full to overflowing. This assumption is consistent with the limited information available from the only historic event, in February 1978, during which the water level inside Roughans Point was higher than the elevation of reach D.

79. Wave heights attacking reach E were reduced by 15 percent. There were several possible adjustments which could have been made to eliminate overprediction of overtopping rates. Among these are (a) reducing the calculated overtopping rate, (b) lowering the still-water level, and (c) reducing the wave heights. The wave heights were selected for reduction because they are the least certain of these possibilities (see "Estimating Error in Stage-Frequency Curves" in Part VI).

80. Wave heights were also lowered for the three northern reaches. At

reach D , the height of waves which propagate from the open ocean was set to zero. There were two justifications for this adjustment. First, due to the orientation of the wall, there is no opportunity for these waves to attack the wall from any but very oblique angles. Second, reach D would be partially sheltered from waves from these oblique angles by the tip of Roughans Point and by Simpson's Pier. At reaches A and C, waves from the open ocean were reuced by 50 percent. As at reach D, these waves would approach from an oblique angle; however, refraction would turn these waves more normal to reaches A and C than at reach D. Since the physical modeling assumed a wave direction normal to the structure, using the full wave height for these waves would result in the overprediction of overtopping rates. The locally generated waves were reduced by 15 percent for all three north wall sections. This can also be justified by the fact that these waves do not always approach normal to the wall sections.

81. The above adjustments were made to the overtopping calculation and flood routing computer codes to match calculated values of interior stage to those observed during the February 1978 storm. The February 1972 storm was then simulated to verify the revised procedure. The results of these two simulations are compared to estimates of actual flooding in Table 9.

Table 9

Comparison of Calculated to Observed Flood Stage

Storm	Calculated ft, NGVD	Observed ft, NGVD
1978	11.9	11.8-12.0
1972	9.6	8.8-9.0

82. The results of this calibration and verification were judged to be acceptable. The 0.6-ft difference between observed and calculated water levels for the 1972 storm seems reasonable when considering that the calculations were based upon a stage-volume relationship determined from 2-ft contour intervals.

Simulation of the Event Ensemble by the Flood Routing Model

83. Following calibration and verification of the flood routing model,

events were simulated for the existing one and five alternative structure combinations. Inputs to the model were the time-histories of overtopping rates for each of four Roughans Point reaches (A, C, D, and E). Six different combinations of the northern and eastern reach structures were modeled. Since the north wall has only two structure classes, "Existing" and "Original Proposal," a combination of northern and eastern structures was given the name of the eastern structure. The "Existing" combination is self-explanatory. The "Original Proposal" combination is made up of the northern and eastern structures proposed before the beginning of modeling (see Figures 28-31 and NED 1983). The other four alternatives, "Wide Berm," "Two Berms," "Wide Berm + 1-ft Cap," and "Wide Berm + 2-ft Cap," combined the eastern structure of the same name (see Figure 32) with the northern "Original Proposal" structure. There were two output files. One file was a time-history of flood stages for each event and structure simulated. The second file contained the maximum stage during each event for each combination of structures simulated. This second file was used to compute the stage-frequency curves.

North Wall Tests

84. During the course of simulating overtopping and flood routing, there was no contribution to overtopping volumes from the "Original Proposal" northern structure. Tests were conducted to determine the effect of lowering the height of the protection along the whole north side of Roughans Point. Since no additional physical model tests were to be run, a method had to be devised to use physical model data from the proposed northern structure (17 ft). Reconsideration of the overtopping rate equation (Equation 8), reveals that changing the height of the northern structure would only change one term in that equation, namely F_c, the freeboard. Since the water level would not be changed, the characteristics of the waves attacking the structure would not be changed. Therefore, even though lower heights were not tested, estimates of the overtopping for lowered structure heights could be made by reducing the freeboard in Equation 8. Using the February 1978 historic event for the initial tests, the northern structure was lowered in 1-ft increments. For this event, overtopping did not start until the structure was lowered to 14 ft NGVD, and large volumes of overtopping did not commence until a structure height of 12 ft NGVD was tested. Using these results, the full ensemble

of 150 events was simulated for northern structure heights of 14, 13, and 12 ft. The results of these tests are presented in Part VII.

PART VI: STAGE-FREQUENCY CURVES

85. In this section, the method for establishing stage-frequency curves will be described for both the still-water locations and for the interior of Roughans Point.

86. The goal of this project was to produce stage-frequency curves for two distinct processes. The first process involved the interaction of storm surge and tide to produce still-water levels at coastal (and river) locations, and the second process combined waves with the surge and tide to produce flood levels behind seawalls due to wave overtopping. Although the simulation of these two processes involved some different steps, development of frequency curves for the two processes once the water levels are determined is essentially the same.

87. Probability was assigned to each of the events selected for simulation, as described in Part II. By assigning the probability to the maximum still-water level caused by the event at each numerical gage location, stage-frequency curves can be constructed by the following method. First, an array of possible stages at each gage location is established with a discretization interval (0.1 ft for this project). Next, for all 150 events, the probability masses assigned to each event are accumulated in the stage interval which brackets the maximum water level that occurred for that event. Exceedances can be determined for any interval by adding the probability of that interval to the sum of the probabilities of the intervals above it. After this was accomplished for the total set of 150 events, the process was repeated for each of the three sets of 50 events. This produced three additional sets of stage versus exceedance relationships which were used for confidence calculations.

88. The range of stages modeled in the still-water level portion of this study was just over 3 ft (from 7.9 to 11.2 ft NGVD). All of the resulting 33 discretization intervals did not receive probability. Some intervals received probabilities from several events causing in places (in the array of stages) a series of heights where no event deposited its probability. This occurrence results in a jagged line when the stage-frequency is plotted.

89. There is no physical reason why adjacent height intervals should have greatly different probabilities. The jagged nature of the raw curves is caused by trying to represent a continuous process (all possible storm events)

with a discrete process (50 storm events). Modeling more events would result not only in a smoother curve but also in greater expense. For example, had 500 events been modeled, it would be highly unlikely that one height interval would receive the probabilities of several events while the three intervals below received none. Therefore, if an economically feasible number of events were to be modeled, the raw output of the stage-frequency generation would require smoothing to adequately represent a continuous curve.

90. Smoothing was accomplished using linear regression of the stage-frequency data when plotted on an appropriate probability paper. Equation 17 is a formula for the construction of Weibull probability paper. Where

$$x_{new} = \left[-\ln\left(x_{old}\right)\right]^{c} \tag{17}$$

the variable x_{old} is the inverse return period, x_{new} is the transformed abscissa value, and c is the variable to be adjusted to best represent the data with a straight line. After numerous trials a c value of 0.80 was chosen. Figure 35 contains a plot of both the raw and regressed stage-frequency curves for the Fox Hill Drawbridge still-water location.

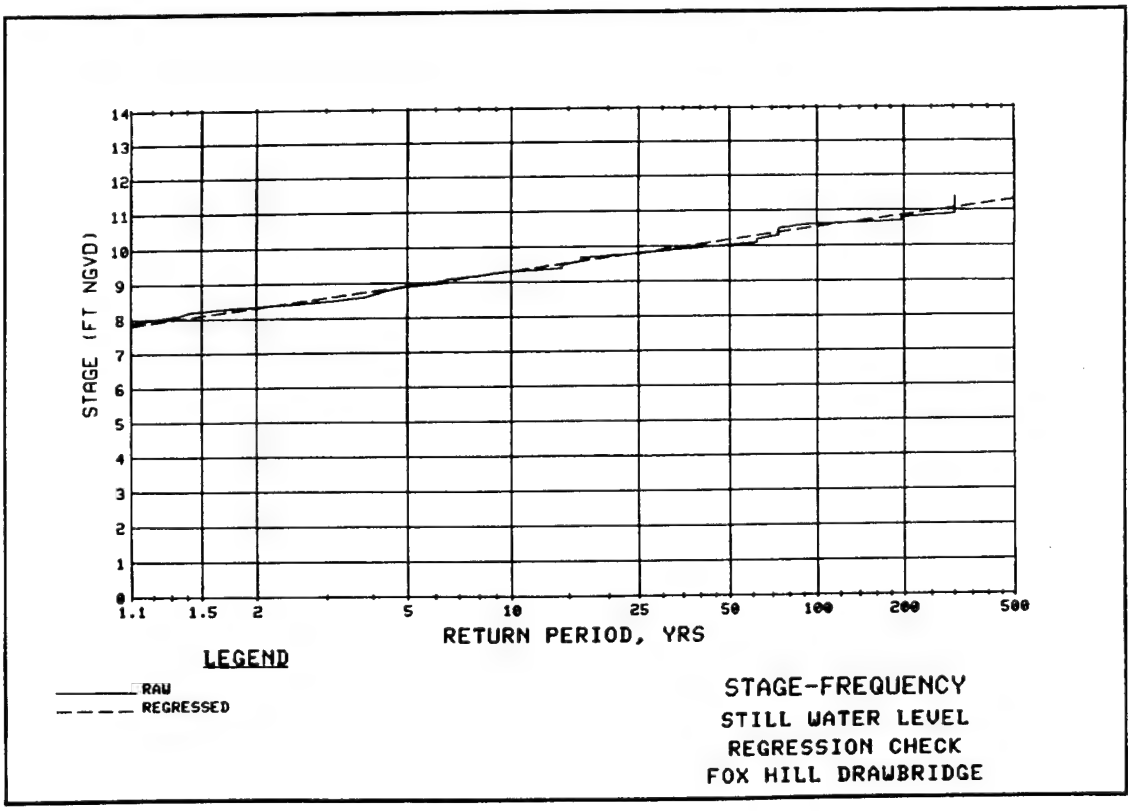

Figure 35. Example of raw and regressed stage-frequency curve

PART VII: RESULTS AND CONCLUSIONS

Roughans Point

91. The stage-frequency curves for the interior flood levels in Roughans Point are presented in Figures 36-40. For these curves it was not possible to regress the total curve as was explained in Part VI. The physics of the problem undergoes a sudden change at higher levels where the effect of weir outflow limits the capacity of the interior of Roughans Point. Also the extreme lower portion of the curves does not conform to the straight line tendency of the middle portion. The lowest possible stage is 3.6 ft NGVD corresponding to the lowest point inside Roughans Point. Consequently, the stage-frequency curves remain at 3.6 ft until the onset of overtopping. Therefore, the linear regression was limited to the middle segment of each curve for the Roughans Point stage-frequency curves. Smoothing for both the lower and higher segments of the curves was done by eye.

92. As explained in paragraph 83, flood levels were calculated for six different combinations of northern and eastern structures. The names of the structure combinations plotted in Figures 36-40 refer to the names of the eastern component. (For the "Existing" and "Original Proposal" structures (NED 1983) refer to Figures 28-31, and for the other alternatives refer to Figure 32.) Three tests lowering the height of the proposed north wall structure were conducted. Since it was determined that there was a negligible difference between the curves with the originally proposed north wall height (17 ft NGVD) and the curves from the highest of the three additional tests (14 ft NGVD), curves resulting from the 17-ft height are not presented. Curves for the six structure combinations are shown in Figures 36-38, with the height of the northern structure in the three figures being 14, 13, and 12 ft, respectively. Note that the 14-, 13-, and 12-ft north structure heights refer only to the alternative structure combinations. For the "Existing" curve, shown on these graphs for comparison purposes, the northern structure is set at the existing height for each structure section.

93. Using Figure 36, several features of the stage-frequency curves for the interior flood levels at Roughans Point will be discussed. The greatest differences among the alternatives occur at the lower return periods. Near the 500-year return period all six curves tend to come together. As was

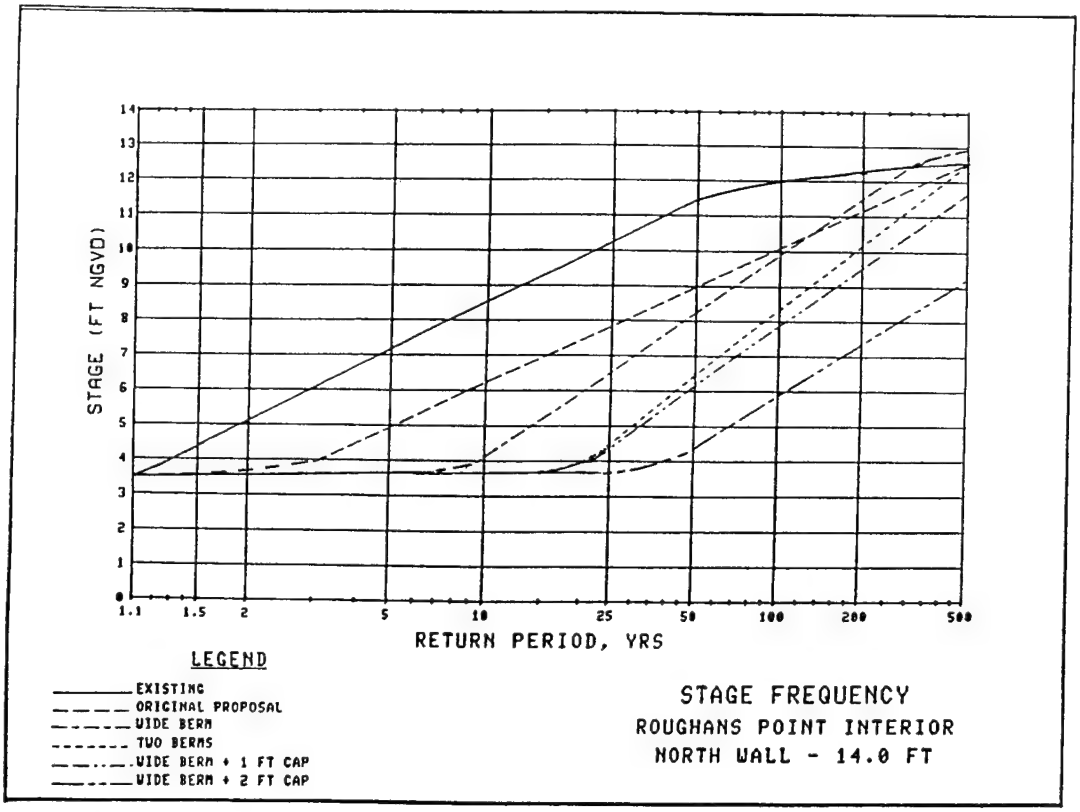

Figure 36. Roughans Point stage frequency, northern structure height = 14 ft

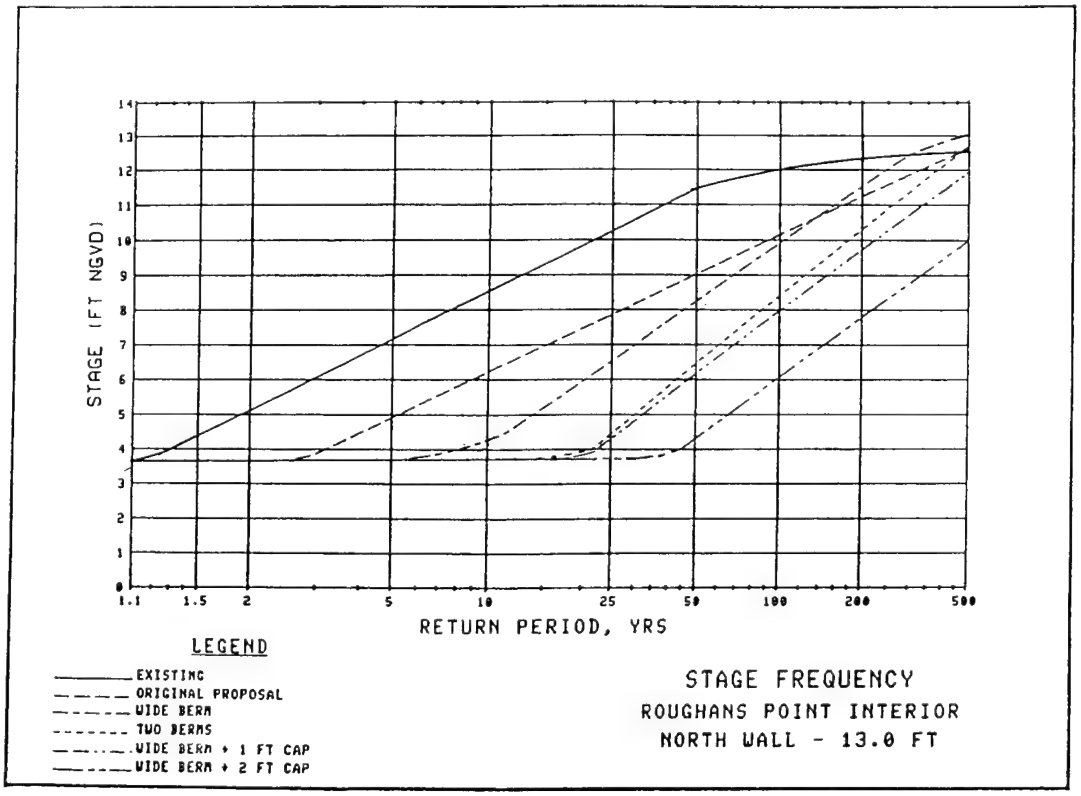

Figure 37. Roughans Point stage frequency, northern structure height = 13 ft

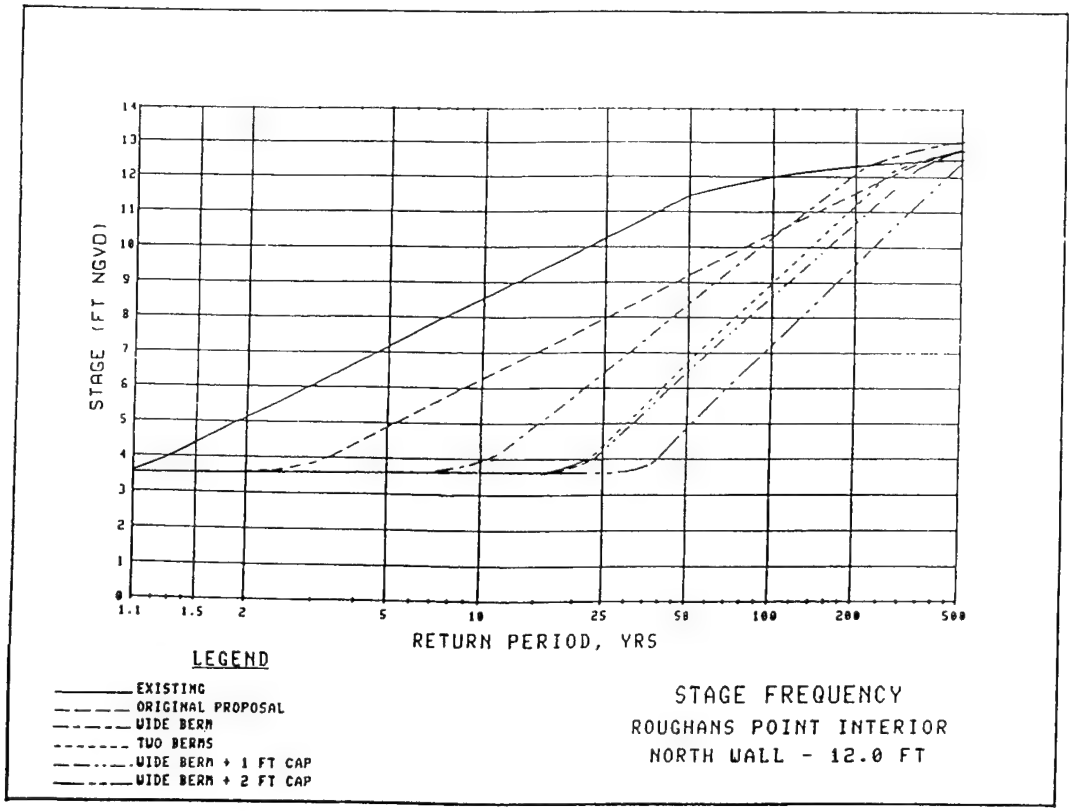

Figure 38. Roughans Point stage frequency, northern structure height = 12 ft

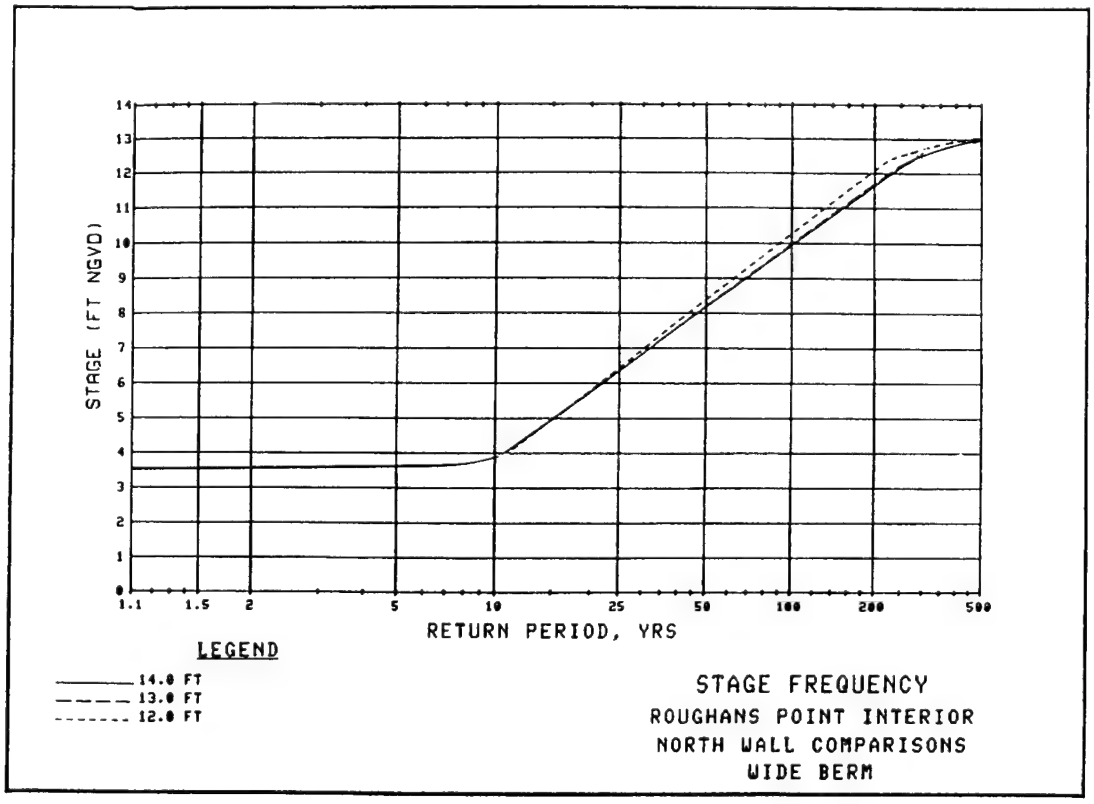

Figure 39. Effect of northern structure height on the "Wide Berm" alternative

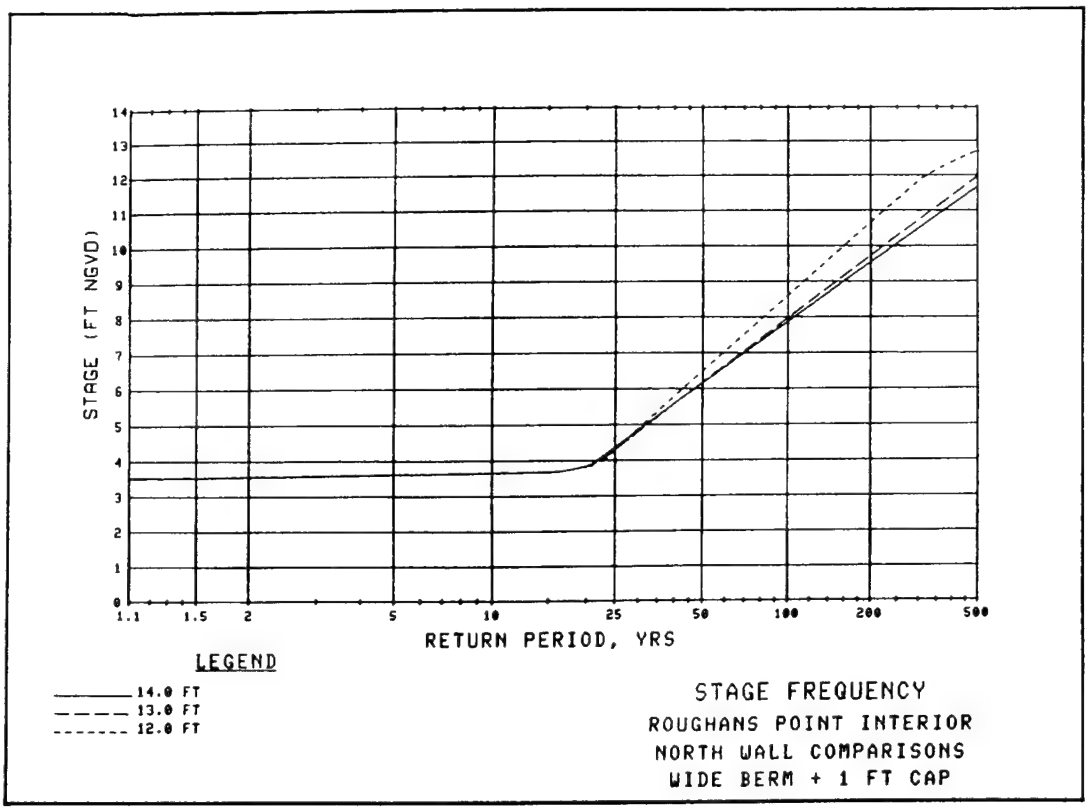

Figure 40. Effect of northern structure height on the "Wide Berm + 1-ft Cap" alternative

discussed in Part V, Roughans Point has a limited volume capacity. When the amount of overtopping surpasses the capacity of the interior, the water pours out over roadways into another drainage area. Therefore, although the various alternatives are still producing very different overtopping rates, the flood levels that result are similar for the highest return periods.

94. Although the "Two Berms" alternative produced results very similar to the "Wide Berm + 1-ft Cap" alternative, the "Two Berms" structure is not a recommended alternative. The physical model tests showed the "Two Berms" structure was not stable. For details see Ahrens and Heimbaugh (in preparation).

95. The wide berm configuration proved to be effective in lowering overtopping at the still-water levels which accompany return periods less than 100 years. Notice, however, that in Figure 36 the "Wide Berm" curve crosses above the "Original Proposal" curve at about 150 years. The berm loses its effectiveness in reducing overtopping as the higher still-water levels submerge it.

96. The effectiveness of the berm is dramatically improved by adding

height to the wall behind it, as is seen in both the "Wide Berm + 1-ft Cap" and the "Wide Berm + 2-ft Cap" alternatives. Studying the overtopping rate equation (Equation 8) shows that the overtopping relationships developed from the physical model are very sensitive to freeboard and, therefore, to structure height.

97. Recommending a height for the north wall is difficult. None of the three heights were actually modeled by the physical model. The final structure selected must, of course, result from a detailed economic analysis. The technique of using the 17-ft north wall physical model results to predict the results for lower revetment heights by lowering freeboard was the best available but must lower confidence in the analysis. The choice seems to be between the 13- and 14-ft heights. The 12-ft height allows significantly greater overtopping to occur. Figures 39 and 40 show the effect of north wall height on the "Wide Berm" and the "Wide Berm + 1-ft Cap", respectively. Since the height of the existing wall sections at A and C (15.3 and 13.7 ft NGVD) is higher than that of the 13-ft trial, the best choice would be a revetment at a 13-ft height with the wall keeping its existing height at A and C, with the height at B being a transition between A and C, and the height at D matching that at C.

Still-Water Locations

98. Stage-frequency curves for 14 locations within the Saugus-Pines River system and the coastal areas bordering Broad Sound are presented in Figures 41-54. Figure 23 shows the location of these 14 numerical gages. Just prior to the completion of the study, additional data were collected by NED during the highest predicted tides of September, October, November, and December 1985 for several locations in the extreme upriver portions of the modeling area (Figure 55). Because of increased interest in flood protection for these areas, it was hoped that the additional data would allow adjustment of the modeling results upstream of where calibration data were previously available. Data were collected also at the Fox Hill Drawbridge calibration gage location, and data for the Boston tide gage were obtained from NOS. These data are summarized in Table 10.

99. Based on the information shown in Table 9, adjustments were made to those numerical gage locations west of the abandoned highway embankment and

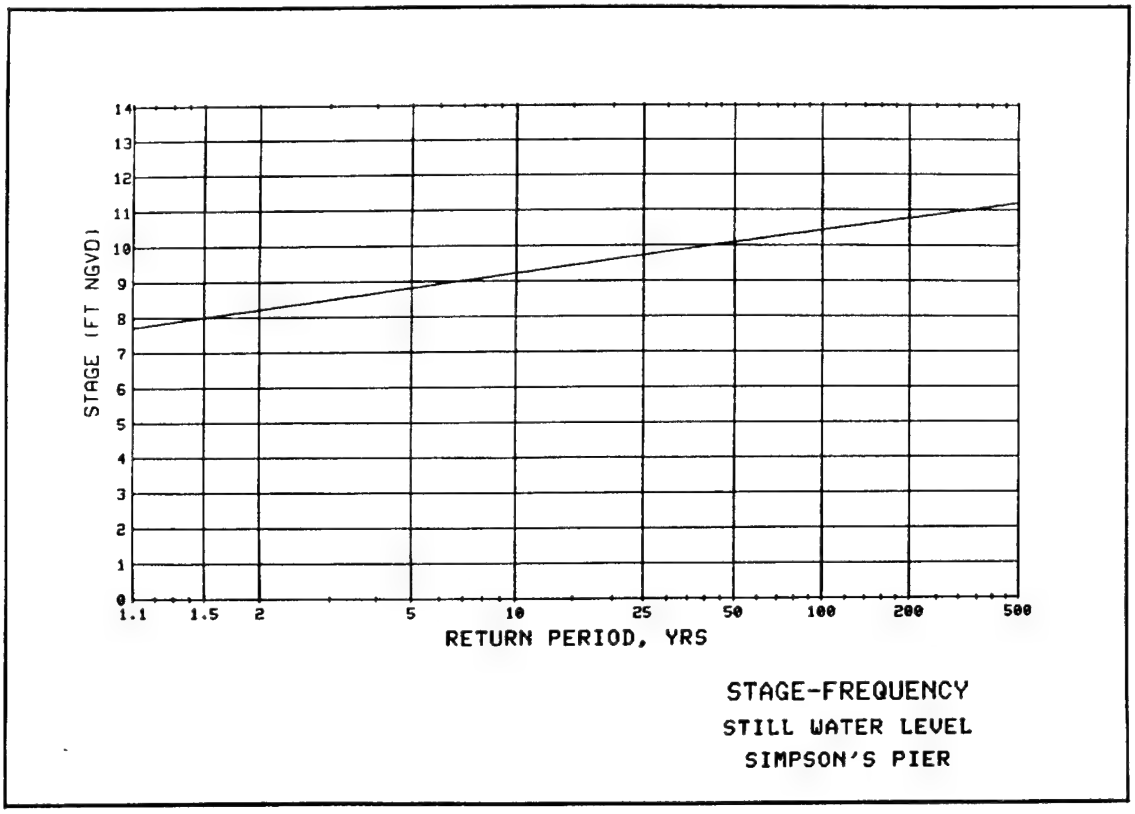

Figure 41. Still-water level stage-frequency curve, Simpson's Pier

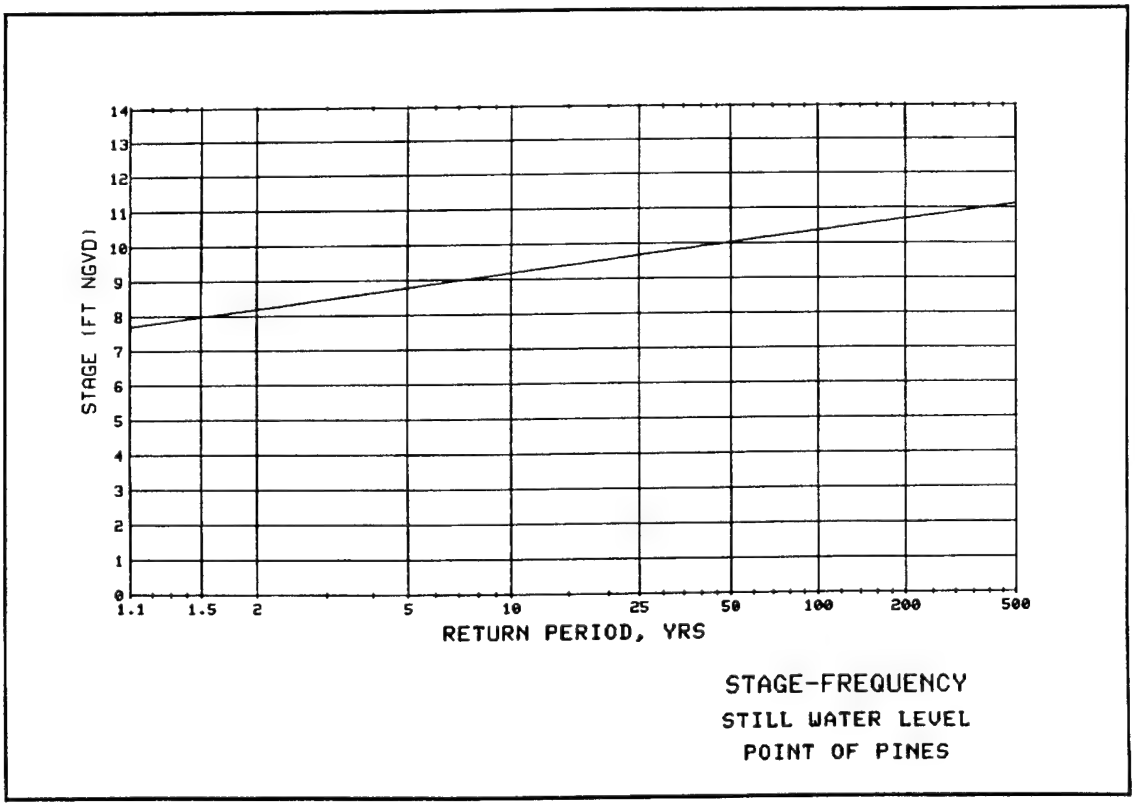

Figure 42. Still-water level stage-frequency curve, Point of Pines

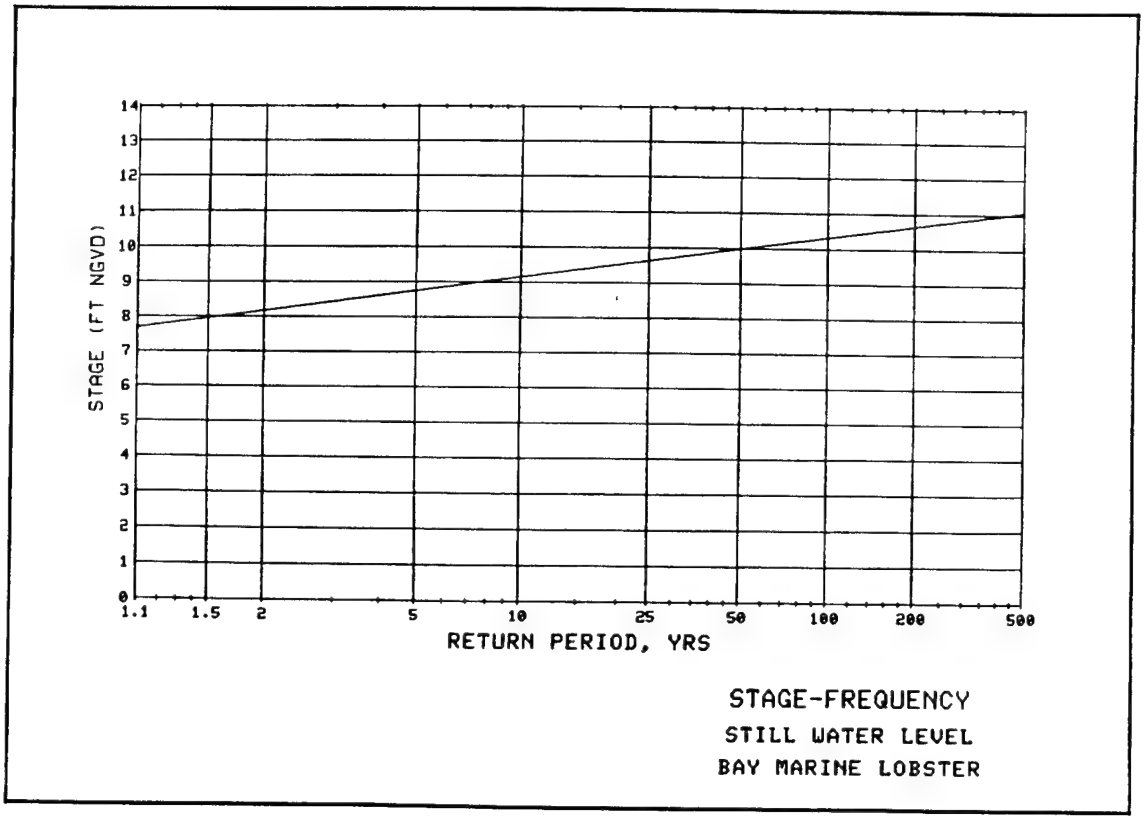

Figure 43. Still-water level stage-frequency curve, Bay Marine Lobster

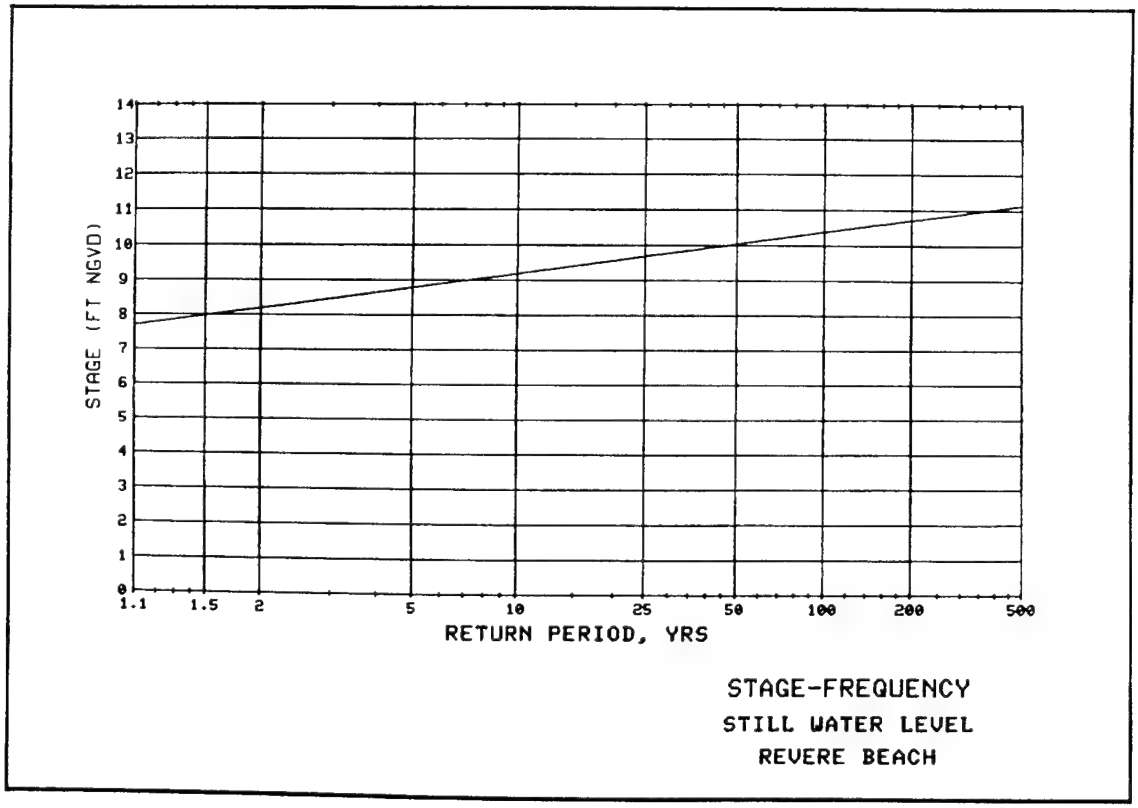

Figure 44. Still-water level stage-frequency curve, Revere Beach

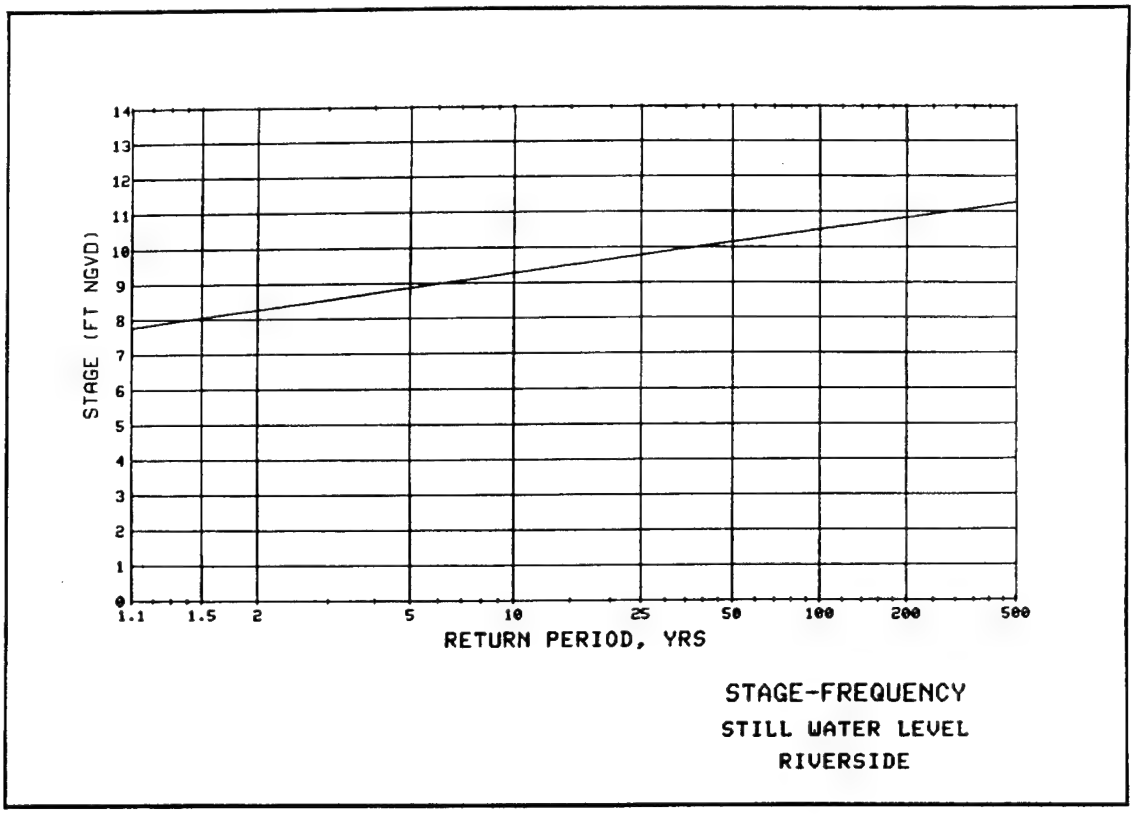

Figure 45. Still-water level stage-frequency curve, Riverside

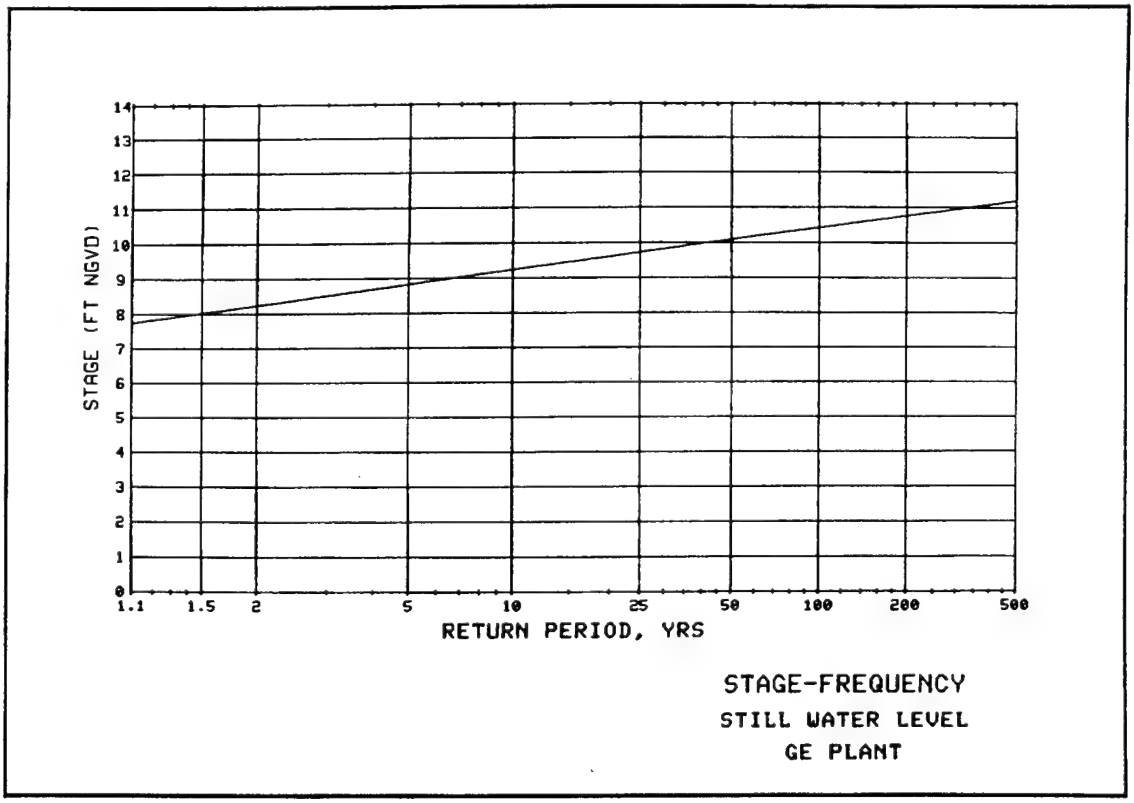

Figure 46. Still-water level stage-frequency curve, GE Plant

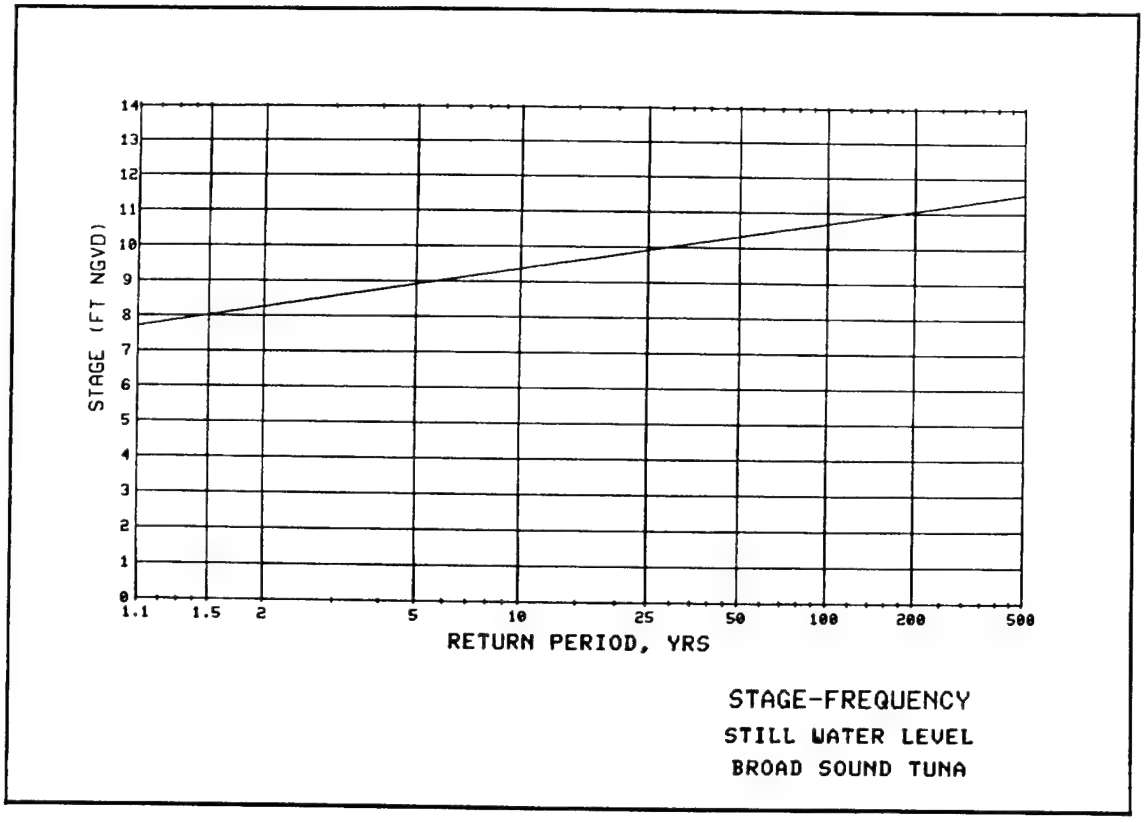

Figure 47. Still-water level stage-frequency curve, Broad Sound Tuna

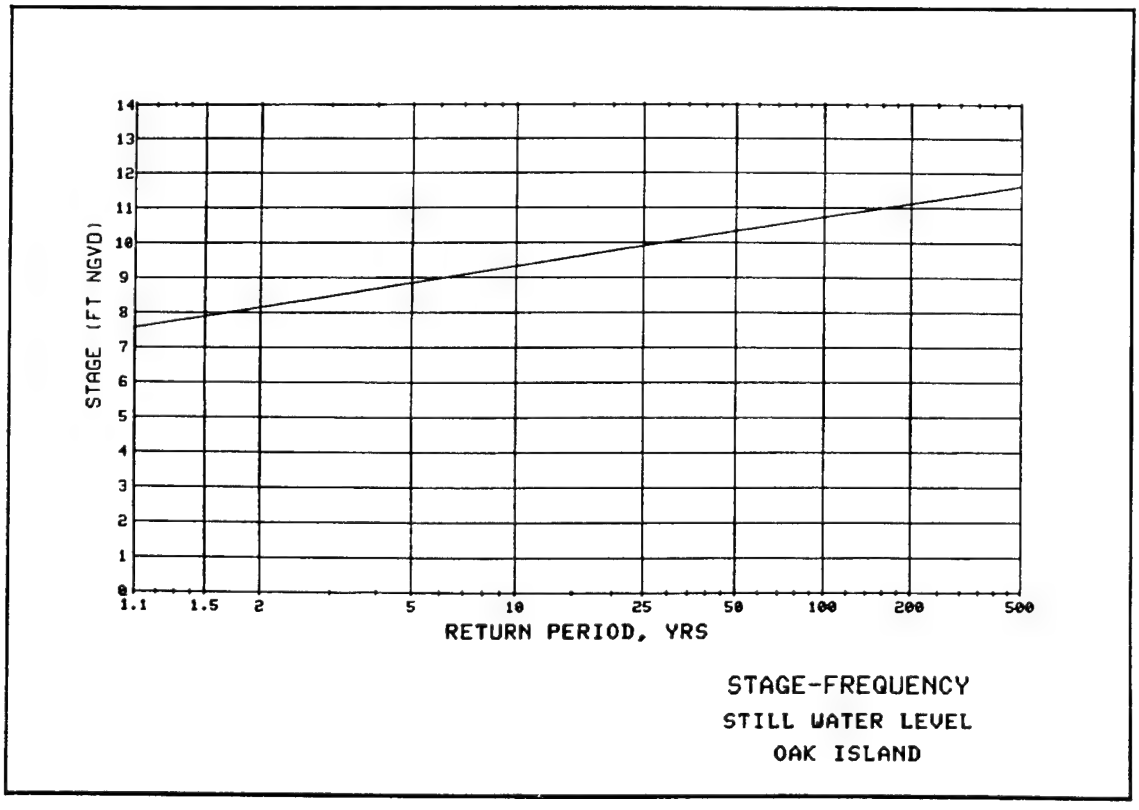

Figure 48. Still-water level stage-frequency curve, Oak Island

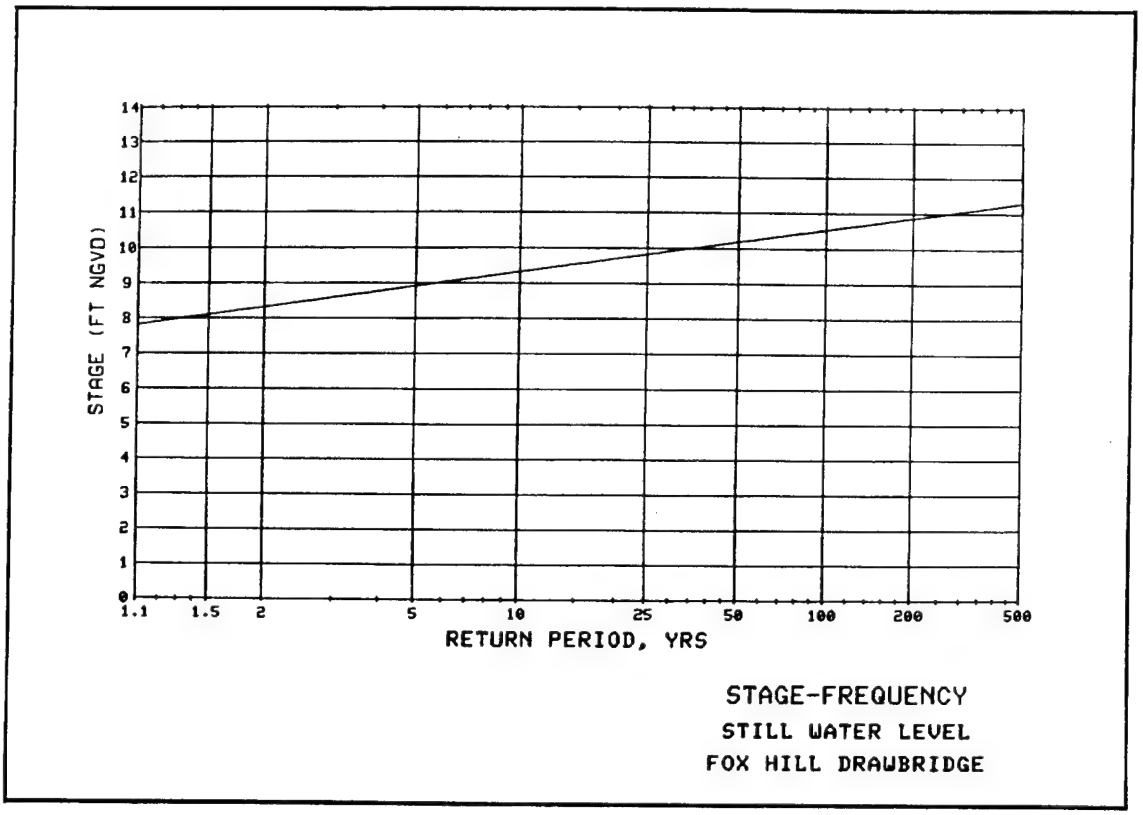

Figure 49. Still-water level stage-frequency curve, Fox Hill Drawbridge

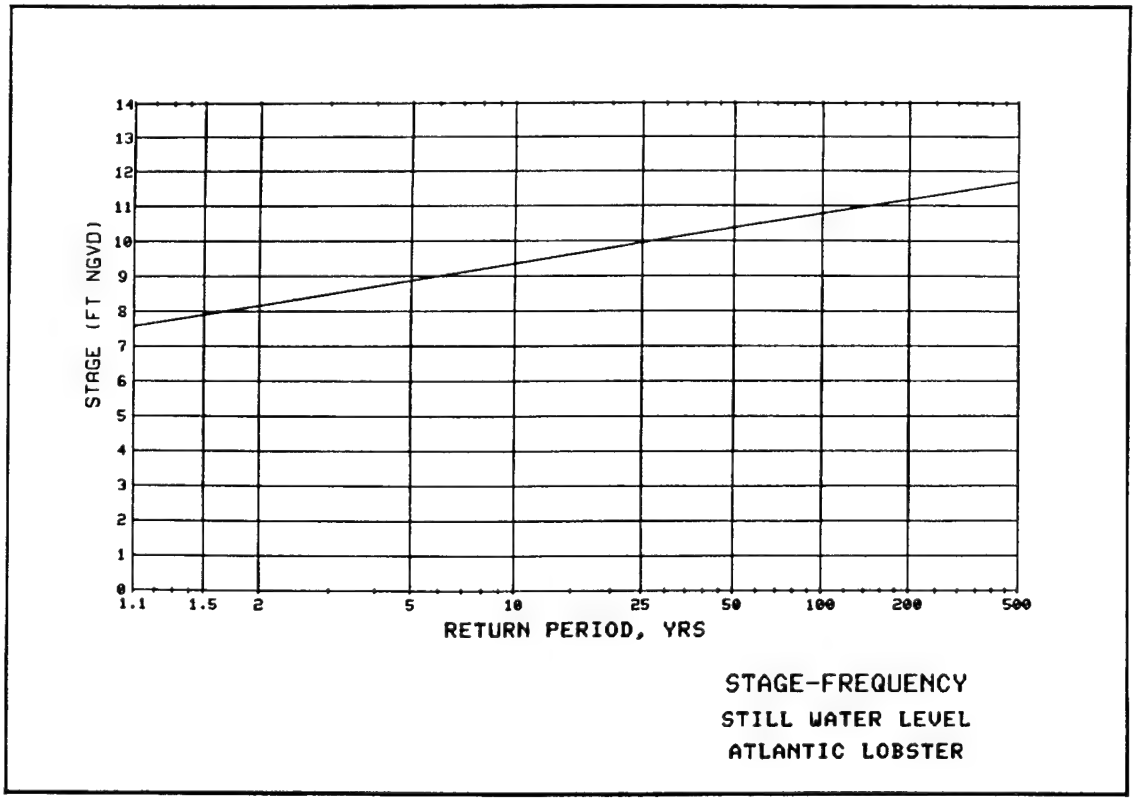

Figure 50. Still-water level stage-frequency curve, Atlantic Lobster

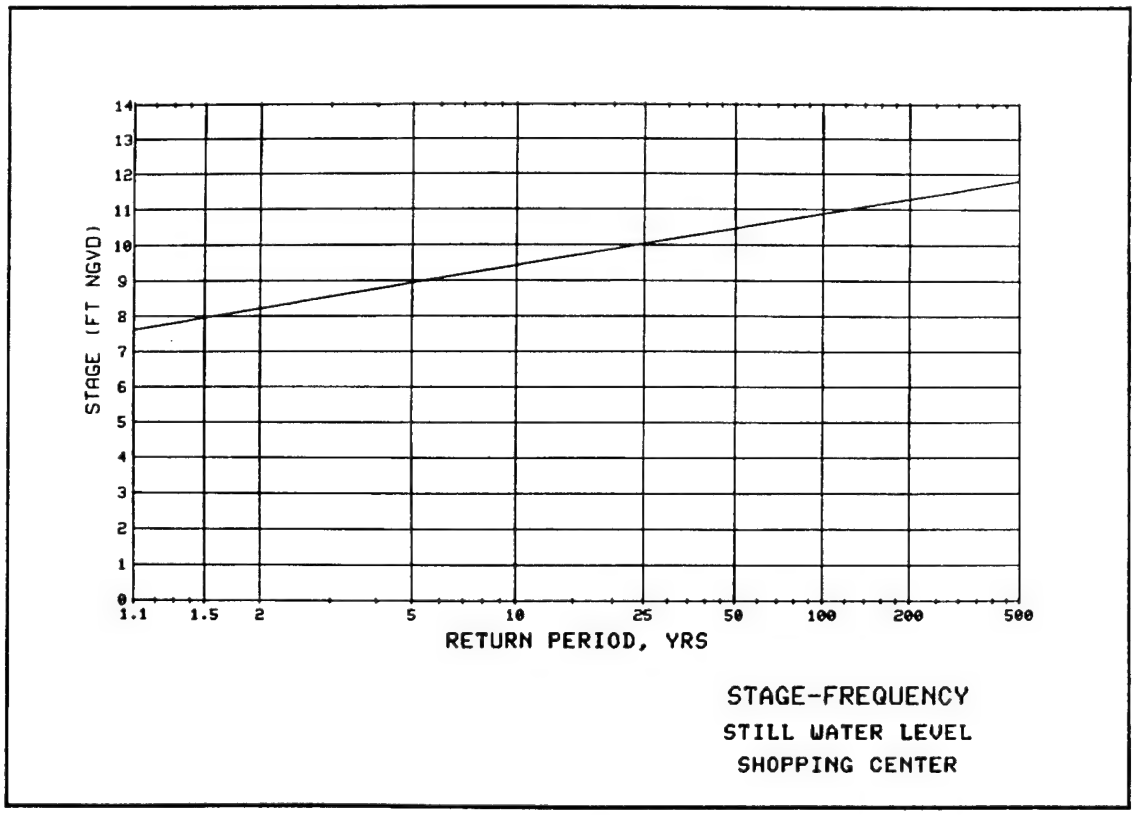

Figure 51. Still-water level stage-frequency curve, Shopping Center

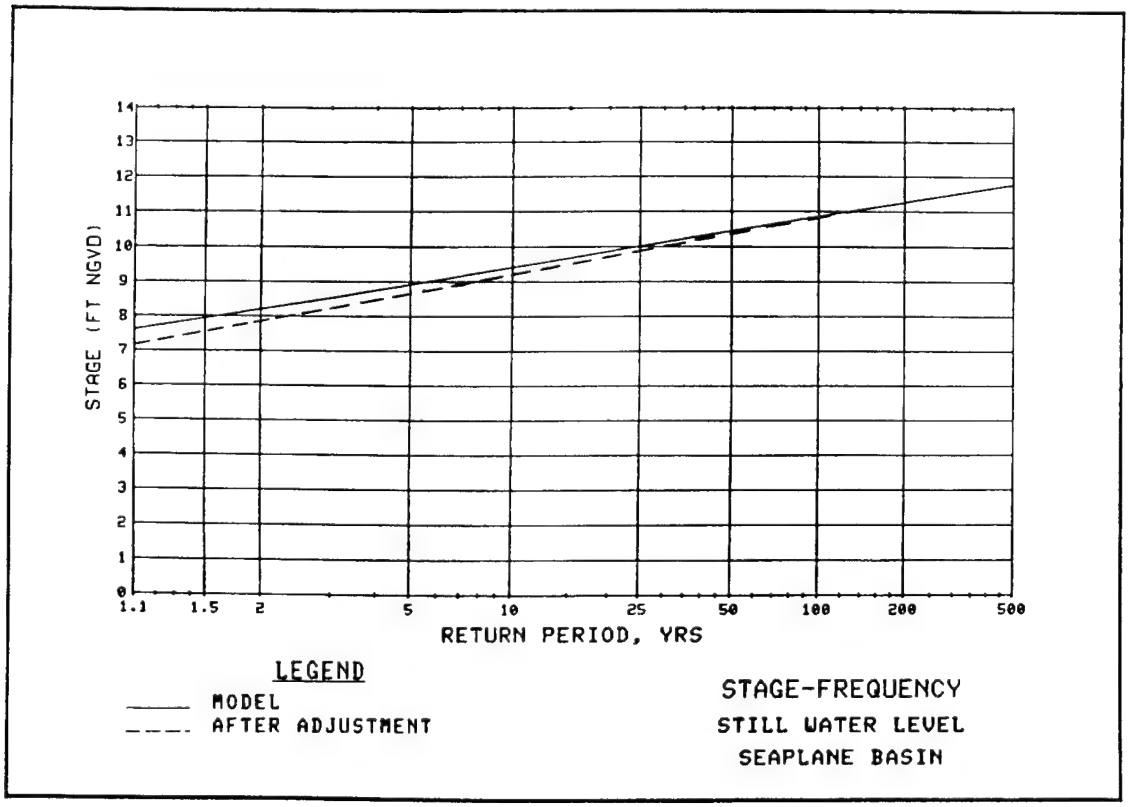

Figure 52. Still-water level stage-frequency curve, Seaplane Basin

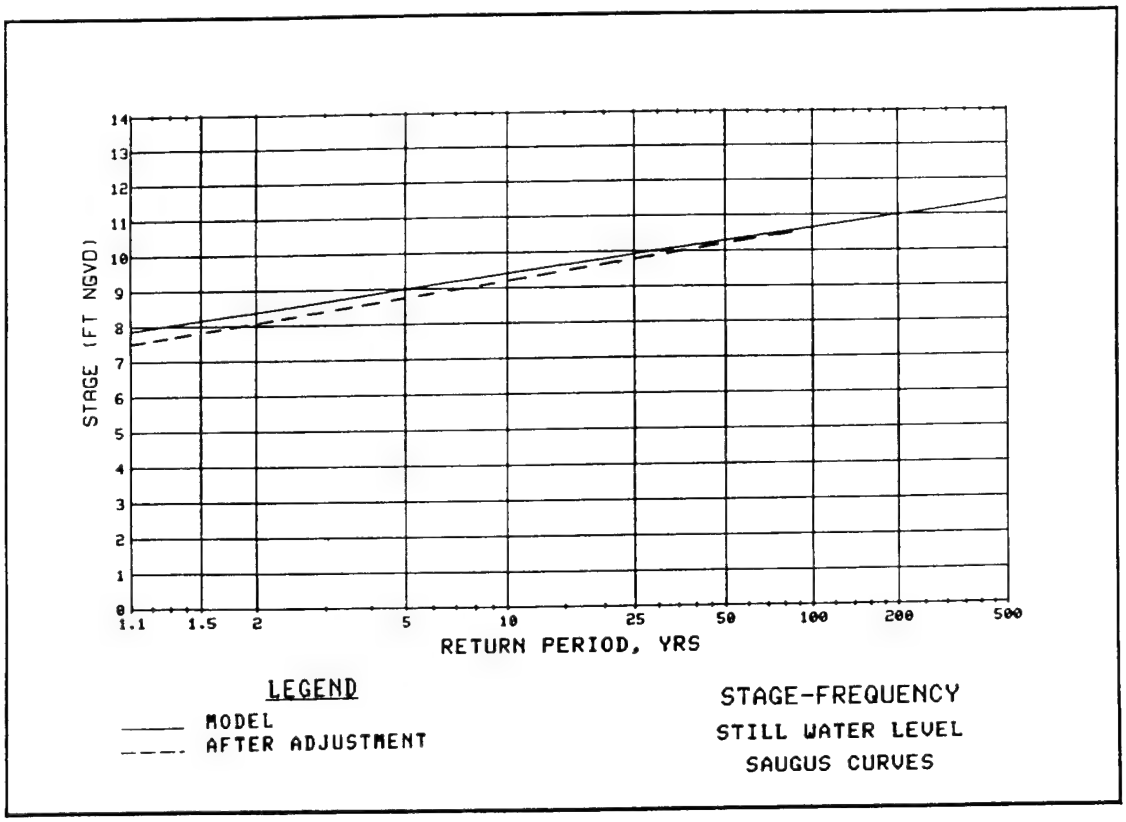

Figure 53. Still-water level stage-frequency curve, Saugus Curves

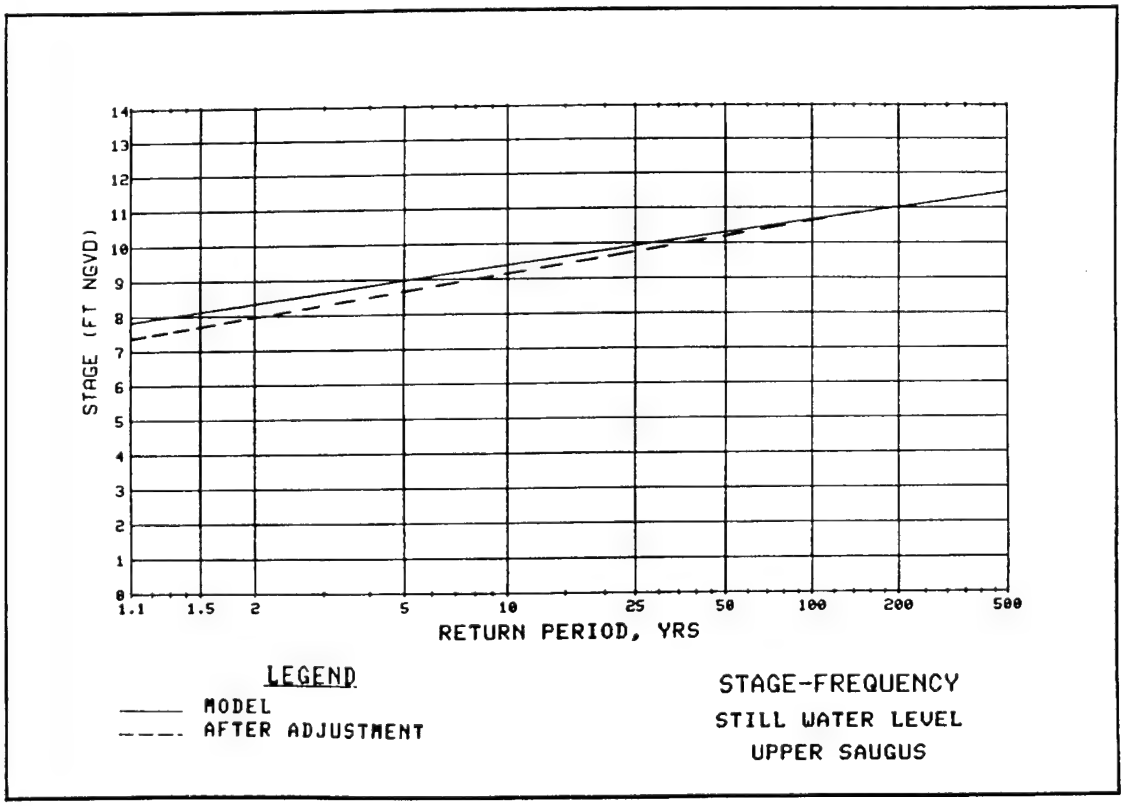

Figure 54. Still-water level stage-frequency curve, Upper Saugus

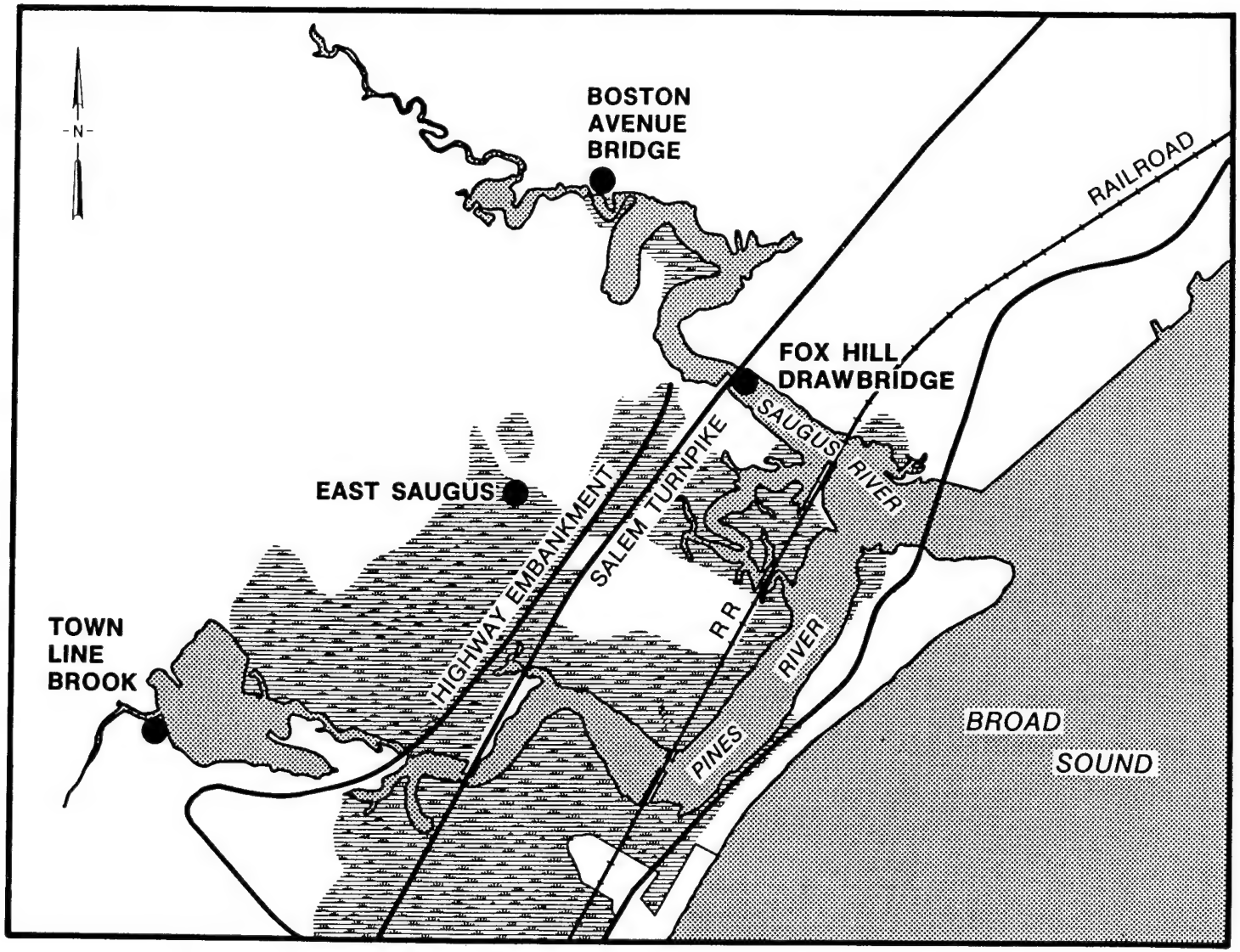

Figure 55. Locations of additional water level data collection

Table 10

Maximum Tide Elevation* Data for Upstream Areas

Location	Date			
	9-17-85	10-15-85	11-13-85	12-12-85
Boston	6.19	7.44	7.20	8.01
Fox Hill Drawbridge	6.55	7.65	7.15	8.1 (est.)
Boston Ave. Bridge	6.1	7.35	6.95	7.9
Town Line Brook	6.1	7.1	6.65	--
East Saugus	--	--	--	6 (est.)

* All elevations are for the maximum elevation and are in feet referenced to NGVD.

upstream of the Fox Hill Draw Bridge. For areas west of the embankment, the curves were lowered by 0.5 ft at 1.5 years, and a straight line was drawn between this level and the original curve at 200 years. The same adjustment was made for the areas west of the drawbridge, except the reduction at 1.5 years was 0.3 ft. The adjustments were phased out at the higher water levels because, as the water level increases, the access of floodwaters to the back locations in the study area improves. The effect of storm surge is to raise the sea level upon which the tide propagates. Unlike a hurrricane surge time-history, which can be sharply peaked because of rapid changes in both speed and direction of the winds, the time-history of almost all the northeaster surges is very broad with any rapid fluctuations in water level confined to several tenths of a foot. At these higher water levels channel cross sections are increased, the effect of bottom friction is lessened because of greater depths, and new paths of access are created from the overtopping of barriers (roadways). All these factors would tend to negate losses seen in Table 9 for higher water levels. The adjustments to the above mentioned areas are shown as the dotted lines in Figures 52-54.

100. Differences among the curves presented in Figures 41-54 are small. This small difference is not surprising considering the small size of the area being modeled. In general, the curves are slightly higher for locations inside the Saugus-Pines River system as compared to locations in Broad Sound. The predominant wind directions during severe northeasters are from the northeast to north. On the inside of the inlet, these directions would tend to

push water up the Pines River away from the inlet, pumping more water into the river system. Curves for locations upstream on the Pines River would be further increased by the effect of the wind setting up the water over the shallow marsh areas. In general there was a small north to south gradient in flood levels with the more southern areas higher by one-half to three-fourths of a foot during the more severe events. For the Broad Sound locations a smaller variation of a few tenths of a foot with the higher levels at the more southern locations also is explained by the direction of the winds.

101. Stage-frequency curves are not presented for the marsh areas west of the highway embankment. Modeling the routing of the floodwaters in these areas is beyond the scope of this study. For lower return periods observations indicate there is a head loss as the waters go north from the Pines River channel across the Saugus Marsh. In these areas, at lower return periods, flow is contained in drainage ditches which are too small to model with the present grid resolution. Also, other subgrid effects such as localized areas of high ground which could thwart the movement of floodwaters are important but were not considered.

102. It is important to emphasize that the effects of ice and snow were not taken into account by the storm surge modeling. It is possible and perhaps even likely that severe northeasters would be accompanied by heavy accumulations of snow and ice formation in the river systems. Snow banks formed from the clearing of roadways could act to divert floodwaters and provide some measure of protection to some areas. Ice could restrict bridge and channel openings and, therefore, reduce the amount of water entering back areas. Ice cover of open water would likely reduce the wind setup of the marsh areas. Although the above mentioned effects indicated the effect of ice and snow would be to reduce flood levels, scenarios are possible where the opposite would be true. For example, ice could divert the flood into areas which would not have been affected without the diversion.

Estimating Error in the Frequency Curves

103. The final products of this study are curves which depict stage versus return period for flood levels at many locations throughout the study area. At any one return period, say 100 years, the curve is merely an estimate of the true flood level. Moreover, this estimate is only a point

estimate which represents a random variable which has a probability distribution. If this probability distribution can be determined, confidence intervals could be calculated by specifying the probability that the true flood level lies between a range of heights about the estimated value. Confidence intervals are relatively easy to determine when dealing with a single data set, for example, confidence intervals about the mean value of a set of data. However, the calculation of stage-frequency curves as done in this study involves multiple data sets and multiple modeling systems. Even if it were possible to determine confidence intervals about each of the processes separately, there would still be the problem of combining separate intervals into one interval for the final stage-frequency curve. The total 90 percent confidence interval would not be the sum of the 90 percent confidence intervals of all the processes. For example, the storm surge model may overpredict, the wave model underpredict, and the probability model assign too low a probability. Consequently, no attempt will be made to place error bounds on the final curves. Instead, a verbal description of the types and, where possible, the magnitudes of the various sources for error will be given. A method has been developed to show curves for the error associated with the process of selecting a limited number of events to be modeled from the infinite number of possible events. Since the physical modeling was not a part of this report, no attempt will be made to determine the potential for error from the physical modeling. The reader will have to analyze the following paragraphs and determine how the possible error will influence any engineering decisions.

104. The modeling of still-water level involved three main parts: data collection and analysis, numerical model calibration, and simulation. The tide gage data used in the project were carefully screened to remove spurious data points; therefore, this information was probably corrected to about 0.1 ft. Calculating accurate tide time-histories was difficult. Five sets of tidal constituents, each based on an analysis done for a different time period, were tested. Due to the large tidal range at Boston, slight errors in the phase of the predicted tide can cause significant errors when calculating the storm surge time-histories. The storm surge time-histories used for combination with tide were edited by eye to remove any errors caused by poor tide prediction. The numerical grid, as shown by the calibration results, had sufficient resolution to accurately model tide in the areas where calibration data were available. WIFM has performed well in numerous studies, and the

calibration and verification in this study produced excellent results. The one-grid system used in this project should prove to be much more accurate than a two-grid system because of the lack of wind data needed to force an outer grid. The major source of potential error in the water level modeling is the lack of storm data for calibration of the model. Implicit in calibrating the model to tide alone is the assumption that the magnitude of the storm surge at the Boston tide gage is very close to the magnitude of the storm surge in the study area for any storm event. Because the two locations are so close to one another in comparison to the size of either the continental shelf or the size of a typical northeaster, this assumption is probably more accurate than the alternative of using a two-grid system. Taking all these factors into account, it is estimated that the accuracy of any one simulation of the storm surge model would be within a few tenths of a foot in areas close to the tide gages and within about one-half foot in those areas west of the highway embankment.

105. The wave modeling portion of the project was less accurate than the water level modeling for four main reasons. First, the state of the art in wave modeling, particularly in shallow water, is not as advanced as in surge modeling. Second, the numerical wave model used is more recent than WIFM and, therefore, less well tested. Third, there were no wave data available for either calibration or verification of the model. And, fourth, the boundary conditions for the wave modeling (the WIS hindcasts which are the best available) were not as accurate as the gage data used for the water level modeling. These four factors are somewhat offset by the fact, that, for all the more severe wave conditions and for many of the times when overtopping occurred at Roughans Point, the waves approaching the wall were depth limited.

106. The flood routing model contained a series of assumptions for calculating outflow from the interior of Roughans Point. For the flood levels bracketed by the 1972 and 1978 floods, the flood routing model should produce good results. However, for extreme floods, the interior water level is heavily dependent upon the volume of water leaving the interior by flowing over roadways and, for existing conditions, over reach D. Therefore, flood levels higher than those produced by the 1978 event are more uncertain than are lower flood levels.

107. The probability model contained several processes which could potentially introduce error into the final curves. These included assigning

probability from the NED Boston stage-frequency curve, selecting events to model, and fitting a curve to the raw modeling results.

108. It is beyond the scope of this report to assign error bounds to the NED stage-frequency curve. However, a simple investigation of the possible error in the curve would be as follows. The curve was based upon 131 years of record, 57 of which were from a continuous record at the NOS tide gage. Because of the relatively long record, the bottom portion of the curve (i.e. return periods of less than 15 years) should be very accurate. The middle portion of the curve (i.e. return periods between 15 and 100 years) is within the length of record and should be accurate to within a few tenths of a foot. The portion of the curve above the 100-year return period would be more uncertain with, of course, the uncertainty increasing with return period. However, because of the extremely flat nature of the curve (there is only a 1-1/4 ft difference between the 50- and 500-year levels), it seems safe to predict that the curve should be accurate to within a half foot even at the 500-year return period.

109. The potential error from the curve fitting process can be best seen in plots of raw versus regressed output. For Fox Hill Drawbridge, the raw and the regressed still-water level stage-frequency curves, previously presented in Figure 35, had a linear regression correlation coefficient of $r = 0.997$. Figure 56 shows the raw versus regressed output for the "Wide Berm + 1-ft Cap" alternative at Roughans Point which had a correlation coefficient of $r = 0.994$. These correlation coefficients are representative of those occurring at all locations. The regression was highly accurate and potentially introduced only minor error into the total process. The lowest correlation coefficient was greater than 0.98 for both the still-water level locations and the interior of Roughans Point.

Determining Error Bands for the Selection Process

110. The selection process that determined which events were selected for modeling was designed specifically for this project. As a result of limited experience with this technique, it is much more difficult to determine the potential error of the selection process as compared to the potential error of the more familiar processes of data collection, data analysis, and numerical modeling. In order to estimate the variability of the selection

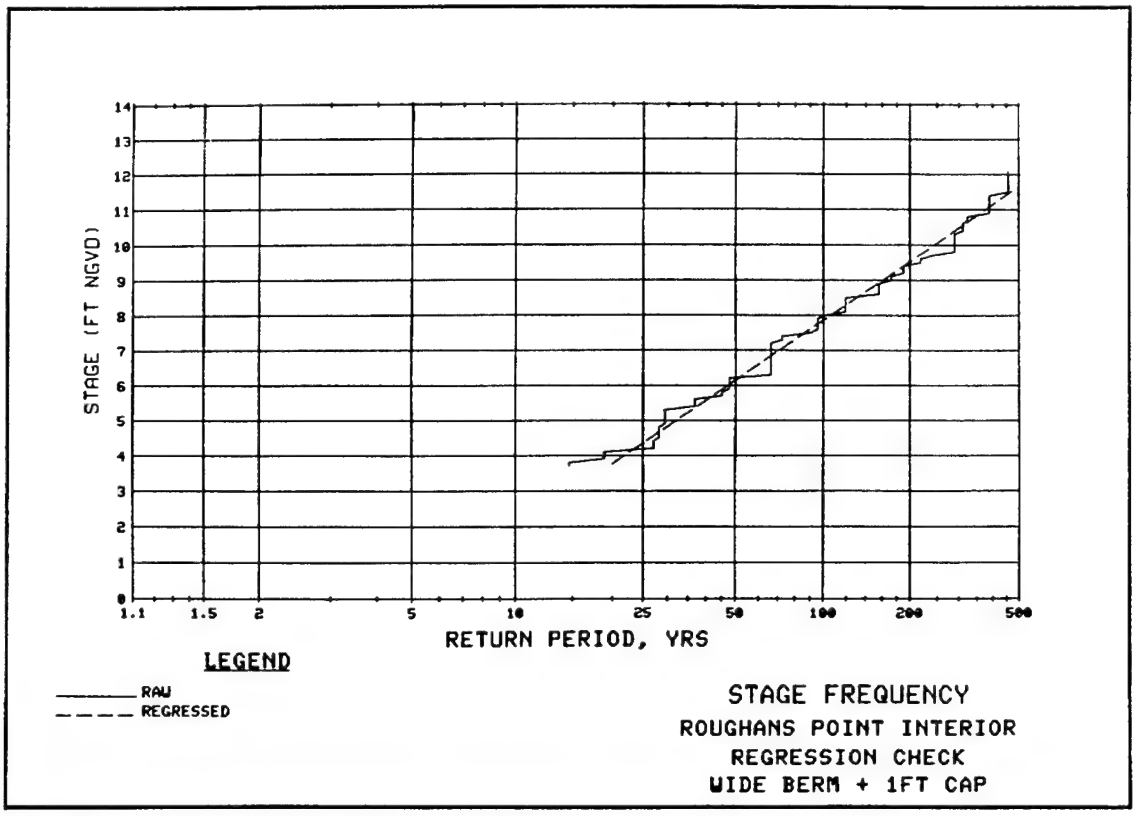

Figure 56. Raw and regressed stage-frequency curves, "Wide Berm + 1-ft Cap"

process, the 150 events were divided into three sets of 50 events each. Each of these sets was processed separately producing three stage-frequency curves. These three curves were generated for each numerical gage for the still-water level locations as well as for each of the six structure combinations at Roughans Point. As was mentioned in Part II, 150 events were more than necessary to produce consistent results for the still-water locations. This assertion was confirmed when stage-frequency curves derived separately from the three sets of 50 events were plotted for each still-water location. For most of the locations there was not a discernible difference between curves from the three sets. Figure 57 contains the three stage-frequency curves for Oak Island which had the greatest variation of all the still-water locations. As can be seen from this figure the variation resulting from selecting a limited number of events to represent all possible events is negligible for the still-water locations.

111. The potential error caused by the selection process is much greater for stage-frequency curves for the interior of Roughans Point than for the stage-frequency curves for the still-water level portion of this project. The flooding levels in the interior of Roughans Point are dependent not only upon

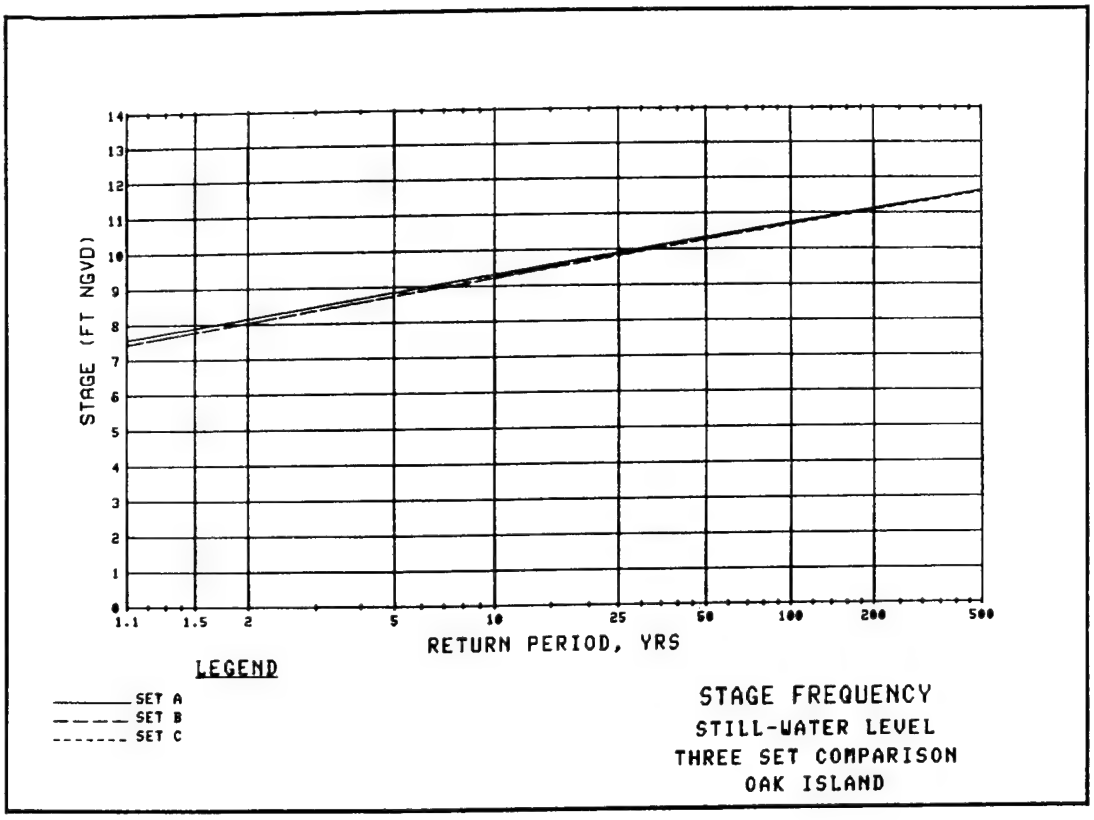

Figure 57. Stage-frequency curves, three-set comparison, Oak Island

the still-water level of the event but also upon the magnitude, direction, and duration of the event's waves. Since the selection process used still-water level as its only criterion, two events which were selected with the same still-water level could have very different wave characteristics and, therefore, could cause very different flood levels at Roughans Point. Stage-frequency curves for the three sets of 50 events are shown in Figures 58 and 59 for the "Wide Berm" and the "Wide Berm + 1-ft Cap" alternatives, respectively, which had the most and the least variation among the three sets, of any of the six Roughans Point structure combinations.

112. Assuming that for any given return period the calculated stage is a normally distributed random variable, an estimate of the probable error PE can be calculated using the three stage-frequency curves generated independently from the three sets of selected events. PE estimates the 50 percent error bounds about the mean value in a series of measurements. Equation 18 states the relationship between PE and standard deviation σ as

$$PE = 0.6745\ \sigma \tag{18}$$

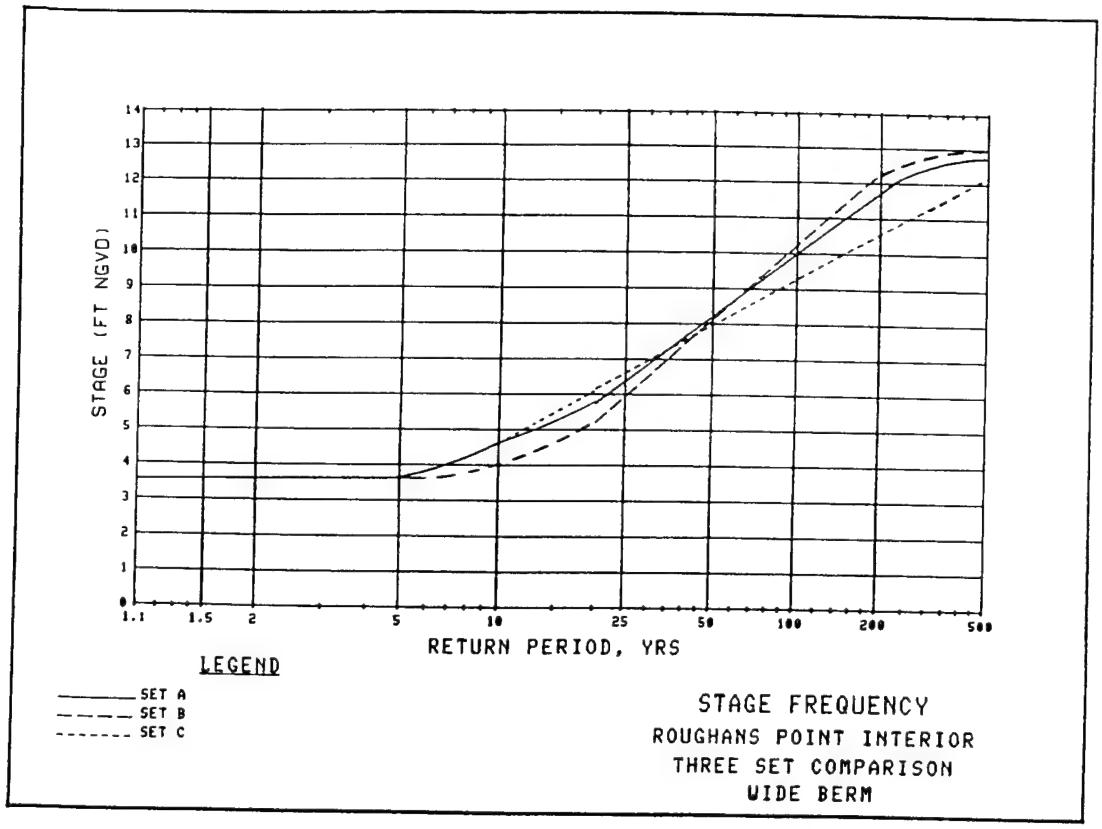

Figure 58. Stage-frequency curves, three-set comparison, "Wide Berm"

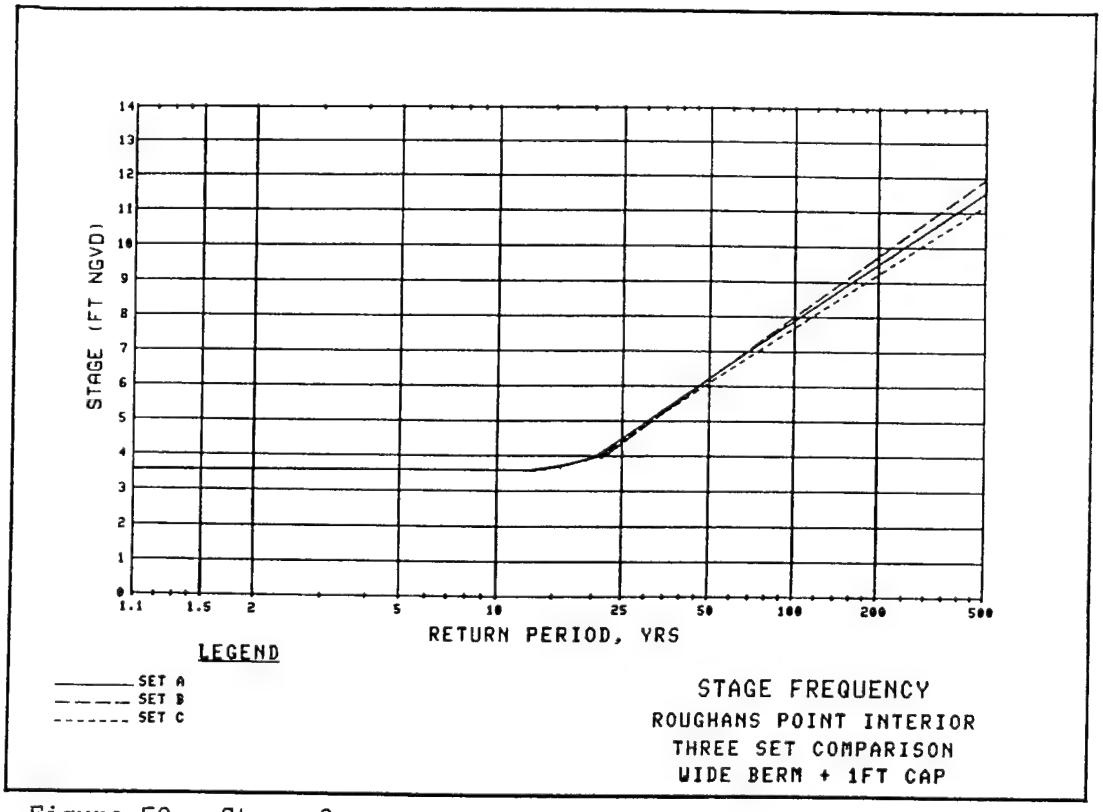

Figure 59. Stage-frequency curves, three-set comparison, "Wide Berm + 1-ft Cap"

Table 11 shows the relationship between the range of stages Ra calculated at any return period and σ, (Beyers 1966).

Table 11
Estimate of Standard Deviation from Range

Sample Size	Estimate of σ
2	0.8862 Ra
3	0.5908 Ra
4	0.4857 Ra

113. A single stage-frequency curve with probable error bands at selected return periods was produced using the following process. First, at each return period where error bounds were desired, the range of simulated stages was determined by ranking the three values and subtracting the smallest from the largest. Second, the PE was estimated using Table 11 and Equation 18. Third, a single curve was produced by processing all 150 events as one set using the methods discussed in Part VI. Finally, the PE bounds were placed upon this combined curve. Figures 60 and 61 show the combined curves with error bounds which correspond to the three curves shown in Figures 58 and 59, respectively. Probable error curves are not presented for any still-water locations. The probable error of the selection process is too small to be seen for the still-water locations because of the small variability shown in Figure 57.

Assessing the Impact of the Standard Project Northeaster

114. The Standard Project Northeaster (SPN) definition can be determined from the definition for the Standard Project Storm (Headquarters, Department of the Army, Office of the Chief of Engineers, 1952) as the northeaster which results from the "most severe combinations of meteorologic" and tidal "conditions that are considered reasonably characteristic of the geographical region involved, excluding extremely rare combinations." For this report two processes are important in considering the specification of an SPN, still-water level and wave overtopping. It is possible that a separate SPN would have to be defined for each process. The SPN which would produce the

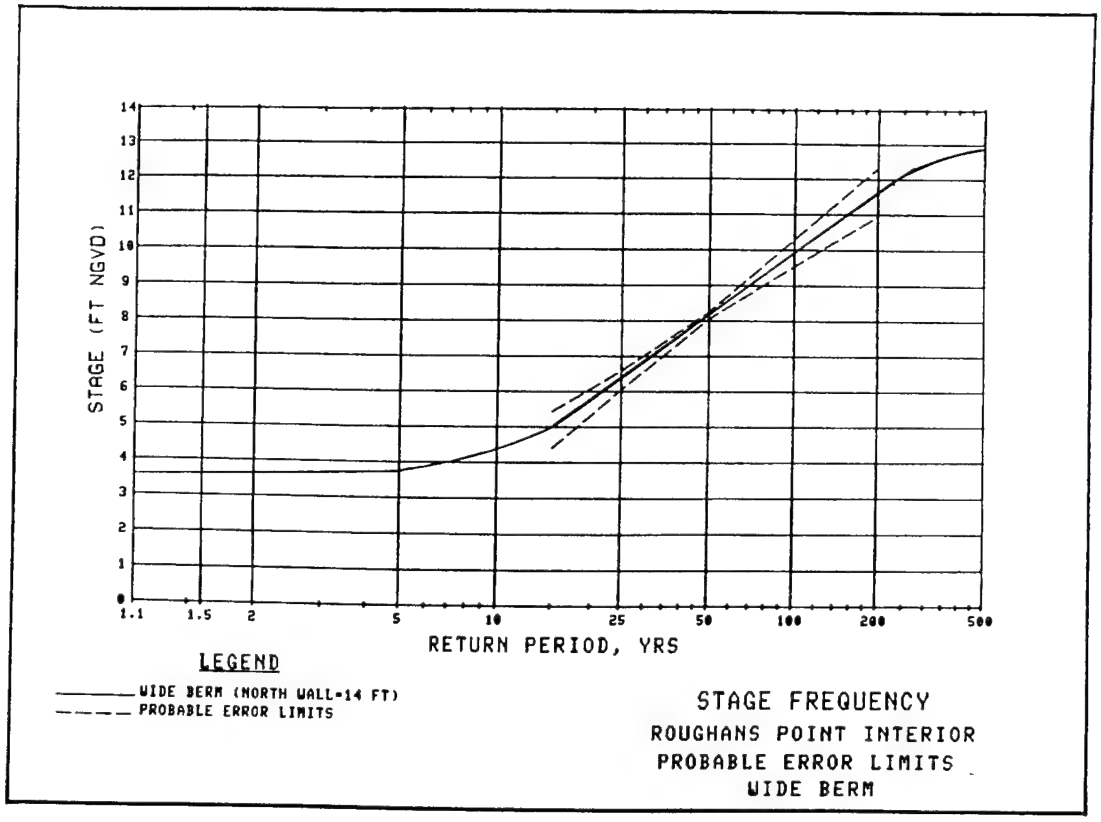

Figure 60. Probable error of the selection process, "Wide Berm"

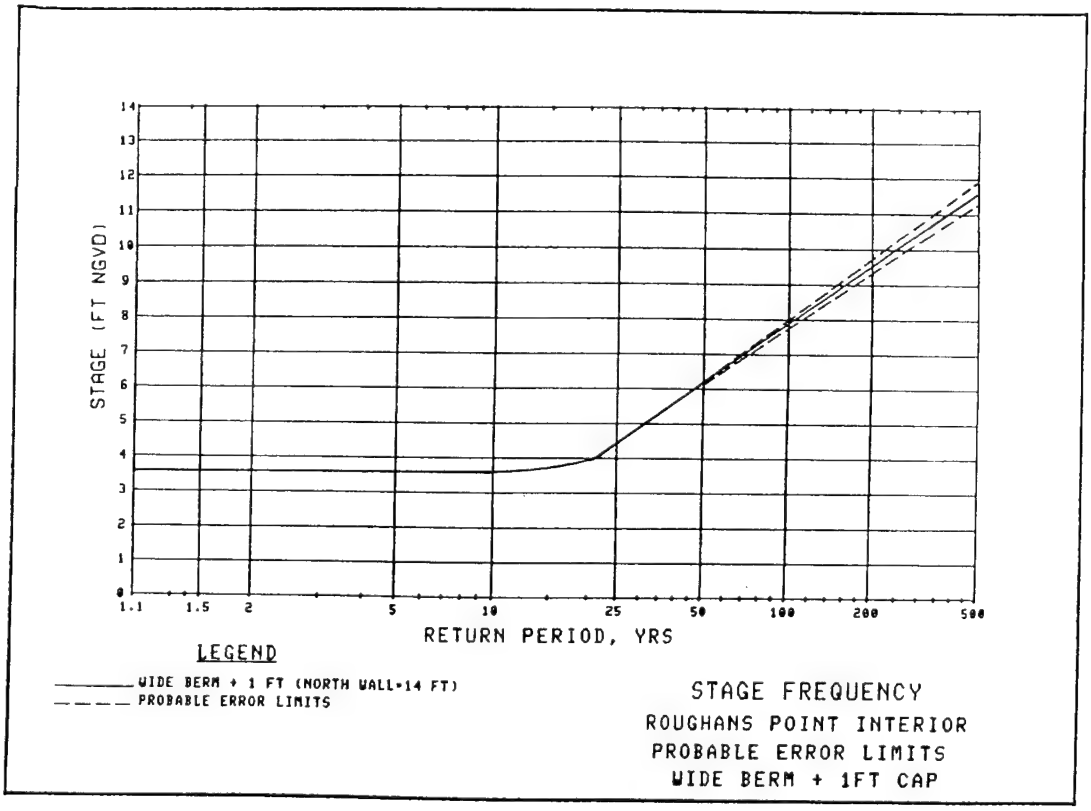

Figure 61. Probable error of the selection process, "Wide Berm + 1-ft Cap"

highest still-water level might not produce the highest waves at Roughans Point and, therefore, not the highest overtopping rates.

115. The SPN still-water level was estimated to be 13.0 ft NGVD (NED 1983) by adding the maximum surge recorded at Boston, about 5 ft, and the maximum probable tide, 7.4 ft NGVD and then rounding up to the next foot of elevation. This resulted in a still-water elevation which was almost 3 ft higher than the maximum ever recorded at the Boston gage. Given the unlikely event that a tide with a maximum elevation near the maximum probable tide were to occur sometime during the maximum surge producing northeaster, the probability that the hour of maximum surge (using hour increments) would occur at the hour of maximum tide is only 1/24 (assuming a semidiurnal tide with unequal highs). Consequently, this combination might fall under the "excluding extremely rare" clause in the definition of the SPN. A better specification of the SPN still-water level might be closer to 12.0 ft NGVD.

116. This report is mainly concerned with the effect of the SPN on interior flooding at Roughans Point and the propagation of the SPN still-water level throughout the study area which can be easily stated regardless of the exact specification of the SPN still-water level. In considering the interior floods at Roughans Point, the effect of an SPN is straightforward; the interior of Roughans Point would fill to overflowing. The interior water level (approximately 1-2 ft higher than the still-water level in Broad Sound) would be determined by how fast the overtopping volumes would flow over roadways at the west boundary of Roughans Point. The evidence seems clear that given a water level on the order of 12-13 ft NGVD and with the waves appropriate for an SPN, all of the proposed alternatives would be swamped. This can best be seen by considering Figure 36. The only alternative which offers significant protection at the highest return periods is the "Wide Berm + 2-ft Cap." However, even this alternative would not offer protection against the SPN. The highest still-water level (in Broad Sound) tested in the simulations was 11.2 ft, roughly a 500-year level. Although the SPN would fall well to the right of the edge of Figure 36, the effect of the SPN can be estimated as follows. The extra foot of still water resulting from the SPN would change a 2-ft cap down to an effective 1-ft cap. Furthermore, the larger and longer waves caused by the effect of deeper water in front of the structure and the higher wind speeds of the SPN would further increase the flood levels. Consequently, the interior levels caused by the SPN with the "Wide Berm + 2-ft

Cap" would be more severe than that shown for the "Wide Berm + 1-ft Cap" at the 500-year return period. It is possible that although the proposed improvements at Roughans Point would offer considerable protection against lesser northeasters, the flood levels for the SPN might be higher after the improvements. Without the improvements, water will begin returning to the ocean over the north wall at approximately 11 ft NGVD. This outflow of water considerably lessens the probability of extreme interior flood levels. With the improvements, this outflow would be prevented by the increased wall heights until much higher water levels. The lack of data to ascertain the relative importance of outflow over the walls versus the outflow at the western edge of the Roughans Point area at extreme interior flood levels makes definitive conclusions difficult.

117. For the still-water locations the numerical storm surge model results showed that the Broad Sound maximum water levels produced by the ensemble storms were efficiently conveyed throughout the Saugus-Pines River system. Differences between outside and inside water levels were always small with the inside level usually slightly higher. The time-history of the SPN surge might be more peaked. This peaked profile would likely suffer more loss through the inlet and channel system, but this loss would be offset by the local wind setup of the shallower water of the flood plain (the cause of the higher interior levels during the simulations). Therefore, the predicted result of the SPN still-water level would be that the whole study area would flood to the level of the SPN in Broad Sound.

Conclusions

118. Stage-frequency curves for 15 possible structure combinations at Roughans Point and for 14 still-water level locations were presented and discussed. The potential error associated with each step of the procedure was discussed. A more formal determination of the probable error of the selection process was presented. Finally the estimated impact of the SPN was discussed for both interior flooding at Roughans Point and the still-water locations.

119. At Roughans Point, where flooding is caused by the overtopping of seawalls by storm waves, physical, numerical storm surge, numerical wave, flood routing, and probability models were needed. Multiple combinations of possible seawall-revetment structures were modeled. Major differences among

the combinations were evident at the lower return periods with the combinations of a wide berm revetment and a cap on the existing seawall for the east wall of Roughans Point providing the greatest protection. At higher return periods the protection differential offered by the various structure combinations tends to diminish. For still-water levels and wave conditions of an SPN, all structure combinations tested would be ineffective at protecting the interior of Roughans Point. Tests were run to determine a structure height for the north wall. These tests indicated that significant overtopping did not begin until the north wall structure was lowered below 13 ft. Since the existing height of the north wall is above this level at several sections, it is recommended that the revetment height be set at 13 ft with the wall height being set so that there is a transition between the existing wall heights. The only height that would be raised would be that of wall D, which would be raised to match wall C.

120. For areas where flooding is due to coastal inundation by the still-water level resulting from the combination of storm surge and astronomical tide, only the storm surge and probability models were necessary. These areas include both open coast and estuarine locations. For these areas flooded by the still-water level, the results of the modeling indicated that the whole study area floods to approximately the same level. The flood levels are efficiently conveyed through the inlet and throughout the flood plain of the Saugus-Pines River system. Inside the inlet there is a small gradient in the still-water level, rising from north to south, which results from local wind setup caused by north to northeast winds which predominate during storm conditions. This local wind setup results in flood levels inside the inlet which vary by one-half to three-fourths of a foot during the more severe storm events. Outside the river system in Broad Sound a smaller north-south gradient exists with differences of only a few tenths of a foot resulting. Data collected after completion of the modeling indicated that losses do occur as the flood levels are conveyed upstream of the Fox Hill Drawbridge on the Saugus River and upstream of the Highway embankment on the Pines River. Stage-frequency curves for these areas were adjusted to accommodate these additional data. The curves were lowered 0.3 and 0.5 ft at the lower return periods for upstream Saugus River and Pines river locations, respectively. These reductions were linearly reduced for higher return periods because higher flood levels would provide greater access to these areas.

REFERENCES

Ahrens, J. P., and Heimbaugh, M. S. In preparation. "Irregular Wave Overtopping of Seawall/Revetment Configurations, Roughans Point Massachusetts," Technical Report, US Army Engineer Waterways Experiment Station, Vicksburg, Miss.

Ahrens, J. P., and McCartney, B. L. 1975. "Wave Period Effect on the Stability of Riprap," Proceedings of Civil Engineering in the Oceans/III, American Society of Civil Engineers, pp 1019-1034.

Beyers, W. H., ed. 1966. Handbook of Tables for Probability and Statistics, The Chemical Rubber Company, Cleveland, Ohio. pp 270-272.

Butler, H. L. 1978. "Coastal Flood Simulations in Stretched Coordinates," Proceedings, 16th International Conference on Coastal Engineering, Hamburg, Germany.

_____. 1983. "Lake Pontchartrain and Vicinity Hurricane Protection Plan, Report 3, Numerical Model Investigation of Plan Impact On the Tidal Prism of Lake Pontchartrain," Technical Report HL-82-2, US Army Engineer Waterways Experiment Station, Vicksburg, Miss.

Corson, W. D., et al. 1981 (Jan). "Atlantic Coast Hindcast, Deepwater, Significant Wave Information," WIS Report 2, US Army Engineer Waterways Experiment Station, Vicksburg, Miss

_____. 1982 (Mar). "Atlantic Coast Hindcast Phase II, Significant Wave Information," WIS Report 6, US Army Engineer Waterways Experiment Station, Vicksburg, Miss.

Harris, D. L. 1981. "Tides and Tidal Datums in the United States," CERC Special Report No. 7, US Army Engineer Waterways Experiment Station, Vicksburg, Miss.

Headquarters, Department of the Army, Office of the Chief of Engineers. 1952. "Standard Project Flood Determinations," Engineer Manual 1110-2-1411, US Government Printing Office, Washington, DC.

Hubertz, J. M. 1985. "A Users Guide to a Steady-State Shallow-Water Directional Spectral Wave Model," Instruction Report CERC-86-1, US Army Engineer Waterways Experiment Station, Vicksburg, Miss.

Hughes, S. A. 1984. "The TMA Shallow-Water Spectrum, Description and Applications," Technical Report CERC-84-7, US Army Engineer Waterways Experiment Station, Vicksburg, Miss.

Jensen, R. E. 1983. "Methodology for the Calculation of Shallow-Water Wave Climate, WIS Report 8," US Army Engineer Waterways Experiment Station, Vicksburg, Miss.

Kitaigorodskii, S. A., Krasitskii, V. P., and Zaslavakii, M. M. 1975. "On Phillips' Theory of Equilibrium Range in the Spectra of Wind Generated Gravity Waves," Journal of Physical Oceanography, Volume 5, pp. 410-420.

Meyers, V. A. 1970. "Joint Probability Method of Tide Frequency Analysis Applied to Atlantic City and Long Beach Island, N. J.," ESSA Technical Memorandum WBTM HYDRO 11, US Department of Commerce, Environmental Science Services Administration, Weather Bureau, Silver Springs, Md.

Prater, M. D., Hardy, T. A., and Butler, H. L. In preparation. "Fire Island to Montauk Point, New York, Storm Surge Model Study," Technical Report, US Army Engineer Waterways Experiment Station, Vicksburg, Miss.

Shore Protection Manual. 1984. 4th edition, 2 volumes, US Army Engineer Waterways Experiment Station, Coastal Engineering Research Center, US Government Printing Office, Washington, DC.

US Army Engineer Division, New England. 1983. "Roughans Point, Revere, Massachusetts-Coastal Flood Protection Study, Interim Report," Vols I and II, Waltham, Mass.

Weggel, J. R. 1977. "Wave Overtopping Equation," Proceedings of the Fifteenth Coastal Engineering Conference, American Society of Civil Engineers, pp 2737-2755.